UNIVERSITÀ DEGLI STUDI DELL'AQUILA

Dipartimento di Scienze Fisiche e Chimiche

Dottorato di Ricerca in Scienze Fisiche e Chimiche

XXXII ciclo

Titolo della tesi

Preparation and physicochemical characterization of *novel* mixed liposomes for medical applications

SSD CHIM/06

Dottorando

Sara Battista

Coordinatore del corso:

Prof. Antonio Mecozzi

Tutore:

Prof.ssa Luisa Giansanti

ANNO ACCADEMICO 2018-2019

Theory is when we know everything
but nothing works.
Praxis is when everything works
but we do not know why.
We always end up by combining
theory with praxis:
nothing works and
we do not know why.

Albert Einstein

Index

Chapter 1

Liposomes

1.1 Introduction

Liposomes are self-assembled colloidal particles that occur naturally and can be prepared artificially,[1] as shown by Bangham and his students in the mid-1960s:[2] they consist of an aqueous volume entrapped by one or more bilayers of (Figure 1).

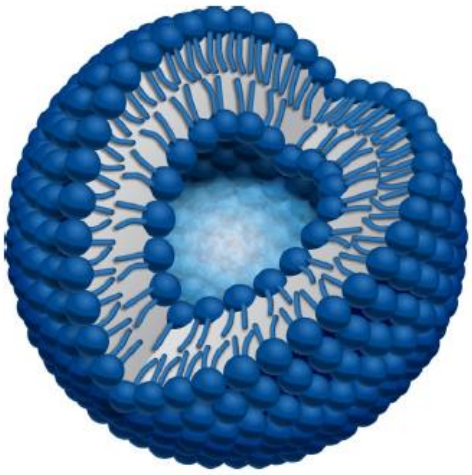

Figure 1. Cross section of an unilamellar liposome

They are generally composed of relatively biocompatible and biodegradable material natural and/or synthetic lipids (phospho- and sphingo-lipids) and may also contain other bilayer constituents such as cholesterol (chol) and hydrophilic polymer conjugated lipids. Liposomes are not a thermodynamically stable state (that would be quickly affected by change in the environment) and do not form 'spontaneously' (without input of external energy); they are only kinetically stable thus, are stable to dilution and preserve their size, shape and encapsulated content better then micelles or microemulsions.[3] The physical properties of liposomes depend on the chemical structure of the amphiphiles used as well as on the method

[1] Lasic, D. D. Liposomes: from Physics to Applications. *Elsevier*, **1993,** 67,1358-1362
[2] Bangham, A. D. Liposome Letters. *Academic Press*, **1983**, 49, 122-124
[3] Lasic, D. D.; Papahadjopulos, D. Medical Applications of Liposome. *Elsevier,* **1998,** 1-5, 1-50

of preparation. Physical instabilities of lipid vesicles involve their aggregation and fusion (leading to precipitation and flat bilayer formation over time). The formation of vesicles can be viewed as a two-step self-assembly process, in which the amphiphile first forms a bilayer, which then, in a second step, closes to form a vesicle. In the classical description, the factor determining the shape of self-assembled amphiphilic structures is the size of either the hydrophobic and the hydrophilic part. Their size determines the curvature of the hydrophobic-hydrophilic interface as described by its mean curvature H and its Gaussian curvature K, which are given by the two radii of curvature R_1 and R_2, as shown in Figure 2.

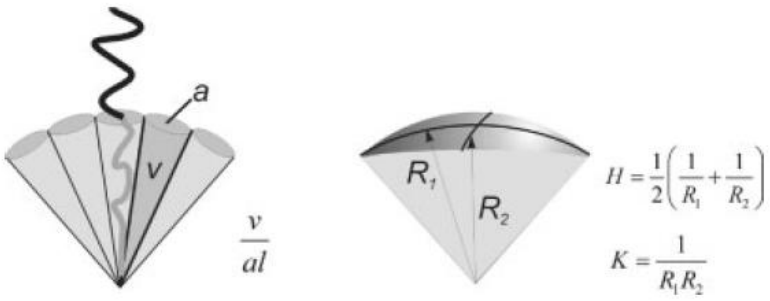

Figure 2. Description of the amphiphile shape in terms of the surfactant parameter v/al and its relation to the interfacial mean curvature (H) and Gaussian curvature (K).

The curvature is related to the surfactant packing parameter by [4]

$$\frac{v}{al} = 1 + Hl + \frac{Kl^2}{3}$$

where v is the hydrophobic volume of the amphiphile, a the interfacial area and l the chain length normal to the interface (Figure 2). Liposomes can be considered as spheres and are characterized by values of packing parameter and curvature shown in Table 1.

[4] S. Hyde. Curvature and the Global Structure of Interfaces in Surfactant Water Systems. *J.Phys.-Paris*, **1990**, 51 (C7), 209-228

Table 1. Packing parameter, mean curvature (H) and Gaussian curvature (K) for aggregation structures of different shapes.

Shape	$v/(al)$	H	K
Sphere	1/3	$1/R$	$1/R^2$
Cylinder	1/2	$1/(2R)$	0
Bilayer	1	0	0

On the basis of their size and number of bilayers, liposomes can also be classified into one of three categories:[5]

- ✓ SUVs (*Small Unilamellar Vesicles*): dimensions between 20 and 100 nm, they are homogeneous and formed by only one bilayer. SUV are enough instable vesicles and tend to fusion; they show a low ratio water/lipid (0.2-2.5 L per mol of lipid).
- ✓ LUVs (*Large Unilamellar Vesicles*) dimensions higher than 0.1 μm, they are formed by only one bilayer and show a high ratio water/lipid (7 L per mol of lipid); they are useful to vehiculate large amounts of hydrophilic drugs.
- ✓ GUVs (*Giant Unilamellar Vesicles*): dimensions between 1 and 200 μm, they are formed by only one bilayer and show a high ratio water/lipid (more than 7 L per mol of lipid); they are mostly used as models for biological membranes.
- ✓ MLVs (*Multilamellar Large Vesicles*): dimensions higher than 0.5 μm, they are quite stable but inhomogeneous for dimensions and lamellarity; they are very easy to prepare and are formed by many bilayers. MLV can incapsulate large amounts of hydrophobic substances and show a good ratio water/lipid (1-4 L per mol of lipid).

It's also possible to obtain multivesicular solutions in which small liposomes are entrapped in bigger ones or oligolamellar liposomes (Figure 3).

[5] Laouini, A.; Jaafar-Maalej, C.; Limayem-Blouza, I.; Sfar, S.; Charcosset, C. Fessi, H. Preparation, Characterization and Applications of Liposomes: State of the Art. *J. Colloid Sci. Biotechnol*. **2012**, 1, 147–168

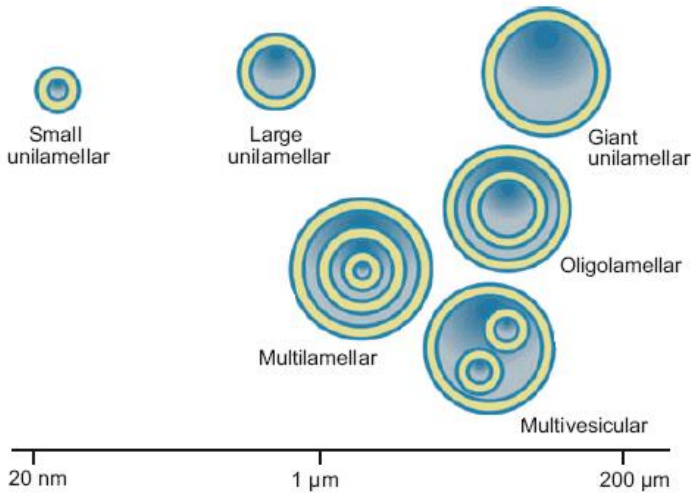

Figure 3. Structural and morphological classification of liposomes.

Liposomes have a characteristic phase transition temperature (Tm) which involves substantial changes in the organization and motion of the fatty acyl chains within the bilayer. Below Tm lipids are in a rigid, well-ordered arrangement ("solid" gel-like phase); above Tm are in a liquid-crystalline ("fluid") phase (Figure 4).

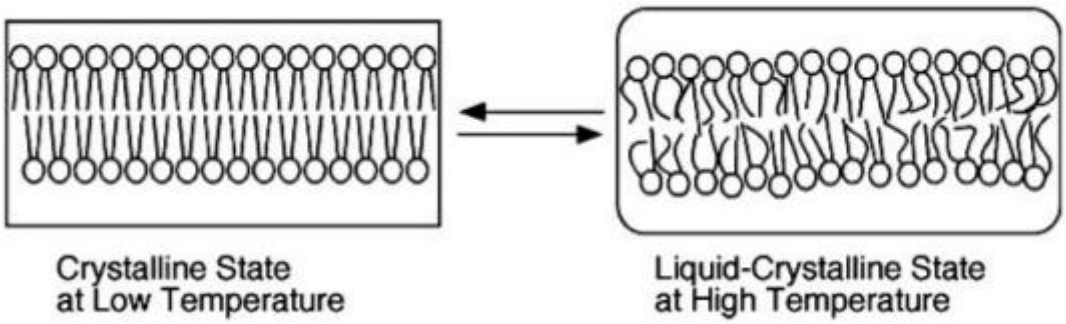

Figure 4. Schematic representation of the lipid arrangement in a planar bilayer below and above the main lamellar chain-melting phase transition temperature (Tm). When a membrane is warmed through the Tm surface area increases and the thickness decreases as the membrane goes through a phase transition. The mobility of the lipid chains increases dramatically. All mechanical treatments of lipid vesicles have to be carried out above Tm, in the fluid state of the membranes.

Below Tm, the saturated hydrophobic chains exist predominately in a rigid, extended all *trans* conformation, similar to their crystalline state. As a result, the surface area per lipid is minimal and the bilayer thickness is maximal. Above Tm,

the chains are rather disordered with a lot of gauche conformations in the hydrocarbon chains, making the bilayer fluid (mechanically treatable), characterized by increased lateral and rotational lipid diffusion rather similar to a liquid; as a result, the surface area per lipid increases and the bilayer thickness decreases by 10 to 15% (Figure 5).

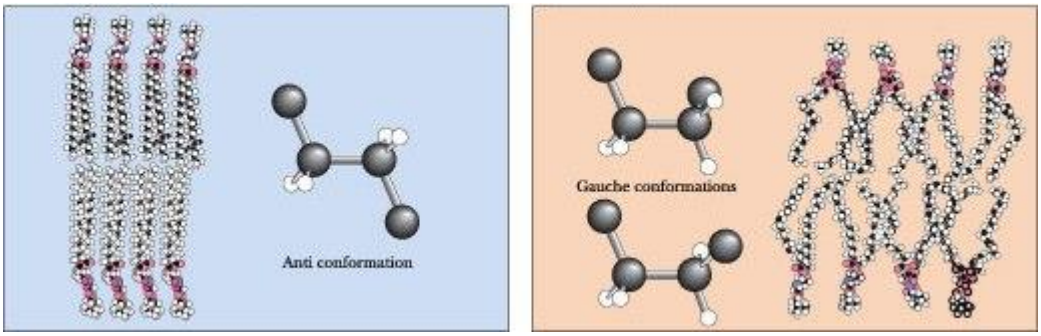

Figure 5. Below the phase transition, lipid chains primarily adopt the *anti*-conformation. Above the phase transition, lipid chains adopt higher-energy conformations, including the gauche conformations shown.

Tm values depend mostly on chain length and on the presence of unsaturation. The curvature of the bilayer (thus liposomes dimensions) and the experimental conditions can also affect Tm to some extent. The presence of chol can lead to a variation or to the disappearance of Tm because there is a loss in cooperativity of the transition. In fact, chol disturbs intermolecular interactions in a complex manner: it either inhibits the formation of the crystalline-analogue state in the case of 1,2-dipalmitoyl-*sn*-glycero-3-phosphocholine (DPPC) or induces the formation of chol-rich and lipid-rich domains.[6] At high concentrations (>30 molar %), chol can totally eliminate the phase transition and decrease the membrane fluidity making liposomes more stable and less leaky after systemic administration.

In analogy to the case of chol, the use of lipid mixtures may result in the formation of domains within the bilayers which are enriched with one of the lipids.[3] The fluidity of liposome can be altered by using phospholipids with different Tm which in turn can vary from –20 to 90°C depending upon the length and the nature

[6] Bakht, O.; Pathak, P.; London, E. Effect of the Structure of Lipids Favoring Disordered Domain Formation on the Stability of Cholesterol-containing Ordered Domains (Lipid Rafts): Identification of Multiple Raft-stabilization Mechanisms. *Biophys J.* **2007**, 93(12), 4307–4318

(saturated or unsaturated) of the fatty acid chains. Presence of high Tm lipids (Tm > 37 °C) makes the liposome bilayer less fluid at the physiological temperature and less leaky. In contrast, liposomes composed of low Tm lipids (Tm < 37 °C) are more susceptible to leakage of drugs encapsulated in aqueous phase at physiological temperatures. The fluidity of bilayers may also influence the interaction of liposomes with cells: liposomes composed of high Tm lipids appear to have a lower extent of uptake by reticuloendothelial system compared to those containing low Tm lipids.

1.2 Applications

Due to their structure, chemical composition and colloidal size (that can be well controlled by preparation methods), liposomes exhibit several properties which may be useful in various applications. The most important properties are colloidal size, rather uniform in size distribution, and special membrane and surface characteristics. They include bilayer phase behaviour, its mechanical properties and permeability, charge density, presence of surface bound or grafted polymers, or attachment of special ligands, respectively. Moreover, due to their amphiphilic character, liposomes are a powerful solubilizing system for a wide range of compounds. In addition to these physico-chemical properties, liposomes exhibit many special biological characteristics, including (specific) interactions with biological membranes and various cells.[7]

Based on these premises, several possible applications of liposomes can be envisaged: to solubilise difficult-to-dissolve substances, dispersants, sustained release systems, delivery systems or microencapsulation systems and microreactors being the most obvious ones. The structure of liposomes offers also a system to compartmentalise chemical reactions and can be used in catalysis or in studies of biomineralization.[8,9] In addition to all these applications, liposomes are very useful

[7] Lasic, D.D. Liposomes. *Am. Sci*. **1992**, 80, 20–31.

[8] Michel, M.; Winterhalter, M.; Darbois, L.; Hemmerle, J.; Voegel, J.C.; Schaaf, P.; Ball, V. Giant Liposome Microreactors for Controlled Production of Calcium Phosphate Crystals. *Langmuir*, **2004**, 20(15), 6127-6133

[9] Kulin, S.; Kishore, R.; Helmerson, K.; Locascio, L. Optical Manipulation and Fusion of Liposomes as Microreactors. *Langmuir*, **2003**, 19-20, 8206-8210

model systems in many fundamental studies from topology, membrane biophysics, photophysics and photochemistry, colloid interactions, cell function, signal transduction, and many others, as summarized in Table 2.[7,10,11]

Table 2. Applications of liposomes in the science

Discipline	Application
Mathematics	Topology of two-dimensional surfaces in three-dimensional space governed only by bilayer elasticity
Physics	Aggregation behaviour, fractals, soft and high-strength materials
Biophysics	Permeability, phase transitions in two-dimensions, photophysics
Physical Chemistry	Colloid behaviour in a system of well-defined physical characteristics, inter- and intra-aggregate forces, DLVO
Chemistry	Photochemistry, artificial photosynthesis, catalysis, microcompartmentalization
Biochemistry	Reconstitution of membrane proteins into artificial membranes
Biology	Model biological membranes, cell function, fusion, recognition
Pharmaceutics	Studies of drug action
Medicine	Drug-delivery and medical diagnostics, gene therapy

One of the most prolific areas of liposome applications is in biochemical investigations of conformation and function of membrane proteins. These are the so-called reconstitution studies and purified membrane proteins, such as ion pumps (sodium potassium- or calcium-ATPases), or glucose transport proteins are reconstituted in their active form into liposomes and then studied. This research has important consequences on our understanding of proteins and cell function.[12,13]

The pharmaceutical applications of liposomes are as drug delivery vehicles, adjuvants in vaccination, signal enhancers/carriers in medical diagnostics and analytical biochemistry, solubilizers for various ingredients as well as support matrix for various ingredients and penetration enhancer in cosmetics.[14] Another important advantage of liposomes is the possibility of modifying their surface for improving specificity towards tissues or for reduced recognition in the

[10] Lipowsky, R. The conformation of membranes. *Nature*, **1992**, 349, 475–481

[11] Routledge, S. J.; Linney, J. A.; Goddard, A. D.; Liposomes as Models for Membrane Integrity. *Biochemical Society Transactions*. **2019**, DOI: 10.1042/BST20190123

[12] Cornelius, F. Functional Reconstitution of the Sodium Pump. Kinetics and Exchange Reactions Performed by Reconstituted Na/K ATPase. *Biochim. Biophys. Acta,* **1991**,1071, 19–66

[13] Villalobo, A. Reconstitution of Ion-motive Transport ATPases in Artificial Lipid Membranes. *Biochim. Biophys. Acta*, **1991**, 1071, 1–48

[14] Daraee, H.; Etemadi, A.; Kouhi , M.; Alimirzalu, S. Application of Liposomes in Medicine and Drug Delivery. *Artif Cells Nanomed Biotechnol*. **2016**, 44(1), 381-91.

bloodstream.[15,16] Antibody-tagged immunoliposomes and long-circulating liposomes grafted with a protective polymer, are two important strategies employed for liposomal drug products to achieve these respective outcomes.[17] Immunoliposomes can increase the accumulation of liposomal drugs in the desired tissues and organs,[18] while PEG-coated long-circulating liposomes can prevent the interaction between liposomes with opsonizing proteins, resulting in a prolonged circulatory time in blood. Applications of liposomes containing drugs or various markers in pharmacology and medicine can be divided into therapeutic and diagnostic ones.

1.2.1 Liposomes as drug delivery systems

Unfortunately, many drugs have a very narrow therapeutic window, meaning that the therapeutic concentration is not much lower than the toxic one. In several cases the toxicity can be reduced or the efficacy enhanced by the use of an appropriate drug carrier which changes the temporal and spatial distribution of the drug, that is its pharmacokinetics and biodistribution. Liposomes as drug delivery systems can offer several advantages over conventional dosage forms especially for parenteral (*i.e*. local or systemic injection or infusion), topical, and pulmonary route of administration.[19,20] Moreover, liposomes exhibit different biodistribution and pharmacokinetics than free drug molecules.[21] In several cases this aspect can be used to improve their therapeutic efficacy.

The benefits of drug loaded liposomes, which can be applied as (colloidal) solution, aerosol, or in (semi) solid forms, such as creams and gels, can be summarized into seven categories:

---

[15] Liu, G. D.; Wang, J.; Wu, H.; Lin Y. Y.; Lin, Y. H. Nanovehicles Based Bioassay Labels. *Electroanalysis*, **2007**, 19, 777–785

[16] Seydack, M. Nanoparticle labels in immunosensing using optical detection methods. *Biosens. Bioelectron.* **2005**, 20, 2454–2469

[17] El-Aneed, A. An overview of current delivery systems in cancer gene therapy. *J. Controlled Release*, **2004**, 94, 1–14

[18] Sugano, M.; Egilmez, N. K.; Yokota, S. J.; Chen, F. A.; Harding, J.; Huang, S. K.; Bankert, R. B. Antibody Targeting of Doxorubicin-loaded Liposomes Suppresses the Growth and Metastatic Spread of Established Human Lung Tumor Xenografts in Severe Combined Immunodeficient Mice. *Cancer Res.* **2000**, 60, 6942–6949

[19] Kellaway, I. W.; Farr, S. J. Liposomes as Drug Delivery Systems to the Lung, *Advanced Drug Delivery Reviews*, **1990**, 5 (1,2) Pages 149-161

[20] Bozzuto, G.; Molinari, A. Liposomes as Nanomedical Devices**,** *Int. J. Nanomedicine*. **2015**, 10, 975–999

[21] Sercombe, L.; Veerati, T.; Moheimani, F.; Wu, S. Y.; Sood, A. K.; Hua, S. Advances and Challenges of Liposome Assisted Drug Delivery. *Front Pharmacol*. **2015**; 6, 286-289

- ✓ improved solubility of lipophilic and amphiphilic drugs: examples include porphyrins, Amphotericin B, Minoxidil, some peptides, and anthracyclines, respectively; furthermore, in some cases hydrophilic drugs, such as anticancer agent Doxorubicin or Acyclovir can be encapsulated in the liposome interior at concentrations several fold above their aqueous solubility. This is possible due to precipitation of the drug or gel formation inside the liposome with appropriate substances encapsulated;[22]
- ✓ passive targeting to the cells of the immune system, especially cells of the mononuclear phagocytic system (in older literature reticuloendothelial system). Examples are antimonials, Amphotericin B, porphyrins and also vaccines, immunomodulators or (immune)suppressors;
- ✓ sustained release system of systemically or locally administered liposomes. Examples are Doxorubicin, cytosine arabinose, cortisones, biological proteins or peptides such as vasopressin;
- ✓ site-avoidance mechanism: liposomes do not dispose in certain organs, such as heart, kidneys, brain, and nervous system and this reduces cardio-, nephro-, and neuro-toxicity. Typical examples are reduced nephrotoxicity of Amphotericin B, and reduced cardiotoxicity of Doxorubicin liposomes;
- ✓ site specific targeting: in certain cases, liposomes with surface attached ligands can bind to target cells ('key and lock' mechanism), or can be delivered into the target tissue by local anatomical conditions such as leaky and badly formed blood vessels, their basal lamina, and capillaries. Examples include anticancer, antiinfection and anti-inflammatory drugs;
- ✓ improved transfer of hydrophilic, charged molecules such as chelators, antibiotics, plasmids, and genes into cells;
- ✓ improved penetration into tissues, especially in the case of dermally applied liposomal dosage forms. Examples include anaesthetics, corticosteroids, and insulin.

In general, liposome encapsulation is considered when drugs are very potent, toxic and have very short life times in the blood circulation or at the sites of local

[22] Lasic, D.D; Frederik, P.M.; Stuart, M.C.A.; Barenholz Y.; McIntosh, T.J. Gelation of Liposome Interior. A Novel Method for Drug Encapsulation, *FEBS Lett.* **1992**, 312, 255–258

(subcutaneous, intramuscular or intrapulmonary) administration. In Table 3 are reported many current applications of liposomes in pharmaceutical industry.

Table 3. Liposomes in the pharmaceutical industry

Liposome Utility	Current Applications	Disease States Treated
Solubilization	Amphotericin B, minoxidil	Fungal infections
Site-Avoidance	Amphotericin B – reduced nephrotoxicity, doxorubicin – decreased cardiotoxicity	Fungal infections, cancer
Sustained-Release	Systemic antineoplastic drugs, hormones, corticosteroids, drug depot in the lungs	Cancer, biotherapeutics
Drug protection	Cytosine arabinoside, interleukins	Cancer, etc.
RES Targeting	Immunomodulators, vaccines, antimalarials, macophage-located diseases	Cancer, MAI, tropical parasites
Specific Targeting	Cells bearing specific antigens	Wide therapeutic applicability
Extravasation	Leaky vasculature of tumours, inflammations, infections	Cancer, bacterial infections
Accumulation	Prostaglandins	Cardiovascular diseases
Enhanced Penetration	Topical vehicles	Dermatology
Drug Depot	Lungs, sub-cutaneous, intra-muscular, ocular	Wide therapeutic applicability

The major drawbacks related to the use of liposomes can be reduced bioavailability of the drug, saturation of the cells of the immune system with lipids and different benefit/risk of some drugs due to their increased interactions with particular cells.[23]

Liposomes in parasitic diseases and infections

Since conventional liposomes are digested by phagocytic cells in the body after intravenous administration, so they are ideal vehicles for the targeting of drug molecules into these macrophages. The best-known examples of this 'Trojan horse-like' mechanism are several parasitic diseases which normally reside in the cell of mononuclear phagocytic system such as leishmaniasis[24] and several fungal infections.[25] The best results reported so far in human therapy are probably liposomes as carriers for Amphotericin B in antifungal therapies. Unfortunately, the drug itself is very toxic and its dosage is limited due to its nephro- and neuro-toxicity. These toxicities are normally correlated with the size of the drug molecule

[23] Çağdaş, M.; Sezer, A. D.; Bucak, S. Liposomes as Potential Drug Carrier Systems for Drug Delivery, DOI: 10.5772/58459

[24] New, R. R. C.; Chance, S. M.; Thomas, S. C.; Peters, W., Nature Antileshmanial Activity of Antimonials Entrapped in Liposomes, **1978**, 272, 55–58

[25] Coukell, A. J.; Brogden, R. N.; Liposomal Amphotericin B. Therapeutic Use in the Management of Fungal Infections and Visceral Leishmaniasis. *Drugs.*, **1998**, 55(4), 585-612

or its complex and obviously liposomes encapsulation prevents accumulation of drug in these organs and drastically reduces toxicity.[26] In addition, often the fungus resides in the cells of the mononuclear phagocytic system and therefore the encapsulation results in reduced toxicity and passive targeting. This liposomal drug is nowadays the drug of choice in disseminated fungal infections which often parallel compromised immune system, chemotherapy, or AIDS and are frequently fatal. Since the lives of the first terminally ill patients, which did not respond to all the conventional therapies, were saved,[26] many patients were very successfully treated with a variety of Amphotericin B formulations. In general, liposomes are able to encapsulated also antiviral drugs[27] such as acyclovir, ribavarin, or azide thymidine (AZT) reducing their toxicity as for Amphotericin B, the first example of approved liposomal drug.

Most of the antibiotics are orally available and liposomes encapsulation can be considered only in the case of very potent and toxic ones which are administered parenterally.[28] The preparation of antibiotics loaded liposomes at reasonably high drug to lipid ratios may not be easy because of the interactions of these molecules with bilayers and the high densities of their aqueous solutions can destabilize the formulation. Several other routes, such as topical or pulmonary (by inhalation) are also considered. For example, Ticarcillin- and tobramycin-resistant strains of *Pseudomonas aeruginosa* were shown to have a markedly increased sensitivity to antibiotics enclosed in liposomes. The liposome-enclosed antibiotic was as effective against the β-lactamase-producing strain as against the non-β-lactamase producing strain.[29]

[26] Lopez-Berestein, G.; Fainstein, V.; Hopter, R.; Mehta, K.R.; Sullivan, M.; Keating, M.; Luna, M.;. Hersh, E. M.; Liposomal Amphotericin B for the Treatment of Systemic Fungal Infections in Patients with Cancer, *J. Infect. Diseases*, **1985**, 151, 704–710

[27] Svenson, C.E.; Popescu, M.C.; Ginsberg, R.C. Liposome Treatments of Viral, Bacterial and Protozoal Infections, *Crit. Rev. Microbiol.* **1988**, 15, 1–31

[28] Alhariri, M.; Azghani, A.; Omri, A. Liposomal Antibiotics for the Treatment of Infectious. *Diseases Expert. Opinion on Drug Delivery*, **2013**, 10(11), 1515–1532

[29] Lagacfi, J.; Dubreuil, M.; Montplaisir, S. Liposome-encapsulated Antibiotics: Preparation, Drug Release and Antimicrobial Activity Against *Pseudomonas Aeruginosa. J. Microencapsulation*, **1991**, 8(1), 53-61

Liposomes in anticancer therapy

Many different liposome formulations of various anticancer agents were shown to be less toxic than the free drug.[30] Anthracyclines are drugs which stop the growth of dividing cells by intercalating into the DNA and therefore kill predominantly quickly dividing cells. These cells are in tumours, but also in gastrointestinal mucosa, hair and blood cells and therefore this class of drugs is very toxic. The most used and studied is Doxorubicin HCl. In addition to the above mentioned acute toxicities its dosage is limited by its cumulative cardiotoxicity. Many different formulations were tried: in most cases the toxicity was reduced about 50%.[31] This includes both short term and chronic toxicities because liposome encapsulation reduces the distribution of the drug molecules towards those tissues.

For the same reason, on the other hand, the efficacy was in many cases compromised due to the reduced bioavailability of the drug, especially if the tumour was not phagocytic, or located in the organs of mononuclear phagocytic system. In some cases, such as systemic lymphoma, the effect of liposome encapsulation showed enhanced efficacy due to the sustained release effect, *i.e.* longer presence of therapeutic concentrations in the circulation[32] while in several other cases the sequestration of the drug into tissues of mononuclear phagocytic system actually reduced its efficacy.

Liposomes in cosmetics

Liposomes can be utilized also in the delivery of ingredients in cosmetics. In addition to the natural lipids, other phospholipids or 'skin lipids', which contain mostly sphingolipids, ceramides, oleic acid, and chol sulphate are also being used. Synthetic lipids, that include mostly non-ionic surfactant lipids which can be chemically more stable, were also used for liposomes preparation in cosmetic. Liposomes itself as a carrier in cosmetics offer advantages because lipids are well hydrated and can reduce the dryness of the skin, which is a primary cause for its

[30] Gabizon, A. Liposomes as a Drug Delivery System in Cancer Therapy. *Drug Carrier Systems,* **1989**, 185–211.

[31] Rafiyath, S. M.; Rasul, M.; Lee, B.; Wei, G.; Lamba, G.; Liu, D. Comparison of Safety and Toxicity of Liposomal Doxorubicin *vs*. Conventional Anthracyclines: a Meta-analysis, *Exp. Hematol.Oncol*. **2012**, 1, 1-18

[32] Storm, G.; Roerdink, F. H.; Steerenberg, P.A.; de Jong, W. H.; Crommelin, D. J. A. Influence of Lipid Composition on the Antitumor Activity Exerted by Doxorubicin Containing Liposomes in a Rat Solid Tumor Model. *Cancer Res.* **1987**, 47, 3366–3372

ageing. Also, liposomes can act as a supply which acts to replenish lipids and, importantly, linolenic acid. In general the rules for topical drug applications and delivery of other compounds are less stringent than the ones for parenteral administration and several hundred cosmetic products are commercially available since Capture (C. Dior) and Niosomes (L'Oréal) were introduced in 1987. They range from simple liposomes pastes which are used as a replacement for creams, gels, and ointments for do-it-yourself cosmetical products to formulations containing various extracts, moisturizers, antibiotics, and to complex products containing recombinant proteins for wound or sunburn healing. Most of the products are anti-ageing skin creams. Waterproof sunscreens, long lasting perfumes, hair conditioners, aftershaves and similar products are also gaining large fractions of the market. Liposomal skin creams already share more than 10% of the over $10 billion market.[33] Table 4 shows some of these products.

As in the case of topical delivery in medical applications, the workers in the field do not agree on the mechanism of action. While some claim enhanced permeability into the skin the others claim mostly that liposomes are a noninteractive, skin-nonirritating, water-based matrix (without alcohols, detergents, oils and other non-natural solubilizers) for the active ingredients.

Table 4. Some liposomal cosmetic formulations currently on the market.[34]

Product	Manufacturer	Liposomes and key ingredients
Capture	Cristian Dior	Liposomes in gel with ingredients
Efect du Soleil	L'Oréal	Tanning agents in liposomes
Niosomes	Lancome (L'Oréal)	Glyceropolyether with moisturizers
Nactosomes	Lancome (L'Oréal	Vitamins
Formule Liposome Gel	Payot (Ferdinand Muehlens)	Thymoxin, hyaluronic acid
Future Perfect Skin Gel	Estee Lauder	TMF, vitamins E, A palmitate, cerebroside ceramide, phospholipid
Symphatic 2000	Biopharm GmbH	Thymus extract, vitamin A palmitate
Natipide II	Nattermann PL	Liposomal gel for do-it-yourself cosmetics
Flawless finish	Elizabeth Arden	Liquid make-up
Inovita	Pharm/Apotheke	Thymus extract, hyaluronic acid, vitamin E
Eye Perfector	Avon	Soothing cream to reduce eye irritation
Aquasome LA	Nikko Chemical Co.	Liposomes with humectant

[33] Skin Care Products Market Size, Share & Trends Analysis Report, By Product (Face Cream, Body Lotion), By Region (North America, Central & South America, Europe, APAC, MEA), And Segment Forecasts, 2019 - 2025

[34] Sundari P. T; Anushree, H. Novel Delivery Systems: Current Trend in Cosmetic Industry. *ejpmr*, **2017**, 4(8), 617-627

According to the manufacturers, liposomes may deliver moisture and a novel supply of lipid molecules to skin tissue in a superior fashion to other formulations. In addition they can entrap a variety of active molecules and can therefore be utilized for skin creams, anti-aging creams, after shave, lipstick, sun screen and make-up. Some of these liposomes can be made very easily by mixing and homogenizing aqueous solutions with molten surfactants. These liposomes can be more stable than their natural analogues and can be easily produced in large quantities and are very inexpensive.

Liposomes in agro-food industry

The ability of liposomes to solubilize compounds with demanding solubility properties, sequester compounds from potentially harmful *milieu* and release incorporated molecules in a sustained and predictable fashion can be used also in the food processing industry.

Lipid molecules, from fats to polar lipids, are one of the fundamental ingredients in almost any food. For instance, lecithin and some other polar lipids are routinely extracted from nutrients, such as egg yolks or soya beans. Traditionally polar lipids were used to stabilize water-in-oil and oil-in-water emulsions and creams, or to improve dispersal of various instant powders in water. With the advent of microencapsulation technology, however, liposomes have become an attractive system because they are composed entirely from food acceptable compounds. The sustained release system concept can be used in various fermentation processes in which the encapsulated enzymes can greatly shorten fermentation times and improve the quality of the product. This is due to improved spatial and temporal release of the ingredients as well as to their protection in particular phases of the process against chemical degradation. A classic example is cheesemaking: the first serious attempts to decrease the fermentation time using cell-wall-free bacterial extracts were encouraging enough to stimulate efforts to improve enzyme presentation. After preliminary studies in which liposome systems were optimized

the cheese ripening times can be shortened by 30–50%.[35,36,37] This means a substantial economic profit knowing that ripening times of some cheeses, such as Cheddar, are about one year during which they require well controlled conditions. In addition, due to the better dispersal of the enzymes the texture of cheeses was even and bitterness and inconsistent flavour due to the proteolysis of enzymes in the early phase of fermentation was much improved.[35,36] In addition to improved fermentation, liposomes are being tried in the preservation of cheeses. Addition of nitrates to cheese milk to suppress the growth of spore-forming bacteria is now being questioned due to health concerns and natural alternatives are under study. Lysozyme is effective but quickly inactivated due to binding to casein. Liposome encapsulation can both preserve potency and increase effectiveness because liposomes become localized in the water spaces between the casein matrix and fat globules of curd and cheese. This also happens to be where most of the spoilage organisms are located.[37] These applications of enhancing natural preservatives, including antioxidants such as vitamins E and C, will undoubtedly become very important due to recent dietary trends which tend to reduce the addition of artificial preservatives and ever larger portion of unsaturated fats in the diet.

In other areas of the agro-food industry, liposomes encapsulated biocides have shown superior action due to prolonged presence of the fungicides, herbicides or pesticides at reduced damage to other life forms.[38] Liposome surface can be made sticky so that they remain on the leafs for longer times and they do not wash into the ground. In these applications inexpensive liposomes produced from synthetic lipids are used.

The same liposomes are being tried in shellfish farms. These animals are susceptible for many parasitic infections. They are filter feeders and they pump large amounts of water through their body. This seems to offset large dilutions of liposomes in the

---

[35] Law, B. A.; King, J. S. Use of Liposomes for Proteinase Addition to Cheddar Cheese. *J. Diary Res.* **1991**, 52, 183–188

[36] Alkhalaf, W.; Piard, J. C.; el Soda, M.; Gripon, J. C.; Desmezeaud, M.; Vassal, L. Liposomes as Proteinases Carriers for the Accelerated Ripening of St. Paulin Type Cheese. *J. Food Sci.* **1988**, 53, 1674–1679

[37] Kirby, C.; Delivery Systems for Enzymes. *Chem. Br.* **1990**, 847–851

[38] Tahibi, A.; Sakurai, J.D.; Mathur, R.; Wallach, D.F.H. Novasome Vesicles in Extended Pesticide Formulation. *Proc. Symp. Contr. Rel. Bioact. Mat.* **1991**, 18, 231–232

pool and the drug molecules as well as some essential nutrients needed in ppm to ppb quantities can be delivered.

Liposomes in bioengineering

Modern genetic engineering and gene recombinant technology is based on the delivery of genetic material, *i.e*. fragments of DNA, into various cells and microorganisms in order to alter their genetic code and force them to produce particular proteins or polypeptides. Nucleic acids used in gene transfer are large, with molecular weights up to several million Daltons, highly charged and hydrophilic and therefore not easy to transfer across cell membranes. Additionally, to classical methods, such as direct injection, phosphate precipitation and others, liposomes were tried as transfection vectors. They can deliver the encapsulated or bound nucleic acid into cells predominantly in two ways: the classical approach is to encapsulate the genetic material into liposomes that act as an endocytosis enhancer. In these cases, the nucleic acid forms a complex with several cationic liposomes and the size of the complex and its adsorption on the cell surface catalyses endocytosis or, possibly, fusion. The third, still unexplored way would be to use fusogenic liposomes or cause fusion upon adsorption of the liposome on the cell surface.

In 1989 transfection was successfully performed using SUVs made from positively charged lipids.[39] Later studies showed better transfection efficiencies by using some of the commercially available cationic lipids.[40] Better transfection efficiencies at reduced toxicity were found by using liposomes containing positively charged chol.[41] Many novel cationic lipids are being synthesised in order to improve transfection, especially *in vivo*.[42] These methods can be used also in gene therapy. The idea is to deliver the non defective gene into the appropriate cells and hope that they will respond. For instance, patients with cystic fibrosis have a defective gene

[39] Felgner, P.; Gadek, T.R.; Holm, M.; Roman, R.; Wenz, M.; Northrop, J.P.; Ringold G.; Danielsen, M. Lipofectin: a Highly Efficient, Lipid Mediated DNA Transfection Procedure. *Proc. Nat. Acad. Sci. USA* **1987**, 84, 7413–7417

[40] Rose, J.K.; Buoncore, L.; Whitt, M.A. A New Cationic Liposome Reagent Mediating Nearly Quantitative Transfection of Animal Cells. *Biotechniques,* **1991**, 10, 520–525

[41] Gao, X.; Huang, L. A Novel Cationic Liposome Reagent for Efficient Transfection of Mammalian Cells. *Biophys. Biochem. Res. Commun*. **1991**, 179, 280–285

[42] Aissaoui, A.; Martin, B.; Kan, E.; Oudrhiri, N. Novel Cationic Lipids Incorporating an Acid-sensitive Acylhydrazone Linker: Synthesis and Transfection Properties. *J. Med. Chem*. **2004**, 47(21), 5210-5223

that encodes the code for a protein critical to a transfer of salts through the cell membrane in the lungs. For example, upon inhalation of the copies of human gene mixed with liposomes, 70% of the cells lining the lungs of mice incorporated the gene and began using it to make proteins in large amounts.[43]

1.2.2 Liposomes as biosensors

Sensors are self-contained integrated devices capable of providing specific quantitative or semiquantitative analytical information. When they possess a biological recognition element (biochemical receptor) that is retained in direct spatial contact with a transduction element they are biosensor:[44] in a common working process the analytes are recognized by biorecognition elements and the recognition event activates a signal through transducers in the biosensor (Figure 6).[45,46]

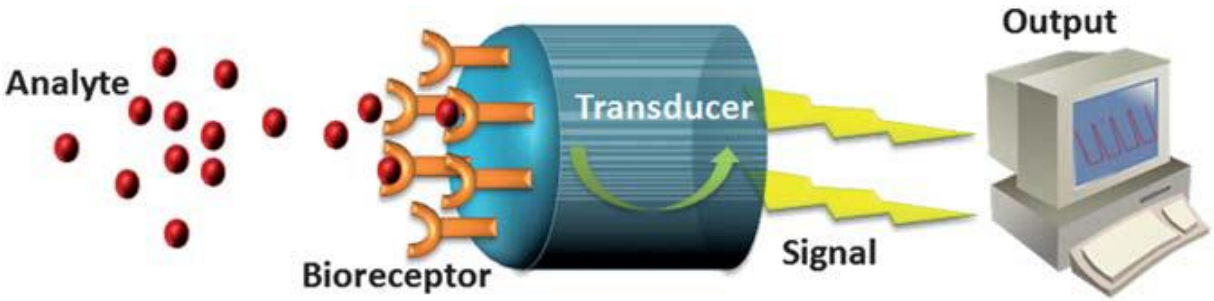

Figure 6. A schematic diagram of components and structure of a generic biosensor.

As an important and necessary component of a biosensor, the transducer is usually required to increase its sensitivity *via* signal amplification.[47] Liposomes have attracted great attention for application in the biosensor field over a number of

[43] Stribling, R.; Brunette, E.; Liggett, D.; Gaenslar, K.; Debs, R. Aerosol Gene Delivery *in Vivo*. *Proc. Nat. Acad. Sci. USA*, **1992**, 89, 11277–11281
[44] Griffin, G. D.; Stratis-Cullum, D. N.; Moselio, S. Encyclopedia of Microbiology, *Academic Press*, **2009**, 88–103
[45] Yun, Y. H.; Eteshola, E.; Bhattacharya, A.; Dong, Z. Y.; Shim, J. S.; Conforti, L.; Kim, D.; Schulz, M. J.; Ahn, C. H.; Watts, N. Tiny Medicine: Nanomaterial-based Biosensors. *Sensors*, **2009**, 9, 9275–9299
[46] Wang, J. Nanomaterial-based Amplified Transduction of Biomolecular Interactions. *Small*, **2005**, 1, 1036–1043
[47] Jain, R.; Dandekar, P.; Patravale, V. Diagnostic Nanocarriers for Sentinel Lymph Node Imaging. *J. Controlled Release*, **2009**, 138, 90–102

decades as a means to amplify the signal.[48,49] Liposomes can encapsulate various signal markers including dyes,[50] enzymes,[51] salts,[52] chelates,[53] DNA,[54,55] electrochemical[56,57,58] and chemiluminescent markers.[59] Consequently, liposomes are an excellent candidate component for biosensors to transduce and amplify signals.[48,49] The relatively low cost of lipids and successful experience from commercialization of liposomal medicines also are important advantages to promote the steps of application and commercialization of liposome-based biosensors. Moreover, the technology for surface modification of liposomes ensures a variety of biorecognition elements can be conjugated to the surface of liposomes,[60,61] including peptide, protein, enzyme, antigen, biotin, avidin and DNA segments.[15,16]

In the broadest sense liposomes have been used as an integral sensing component in a number of different ways. A wide range of signal markers have been encapsulated in liposomes for amplification purposes, including enzymes, fluorescent dyes, electrochemical and chemiluminescent markers. The ability to conjugate the bilayer

---

[48] Rongen, H. A. H.; Bult A.; van Bennekom, W. P. Liposomes and Immunoassays. *J. Immunol. Methods*, **1997**, 204, 105–133

[49] Edwards K. A.; Baeumner, A. J. Analysis of Liposomes. *Talanta*, **2006**, 68, 1421–1431

[50] Ho, R. J. Y.; Huang, L. Phosphatodylethanolamine Liposomes: Drug Delivery, Gene Transfer and Immunodiagnostic Applications. *J. Immunol.* **1985**, 134, 4035–4040

[51] Ceccoli, J.; Rosales, N.; Tsimis J.; Yarosh, D. B. Treatment of Human Melanocytes and S91 Melanoma Cells With the DNA Repair Enzyme T4 Endonuclease V Enhances Melanogenesis After Ultraviolet Irradiation. *J. Invest. Dermatol.* **1989**, 93, 190–194

[52] Orcutt K. M.; Wells, M. L. A Liposome-based Nanodevice for Sequestering Siderophore-bound Fe. *J. Membr. Sci.* **2007**, 288, 247–254

[53] Zhan, W.; Bard, A. Immunoassay of Human C-reactive Protein by Using $Ru(bpy)_3^{2+}$-encapsulated Liposomes as Labels. *J. Anal. Chem.*, **2007**, 79, 459–463

[54] Filion, M. C.; Phillips, N. C. Major Limitations in the Use of Cationic Liposomes for DNA Delivery. *Int. J. Pharm.* **1998**, 162, 159–170

[55] Kao, G. Y.; Chang, L. J.; Allen, T. M. Use of Targeted Cationic Liposomes in Enhanced DNA Delivery to Cancer Cells. *Cancer Gene Ther.* **1996**, 3, 250–256

[56] Chumbimuni-Torres, K. Y.; Wu, J.; Clawson, C.; Galik, M.; Walter, A.; Flechsig, G. U.; Bakker, E.; Zhang, L. F. Wang, J. Amplified Potentiometric Transduction of DNA Hybridization Using Ion-loaded Liposomes. *Analyst*, **2010**, 135, 1618–1623

[57] Edwards, A. J.; Durst, R. A. Flow-injection Liposome Immunoanalysis (FILIA) with Electrochemical Detection. *Electroanalysis*, **1995**, 7, 838–845

[58] Shukla, S.; Leem; H.; Kim, M. Development of a Liposome-based Immunochromatographic Strip Assay for the Detection of *Salmonella*., *Anal. Bioanal. Chem.* **2011**,401, 2581–2590

[59] Rakthong, P.; Intaramat, A.; Ratanabanangkoon, K. Luminol Encapsulated Liposome as a Signal Generator for the Detection of Specific Antigen-antibody Reactions and Nucleotide Hybridization. *Anal.Sci.* **2010**, 26, 767–772

[60] Zhu, J. M.; Yan, F.; Guo Z. W.; Marchant, R. E. Surface Modification of Liposomes by Saccharides: Vesicle Size and Stability of Lactosyl Liposomes Studied by Photon Correlation Spectroscopy. *J. Colloid Interface Sci.* **2005**, 289, 542–550

[61] Lestini, B. J.; Sagnella, S. M.; Xu, Z.; Shive, M. S.; Richter, N. J.; Jayaseharan, J.; Case, A. J.; Kottke-Marchant, K.; Anderson, J. M.; Marchant, R. E. Recent Advances of Membrane-cloaked Nanoplatforms for Biomedical Applications. *J. Controlled Release*, **2002**, 78, 235–247

lipid with a variety of biorecognition elements also ensures that liposomes are able to recognize various analytes for transduction of the signal. A number of different types of liposome-based assays have been reported using liposomes as a signal amplifier, including liposome immunoassay, liposome immunolysis assay, liposome immunosorbent assay, flow-injection liposome immunoanalysis and cytolysin-mediated liposome immunoassay, *etc*. Liposomes have also been combined with other analytical techniques such as micro-cantilever,[62] surface plasmon resonance[63] and quartz crystal microbalance (QCM),[64] to quantitatively or semi-quantitatively detect analytes.

Liposomes have also attracted much attention in cytologic research because they can be a useful simplified cell membrane model. In this context liposome-based biosensors have been utilized to monitor the simulated physiological processes of cells and to detect the interaction between bioreceptor and ligand based on liposomal cell model.[65] Furthermore, the liposomal bilayer membrane has also been widely used as a supporting film to coat electrodes, substrates, and novel metal films (Au, Ag) in biosensors.[66]

Increased sensitivity and lower limit of detection for biosensors have been pursued through various strategies in bioanalysis and clinical diagnosis. Signal amplification is one of most efficient strategies to realize this goal in a biosensor. The ability to amplify a one-to-one biological binding event into a one-to many signals provides the opportunity for physicochemical amplification of the signal by orders of magnitude. In this sense, liposomes have potential to act as excellent signal amplifiers when the ability to bind and/or encapsulate multiple signaling entities to a single liposome is combined with traditional assays. Consequently, low detection

---

[62] Braun, T.; Ghatkesar, M. K.; Backmann, N.; Grange, W.; Boulanger, P.; Letellier, L.; Lang, H. P.; Bietsch, A.; Gerber, C.; Hegner, M. Quantitative Time-resolved Measurement of Membrane Protein-ligand Interactions Using Microcantilever Array Sensors. *Nat. Nanotechnol.* **2009**, 4, 179–185

[63] Lombardi, D.; Cuenoud, B.; Wunderli-Allenspach, H.; Kramer, S. D. Interaction Kinetics of Salmeterol with Egg Phosphatidylcholine Liposomes by Surface Plasmon Resonance. *Anal. Biochem.* **2009**, 385, 215–223

[64] Alfonta, L.; Singh, A. K.; Willner, I. Liposomes Labeled With Biotin and Horseradish Peroxidase: a Probe for the Enhanced Amplification of Antigen-antibody or Oligonucleotide-DNA Sensing Processes by the Precipitation of an Insoluble Product on Electrodes. *Anal. Chem.* **2001**, 73, 91–102

[65] Bilek, G.; Kremser, L.; Wruss, J.; Blaas, D.; Kenndler, E. Analysis of Common Cold Virus (Human Rhinovirus Serotype 2) by Capillary Zone Electrophoresis: the Problem of Peak Identification. *Anal. Chem.* **2007**, 79, 1620–1625

[66] Gustafson, I. Investigating the Interaction of the Toxin Ricin and its B-chain With Immobilised Glycolipids in Supported Phospholipid Membranes by Surface Plasmon Resonance. *Colloids Surf. B*, **2003**, 30, 13–24

limits are often achieved in liposome-based biosensors or assays for analytes including hormones, viruses, bacteria, DNA/RNA segments, pesticides, tumor markers, proteins, antibodies and some drugs. Many different formats have employed liposomes as the amplifying component; these are introduced below in context with the class of signaling molecule incorporated into the liposomes to amplify the output signal.

Colorimetric signaling

Colorimetry is a simple method that has been widely applied in biochemical analysis and sensors.[67] There are several advantages of colorimetry, including low cost, simple instrumentation (or in the case of visual detection, no instrumentation) compared with other methods, and a qualitative or semi-qualitative test can be conducted often by the naked eye. However, the disadvantage of colorimetry is that it generally has low sensitivity. Therefore, dye-encapsulated liposomes have been employed as amplifiers of the signal to increase the sensitivity of colorimetric-based biosensors.

Fluorescence

Fluorescent dyes are widely used as encapsulated agents in liposome-based biosensors for signal amplification. Homogeneous liposome immunoassays are desired for convenience (no separating or washing step required) and potential commercial value. Fluorescence enhancement from self-quenching dyes (calcein and carboxyfluorescein *etc.*) and fluorescence resonance energy transfer[68] are efficient strategies to realize homogeneous immunoassays. For the fluorescence enhancement strategy, lysis and destabilization of liposomes using a cytolytic reagent is usually utilized to enhance fluorescence intensity, through the leakage of encapsulated self-quenching dyes from liposomes for homogeneous liposome immunoassays.

[67] Wen, H. W.; DeCory, T. R.; Borejsza-Wysocki, W.; Durst, R. A. Investigation of Neutravidin-tagged Liposomal Nanovesicles as Universal Detection Reagents for Bioanalytical Assays. *Talanta*, **2006**, 68, 1264–1272

[68] Chen, R. F.; Knutson, J. R. Mechanism of Fluorescence Concentration Quenching of Carboxyfluorescein in Liposomes: Energy Transfer to Nonfluorescent Dimers. *Anal. Biochem.* **1988**, 172, 61–77

Chemiluminescence

Chemiluminescent immunoassay (CLIA) has been widely used and successfully commercialized in clinical diagnosis. There are two main types of CLIA, enzyme chemiluminescent immunoassay (ECLIA) and electrogenerated chemiluminescent immunoassay. Enzyme and Ru^{2+} chelate are utilized to generate chemiluminescence (CL) through catalyzing CL substrate and electronic excitation in ECLIA and electrogenerated CLIA, respectively. Liposomes provide an opportunity for amplification of CL signals in CLIA through encapsulation of enzyme, CL substrate[69] and Ru^{2+} chelate,[70] or embedding enzymes onto the surface of liposomes. Liposome-based CLIA was successfully utilized to increase the sensitivity of the CL sensor and to detect trace analytes. Obviously from the above discussion, marker encapsulation is an important amplification strategy, however, liposomes may also be utilized to respond to the environment and provide amplification that is not dependent on release of an encapsulated entity. For example, liposomes prepared using polydiacetylene lipids[71] can respond to the interaction between analyte and liposome through a change of colour. Liposomes can also be used to quantify analytes when coupled to other special analytical techniques including surface plasmon resonance and QCM. This section will review the construction of non-marker encapsulated liposome systems as assays or biosensors.

1.3 Preparation techniques

The correct choice of liposome preparation method depends on the following parameters:

1) the physicochemical characteristics of the material to be entrapped and those of the liposomal components;
2) the nature of the medium in which the lipid vesicles are dispersed;

[69] Ratanabanangkoon, K.; Rakthong, P.; Intaramat, A. Luminol Encapsulated Liposome as a Signal Generator for the Detection of Specific Antigen-antibody Reactions and Nucleotide Hybridization. *Anal. Sci.* **2010**, 26, 767–772
[70] Mao, L.; Yuan, R.; Chai, Y. Q.; Zhuo Y.; Xiang, Y. Label-free Supersandwich Electrochemiluminescence Assay for Detection of Sub-nanomolar Hg^{2+}. *Biosens. Bioelectron.* **2011**, 26, 4204–4208
[71] Reppy M. A.; Pindzola, B. A. Biosensing With Polydiacetylene Materials: Structures, Optical Properties and Applications. *Chem. Commun.* **2007**, 4317–4338

3) the effective concentration of the entrapped substance and its potential toxicity;

4) additional processes involved during application/delivery of the vesicles;

5) optimum size, polydispersity and shelf-life of the vesicles for the intended application and reproducibility and possibility of large-scale production of liposomal products.

1.3.1 Hydration of a thin lipid film (TFH)

After the solubilization of liposomes components in organic solvent and the subsequent removal of the solvent, a dry lipid film is deposited on the flask wall. Its hydration by adding an aqueous buffer solution under stirring leads to the formation of multilamellar liposomes (MLVs). This method is widespread and easy to handle, however, MLVs are heterogeneous both in size and lamellarity. Thus, liposome size reduction techniques, such as sonication for SUVs formation or extrusion through polycarbonate filters forming LUVs[72,73] can be used to produce smaller and more uniformly sized vesicles (Figure 7).

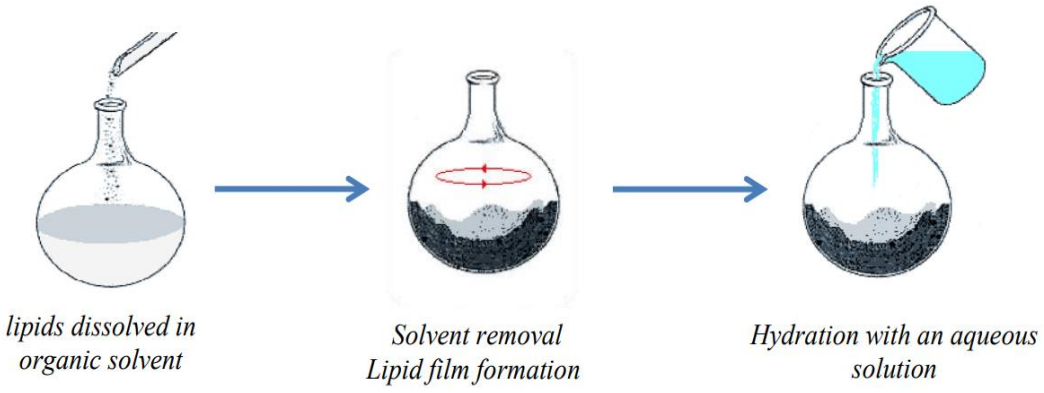

Figure 7. Liposome preparation by TFH

[72] Olson, F.; Hunt, C.A.; Szoka, F.C.; Vail, W.J.; Papahadjopoulos, D. Preparation of Liposomes of Defined Size Distribution by Extrusion Through Polycarbonate Membranes. *Biochim. Biophys. Acta*, **1979**, 557(1), 9-23

[73] Mui, B.; Chow, L.; Hope, M. J. Extrusion Technique to Generate Liposomes of Defined Size. *Methods Enzymol.* **2003**, 367, 3-14

1.3.2 Solvent (ether or ethanol) injection technique

The solvent injection methods involve the dissolution of the lipid into an organic solvent (ethanol or ether), followed by the injection of the lipid solution into aqueous media, where lipids will assemble into liposomes.[74] This method permits to obtain a narrow distribution of small liposomes (under 100 nm) in one step, without extrusion or sonication.[75]

1.3.3 DELOS-Susp (depressurization of an expanded liquid organic solution-suspension)

Supercritical fluids are non-condensable fluids, which are very dense at certain temperatures and pressures beyond the critical values. As the line between the liquid and gas phase disappears, supercritical fluids have many particular characteristics compared with conventional fluids. Among these characteristics, solvents with special properties have attracted a great deal of interest from researchers. Remarkably, supercritical carbon dioxide (scCO2) is an excellent organic solvent substitute. In spite of its low cost, it is non-toxic and is not inflammable. In addition, it has a relatively low critical temperature and pressure (31 °C and 73.8 bar) with the dissolution properties analogous to those of nonpolar solvents.[76]

Among the methods based on supercritical fluid technology, DELOS-Susp one is useful for the straightforward synthesis of cholesterol-rich SUVs with controlled size distribution, uniform shapes, and good stability in time has been achieved.[77] In addition, recent studies have shown that vesicular systems prepared by this method have a vesicle-to-vesicle homogeneity degree, regarding membrane supramolecular organization, more than double than those prepared by thin-film hydration.[78] It's

---

[74] Szebeni, J.; Breuer, J. H.; Szelenyi, J.G.; Bathori, G.; Lelkes, G.; Hollan, S.R. Oxidation and Denaturation of Hemoglobin Encapsulated in Liposomes. *Biochim. Biophys. Acta*, **1984**, 798, 60-67

[75] Stano, P.; Bufali, S.; Pisano, C.; Bucci, F.; Barbarino, M.; Santaniello, M.; Carminati, P.; Luisi, P. L. Novel Camptothecin Analogue (Gimatecan)-containing Liposomes Prepared by the Ethanol Injection Method. *J. Liposome Res.* **2004**, 14, 87-109

[76] Lesoin, L.; Boutin, O.; Crampon, C. CO_2/Water/Surfactant Ternary Systems and Liposome Formation Using Supercritical CO_2: a Review. *Colloids Surf. Physicochem. Eng. Asp.* **2011**, 377, 1-14

[77] Cano-Sarabia, M.; Ventosa, N.; Sala, S.; Patiño, C.; Arranz, R.; Veciana, J. Preparation of Uniform Rich Cholesterol Unilamellar Nanovesicles Using CO_2-expanded Solvents. *Langmuir*, **2008**, 24, 2433-2437

[78] Elizondo, E.; Larsen, J.; Hatzakis, N. S.; Cabrera, I.; Bjornholm, T.; Veciana, J.; Stamou, D.; Ventosa, N. Influence of the Preparation Route on the Supramolecular Organization of Lipids in a Vesicular System. *J. Am. Chem. Soc.* **2012**, 134, 1918-1921

known the potential of the DELOS-Susp method as a simple, robust, scalable, and one-step process to prepare a variety of SUV-biomolecule conjugates with high structural homogeneity. The whole procedure (as shown in Figure 8) includes the loading (a) of an organic solution of the lipidic membrane components and the desired hydrophobic active compounds/molecules into an autoclave at a working temperature (T*w*) and atmospheric pressure; the addition of CO_2 (b) to produce a CO_2-expanded solution, at a given X_{CO_2}, working pressure (P*w*), and T*w*, where the hydrophobic active and membrane components remain dissolved; and finally, the depressurization (c) of the expanded solution over an aqueous solution, which might contain membrane surfactants and hydrophilic biomolecules, to produce an aqueous dispersion of the nanovesicle bioactive(s) conjugates with vesicle-to-vesicle homogeneity regarding size and morphology.

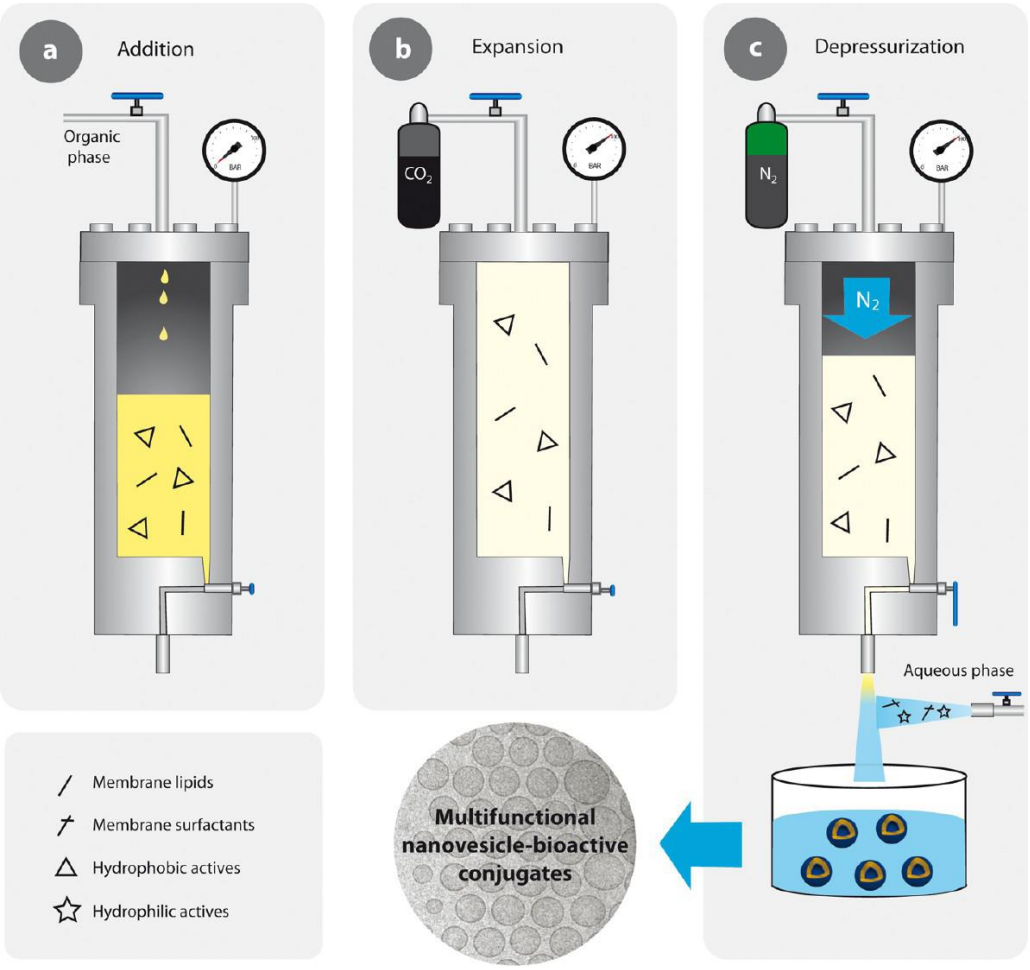

Figure 8. Schematic representation of the DELOS-SUSP method for the efficient preparation of multifunctional nanovesicle-bioactive conjugates.

1.3.4 Reverse-phase evaporation (Rev) method

In this method a lipid film is prepared by evaporating organic solution containing the proper amount of lipid components under reduced pressure. The lipids are re-dissolved in a second organic phase, usually constituted by diethyl ether and/or isopropyl ether. Large unilamellar and oligolamellar vesicles are formed when an aqueous buffer is introduced into this mixture. The organic solvent is subsequently removed under a gentle stream of nitrogen.

Liposomes obtained by the methods described above, except for the ones prepared by DELOS-susp methodology are heterogeneous for dimensions and number of lamellae. Liposomes lamellarity can be reduced upon repetitively freezing the MLVs suspension in liquid nitrogen (at −195 °C) and thawing it at a temperature above Tm. The vesicle suspension may undergo certain physico-chemical changes thereby often equilibrating the vesicles aqueous interior and the external bulk aqueous phase. This process results in an increased entrapment yield and possibly leads to an elimination -through fusion processes- of very small vesicles possibly present, depending on the lipid used and depending on the salt content. Typically, freezing-thawing cycles are repeated 3–6 times.

Chapter 2

Liposomes as drug delivery systems

2.1 (+)-Usnic acid

2.1.1 Introduction

Usnic acid was first isolated as a prominent secondary lichen metabolite by the German scientist Knop in 1844.[79] When extracted from lichens, it is yellow and crystalline in appearance. Lichens are symbiotic organisms of fungi and algae that comprise about 17,000 species, which synthesize numerous metabolites.[80,81] Lichens and their metabolites exert a wide variety of biological functions and have been used in perfumery, cosmetics, ecological applications, and pharmaceuticals. The significance of lichens and their metabolites was summarized in a review article by Huneck.[82] It is estimated that lichens cover approximately 8% of the earth surface. Usnic acid has been identified in many lichen genera including species of *Alectoria, Cladonia, Evemia, Lecanora, Parmelia, Ramalina,* and *Usnea*. Traditionally, *Usnea* species such as the pendulous "beard" lichens, *U. barbata* (Figure 9)*, U. florida* and *U. longissima* have been used as a source of usnic acid in herbal medicine and their usnic acid content ranges from 1–3% of dry weight[80,83] Usnic acid is synthesized within the mycobiont (fungal part) of the lichen and is then deposited onto the outer surface of the photobiont.[84] The first recorded use of the *Usnea* species in Traditional Chinese Medicine (TCM) dates to 101 B.C., when it was used as an antimicrobial agent under the Chinese name of Song Lo. Song Lo tea or decoction for internal and external use has also been recorded for detoxification of the liver, treatment of

[79] Guo, L.; Shi, Q.; Fang, J. L.; Mei, N.; Ali, A. A.; Lewis, S. M.; Leakey, J. E. A.; Frankos, V. H. Review of Usnic Acid and *Usnea Barbata* Toxicity *J. Environ. Sci. Health C. Environ. Carcinog. Ecotoxicol. Rev.* **2008**, 26(4), 317–338

[80] Cocchietto, M.; Skert, N.; Nimis, P. L.; Sava, G. A Review on Usnic Acid, an Interesting Natural Compound. *Naturwissenschaften*, **2002**, 89, 137–146

[81] Shibamoto, T.; Wei, C. I. Mutagenicity of Lichen Constituents. *Environ. Mutagen.* **1984**, 6, 757–762

[82] Huneck, S. The Significance of Lichens and Their Metabolites. *Naturwissenschaften,* **1999**, 86, 559–570

[83] Cansaran, D.; Kahya, D.; Yurdakulola, E.; Atakol, O.; Identification and Quantitation of Usnic Acid from the Lichen *Usnea Species* of *Anatolia* and Antimicrobial Activity. *Z. Naturforsch C,* **2006**, 61, 773–776

[84] Romagni, J. G; Meazza, G.; Nanayakkara, N. P.; Dayan, F. E. The Phytotoxic Lichen Metabolite, Usnic Acid, is a Potent Inhibitor of Plant *p*-hydroxyphenylpyruvate Dioxygenase. *FEBS Lett.* **2000**, 480, 301–305

malaria, wounds, snake bite, cough, and so on. However, despite its long history, Song Lo is classified as a rarely used herb in TCM.

Figure 9. *Usnea Barbata*

Usnea species have been used as antimicrobial agents in many countries and were being developed as a modern pharmaceutical just prior to the advent of the penicillin antibiotics.[80] In Germany, pure usnic acid has been formulated and used in cosmetics and pharmaceuticals under the trade names of "Omnigran a, Granobil, and Usnagren A".[85] In Finland, "ramalina thrausta" was used internally to treat sore throat and toothache and externally to treat wounds and athlete's foot.[86] In Italy, usnic acid has been used in vaginal creams, foot creams, powders, and shampoo.[87] In Argentina, "Barba del la Piedra" (*Usnea densirostra*) has been sold to treat many ailments.[88] In these preparations, usnic acid is employed either as the active principle or has functioned as a preservative. In the United States, *Usnea* can be obtained in bulk powder or as dried lichen from several herbal supply companies. It is widely available in dietary supplement stores either alone or in combination with other herbs such as *Echinacea* as tinctures in alcoholic or alcohol-free preparations.

Usnic acid (full name: 2,6-diacetyl- 7,9-dihydroxy-8, 9 b-dimethyl-dibenzofuran-1,3(2H,9bH)-dione) exists in two enantiomers; (+) D-usnic acid and (−) L-usnic acid, indicating an R or S projection of the angular -CH_3 group at position 9b (Figure 9a).

[85] Sweetman, S. C. Martindale: The Complete Drug Reference. *London: Pharmaceutical Press*, **2004**

[86] Ingolfsdottir, K. Usnic Acid. *Phytochemistry*, **2002**, 61, 729–736

[87] Rafanelli, S.; Bacchilega, R.; Stanganelli, I.; Rafanelli, A. Contact Dermatitis from Usnic Acid in Vaginal Ovules. *Contact Dermatitis,* **1995**, 33, 271–272

[88] Correche, E. R.; Carrasco, M.; Escudero, M. E.; Velazquez, L.; de Guzman, A. M. S.; Giannini, F.; Enriz, R. D.; Jauregui, E. A.; Cenal, J. P.; Giordano, O. S. Study of the Cytotoxic and Antimicrobial Activities of Usnic Acid and Derivatives. *Fitoterapia*, **1998**, 69, 493–501

The enantiomers have been identified as showing different biological activities.[84] In addition, two other natural isomers (+) and (−) isousnic acids [2,8-diacetyl-7,9-dihydroxy-6,9b-dimethyldibenzofuran-1,3(2H,9bH)-dione] are also found in lichens (Figure 10b).

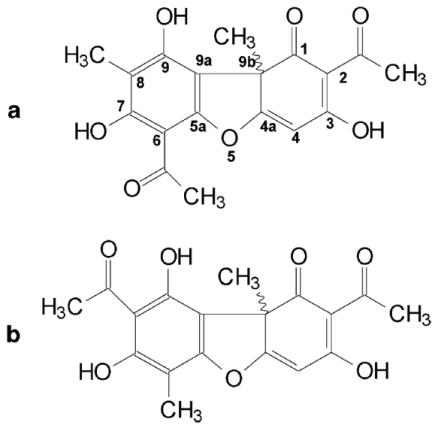

Figure 10. Structure of usnic (a) and isousnic (b) acids.

Of the three hydroxyl groups present in the usnic acid molecule, the enolic hydroxyl at the 3 position (Figure 10a) has the strongest acidic character (pK_a 4.4) due to both the inductive effect of the keto groups in 1 and 2 positions and the resonance effect of the keto group in 2 position, whereas the hydroxyl groups at positions 9 and 7 are less acidic with pK_a values of 8.8 and 10.7, respectively.[86] Usnic acid is highly lipophilic in both neutral and anionic forms because of its β-triketone groups that delocalize the negative charge of the anion by resonance stabilization[89] (Figure 11).

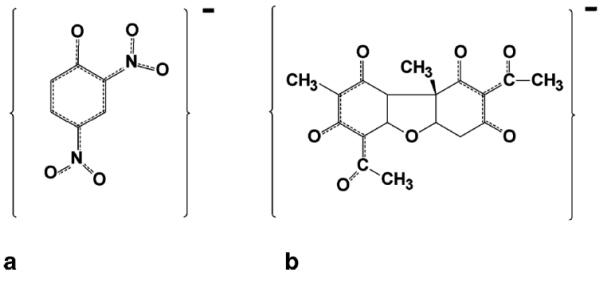

Figure 11. Structures of the monoanionic forms of (a) 2,4-dinitrophenol and (b) (+)-usnic acid showing the resonance stabilization of their negative charges by delocalization of π orbital electrons as shown by the dashed lines.

[89] Sharma, R. K.; Jannke, P. J. Acidity of Usnic Acid. *Indian Journal of Chemistry*, **1966**, 4, 16–18

Because of this lipophilicity, usnic acid and the usneate anion behave as a membrane uncoupler in a similar manner to 2,4-dinitrophenol.[90] According to chemiosmotic theory, such molecules easily diffuse through biological membranes in their charged and neutral forms, which results in the breakdown or uncoupling of ion gradients.[90] Usnic acid can pass through the inner-mitochondrial membranes by passive diffusion into the matrix where it is ionized, releasing a proton into the matrix. The resulting usneate anion can then diffuse back into the inter-membrane space, where it binds to a proton on the acidic side of the inner-membrane proton gradient to re-form usnic acid, which can then diffuse back into the matrix. The resulting cycle causes proton leakage that eventually can dissipate the proton gradient across the inner-membrane, disrupting the tight coupling between electron transport and adenosine triphosphate synthesis. This mitochondrial uncoupling activity of usnic acid has been demonstrated in vitro in several studies[91,92,93,94] and it is thought to play a major role in its hepatotoxicity. However, usnic acid also produces the same uncoupling actions on bacterial cell membranes, process at the base of its antimicrobial activity.

Pharmacological activity

During the 1980s, interest in usnic acid as an antimicrobial was renewed because of increasing experience of multidrug resistance caused by overuse of synthetic antibiotics.[80] It has been shown that both the optical enantiomers of usnic acid are active against Gram-positive bacteria and mycobacteria[86] and several research studies and clinical trials have confirmed the antibacterial properties of this molecules. For example, in preliminary clinical trials, a mouthwash containing 1% of UA was administered to volunteers. The samples of oral bacterial flora were examined at regular intervals. It was reported that the growth of *Streptococcus*

[90] Mitchell, P. Vectorial Chemistry and the Molecular Mechanics of Chemiosmotic Coupling: Power Transmission by Proticity. *Biochem. Soc. Trans.* **1976**, 4, 399–430

[91] Abo-Khatwa, A. N.; al Robai, A. A. al Jawhari, D. A. Lichen Acids as Uncouplers of Oxidative Phosphorylation of Mouse-liver Mitochondria. *Nat. Toxins,* **1996**, 4, 96–102

[92] Han, D.; Matsumaru, K.; Rettori, D.; Kaplowitz, N. Usnic Acid-induced Necrosis of Cultured Mouse Hepatocytes: Inhibition of Mitochondrial Function and Oxidative Stress. *Biochem. Pharmacol*. **2004**, 67, 439–451

[93] Pramyothin, P.; Janthasoot, W.; Pongnimitprasert, N.; Phrukudom, S.; Ruangrungsi, N. Hepatotoxic Effect of (+)Usnic Acid from *Usnea Siamensis Wainio* in Rats, Isolated Rat Hepatocytes and Isolated Rat Liver Mitochondria. *J. Ethnopharmacol.* **2004**, 90, 381–387

[94] Shibamoto, T.; Wei, C. I. Mutagenicity of Lichen Constituents. *Environ. Mutagen*. **1984**, 6, 757–762

mutans involved in the etiology of dental caries, was selectively suppressed.[95] Using standardized assays, the in vitro susceptibility of pathogenic Gram positive and anaerobic bacteria toward usnic acid has been confirmed.[86] Usnic acid has been shown to suppress the growth of Gram-positive organisms that are mainly responsible for body odor.

Ethoxydiglycol extracts of lichens containing 10% usnic acid on a wet weight basis have been demonstrated to have preservative potential in moisturizing cream.[86] Usnic acid was found to be effective against *Mycobacteriurn aureurn*.[96] In in vitro assays, usnic acid and its salt inhibited the growth of *Mycobacteriurn tuberculosis* at relatively low concentrations.[97] Partially purified usnic acid from Song Lo has also been therapeutically tested in China for tuberculosis and chronic bronchitis.[98] Other recent–studies have shown that usnic acid is active against *methicillin-resistant Staphylococcus aureus*,[99,100] and its potential use in the sterilization of surgical implants is being investigated.[101]

During a short-term treatment with usnic acid salt,[102] patients with *Tineapedis* exhibited a significant improvement in their clinical conditions.[86]

(−)-Usnic acid exhibited a significant inhibitory effect against the pathogenic protozoan *Trichornonas vaginalis* at comparatively lower concentrations than metronidazole.[103] The compound also showed leishmanicidal properties both in

---

[95] Ghione, M.; Parrello, D.; Grasso, L. Usnic Acid Revisited, its Activity on Oral Flora. *Chemioterapia,* **1988**, 7,302–305

[96] Ingolfsdottir, K.; Chung, G.A.; Skulason, V. G.; Gissurarson, S.R.; Vilhelmsdottir, M. Antimycobacterial Activity of Lichen Metabolites *in Vitro*. *Eur. J. Pharm. Sci.* **1998,** 6, 141–144

[97] Krishna, D. R.; Venkataramana, D. Pharmacokinetics of D(+)-usnic Acid in Rabbits After Intravenous and Oral Administration. *Drug. Metab. Dispos.* **1992**, 20, 909–911

[98] Frankos, V. H. NTP Nomination for Usnic Acid and *Usnea barbata*. **2004**, http://ntp-server.niehs.nih.gov/

[99] Lauterwein, M.; Oethinger, M.; Belsner, K.; Peters, T.; Marre, R. *In Vitro* Activities of the Lichen Secondary Metabolites Vulpinic Acid, (+)-Usnic Acid, and (−)-Usnic Acid Against Aerobic and Anaerobic Microorganisms. *Antimicrob. Agents Chemother.* **1995**, 39, 2541–2543

[100] Elo, H.; Matikainen, J.; Pelttari, E. Potent Activity of the Lichen Antibiotic (+)-Usnic Acid Against Clinical Isolates of Vancomycin-resistant *Enterococci* and Methicillin-resistant *Staphylococcus Aureus*. *Naturwissenschaften*, **2007**, 94, 465–468

[101] Francolini, I.; Norris, P.; Piozzi, A.; Donelli, G.; Stoodley, P. Usnic Acid, a Natural Antimicrobial Agent Able to Inhibit Bacterial Biofilm Formation on Polymer Surfaces. *Antimicrob. Agents Chemother.* **2004**, 48, 4360–4365

[102] CFSAN. Letter to Distributor of Hazardous Ddietary Supplement LipoKinetix. **2001**, http://www.cfsan.fda.gov/~dms/ds-ltr26.html

[103] Wu, J.; Zhang, M.; Ding, D.; Tan, T.; Yan, B. Effect of *Cladonia Alpestris* on *Trichomonas Vaginalis in Vitro*. *Chinese J. Parasitic Dis.* **1995**, 13, 126–129

vitro and in vivo studies; intralesional administration produced a reduction in lesion weight and parasite body burden.[104]

In a cancer chemoprevention assay, UA isolated from *Usnea longissima* was found to be significantly effective against tumor-promoter–induced Epstein-Barr virus with an ED5O of 1 .0 µg/mL.[105] UA also inhibited the cytopathologic effects of herpes simplex type I and polio type 1 viruses in the infected kidney cells of the African green monkey.[80] In a clinical trial, the effect of an intravaginal formulation containing usnic acid and zinc sulfate as an adjuvant therapy to radio surgical treatment was evaluated in 100 women with genital infections of human papilloma virus. The treatment significantly improved the time of re-epithelization one month after the radio surgery.[106]

(−)-Usnic acid caused moderate inhibition in the murine P388 leukemia assay and also exhibited cytotoxic activity against cultured Ll210 cells; it was inferred that p-tri-ketone moiety was essential for the optimum activity.[107] On the other hand, UA (50 µg/mL) reduced the cell counts of leukemic (K−562) and endometrial carcinoma cell culture (HEC-50).[108,109]

In an acute rat paw edema and a chronic rat cotton pellet assay at 100 mg/kg oral dose level, the anti-inflammatory action of UA was comparable with ibuprofen at the same dose level.[110]

In two mice studies, the analgesic and antipyretic effects of usnic acid were evaluated.[79] At 100 mg/kg oral dose level, usnic acid exhibited a significant analgesic effect as indicated in acetic acid-induced writhing and tail pressure tests.

---

[104] Fournet, A.; Ferreira, M. E.; Rojas, A.; Torres, O.; Inchausti, A.; Yaluff, G.; Quilhot, W.; Fernandez, E.; Hidalgo, M. E. Activity of Compounds Isolated from Chilean Lichens Against Experimental Cutaneous *Leishmaniasis*. *Comp. Biochem. Physiol. C Pharmacol. Toxicol. Endocrinol.* **1997**, 116, 51–54

[105] Yamamoto, Y.; Miura, Y.; Kinoshita, Y.; Higuchi, M.; Yamada, Y.; Murakami, A.; Ohigashi, H.; Koshimizu, K. Screening of Tissue Cultures and Thalli of Lichens and Some of Their Active Constituents for Inhibition of Tumor Promoter-induced *Epstein-Barr* Virus Activation. *Chem. Pharm. Bull. (Tokyo)*, **1995**, 43, 1388–1390

[106] Scirpa, P.; Scambia, G.; Masciullo, V.; Battaglia, F.; Foti, E.; Lopez, R.; Villa, P.; Malecore, M.; Mancuso, S. A Zinc Sulfate and Usnic Acid Preparation Used as Post-surgical Adjuvant Therapy in Genital Lesions by *Human Papillomavirus*. *Minerva Ginecol.* **1999**, 51, 255–260

[107] Takai, M.; Uehara, Y.; Beisler, J. A. Usnic Acid Derivatives as Potential Antineoplastic Agents. *J. Med. Chem.* **1979**, 22, 1380–1384

[108] Cardarelli, M.; Serino, G.; Campanella, L.; Ercole, P.; De Cicco, N. F.; Alesiani, O.; Rossiello, F. Antimitotic Effects of Usnic Acid on Different Biological Systems. *Cell. Mol. Life Sci.* **1997**, 53, 667–672

[109] Kristmundsdóttir, T.; Aesa Aradóttir, H.; Ingólfsdóttir, K.; Ögmundsdóttir, H.M. Solubilization of the Lichen Metabolite (+)-Usnic Acid for Testing in Tissue Culture. *J. Pharm. Pharmacol.* **2002**, 54, 1447–1452

[110] Vijayakumar, C. S.; Viswanathan, S.; Reddy, M. K.; Parvathavarthini, S.; Kundu, A. B.; Sukumar, E. Anti-inflammatory Activity of (+)-Usnic Acid. *Fitoterapia,* **2000**, 71, 564–566

At oral dose levels up to 300 mg/kg, usnic acid also expressed significant antipyretic activity determined through lipopolysaccharide-induced hyperthermia. The *in vivo* toxicities of usnic acid have been reported in both animals and plants, even though data are sparse. In several experimental animal or wild animal species. The first investigation showing that usnic acid could cause weight loss with the possibility of general toxicity, although this possibility was largely ignored in the ensuing decades, was reported in 1950.[111] No apparent organ-specific toxicities in the liver, spleen, or lung were observed in this report. According to more recent investigations, usnic acid caused no apparent general toxicity, as evidenced by the negative observations in clinical signs or changes of body weight. However, strong hepatotoxicity, including elevated serum transaminase activity and extensive liver necrosis, were observed. No toxicity in other organs such as the kidney and spleen were detected.[112,113] Another study showed a remarkable swelling of the liver mitochondria and endoplasmic reticulum, although no changes in serum transaminase activity were observed, indicating that mild hepatotoxicity occurred at low doses.[93] On the other hand, at higher doses the treatment with usnic acid showed some toxicity.[114] Other clinical signs such as lethargy and anorexia, increase of serum lactate dehydrogenase, aspartate aminotransferase and creatine kinase, changes in the skeletal muscle or even death can be induced by usnic acid at high dosage on domestic sheep.[115] This is in sharp contrast with mice, rats, and humans, in which the liver is considered to be the most vulnerable organ with usnic acid insults. Usnic acid is also the assumed toxicant associated with some 400–500 cow elk deaths occurred in Wyoming in 2004.[116] Usnic acid also serves as a strong

---

[111] Marshak, A.; Kuschner, M. The Action of Streptomycin and Usnic Acid on the Development of *Tuberculosis* in Guinea Pigs. *Public Health Rep.* **1950**, 65, 131–144

[112] Ribeiro-Costa, R. M.; Alves, A. J.; Santos, N. P.; Nascimento, S. C.; Goncalves, E. C.; Silva, N. H.; Honda, N. K.; Santos-Magalhaes, N. S. *In Vitro* and *in Vivo* Properties of Usnic Acid Encapsulated into PLGA-microspheres. *J. Microencapsul.* **2004**, 21, 371–384

[113] da Silva Santos, N. P.; Nascimento, S. C.; Wanderley, M. S.; Pontes-Filho, N. T.; da Silva, J. F.; de Castro, C. M.; Pereira, E. C.; da Silva, N. H.; Honda, N. K.; Santos-Magalhaes, N. S. Nanoencapsulation of Usnic Acid: an Attempt to Improve Antitumour Activity and Reduce Hepatotoxicity. *Eur. J. Pharm. Biopharm.* **2006**, 64, 154–160

[114] Odabasoglu, F.; Cakir, A.; Suleyman, H.; Aslan, A.; Bayir, Y.; Halici, M.; Kazaz, C. Gastroprotective and Antioxidant Effects of Usnic Acid on Indomethacin-induced Gastric Ulcer in Rats. *J. Ethnopharmacol.* **2006**, 103, 59–65

[115] Dailey, R. N.; Montgomery, D. L.; Ingram, J. T.; Siemion, R.; Vasquez, M.; Raisbeck, M. F. Toxicity of the Lichen Secondary Metabolite (+)-Usnic Acid in Domestic Sheep. *Vet. Pathol.* **2008**, 45, 19–25

[116] Cook, W. E.; Raisbeck, M. F.; Cornish, T. E.; Williams, E. S.; Brown, B.; Hiatt, G.; Kreeger, T. J. Paresis and Death in Elk (*Cervus elaphus*) Due to Lichen Intoxication in Wyoming. *J. Wildl. Dis.* **2007**, 43, 498–503

toxicant toward certain insects such as mosquitoes on their 3rd-4th stages, suggesting that it might be developed as a novel natural insecticide.[117] In addition to the toxicity toward animals, usnic acid displays phytotoxicity on the growth of onion and lettuce, possibly by the inhibition of plant *p*-hydroxyphenylpyruvate dioxygenase, indicating the potential usage as an herbicide.[84]

The idea of utilizing chemicals with mitochondrial uncoupling activity for weight loss originated in the early 1930s after it was noticed that munition workers exposed to 2,4-dinitrophenol lost weight.[118] Subsequently, 2,4-dinitrophenol was formulated into an anti-obesity drug that was prescribed by some physicians or directly marketed to the public with some claims of efficacy. However, many serious side effects were also recorded, including liver, heart, and muscle toxicity and cataract formation so that in 1938, the FDA finally declared 2,4-dinitrophenol too toxic to be used under any circumstances. Following this, reports of 2,4-dinitrophenol misuse became less frequent. Interest in uncoupling chemicals has resurfaced primarily in the body-building community with the advent of the Internet and the passage of "Dietary Supplement Health and Education Act" resulting in the clandestine trade of 2,4-dinitrophenol[119,120] and the open marketing of usnic acid and other natural products in dietary supplements formulated for weight loss.[98] Such formulations generally contain relatively high usnic acid concentrations, either alone or in combination with other ingredients, and their use has been reported to be associated with hepatotoxicity.[121]

---

[117] Cetin, H.; Tufan-Cetin, O.; Turk, A. O.; Tay, T.; Candan, M.; Yanikoglu, A.; Sumbul, H. Insecticidal Activity of Major Lichen Compounds, (−)- and (+)-Usnic acid, Against the Larvae of House Mosquito, *Culex Pipiens. L. Parasitol. Res.* **2008**, 102, 1277–1279

[118] Colman, E. Dinitrophenol and Obesity: an Early Twentieth-century Regulatory Dilemma. *Regul. Toxicol. Pharmacol.* **2007**, 48, 115-117

[119] Miranda, E. J.; Mc Intyre, I. M.; Parker, D. R.; Gary, R. D.; Logan, B. K. Two Deaths Attributed to the Use of 2,4-Dinitrophenol. *J. Anal. Toxicol.* **2006**, 30, 219–222

[120] Hsiao, A. L.; Santucci, K. A.; Seo-Mayer, P.; Mariappan, M. R.; Hodsdon, M. E.; Banasiak, K. J.; Baum, C. R. Pediatric Fatality Following Ingestion of Dinitrophenol: Postmortem Identification of a "Dietary Supplement". *Clin. Toxicol*. **2005**, 43, 281–285

[121] Favreau, J. T.; Ryu, M. L.; Braunstein, G.; Orshansky, G.; Park, S. S.; Coody, G. L.; Love, L. A.; Fong, T. L. Severe Hepatotoxicity Associated with the Dietary Supplement LipoKinetix. *Ann. Intern. Med.* **2002**, 136, 590–595

2.1.2 *Aim of the work*

Many natural compounds including UA show pharmacological activities (as explained above) but cannot be used for therapeutic applications because of their low water solubility and/or stability and/or their toxicity. In fact, as explained above, UA shows a water solubility lower than 10 mg/100 mL at 25° C,[109] and a dose-dependent hepatotoxicity[109] that hamper its potential pharmaceutical applications. To circumvent these limitations, UA can be included in liposomes because these drug carriers offer many advantages featuring biocompatibility, low toxicity and the capability of loading both hydrophilic and hydrophobic molecules protecting them from biological degradation and eventually delivering them to the target. Further, liposomes can enhance drug cellular uptake and slow down clearance rate.[122] For these reasons liposomes can be considered the most promising drug delivery systems[123] and many formulations are yet on the market or in clinical trials. Recently it was reported that UA included in glucosylated liposomes show antibiotic activity on biofilm of *S. epidermidis*. In particular, it was shown that the presence of both cationic charge and surface decoration with targeting glucose residues were crucial for biological activity.[124]

Here we report an investigation on the entrapment efficiency (E.E.) of UA in liposomes formulated with three different phospholipids (PCs) featuring different alkyl chain lengths and extent of saturation/unsaturation, namely 1,2-dimyristoyl-*sn*-glycero-3-phosphatidylcholine (DMPC), 1,2-dioleooyl-*sn*-glycero-3-phosphatidylcholine (DOPC) and 1,2-dipalmitoyl-*sn*-glycero-3-phosphatidylcholine (DPPC) in the presence and in the absence of cholesterol (chol). UA was loaded by passive and active loading. It is known that the nature of PC and the loading technique can have a crucial effect on liposomes properties[125,126,127] and on their

[122] Alavi, M.; Karimi, N.; Safaei, M. Application of Various Types of Liposomes in Drug Delivery Systems. *Adv. Pharm. Bull.* **2017** 7(1), 3-9.

[123] Bulbake, U.; Doppalapudi, S.; Kommineni, N.; Khan, W. Liposomal Formulations in Clinical Use: an Updated Review. *Pharmaceutics,* **2017**, 9(2) 12-45

[124] Francolini, I.; Giansanti, L.; Piozzi, A.; Altieri, B.; Mauceri, A.; Mancini, G. Glucosylated Liposomes as Drug Delivery Systems of Usnic Acid to Address Bacterial Infections. *Colloids Surf B Biointerfaces,* **2019**, 181, 632-638

[125] Gradella Villalva, D.; Giansanti, L.; Mauceri, A.; Ceccacci, F.; Mancini, G. Influence of the State of Phase of Lipid Bilayer on the Exposure of Glucose Residues on the Surface of Liposomes. *Coll. Surf. B: Biointer*. **2017**, 159, 557–563

ability to entrap a solute.[128,129,130] Physicochemical properties and UA loading capability of liposomes composed of DMPC and any of the pyrrolidinium-based amphiphiles (PAs) **1**-**4** reported in Figure 12 were then investigated in detail.

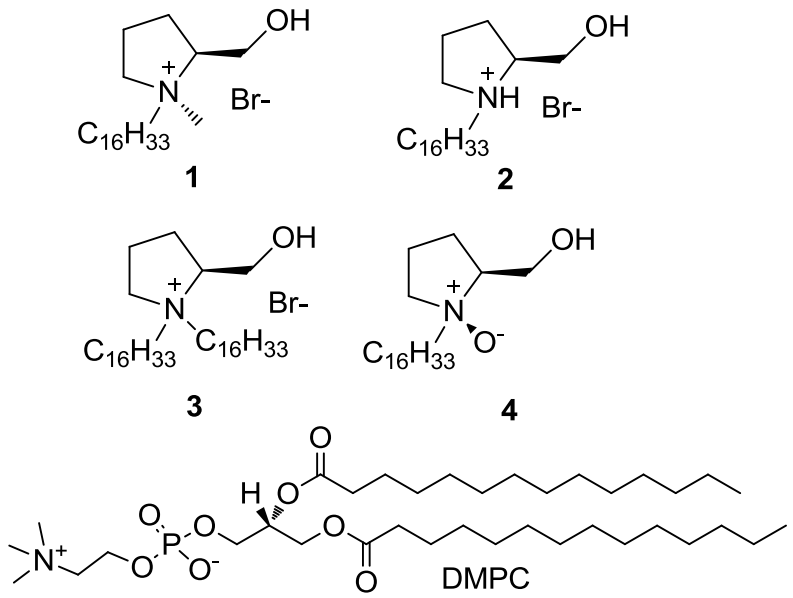

Figure 12. Pyrrolidinium-based amphiphiles (PAs) **1**-**4** and DMPC.

In fact, it is well known that the structural characteristics of the components of lipidic self-assembled systems influence the morphology and physicochemical behavior of the aggregates[131,132] and are strictly related to that their "classical" performance properties (*i.e.* wetting and foaming ability, solubilization and

[126] Gradella Villalva, D.; Diociaiuti, M.; Giansanti, L.; Petaccia, M.; Besker, N.; Mancini, G. Molecular Packing in Langmuir Monolayers Composed of a Phosphatidylcholine and a Pyrene Lipid. *J. Phys. Chem. B,* **2016**, 120, 1126–1133

[127] Scindia, Y.; Silbert, L.; Volinsky, R.; Kolusheva, S.; Jelinek, R. Colorimetric Detection and Fingerprinting of Bacteria by Glass-supported Lipid/Polydiacetylene Films. *Langmuir,* **2007**, 23, 4682–4687

[128] Giuliani, C.; Altieri, B.; Bombelli, C.; Galantini, L.; Mancini, G.; Stringaro, A. Remote Loading of Aloe Emodin in Gemini-based Cationic Liposomes. *Langmuir,* **2015**, 31, 76-82

[129] Giansanti, L.; Condello, M.; Altieri, B.; Galantini, L.; Meschini, S.; Mancini, G. Influence of Lipid Composition on the Ability of Liposome Loaded Voacamine to Improve the Reversion of Doxorubicin Resistant Osteosarcoma Cells. *Chem. Phys. Lipids,* **2019,** 223, 104781

[130] Som, A.; Tew, G. N. Influence of Lipid Composition on Membrane Activity of Antimicrobial Phenylene Ethynylene Oligomers. *J. Phys. Chem. B,* **2008**, 112, 3495–3502

[131] Israelachvili, J. N.; Mitchell, D. J. Theory of Self-assembly of Hydrocarbon Amphiphiles into Micelles and Bilayers *J. Chem. Soc.* **1976**, 72, 1525-1568

[132] Oliver, R. C.; Lipfert, J.; Fox, D. A.; Lo, R. H.; Doniach, S.; Columbus, L. Dependence of Micelle Size and Shape on Detergent Alkyl Chain Length and Headgroup. *PLOS ONE*, **2013**, 8(5), 62488.

detergency).[133,134,135] For example, the length and the charge of the surfactant can significantly affect the properties of the aggregates it forms.[136,137,138,139] Amino acid surfactants as alternatives to conventional surfactants have attracted widespread attention over the last decade.[140,141,142] Cationic amino acid surfactants exhibit good antibacterial activity against a broad spectrum of microorganisms[143,144,145] thanks to electrostatic and hydrophobic interaction with bacterial cell wall.[146,147] These agents can also lead to membrane disruption[148] with consequent release of electrolytes and nucleic materials and cell death. In particular, proline-based surfactants possess interesting physicochemical and biological activities. Proline, being a cyclic secondary amine, shows an exceptional conformational rigidity compared to other amino acids. However, there have been limited studies on antibacterial properties of

---

133 Azira, H.; Tazerouti, A.; Canselier, J. P. Study of Foaming Properties and Effect of the Isomeric Distribution of Some Anionic Surfactants. *J. Surfact. Deterg.* **2008**, 11, 279–286

134 Sehgal, P.; Doe, H.; Bakshi, M. S. Solubilization of Phospholipid Vesicular Structures into Mixed Micelles of Zwitterionic Surfactants. *J. Surfact. Deterg.* **2003**, 6(1), 31-37

135 Lichtenberg, D.; Robson, R. J.; Dennis, E. A. Solubilization of Phospholipids by Detergents Structural and Kinetic Aspects. *Biochimica et Biophysica Acta (BBA) - Reviews on Biomembranes,* **1983**, 737(2), 285-304

136 Ceccacci, F.; Giansanti, L.; Mancini, G.; Mauceri, A.; Scipioni, A.; Sperduto, C. Transcription of Chirality from Molecules to Complex Systems: the Role of Hydrophobic Interactions. *Supramol. Chem.* **2013**, 25 (9-11), 741-747

137 Costas-Costas, U.; Bravo-Diaz, C.; Gonzalez-Romero, E. Kinetics and Mechanism of the Reaction Between Ascorbic Acid Derivatives and an Arenediazonium Salt: Cationic Micellar Effects. *Langmuir*, **2005**, 21, 10983-10991.

138 Ceccacci, F.; Giansanti, L.; Levi Mortera, S.; Mancini, G.; Sorrenti, A.; Villani, C. Enantiodiscrimination of Bilirubin-IX Alpha Enantiomers in Biomembrane Models: Has Chirality a Role in Bilirubin Toxicity? *Bioorganic. Chem.* **2008**, 36(5), 252-254

139 Joshi, J. V.; Aswal, V. K.; Bahadur P.; Goyal, P. S. Role of Counterion of the Surfactant Molecule on the Micellar Structure in Aqueous Solution. *Current Science,* **2002**, 83(1), 47-49

140 Pinazo, A.; Pons, R.; Perez, L.; Infante, M. R. Amino Acids as Raw Material for Biocompatible Surfactants. *Ind. Eng. Chem. Res.* **2011**, 50, 4805–4817

141 Chandra, N.; Tyagi, V. K. Synthesis, Properties and Applications of Amino Acid Based Surfactants: a Review. *J. Dispers. Sci. Technol.* **2013**; 34, 800–808

142 Moran, M. C.; Pinazo, A.; Perez, L.; Clapes, P.; Angelet, M.; Garcia, M. T.; Vinardell, M. P.; Infante, M. R. Green Amino Acid-based Surfactants. *Green Chem.* 2004, 6, 233–240.

143 Castillo, J. A.; Pinazo, A.; Carilla, J.; Infante, M. R.; Alsina, M. A.; Clapes, H. I. Interaction of Antimicrobial Arginine-based Cationic Surfactants with Liposomes and Lipid Monolayers. *Langmuir*, **2004**, 20, 3379–3387

144 Lukac, M.; Lacko, I.; Bukovsky, M.; Kyselova, Z.; Karlovsta, J.; Horvath, B.; Devinsky, F. Synthesis and Antimicrobial Activity of a Series of Optically Active Quaternary Ammonium Salts Derived From Phenylalanine. *Cent. Eur. J. Chem.* **2010**, 8, 194–201

145 Perez, L.; Pinazo, A.; Garcia, M. T.; Lozano, M.; Manresa, A.; Angelet, M.; Vinardell, M. P.; Mitjans, M.; Pons, R.; Infante, M. R. Cationic Surfactants From Lysine: Synthesis, Micellization and Biological Evaluation. *Eur. J. Med. Chem.* **2009**, 44, 1884–1892

146 Joondan, N.; Jhaumeer-Laulloo, S.; Caumul, P. A Study of the Antibacterial Activity of *L*-Phenylalanine and *L*-Tyrosine Esters in Relation to Their CMCs and Their Interactions With 1,2-dipalmitoyl-*sn*-glycero-3-phosphocholine, DPPC as Model Membrane. *Microbiol. Res.* **2014**, 169, 675–685

147 Joondan, N.; Caumul, P.; Akerman, M.; Jhaumeer-Laulloo, S. Synthesis, Micellisation and Interaction of Novel Quaternary Ammonium Compounds Derived From *L*-Phenylalanine With 1,2-dipalmitoyl-*sn*-glycero-3-phosphocholine as Model Membrane in Relation to Their Antibacterial Activity, and Their Selectivity Over Human Red Blood Cells. *Bioorg. Chem.* **2015**, 58, 117–129

148 Faustino, C. M. C.; Calado, A. R. T.; Garcia-Rio, L. Mixed Micelle Formation Between Amino-acid Based Surfactants and Phospholipids. *J. Colloid Interface Sci.* **2011**, 329, 493–498

proline-based surfactants. In particular *L*-prolinol derivatives are surfactants that, as other proline-based ones, bear a polar headgroup featuring a pyrrolidine ring; this moiety confers to them a lower conformational freedom with respect to the corresponding acyclic analogue, together with a different balance as a whole between the hydrophilic and the hydrophobic region of the molecules.[149] The possibility of modifying the pyrrolidine skeleton and the length of the alkyl chains, thus the physicochemical properties of the surfactant, makes pyrrolidinium based surfactants interesting in many research fields.[150,151,152,153] It was previously shown that the differences in the molecular structure of **1-3**, besides affecting liposomes physicochemical features, also influenced the drug delivery efficiency toward bacterial cells.[153] The biological activity of mixed liposomes containing PAs **1-4** was evaluated on *Staphylococcus aureus* bacterial cells.

2.1.3 Experimental section

Materials

DMPC, DOPC and DPPC were purchased from Avanti Polar Lipids (Alabaster, AL) and used without further purification (purity > 99%). Phosphate-buffered saline (PBS) tablets (0.01 M phosphate buffer, 0.0027 M KCl, 0.137 M NaCl, pH=7.4 at 25°C), Mueller Hinton, UA, chol, 4-heptadecyl-7-hydroxycoumarin (HC), calcium acetate and dialysis tubing cellulose membrane D 9527 were purchased from Sigma-Aldrich (Milano, Italy). PAs **1-4** were prepared and purified as previously described.[154,155,156] Methicillin sensible *Staphylococcus aureus* reference strain from the American Type Culture Collection (ATCC 29213) was used as control organism.

---

[149] Karukstis, K. K.; Mc Donough, J. R. Characterization of the Aggregates of *N*-alkyl-*N*-methylpyrrolidinium Bromide Surfactants in Aqueous Solution. *Langmuir*, **2005**, 21, 5716-5721

[150] Zhao, M. W.; Zheng, L. Q. Micelle Formation by *N*-alkyl-*N*-methylpyrrolidinium Bromide in Aqueous Solution. *Phys. Chem. Chem. Phys.* **2011**, 13, 1332-1336

[151] Cai, B.; Li, X.; Yang, Y.; Dong, J. Surface Properties of Gemini Surfactants with Pyrrolidinium Headgroups. *J. Coll. Int. Sci.* **2012**, 370, 111–116

[152] Tian, Y.; Wei, R.; Cai, B.; Dong, J.; Deng, B.; Xiao, Y. Cationic Gemini Pyrrolidinium Surfactants Based Sweeping-micellar Electrokinetic Chromatography for Simultaneous Detection of Nine Organic Pollutants in Environmental Water. *Journal of Chromatography A*, **2016**, 1475, 95–101

[153] Bombelli, C.; Bordi, F.; Ferro, S.; Giansanti, L.; Jori, G.; Mancini, G.; Mazzuca, C.; Monti, D.; Ricchelli, F.; Sennato, S.; Venanzi, M. New Cationic Liposomes as Vehicles of *m*-Tetrahydroxyphenylchlorin in Photodynamic Therapy of Infectious Diseases. *Mol. Pharmaceutics*, **2008**, 5(4), 672–679

[154] Borocci, S.; Ceccacci, F.; Galantini, L.; Mancini, G.; Monti, D.; Scipioni, A.; Venanzi, M. Deracemization of an Axially Chiral Biphenylic Derivative as a Tool for Investigating Chiral Recognition in Self-assemblies. *Chirality*, **2003**, 15(5), 441-447

Liposomes preparation

Liposomes were prepared according to thin film methodology. Briefly, the proper amount of PC in the presence or in the absence of chol (molar ratio: 7/3) or of DMPC and one PAs **1-4** (molar ratio: 9/1) were dissolved in $CHCl_3$ on the inside wall of a round-bottom flask. The lipid films obtained after solvent evaporation were stored overnight under reduced pressure (0.4 mbar), then aqueous PBS (in the case of protocol 1) or 170 mM calcium acetate solution at pH 6 (in the case of protocol 2) was added to obtain a lipid dispersion of the desired concentration. The solutions containing multilamellar vesicles (MLV) were heated at 50°C and vortex-mixed. With the exception of samples used for differential scanning calorimetry (DSC) measurements, the suspensions were then sonicated for 4 minutes at 72 W (cycles: 0.5 s) under cooling condition of an ice-water bath, using a Hielscher UP100-H ultrasonic processor with microtip probe (7 mm) to obtain small unilamellar vescicles.

Inclusion of UA in liposomes and evaluation of E.E

Protocol 1: passive loading was performed by adding a proper volume of a solution of UA 37.5 mM in DMSO to preformed liposomes (5 mM) to obtain 1:20 UA/lipid ratio (total UA concentration 0.25 mM). Being the volume of the added organic solvent ≤1% of the total volume, its effect on the stability of preformed liposomes is neglectable. The solutions were incubated for 1h at 30°C, 40°C or 60°C in the case of DOPC, DMPC or DPPC based liposomes, respectively.

Protocol 2 (only in the case of PC liposomes): active loading of UA was performed applying a pH transmembrane gradient according to a described procedure.[157] Briefly, lipid films were hydrated using a 170 mM calcium acetate solution at pH 6 to obtain liposomes 5 mM. The transmembrane pH gradient was generated by a transmembrane difference in calcium acetate concentration obtained removing the

[155] Barenholz, Y.; Bombelli, C.; Bonicelli, M. G.; Di Profio, P.; Giansanti, L.; Mancini, G.; Pascale, F. Influence of Lipid Composition on the Thermotropic Behavior and Size Distribution of Mixed Cationic Liposomes. *J. Coll. Int. Sci.* **2011**, 356, 46-53

[156] Battista, S.; Campitelli, P.; Carlone, A.; Giansanti, L. Influence of Structurally Related Micelle Forming Surfactants on the Antioxidant Activity of Natural Substances. *Chem. Phys. Lipids*, **2019**, 225, 104818

[157] Clerc, S.; Barenholz, Y. Loading of Amphipathic Weak Acids into Liposomes in Response to Transmembrane Calcium Acetate Gradients. *Biochim. et Biophys. Acta*, **1995**, 1240, 257-265

salt from the bulk by dialysis (the external medium was exchanged 4 times in 2 hours with a volume of 170 mM sodium sulfate equal to 25 fold the volume of liposomes dispersion). A proper amount of UA dissolved in DMSO was then added to the preformed liposome suspension to obtain a 1:20 UA/lipid molar ratio (total UA concentration 0.25 mM) and the solution was incubated for 1h at 30°C, 40°C or 60°C in the case of DOPC, DMPC or DPPC based liposomes, respectively.

The removal of unentrapped UA was carried out in both procedures by dialysis exchanging 4 times in 1 hour the external medium with a volume equal to 25 fold the one of liposomes dispersion of PBS (in the case of protocol 1) or 5% glucose (in the case of protocol 2). E.E. was evaluated before and after removal of free UA by UV measurements (absorbance at 290 nm) of samples obtained by adding 1.5 mL of methanol to 1.5 mL of liposome suspension, using a Varian Cary 50 UV-vis spectrophotometer (Agilent).

DLS and Zeta potential measurements

DLS and electrophoretic mobility measurements by means of the laser Doppler electrophoresis technique were carried out at 25°C on 1 mM DMPC/**1(-4)** liposome solutions (prepared according to protocol 1) before and after UA inclusion using a Malvern Zetasizer apparatus equipped with a 5 mW He-Ne laser operating at 633 nm and a digital logarithmic correlator. To obtain the size distribution the measured autocorrelation functions were analyzed by means of the non-negative least square (NNLS) algorithm. The distribution of the diffusion coefficients D of the particles was converted in a distribution of apparent hydrodynamic diameters D_H using the Stokes–Einstein relationship $D_H = kT/3\pi\eta D$, where kT is the thermal energy and η the solvent viscosity. Reported D_H values correspond to the average values over several measurements and were obtained from intensity weighted distributions. The measurements of the electrophoretic mobility to determine Zeta potential were carried out by means of the laser Doppler electrophoresis technique. Analysis of the Doppler shift in the Zetasizer Nano series was done by using phase analysis light scattering (PALS) implemented with M3 (mixed mode measurement). Low applied voltages were used to avoid the risk of effects due to Joule heating. Zeta potential

was inferred from the electrophoretic mobility data by using the Henry equation under the Smoluchowsky approximation. All values reported were the average of 3 consecutive measurements of the same samples.

*Determination of thermotropic properties of DMPC/**1**(-**4**) liposomes*

Differential scanning calorimetry (DSC) measurements were carried out on 30 µL of MLV. DMPC/**1**(**-4**) liposomes (1 mg/10 µL, ≈ 150 mM in total lipids) in PBS before and after incubation with 3 µL of a DMSO solution 37.5 mM in UA or with 3 µL of DMSO devoid of UA. Liposomes containing DMSO (in the presence and in the absence of UA) were incubated 1 h at 40 °C before DSC measurements. Two heating scans were recorded at the rate of 5 °C/min and two subsequent heating scans were recorded at the rate 1 °C/min. Under the experimental conditions, reproducible thermal recordings were obtained. Uncertainty on temperatures is 0.1 °C.

Evaluation of the antimicrobial activity of liposomal UA

The antimicrobial susceptibility of *S. aureus* ATCC 29213 to UA loaded in liposomes was determined in accordance with the CLSI guidelines.[158] In detail, 50 µL of bacterial suspension in 0.9% saline solution (NaCl) at a concentration of 10^6 CFU/mL were added to the wells of a 96-well microtitre plate containing 50 µL of two-fold serially diluted free UA and liposomes loaded with UA in cation-adjusted Mueller–Hinton. Positive control wells were prepared with colture medium and bacterial suspension. Microtitre plates were incubated for 18 h at 35°C. The growth in each well was quantified spectrophotometrically at 595 nm by a microplate reader iMark, BioRad (Milan, Italy). The minimum inhibitory concentration (MIC) for UA and UA loaded in liposomes was defined as the concentration of drug that reduces growth by 80% compared to untreated organisms. The MIC value was determined as the median of three independent experiments.

[158] CLSI. Performance Standards for Antimicrobial Susceptibility Testing. 27th ed. CLSI supplement M100. Wayne, PA: Clinical and Laboratory Standards Institute; **2017**

Evaluation of interaction between liposomes and bacteria by fluorescence measurements

The interaction between DMPC/**1**(**-4**) liposomes and bacterial cells (bacterial inoculum 5×10^5 CFU/mL) was qualitatively evaluated by estimating the variation of surface potential of the liposomes upon incubation with the pathogens. The variation of surface potential was investigated by exploiting the differences in the excitation spectra of HC, a fluorescent probe associated to lipid bilayer.[159] HC containing liposomes were prepared according to protocol 1 adding a proper volume of HC dissolved in THF to the lipid chloroform solution to obtain 50 µM HC and 10 mM total lipid concentration. The measurements were performed on liposomes devoid of UA before and after incubation (18 h) with bacterial cells as described in the previous paragraph. Fluorescence excitation spectra of HC embedded in lipid bilayer were recorded at 25°C by scanning the excitation wavelength between 300 and 400 nm and at an emission wavelength of 450 nm, using a Perkin Elmer LS 50 spectrofluorimeter, on a solution containing 30 µL of liposomes and bacteria suspension or 30 µL of liposomes not previously incubated with bacteria (the blank sample) and 2970 µL of Mueller-Hinton medium used in biological experiments.

2.1.4 Results and discussion

The effect of liposomes components (both the PC and the synthetic amphiphiles) and of the loading technique on E.E. of UA and on liposomes properties was investigated at the aim of correlating them to be antibacterial activity of liposome loaded drug.

At first we investigated liposomes composed of mere PC, in the presence and in the absence of chol (at 2:1 molar ratio) to evaluate the effect of the extent of saturation/unsaturation, of chain length and of loading technique on the entrapment of UA. The E.E. was investigated by UV measurements after removal of the unentrapped UA by dialysis. Before applying the chosen protocol with liposomes suspensions we verified that the amount of free UA corresponding to 100% E.E. was completely removed from the solution. UA was loaded in liposome

[159] Zuidan, N.J.; Barenholz, Y. Electrostatic Parameters of Cationic Liposomes Commonly Used for Gene Delivery as Determined by 4-heptadecyl-7-hydroxycoumarin. *Biochim. Biophys. Acta,* **1997**, 1329, 211-222

by two different procedures, *i.e.* passive and remote loading. In the first procedure UA, scarcely soluble in water, was solubilized in DMSO and then was added to preformed liposomes in PBS (organic solvent ≤1% of the volume of aqueous solution); in the second procedure, that can be used for weak acid or basic compounds,[157] a pH gradient between the liposome internal aqueous phase and the bulk was generated to act as a driving force for drug active loading. In particular the pH of the bulk was such (pH 6) to switch the deprotonation equilibrium toward the neutral form of UA, whereas the pH of the liposome internal pool (pH ≈ 8) was set higher than that of the bulk. The higher affinity of neutral molecules for lipid bilayer promote the binding of UA from the bulk and the crossing of lipid bilayer, once it reaches the internal liposomes compartment (at higher pH) it is deprotonated and entrapped inside the aggregates. The E.E. obtained using the two procedures are reported in Table 5.

Table 5. E.E. of PC and PC/chol liposomes obtained using passive or active loading by incubation of UA with preformed liposomes. Error in determination is ≤ 5%.

PC/chol	Passive Loading (Protocol 1)	Active Loading (Protocol 2)
DMPC (10/0)	100	--
DMPC (7/3)	82	77
DPPC (10/0)	60	--
DPPC (7/3)	71	43
DOPC (10/0)	38	--
DOPC (7/3)	29	25

It is evident that in all cases active loading yielded lowest E.E., this being in agreement with what observed in a previous investigation on the inclusion of UA in glycosylated liposomes.[124] In order to rule out that this result could be due to the lack of a well-established pH gradient across the lipid membrane, the presence of the pH imbalance between the internal aqueous core of liposomes and the bulk was

verified by exploiting pyranine, a fluorescence pH-sensitive probe (data not shown), according to a procedure described in the literature.[157] The obtained result can be explained considering the high lipophilicity of UA also in its deprotonated form (due to the possibility of stabilizing the negative charge by resonance on the β-triketone groups).[79] This might cause the failure of the active loading that is based on the different permeability of lipid bilayer toward neutral and charged form of the drug. Another hypothesis is that in the bulk (at pH= 6), the scarcely soluble neutral form of UA aggregates as suggested by a slight reduction (5%) of the value of the maximum in the absorbance spectrum reducing the pH of the bulk to 5, value at which precipitation of UA begins occurs. Aggregation and precipitation obviously subtract UA from association with lipid bilayer.

While the presence of chol is crucial to maintain a pH gradient across the lipid membrane, passive loading was investigated also in the absence of chol, and actually higher E.E. were observed in the case of liposomes devoid of chol. Highest E.E. were observed in the case of DMPC liposomes, whereas lowest E.E. were observed in the case of DOPC liposomes. Therefore, on the one hand we observed that the extreme fluidity of DOPC disfavors the association of UA, on the other that also the rigidity ascribed by chol to lipid membrane as well as he high extent of lipid packing featured by DPPC liposomes are not optimal conditions. Moreover, deprotonated UA forms persistent hydrogen bonds with DPPC and most of all with DOPC when included in liposomes. The occurrence of these interactions brings to the destabilization of lipid bilayer and promotes the transition to a non lamellar state, thus reducing liposomes stability.[160] Obviously, this phenomenon could contribute to explain the fact that in the case of DOPC the lowest E.E. of UA was observed. The high extent of UA association with DMPC liposomes depends on the fact that in DMPC bilayer a good compromise between rigidity and fluidity of the bilayer is achieved, so the best matching of the grooves within lipid bilayer with the topology of UA molecules occurs.

[160] Nadvorny, D.; Bosco, J.; Da Silva, P.; Lins, R. D. Anionic Form of Usnic Acid Promotes Lamellar to Nonlamellar Transition in DPPC and DOPC Membranes. *J. Phys. Chem. B*, **2014**, 118, 3881-3886

Based on these results we selected DMPC as phospholipid component in the formulation of mixed liposomes containing one of the four synthetic amphiphiles, **1-4**, derived from *L*-prolinol, and used passive loading procedure to load UA.

E.E. of UA, the size and zeta potential of of DMPC and DMPC/PA formulations are reported in Table 6.

Table 6. Physicochemical and biological features of the DMPC and DMPC/PA formulations at 9/1 molar ratio.

Formulation	E.E. (%)	size (nm)[b]	Zeta potential[b] (mV)	Zeta potential with UA (mV)	biological activity[c] (μg/mL)
DMPC	100%	82 ± 3	-2 ± 1	-7 ± 2	8
DMPC/**1**	85%	70 ± 8	21 ± 2	12 ± 2	toxic[b]
DMPC/**2**	82%	69 ± 5	13 ± 3	8 ± 2	8
DMPC/**3**	87%	78 ± 8	14 ± 2	12 ± 2	absent
DMPC/**4**	96%	71 ± 6	13 ± 2	9 ± 1	toxic[b]

[a] A minor larger size population (from ≈ 500 nm to ≈ 1 μm) is present in all samples; similar results were obtained investigating UA loaded liposomes. [b]Data referred to void liposomes. Similar results were obtained with UA loaded liposomes. [c]UA liposomal MIC in the range 8-16 μg/mL; MIC of free UA is 8 μg/mL in the same range. The reported MICs correspond to the average values over 5 independent measurements.

The E.E. was very high (> 80%) in all cases without relevant variations due to the different nature of PS. Size and size distribution of the investigated liposomes did not showed any dependence on PA molecular structure because all liposomes showed a D_H of ~70-80 nm, both in the presence and in the absence of UA (data not shown). A minor population (less than 5%) with dimensions in the range 0.5-1 μm was also observed, a phenomenon that generally occurs upon sonication.[161,162] The stability of the samples over time was not evaluated but it was observed that maintain their features for at least one week .

[161] Zasadzinski, J. A. N. Transmission Electron Microscopy Observations of Sonication-induced Changes in Liposome Structure. *Biophys. J.* **1986**, 49, 1119-1130

[162] Hamilton, R. L. Jr.; Goerke, J.; Guo, L. S. S.; Williams, M. C.; Havel, R. J. Unilamellar Liposomes Made with the French Pressure Cell: a Simple Preparative and Semiquantitative Technique. *J. Lipid Res.* **1980**, 21, 981-992

Liposome zeta potential in the presence and in the absence of UA was also measured (Table 2). The value of zeta potential of DMPC/PA liposomes, both in the presence and in the absence of UA, resulted all higher than that of DMPC liposomes. This was unexpected in the case of DMPC/**4** liposomes because the PA component is zwitterionic as well as DMPC. Actually similar results were obtained in the study of liposomes containing **4** or its homologues:[163] evidently lipid organization involves the better exposure of cationic residues better than the anionic ones. The value of zeta potential of DMPC/**2** liposomes suggests a partial protonation of the tertiary amine group of **2**. Liposomes containing **1**, the cationic analogue of **2**, as expected showed the highest positive zeta potential, about ten millivolt higher than liposomes containing **2** or **3**, the corresponding twin cationic surfactant. In the latter case it is reasonable that reduced lipid packing due the presence of two alkyl chains brings a different lipid organization and/or to a stronger interaction with counterions with consequent influence on zeta potential. The differences observed among the four mixed formulation are due to different lipid organization and packing that involves a minor or major exposure of the cationic residues. Interestingly zeta potential of formulations containing UA, with the sole exception of DMPC/**3** liposomes, are lower than those of empty liposomes, as observed in other cases,[124,160,163,164] thus suggesting that UA is localized on the surface of liposomes and neutralizes part of their charges. This is not surprising because, though UA is a lipophilic molecule, in the experimental conditions, *i.e.* pH=7.4, it is mostly in its deprotonated form and as such can interact with charged lipid headgroups without penetrating deeply in the lipid bilayer. In the case of DMPC/**3** liposomes, it is evident that the twin nature of the PA component involves the low extent of lipid packing and the formation of deeper grooves that can accomodate UA.

The thermotropic behavior and lipid organization of mixed formulations were investigated by DSC measurements on MLV because unilamellar vescicles tend to

[163] Battista, S.; Campitelli, P.; Galantini, L.; Köber, M.; Vargas-Nadal, G.; Ventosa, N.; Giansanti, L. Use of *N*-oxide and Cationic Surfactants to Enhance Antioxidant Properties of (+)-Usnic Acid Loaded Liposomes. *Coll. Surf. A,* **2019**, under revision

[164] Funun, M. Classification and Application of Colloidal Drug Delivery Systems in Tumor Targeting. *Colloids in Drug Delivery*, **2016**, 18, 417-419

fuse upon heating and this increases the complexity of the thermograms.[165] DSC thermograms give directly the transition temperature, Tm whereas the ΔH associated to the transition can be assessed by integrating the area of the corresponding peak. In an ideal system lipid molecules are perfectly ordered and undergo the transition from the gel to the liquid-crystal phase at the same temperature. In real systems, defects in lipid packing, calorimetric lags and finite scan rates cause a broadening of the peak associated to a transition over finite ranges of temperature.[166] The width at half-height of the transition ($\Delta T_{1/2}$). In fact, the cooperativity of the transition (*i.e.* how the transition of a molecule from a state to another affects the transition of the surrounding molecules) can also be estimated by calculating the cooperative unit (CU) according to equation 1[167]

$$CU = \Delta H_{vH}/\Delta H_{exp} \qquad (1)$$

where ΔH_{vH} is the van't Hoff enthalpy variation and ΔH_{exp} is the experimental enthalpy variation obtained by integration of the peak associated to the transition. ΔH_{vH} can be calculated using equation 2[168]

$$\Delta H_{vH} = 6.9\ T^2/\ \Delta T_{1/2} \qquad (2)$$

Also the shape of the peaks also contain useful information on the interaction of lipids, on their miscibility (in the case of mixed formulations), on the presence of domains and on the location and on the influence of molecules included in the lipid bilayer on these features.

The thermograms and the relative thermodynamic parameters are reported in Figure 13 and Table 7, respectively.

[165] Chiu, M. H.; Prenner, E. J. Differential Scanning Calorimetry: an Invaluable Tool for a Detailed Thermodynamic Characterization of Macromolecules and Their Interactions. *J. Pharm. Bioallied. Sci.* **2011,** 3(1), 39-59

[166] Sturtevant, J. M. The Effects of Water-soluble Solutes on the Phase Transitions of Phospholipids. *Proc. Natl. Acad. Sci. USA,* **1982**, 79, 3963-3967

[167] Biltonen, R. L.; Lichtenberg, D. The Use of Differential Scanning Calorimetry as a Tool to Characterize Liposome Preparations. *Chem. Phys. Lipids,* **1993**, 64, 129-142

[168] Sturtevant, J. Biochemical Applications of Differential Scanning Calorimetry. *Ann. Rev. Phys. Chem.* **1987**, 38, 463-488

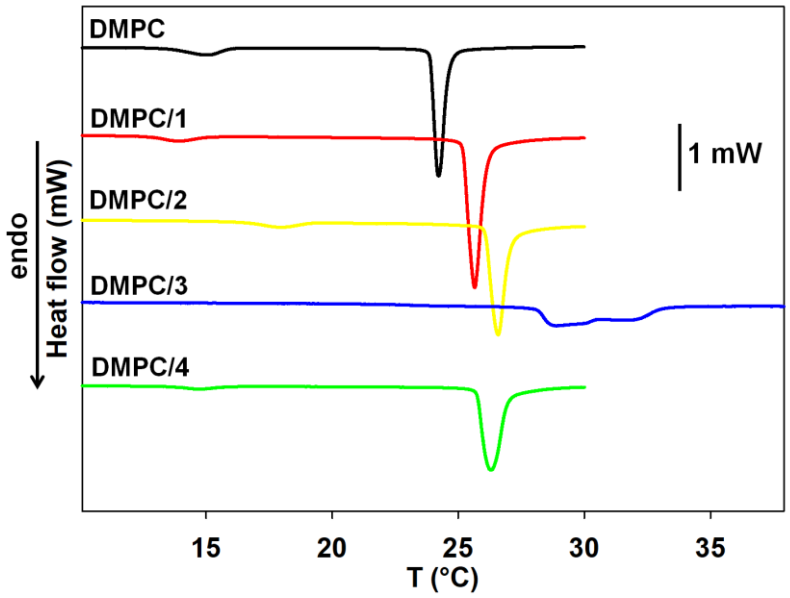

Figure 13. Thermograms of DMPC and DMPC/PA MLV. Scan rate is 1° C/min.

Table 7. Thermodynamic parameters of empty DMPC and DMPC/PA MLV obtained by DSC measurements.

Formulation	pretransition		main transition		
	T (°C)	ΔH_m(kJ/mol)	T(°C)	ΔH_m (kJ/mol)	CU
DMPC	15.1	3.17	24.2	19.15	96
DMPC/**1**	13.9	2.04	25.7	27.54	59
DMPC/**2**	18.0	2.29	26.6	21.99	42
DMPC/**3**	-	-	≈29; ≈33[a]	19.65	-
DMPC/**4**	14.8	1.09	26.3	20.67	44

[a] Onset and endset temperature 28.1 °C and 31.7 °C, respectively.

It can be observed that the inclusion of the synthetic PA induces a shift of Tm to higher values with respect to Tm of DMPC liposomes to an extent that depends on the molecular structure of the PA. The main transition temperature corresponds to

the passage of the hydrocarbon chains from all *trans* conformation typical of the rigid gel state to *gauche* conformation of the disordered fluid-like liquid-crystalline state. This transition is linked to van der Waals interactions among lipid chains in the gel phase and thus is strictly related to lipid packing. The fact that Tm values of DMPC/**1**(**2**,**4**) liposomes increases suggest that the presence of PA in the lipid bilayer involves an increase of lipid compaction and, as a consequence, of attractive Van der Waals contact among lipids. This is confirmed by the decrease of the experimental ΔH. The most evident variations were observed in the case of DMPC/**3** liposomes thermogram: the main transition occurs in a very broad range of temperature and at least two peaks are present. This evidence indicates the formation of domains and low lipid miscibility and supports the hypothesis of a peculiar lipid organization of DMPC/**3** liposomes deduced from zeta potential values. The evident broadening of the peak associated to the transition of DMPC/**3** liposomes and the relatively low value of ΔH indicates that the increase of Tm with respect to DMPC ones is not attributable to an enhanced lipid packing but is reasonably due to the fact that the vesicles formed by this liposomes-forming lipid feature a Tm of ≈ 70°C.[154] This thermotropic behavior is not surprising considering that **3** is a twin bulky surfactant, thus its inclusion in DMPC bilayer can affect lipid packing in a more substantial manner with respect to the other PAs.

Also the pretransition, linked to the formation of a two-dimensional arrangement with periodic ripples associated to a cooperative rotation of headgroups, is shifted in a PA dependent manner and completely disappears when liposomes contain twin PA **3**. This is not surprising because the pretransition is very sensitive to any kind of perturbation and in DMPC/**3** lipid compaction and order are very low. Differently from what observed in the case of the main transition, ΔH values strongly depend on the different polar lipid headgroup. The highest reduction with respect to DMPC liposomes was observed in the case of DMPC/**4** liposomes (≈ 65%). This evidence supports the hypothesis of the folding of the pyrrolidinium ring bearing the *N*-oxide moiety. In fact, this conformation makes the polar headgroup of **4** more bulky with respect to the ones of the other single-tailed PAs **1** and **2**. As a consequence, **4** exerts the highest disturbing effect on the packing of the headgroup

in the polar region (and thus on the cooperativity of the pretransition) with respect to **1** and **2**.

The heterogeneity among lipid components in the membrane lowers also the cooperativity of the main transition with respect to DMPC liposomes as indicated by the net decrease of CU values. In fact, CU can be considered as the number of lipids undergoing the main transition at the same time (*i.e.* at the same temperature). Thus, despite in general lipid packing increases with respect to DMPC, the structural differences among DMPC and each PA causes a reduction of the cooperativity of the movements occurring during the transition.

The influence of UA on lipid packing and on liposomes thermotropic behavior was also investigated, as reported in Table 8 and Figure 14.

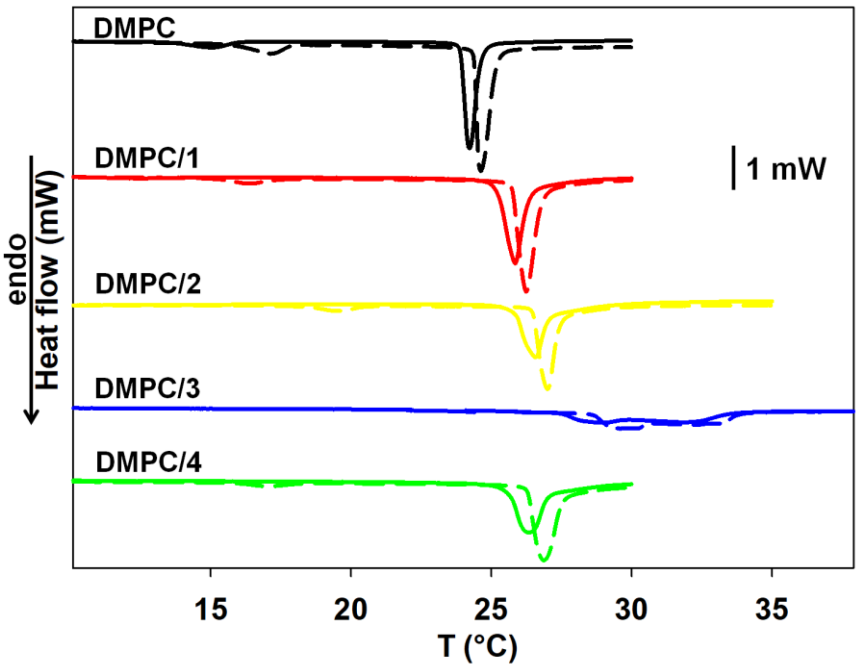

Figure 14. Thermograms of DMPC and DMPC/PA MLV including incubated 1 h at 40°C with a solution of UA in DMSO (final volume 4% with respect to PBS) to obtain a final molar ratio lipids/UA 1/20 (continuous line) and of the same formulations incubated 1 h at 40°C with 4% DMSO without UA (dotted line). Scan rate is 1° C/min.

In this case we compared the results obtained in the presence of UA with those obtained after liposomes incubation with 10% DMSO in the absence of UA at 40°C.

In fact, to have in solution a concentration of UA more similar to the one used in experiments with unilamellar vescicles, 10 µL of a solution of UA dissolved in DMSO (at UA maximum solubility) were added to 100 µL of MLV 1 mg/10 µL in PBS. This volume of DMSO exceeded the maximum allowable percentage of organic solvent (1% of total volume) that surely does not interfere with liposomes stability. By comparing thermograms obtained studying preformed liposomes incubated with DMSO or DMSO + UA it was verified liposomes stability in the experimental conditions (it was demonstrated that only one week after the preparation the amount of DMSO begins to disturb the lipid packing of the bilayer).

Table 8. Thermodynamic parameters of DMPC and DMPC/PA MLV including UA obtained by DSC measurements. Values reported in brackets are relative to samples devoid of UA after 1h incubation at 40°C in the presence of 4% of DMSO.

Formulation	pretransition		main transition		
	T (°C)	ΔH_m (kJ/mol)	T(°C)	ΔH_m (kJ/mol)	CU
DMPC	- (17.1)	- (4.25)	24.2 (24.6)	21.68 (23.46)	70 (73)
DMPC/**1**	- (16.4)	- (2.54)	25.9 (26.2)	25.47 (20.56)	52 (73)
DMPC/**2**	- (19.5)	- (2.28)	26.6 (27.0)	21.64 (21.04)	53 (75)
DMPC/**3**	- -	- -	≈29; ≈32[a] (≈29; ≈33)[b]	19.61 (20.97)	- -
DMPC/**4**	-	-	26.4 (26.9)	21.86 (23.67)	42 (42)

[a] Onset and endset temperature in the absence of UA are 26.2 °C and 33.8 °C, respectively. [b]Onset and endset temperature in the presence of UA 24.9 °C and 31.7 °C, respectively.

Moreover it was proved that the observed variations are due to the presence of UA and not to the presence of DMSO.

It is evident that, with exception of DMPC/**3** liposomes, the presence of UA induces a reduction of Tm, the almost complete disappearance of the pretransition and a neat decrease of ΔH and of CU. It is evident that UA is located near the headgroups (the pretransition, very sensitive to the presence of a solute in headgroup region,[169] is no longer observable), in agreement with what deduced by zeta potential results, and in the external region of the bilayer. In fact, the intercalation of UA in the bilayer reduces van der Waals interactions among lipid chains interfering with the thermal profile of the transition. Obviously, the perturbation of lipid organization and packing interferes not only with Tm values, but also with the extent of ΔH associated to the transition because of an expansion of the available space between lipid chains. The enhancement of their mobility reduces their tendency to act in a concerted manner thus also reducing the cooperativity of the transition.[170] In the case of DMPC/**3** liposomes only a slight variation of Tm and ΔH are observed, but the bilayer is disordered and inhomogeneous yet in the absence of UA, thus its influence on lipid packing in this sample is less relevant.

The antibacterial activity of liposomal UA was also evaluated on Methicillin sensible *Staphylococcus aureus* (Table 6). Empty DMPC/**1** and DMPC/**4** at concentration > to 10^{-4} M formulations are toxic. It is reasonable to hypothesize that the too high zeta potential of DMPC/**1** liposomes and the peculiar exposure of the charged group in DMPC/**4** liposomes induce a strong interaction with bacteria that brings to the disruption of their cell membrane. UA delivered by DMPC and DMPC/**2** liposomes ~1 mM showed the same minimum inhibitory concentration (MIC) of free UA (8 μg/mL) whereas UA delivered by DMPC/**3** liposomes at the same concentration was not active; it is reasonable to ascribe this difference to the peculiar lipid organization of the latter formulation that either reduces its ability to interact with the bacterial cell and/or to deliver effectively the active principle. To

[169] Fa, N.; Ronkart, S.; Schanck, A.; Deleu, M.; Gaigneaux, A.; Goormaghtigh, E.; Mingeot Leclercq, M. P. Effect of the Antibiotic Azithromycin on Thermotropic Behavior of DOPC or DPPC Bilayers. *Chem. Phys. Lipids,* **2006**, 144, 108-116

[170] Castile, J. D.; Taylor, K.M.G.; Buckton, G. A High Sensitivity Differential Scanning Calorimetry Study of the Interaction Between Poloxamers and Dimyristoylphosphatidylcholine and Dipalmitoylphosphatidylcholine Liposomes. *Int. J. Pharm.* **1999**, 182, 101-110

rationalize the observed differences we investigated qualitatively the effect of liposomes-bacteria interaction by incubating cells with liposomes including HC (and devoid of UA). HC is a 7 hydroxycoumarin derivative that exhibits fluorescence only when included in the lipid bilayer because in water gives self-quenching due to aggregation. HC is located at liposomes interface and its excitation fluorescence spectrum varies as a function of the surface potential of the aggregates. In Figure 15 HC excitation spectra before and after 18 h incubation of DMPC/**2**, DMPC/**3** or DMPC/**4** liposomes (i.e. an active, an inactive and a toxic formulation, respectively) with bacterial cells are reported as an example. DMPC and DMPC/**1** liposomes showed the same behavior of DMPC/**2** and DMPC/**4**, respectively (data not shown). Liposomes concentration corresponds to the one at which UA is active when included in DMPC and DMPC/**2** liposomes (i.e. ≈ 1 mM). It can be clearly observed that upon incubation with bacteria in the case of DMPC/2 liposomes (the active formulation chosen as an example) the peak at 330 nm decreases of ≈ 30% whereas fluorescence intensity at higher wavelength slightly increases: these variations indicate that the probe experiences a different microenvironment upon the incubation of liposomes with bacteria, due to the interaction between the aggregates and the cell. Incubation of bacteria with DMPC/**4** liposomes (the toxic formulation chosen as an example) induces a neat decrease of both peaks, especially of the one at 330 nm, indicating a strong interaction of DMPC/**4** liposomes with bacterial membrane that, at higher liposomes concentration, brings to its disruption and to pathogens death also in the absence of UA. Inactive DMPC/**3** liposomes show a net decrease of intensity of the peak at 330 nm: this finding indicates that they can interact with bacteria without killing them but, for reasons probably related to their peculiar lipids organization, they cannot actively release the entrapped UA to the cells. It is noteworthy that these three formulations feature similar zeta potentials, characteristic often indicated as the most important parameter in determining the ability of liposomal carrier to interact with cells. Anyway, the completely different UA efficacy when included in each of them demonstrates that this simplistic statement can be misleading and that the ability of a formulation to interact with the biological milieu

depends on a complex equilibrium among several factors strictly related to physicochemical properties of both the delivery systems and the target cells.

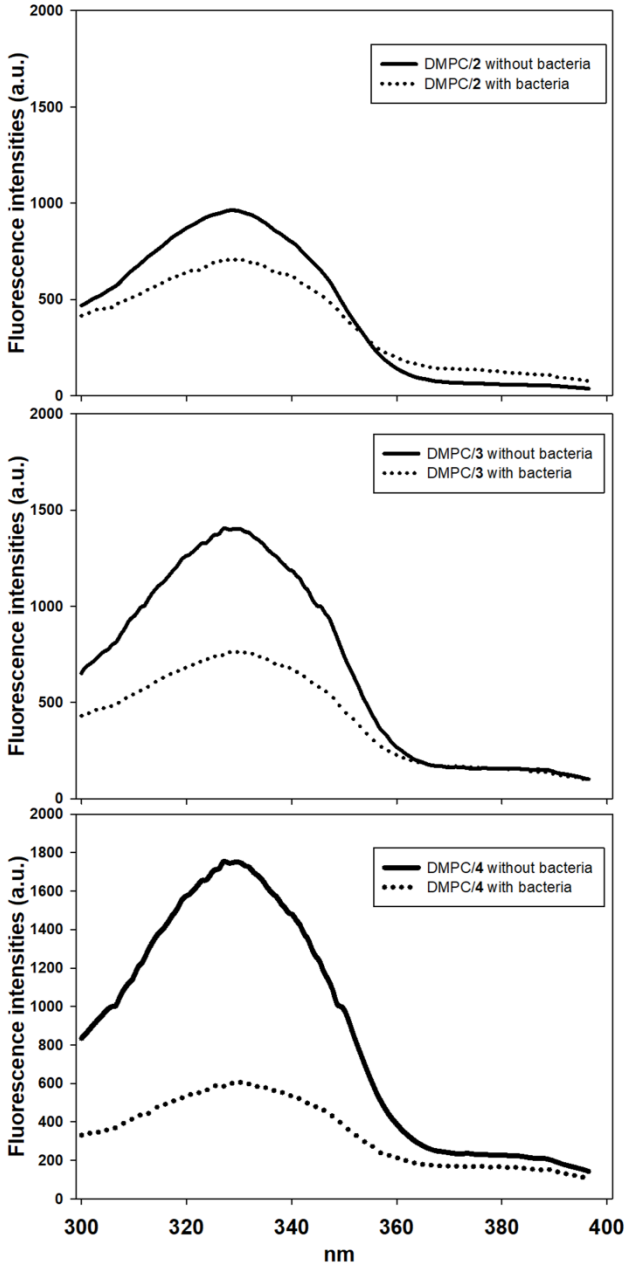

Figure 15. Comparison of HC fluorescence spectra included in DMPC/**2(-4)** liposomes in the presence or in the absence of bacteria after 18 h of incubation.

2.1.5 Conclusions

Liposomes composed of different PCs or DMPC and structurally related synthetic surfactants derived from *L*-prolinol were investigated to evaluate *i*) the best UA loading methodology and *ii*) the relation between the molecular structure of liposomes components and their physicochemical and biological properties. The

fact that despite UA is a weak acid a higher E.E. was observed by using simple incubation on DMPC preformed liposomes than with active loading by pH gradient technique demonstrates that beside drug charge, characteristic such as drug lipophilicity and fluidity of the bilayer must not be neglected in the choice of PC and loading method. The finding that some mixed formulations feature the same bactericidal activity as free UA enlarges the prospective of this active principle that, besides antibacterial properties, displays many pharmacological properties. As a whole, in the investigation on mixed liposomes we demonstrated that also subtle differences in the structure of liposomes components (even the minor one) can affect the aggregates features and, as a consequence, their ability to interact with bacterial cells. Our results confirm that it is possible to optimize the delivery of a drug to bacterial cells by controlling liposomes composition. The possibility of correlating the molecular structure of lipids with the physicochemical and the biological properties of liposomes is critical for a rational and systematic approach to the design of liposomes as drug delivery systems.

2.2 Curcuminoids

2.2.1 Introduction

Curcumin (1,7-bis(4-hydroxy-3-methoxyphenyl)-1,6-heptadiene-3,5-dione) is a natural polyphenol and the principal constituent of turmeric *i.e.*, the ground rhizomes of *Curcuma longa*, which contains two other curcuminoids: desmethoxycurcumin and bis-desmethoxycurcumin.[171] Turmeric is widely used as a spice mostly in Asian countries. It is also used to treat acne, psoriasis, dermatitis and rash. Traditionally, turmeric was suspended in whole milk or buttermilk that dissolved it in fat fractions and/or stabilized curcumin.[172] Over the past few decades, preclinical and clinical studies have revealed that curcumin is active against variety of diseases, such as cancer and pulmonary diseases, as well as neurological, liver, metabolic, autoimmune and cardiovascular diseases, and numerous other chronic ailments.[173,174,175,176] Over 116 clinical studies on curcumin in humans were registered with the US National Institutes of Health in 2015 encompassing a number of conditions, such as cancer, cognitive disorders, gastrointestinal diseases and psychiatric conditions without exerting any toxic effects.[177,178,179,180] One of the puzzling questions is how curcumin can be so effective in the treatment of diseases, since it has a very low water solubility and bioavailability. For example, the oral dose of 8 g/day in humans translates to low

[171] Manolova, Y.; Deneva, V.; Antonov, L.; Drakalska, E.; Momekova, D.; Lambov, N. The Effect of the Water on the Curcumin Tautomerism: a Quantitative Approach. *Spectrochim. Acta A Mol. Biomol. Spectrosc.* **2014**, 132, 815-820

[172] Fu, S.; Shen, Z.; Ajlouni, S.; Nig, K.; Sanguansri, L.; Augustin, M. A. Interactions of Buttermilk with Curcuminoids. *Food. Chem.* **2014**, 149, 47-53

[173] Gostner, J.; Ciardi, C.; Becker, K.; Fuchs, D.; Sucher, R. Immunoregulatory Impact of Food Antioxidants. *Curr. Pharm. Des.* **2014**, 20, 840-849

[174] Gupta, S. C.; Kismali, G.; Aggarwal, B. B. Curcumin, a Component of Turmeric: from Farm to Pharmacy. *Biofactors,* **2013**, 39, 2-13

[175] Maruta, H. Herbal Therapeutics That Block the Oncogenic Kinase PAK1: a Practical Approach Towards PAK1-dependent Diseases and Longevity. *Phytother. Res.* **2014**, 28, 656-672

[176] Srinivasan, K. Antioxidant Potential of Spices and Their Active Constituents. *Crit. Rev. Food Sci. Nutr.* **2014**, 54, 352-372

[177] Current Clinical Trials on Curcumin. *US National Institutes of Health, Clinical Trial Registry*, **2015**

[178] Bar-Sela, G.; Epelbaum, R.; Schaffer, M. Curcumin as an Anticancer Agent: Review of the Gap Between Basic and Clinical Applications. *Curr. Med. Chem.* **2010**, 17, 190-197

[179] Chainani-Wu, N. Safety and Anti-inflammatory Activity of Curcumin: a Component of Tumeric (*Curcuma longa*). *J. Altern. Complement. Med.* **2003**, 9, 161-168

[180] Goel, A.; Kunnumakkara, A. B.; Aggarwal, B. B. Curcumin as 'Curecumin': From Kitchen to Clinic. *Biochem. Pharmacol.* **2008**, 75, 787-809

nanogram levels of circulating curcumin in plasma (only 22-41 ng/ml).[181,182] Moreover, curcumin is not stable under various conditions, such as aqueous phosphate buffer or serum-free medium at 37˚C, degrading to the bioactive compounds, including ferulic acid, feruloylmethane and vanillin, which may be responsible for its biological activities rather than curcumin itself.[181,183] In view of the very low bioavailability of curcumin as observed in clinical studies, the role of the degradation or condensation products should be taken into consideration when evaluating the activity of curcumin in various diseases.

Physico-chemical properties of curcumin

Curcumin is, practically insoluble in water at a neutral and lower pH, but is soluble in acetone, dichloromethane, methanol, ethanol, alkali and oils. The water solubility of curcumin may be increased by its incorporation into various surfactants, such as sodium dodecyl sulfate, polysaccharides, polyethylene glycol and cyclodextrins, as well as others.[183,184] In addition, in aqueous solutions and at an alkaline pH, the acidic phenol group in curcumin dissociates its hydrogen, forming the phenolate ion(s) that render the solubility of curcumin in water somewhat possible.[185,186,187,188] Curcumin exhibits *keto-enol* tautomerism (Figure 16) and the high conjugation of its molecular structure is responsible for the yellow color of turmeric. The *enol* form is more energetically stable in the solid phase and, depending on the solvent, up to 95% can be in the *enol* form.[171] Three reactive functional groups, namely the diketone moiety and the two phenolic groups, determine the biological activity of

[181] Dhillon, N.; Aggarwal, B. B.; Newman, R. A.; Wolff, R. A.; Kunnumakkara, A. B.; Abbruzzese, J. L.; Nig, C. S.; Badmaev, V.; Kurzrock, R. Phase II Trial of Curcumin in Patients With Advanced Pancreatic Cancer. *Clin. Cancer Res.* **2008**, 14, 4491-4499

[182] Shen, L.; Ji, H. F. Contribution of Degradation Products to the Anticancer Activity of Curcumin. *Clin. Cancer Res.* 2009, 15, 7108-7109

[183] Wang, Y. J.; Pan, M. H.; Cheng, A. L.; Lin, L. I.; Ho, Y. S.; Hsieh, C. Y.; Lin, J. K. Stability of Curcumin in Buffer Solutions and Characterization of its Degradation Products. *J. Pharm. Biomed. Anal.* **1997**, 15, 1867-1876

[184] Tønnesen, H. H. Solubility, Chemical and Photochemical Stability of Curcumin in Surfactant Solutions. Studies of Curcumin and Curcuminoids. *Pharmazie,* **2002**, 57, 820-824

[185] Schneider, C.; Gordon, O. N.; Edwards, R. L.; Luis, P. B. Degradation of Curcumin: from Mechanism to Biological Implications. *J. Agric. Food Chem.* **2015**, 63, 7606-7614

[186] Tønnesen, H. H.; Karlsen, J.; van Henegouwen, G. B. Studies on Curcumin and Curcuminoids. Photochemical Stability of Curcumin. *Z. Lebensm. Unters. Forsch.* **1986**, 183, 116-122

[187] Metzler, M.; Pfeiffer, E.; Schulz, S. I.; Dempe, J. S. Curcumin Uptake and Metabolism. *Biofactors*, **2013**, 39, 14-20

[188] Mohanty, C.; Sahoo, S. K. The *in Vitro* Stability and *in Vivo* Pharmacokinetics of Curcumin Prepared as an Aqueous Nanoparticulate Formulation. *Biomaterials,* **2010**, 31, 6597-6611

curcumin. The biologically important chemical reactions of curcumin are hydrogen donation and radical processes, reversible and irreversible nucleophilic addition (Michael reaction), hydrolysis, degradation and as substrate in enzymatic reactions.[189]

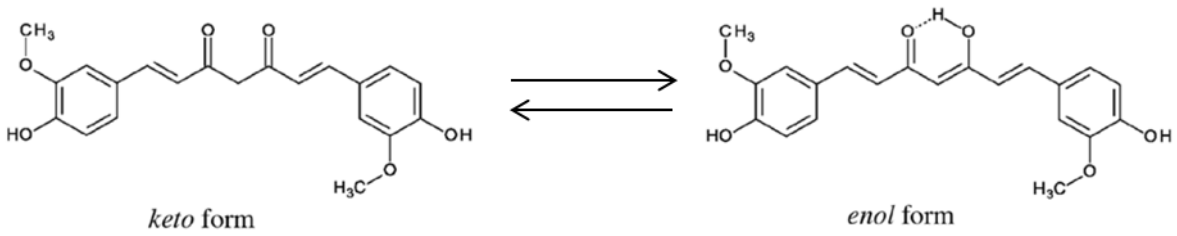

Figure 16. *Keto-enol* tautomerism of curcumin.

Curcumin and 728 analogs were tested for pharmacological properties (mostly anticancer activity) on different cell lines.[190] Some analogs exhibit antioxidant, anti-mutagenic and anti-HIV activities, anti-angiogenic, anti-malaria and anti-tuberculosis activities or anti-inflammatory activities (cyclooxygenases COX inhibitors).[177,191] The anticancer properties of curcuminoids depend on the presence of OH groups in the phenolic ring (entries 4 and 4') that are electron donor to free radicals. The methoxy group at position 3 and 3' seems to be responsible for the antioxidant properties of curcuminoids whereas substitution in the 2 and 2' positions increases all activities than the unsubstituted analogs. Cyclization of the keto-enol group and introduction of heteroatoms (oxygen and nitrogen) leads to the formation of compounds with enhanced antitumor and anti-angiogenic activities. Attaching solubilizing groups to the OH group in position 4 and 4' induces some cytotoxicity in curcuminoids. The elimination of one of the methoxy groups makes curcumin effective against tuberculosis[177] whereas their conversion to hydroxyl

[189] Priyadarsini, K. I. The Chemistry of Curcumin: from Extraction to Therapeutic Agent. *Molecules,* **2014**, 19, 20091-20112

[190] Agrawal, D. K.; Mishra, P. K. Curcumin and its Analogues: Potential Anticancer Agents. *Med. Res. Rev.* **2010**, 30, 818-860

[191] Mazumder, A.; Neamati, N.; Sunder, S.; Schulz, J.; Pertz, H.; Eich, E.; Pommier, Y. Curcumin Analogs with Altered Potencies Against HIV-1 Integrase as Probes for Biochemical Mechanisms of Drug Action. *J. Med. Chem.* **1997**, 40, 3057-3063

groups increases its anti-HIV activity.[177] The structure-activity relations described above are summarized in Figure 17.

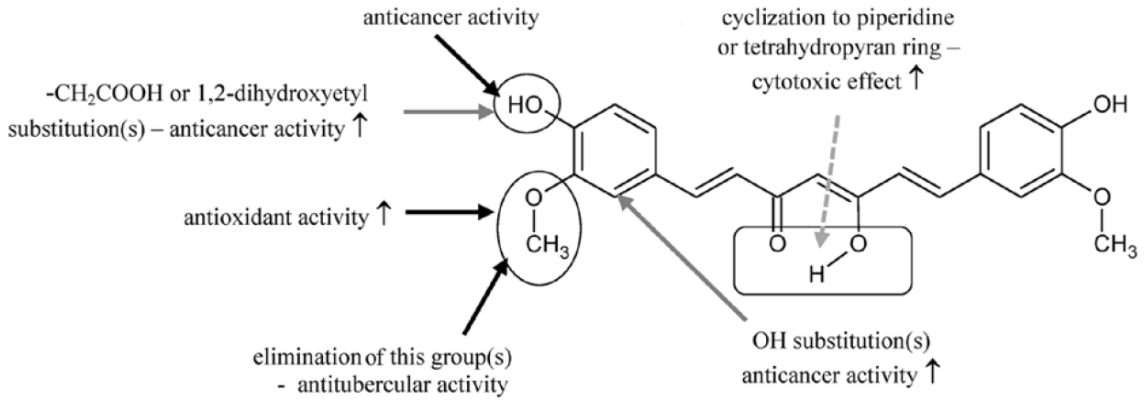

Figure 17. Structure-activity relationships of curcumin analogs.

Alkaline degradation and autoxidation of curcumin

About 90% of curcumin at basic pH and at 37˚C degrades in 30 min giving trans-6-(4-hydroxy-3-methoxyphenyl)-2,4-dioxo-5-hexenal, vanillin, ferulic acid and feruloyl methane (Figure 18, A-D).[183] This phenomenon can explain the biological activity of curcumin, since the degradation products have better aqueous solubility than curcumin as reflected by their respective logP values: 1.42 for ferulic acid and 1.09 for vanillin, lower than the *keto* and *enol* form of curcumin, which are respectively 2.56 and 2.17.[182] Moreover, it has been reported that ferulic acid inhibits COX-1 and COX-2 and suppresses the activation of nuclear factor-κB (NF-κB), important targets in the prevention of cancer development.[182,192,193] Vanillin as well can inhibit COX-2 gene expression and NF-κB activation.[182,194] Curcumin degradation products can also inhibit xanthine oxidase, that is involved in the pathogenesis of many diseases, more than curcumin itself because of its lower

[192] Jayaprakasam, B.; Vanisree, M.; Zhang, Y.; Dewitt, D. L.; Nair, M. G. Impact of Alkyl Esters of Caffeic and Ferulic Acids on Tumor Cell Proliferation, Cyclooxygenase Enzyme, and Lipid Peroxidation. *J. Agric. Food Chem.* **2006**, 54, 5375-5381

[193] Jung, K. J.; Go, E. K.; Kim, J. Y.; Yu, B. P.; Chung, H. Y. Suppression of Age-related Renal Changes in NF-kappaB and its Target Gene Expression by Dietary Ferulate. *J. Nutr. Biochem.* **2009**, 20, 378-388

[194] Murakami, Y.; Hirata, A.; Ito, S.; Shoji, M.; Tanaka, S.; Yasui, T.; Machino, M.; Fujisawa, S. Re-evaluation of Cyclooxygenase-2-inhibiting Activity of Vanillin and Guaiacol in Macrophages Stimulated with Lipopolysaccharide. *Anticancer Res.* **2007**, 27, 801-807

ability to fit in the binding pocket.[182,195,196] The prevailing degradation reaction is not the cleavage of the heptadienedione chain (resulting in vanillin, ferulic acid and feruloylmethane as products)[197] but a spontaneous autoxidation due to free radical-driven incorporation of oxygen.[198]185 Different product profiles of curcumin autoxidation reactions are dependent on time: in reactions between 20-45 minutes spiroepoxide and vinylether are the major products (Figure 18, E-G) and dihydroxy, ketohydroxy and hemiketal cyclopentadiones are minor products. Degradation between 30 min and 4 h also produces the bicyclopentadiones as major products and, several unidentified chemicals.

Naturally occurring polyphenols as curcumin interact with topoisomerase II, increasing the levels of topoisomerase II-mediated DNA cleavage. Topoisomerase poisons are used in anticancer and antibacterial therapies. Curcumin, bicyclopentadione, vanillin, ferulic acid and feruloylmethane have no effect on DNA cleavage of human topoisomerase IIα and IIβ.[199] However, intermediates of the curcumin oxidation pathway increased the level of DNA cleavage by both enzymes ~4-5-fold. Moreover, under conditions that promote oxidation, curcumin enhanced topoisomerase II-mediated DNA cleavage even further.[199] Also a stable spiroepoxide product of curcumin oxidation was able to poison recombinant human topoisomerase IIα; this process was significantly increased in the presence of potassium ferricyanide, indicating that oxidative conversion was needed to achieve full DNA cleavage activity and that curcumin oxidative metabolites may be responsible for its biological effects.[197]

---

[195] Chang, Y. C.; Lee, F. W.; Chen, C. S.; Huang, S. T.; Tsai, S. H.; Huang, S. H.; Lin, C. M. Structure-activity Relationship of C6-C3 Phenyl-propanoids on Xanthine Oxidase-inhibiting and Free Radical-scavenging Activities. *Free Radic. Biol. Med.* **2007**, 43, 1541-1551

[196] Shen, L.; Ji, H. F. Insights into the Inhibition of Xanthine Oxidase by Curcumin. *Bioorg. Med. Chem. Lett.* **2009**, 19, 5990-5993

[197] Gordon, O. N.; Schneider, C. Vanillin and Ferulic Acid: not the Major Degradation Products of Curcumin. *Trends Mol. Med.* **2012**, 18, 361-363, author reply 363-364

[198] Griesser, M.; Pistis, V.; Suzuki, T.; Tejera, N.; Pratt, D. A.; Schneider, C. Autoxidative and Cyclooxygenase-2 catalyzed Transformation of the Dietary Chemopreventive Agent Curcumin. *J. Biol. Chem.* **2011**, 286, 1114-1124

[199] Ketron, A. C.; Gordon, O. N.; Schneider, C.; Osheroff, N. Oxidative Metabolites of Curcumin Poison Human Type II Topoisomerases. *Biochemistry*, **2013**, 52, 221-227

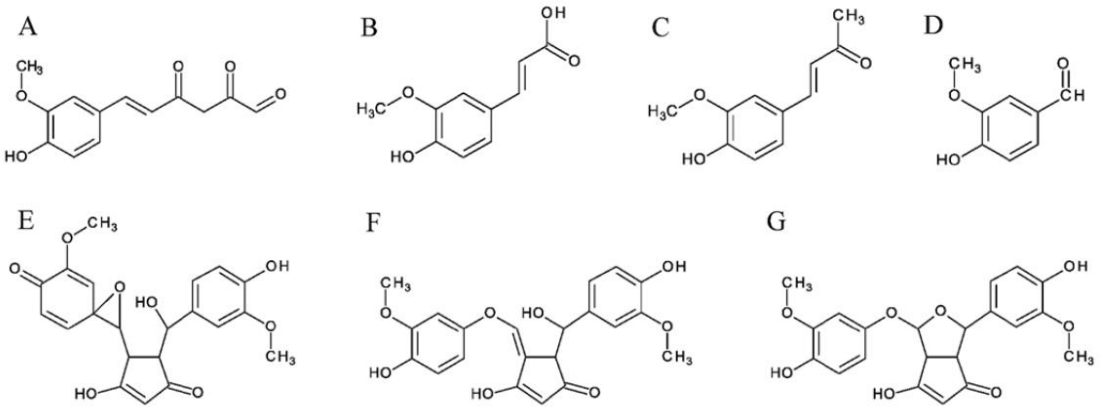

Figure 18. Degradation of curcumin to: (A) trans-6-(4-hydroxy-3-methoxyphenyl)-2,4-dioxo-5-hexenal; (B) ferulic acid; (C) feruloyl methane; (D) vanillin; (E) spiroepoxide; (F) vinylether; (G) bicyclopentadione.

Photodegradation of curcumin

Turmeric stains as curcuminoids can be decomposed by exposure to sunlight because they absorb strongly in the visible wavelength range with consequent degradation and modification. The photodegradation of curcumin takes place in solid state and in different organic solvents, but the composition, degradation kinetics and the relative abundance of the degradation products differ as a function of the physical state and the conditions.[183,184,200,201,202] The photochemical degradation of solid state curcumin exposed to sunlight for 120 h yielded vanillin (34%), ferulic aldehyde (0.5%), ferulic acid (0.5%), vanillic acid (0.5%) and three unidentified compounds. The photodegradation of dissolved curcumin depends on the solvent and wavelength. Exposure to visible light inflicts more degradation than UV light; the irradiation of curcumin in 254-nm in methanol has been shown to produce three unspecified degradation products, whereas irradiation with daylight produces five unspecified degradation chemicals products.[184] Irradiation with light (400-750-nm) for 4 h was shown to be associated with cyclization at one of the o-methoxyphenyl groups, producing 7-hydroxy-1-[(2E)-3-(4-hydroxy-3-

[200] Ansari, M. J.; Ahmad, S.; Kohli, K.; Ali, J.; Khar, R. K. Stability-indicating HPTLC Determination of Curcumin in Bulk Drug and Pharmaceutical Formulations. *J. Pharm. Biomed. Anal.* **2005**, 39, 132-138

[201] Heger, M.; van Golen, R. F.; Broekgaarden, M.; Michel, M. C. The Molecular Basis for the Pharmacokinetics and Pharmacodynamics of Curcumin and its Metabolites in Relation to Cancer. *Pharmacol. Rev.* **2013**, 66, 222-307

[202] Tønnesen, H. H.; de Vries, H.; Karlsen, J.; Beijersbergen van Henegouwen, G. Studies on Curcumin and Curcuminoids. Investigation of the Photobiological Activity of Curcumin Using Bacterial Indicator Systems. *J. Pharm. Sci.* **1987**, 76, 371-373

methoxyphenyl)prop-2-enoyl]-6-methoxy naphthalen-2(1H)-one in isopropanol, methanol and chloroform, but not in acetonitrile and ethyl acetate.[184,202] The photodegradation of curcumin involves the formation of the excited states and generation of singlet oxygen that is responsible for the photobiological and photodynamic activity of curcumin.[189,202] Thus, the degradation of curcumin following photoexcitation must proceed though the triplet excited state of curcumin.[189] Curcumin is photoactivated by blue light (420-480 nm) that has limited tissue penetration. That property makes curcumin an ideal surface antibacterial agent skin disinfection, particularly because it does not affect deeper healthy tissue.[203,204,205]

2.2.2 Aim of the work

Curcumin (> 80%) and its analogs devoid of one or both the methoxy groups (*i.e.* demethoxycurcumin and bisdemethoxycurcumin, respectively) are the three main curcuminoids (CUR) present in the purified extract of *Curcuma longa* that we used in this work (Figure 19). As explained above, curcumin has been extensively investigated for its biological and pharmacological activities. Unfortunately, the low water solubility of curcumin and its derivatives together with their chemical and photochemical instability has hampered their pharmaceutical applications. To circumvent these limitations their inclusion in many drug delivery systems such as liposomes, cyclodextrins, biopolymers, dendrimers, nanogels or their conjugation with metallic nanoparticles was successfully investigated.[206] Most of these systems improved their stability and solubility in aqueous media with a significant increase of their bioavailability and, as a consequence, of their biological effect. Anyway, despite the huge number of investigations on the biological and pharmacological effects of curcumin and its derivatives, studies describing with a systematic

[203] Leite, D. P.; Paolillo, F. R.; Parmesano, T. N.; Fontana, C. R.; Bagnato, V. S. Effects of Photodynamic Therapy with Blue Light and Curcumin as Mouth Rinse for Oral Disinfection: a Randomized Controlled Trial. *Photomed. Laser Surg.* **2014**, 32, 627-632

[204] Mahdi, Z.; Habiboallh, G.; Mahbobeh, N. N.; Mina, Z. J.; Majid, Z.; Nooshin, A. Lethal Effect of Blue Light-activated Hydrogen Peroxide, Curcumin and Erythrosine as Potential Oral Photosensitizers on the Viability of *Porphyromonas Gingivalis* and *Fusobacterium Nucleatum*. *Laser Ther.* **2015**, 24, 103-111

[205] Yin, R.; Hamblin, M. R. Antimicrobial Photosensitizers: Drug Discovery Under the Spotlight. *Curr. Med. Chem.* **2015**, 22, 2159-2185

[206] Ghalandarlaki, N.; Alizadeh, A. M.; Ashkani-Esfahani, S. Nanotechnology-Applied Curcumin for Different Diseases Therapy. *BioMed Res. Int.* **2014**, 394264-394287

approach the relation between the properties of the drug delivery systems and their efficacy are relatively scarce.

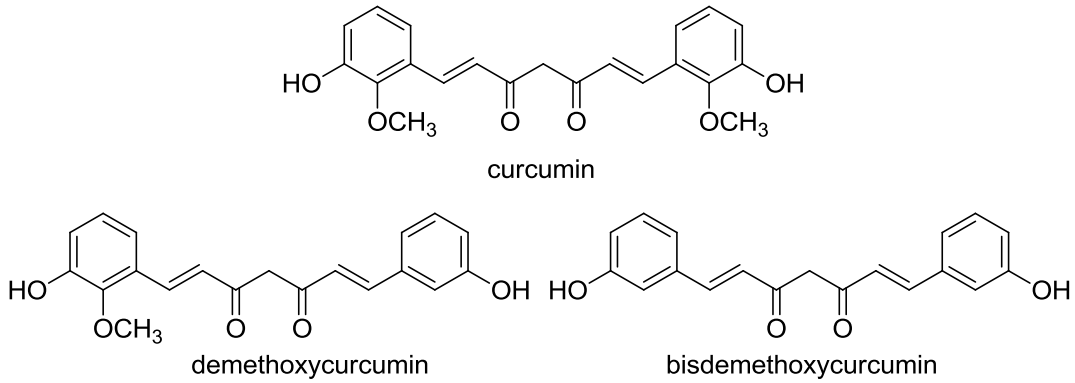

Figure 19. Molecular structures of CUR components

In this chapter an investigation on the inclusion of CUR on liposomes composed of unsaturated (1,2-dioleoyl-*sn*-glycero-3-phosphocholine, DOPC) or saturated phosphocholine (PC) differing for the length of the alkyl chains (1,2-dimyristoyl-*sn*-glycero-3-phosphocholine, DMPC, 1,2-dipalmitoyl-*sn*-glycero-3-phosphocholine, DPPC, or 1,2-dipalmitoyl-*sn*-glycero-3-ethylphosphocholine chloride salt, EPC, Figure 20) in the presence and in the absence of 33% of chol is reported. This study was aimed to deepen our knowledge on the interaction of CUR with lipid bilayers in the attempt to correlate their biological activity to the properties of liposomes as drug delivery systems. The influence of the lipidic composition on the entrapment efficiency of the three CUR and on their stability at physiological and basic pH was evaluated by HPLC measurements. In fact, as explained above CUR in solution can be present in the *keto* and *enol* tautomers, characterized by different stability, solubility and, in some cases, biological activity,[207,208] in a ratio depending on the condition.[209] Literature reports demonstrate that the three free CUR show a different pH-dependence of degradation rate (because of different intramolecular charge

[207] Yanagisawa, D.; Shirai, N.; Amatsubo, T.; Taguchi, H.; Hirao, K.; Urushitani, M.; Morikawa, S.; Inubushi, T.; Kato, M.; Kato, F.; Morino, K.; Kimura, H.; Nakano, I.; Yoshida, C.; Okada, T.; Sano, M.; Wada, Y.; Wada, K.; Yamamoto, A.; Tooyama, I. Relationship Between the Tautomeric Structures of Curcumin Derivatives and Their αβ-binding Activities in the Context of Therapies for Alzheimer's Disease. *Biomaterials*, **2010**, 31, 4179-4185

[208] Gupta, S. C.; Prasad, S.; Kim, J. H.; Patchva, S.; Webb, L. J.; Priyadarsini, I. K.; Aggarwal. B. B. Multitargeting by Curcumin as Revealed by Molecular Interaction Studies. *Nat. Prod. Rep.* 2011, 28(12), 1937-1955

[209] Priyadarsini. I. K. Photophysics, Photochemistry and Photobiology of Curcumin: Studies from Organic Solutions, Bio-mimetics and Living Cells. *J. Photoch. Photobiol. C: Photochem. Rev.* **2009**, 10, 81–95

distribution) in water-methanol mixtures[210] (used to simulate their environmental conditions when embedded in the apolar region of supramolecolar systems) to prevent their alkaline degradation.[211,212]

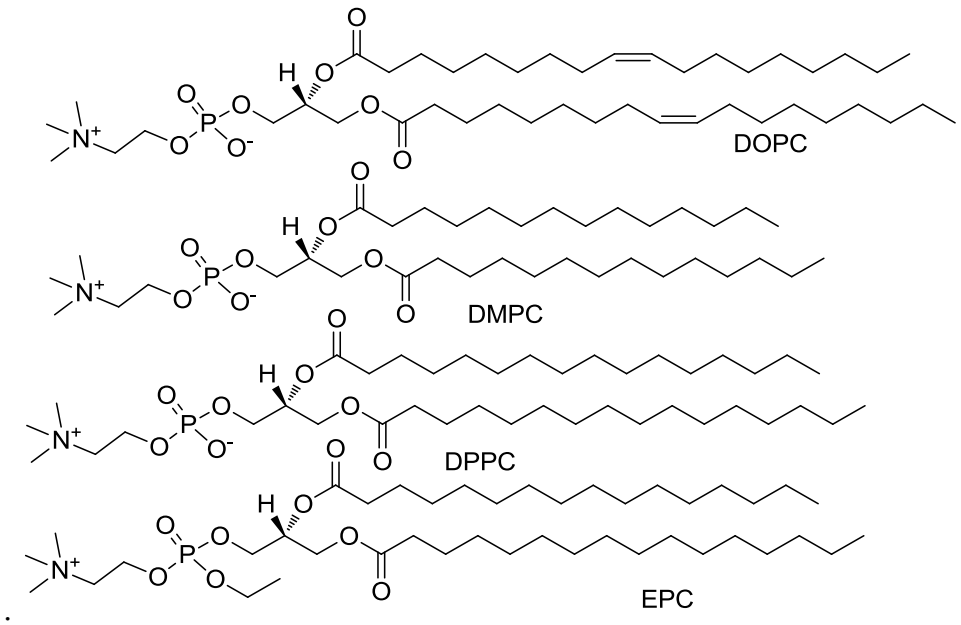

Figure 20. Molecular structures of lipids

After the investigation of size and zeta potential of the formulations, the localization of the CUR in the bilayer was assessed by fluorescence quenching measurements that allow to evaluate the accessibility of CUR, the fluorophore, to the quencher molecule, *i.e.* the proximity of CUR to liposomes surface, and to better understand their interaction with lipid bilayer and the influence of lipid composition. Through DSC measurements, besides CUR location, its influence on the properties of the bilayer was also evaluated. Antimicrobial efficacy measurements of loaded CUR allowed to estimate the influence of the bilayer composition on the properties of the extract and also to analyze if there was a synergistic effect of the components of CUR if compared to only curcumin.

[210] D'Archivio, A. A.; Maggi, M. A. Investigation by Response Surface Methodology of the Combined Effect of pH and Composition of Water-methanol Mixtures on the Stability of Curcuminoids. *Food Chem.* **2017**, 219, 414-418

[211] Leung, M. H. M.; Colangelo, H.; Kee, T. W. Encapsulation of Curcumin in Cationic Micelles Suppresses Alkaline Hydrolysis. *Langmuir,* **2008,** 24, 5672-5675

[212] Chen, X.; Zou, L.; Niu, J.; Liu, W.; Peng S.; Liu, C. The Stability, Sustained Release and Cellular Antioxidant Activity of Curcumin Nanoliposomes. *Molecules,* **2015**, 20, 14293-14311

2.2.3 Experimental section

Materials

All lipids used for liposome preparation were purchased from Avanti Polar Lipids (Alabaster, AL) and used without further purification. Phosphate buffered saline (PBS) tablets (0.01 M phosphate buffer, 0.0027 M KCl, 0.137 M NaCl, pH=7.4 at 25 °C), chol, methyl viologen dichloride hydrate (MV), Mueller Hinton, KI, Na_2SO_3, dialysis tubing cellulose membrane D 9527 and HPLC-grade methanol and acetonitrile were obtained from Sigma Aldrich. Double deionized water was prepared using a Milli-Q filtration/purification system (Millipore, Bedford, MA, USA). Basic buffer at pH=8.6 was prepared using borax and boric acid. CUR was obtained from a provider of food ingredients.

Methicillin sensible *Staphylococcus aureus* reference strain from the American Type Culture Collection (ATCC 29213) was used as control organism.

Liposomes preparation

Lipid films were prepared on the inside wall of a round-bottom flask by evaporation of solutions containing the proper amount of PC (dissolved in $CHCl_3$) and CUR at 100:1 molar ratio in the presence or in the absence of 33 molar percentage of chol (dissolved in $CHCl_3$). The obtained films were stored overnight under reduced pressure (0.4 mbar), then PBS was added to obtain a 1 mM lipid dispersion. In the case of zeta potential measurements PBS buffer 15 mM was used to reduce the Joule-heating effect. The solutions were heated at 50 °C and vortex-mixed, then the suspensions were sonicated for 4 minutes at 72W (cycles 0.5s) under cooling condition of an ice-water bath, using a Hielscher UP100-H ultrasonic processor with microtip probe (7 mm). To remove unentrapped CUR dialysis exchanging 4 times the external medium PBS solution (25 fold the liposome dispersion volume) in two hours was carried out.

DLS and zeta potential measurements

DLS and zeta potential of the different formulations were evaluated as described above (see Chapter 2 section 1.3).

Evaluation of E.E. and degradation of CUR

The amount of CUR in solution before and after dialysis was measured on solutions composed of 100 µL of liposomes suspension and 500 µL of CH_3OH by HPLC measurements using a chromatographic system that consists of two Model 510 pumps (Waters, Milford, MA, USA), a Pump Control Module II (Waters), a Model 7725i sample injector (Rheodyne, Cotati, CA, USA) equipped with a 20 µL loop and a Model 996 (Waters) diode array detector as previously described. The E.E. for each formulation was evaluated by the ratio between the area of the peak corresponding to each CUR before and after dialysis. The stability of the CUR was evaluated by comparing the area of the peak corresponding to each CUR soon after the dialysis and after 3 hours of incubation at room temperature in PBS buffer and in borax/boric acid buffer at pH 8.6. The E.E. of each formulation was also evaluated by recording fluorescence (λ_{exc} = 425 nm, λ_{em} = 485 nm) spectra on a Perkin Elmer LS 50 spectrofluorimeter spectra before and after dialysis to remove free CUR.

Fluorescence quenching measurements

The localization of CUR in the bilayer was carried out by fluorescent quenching experiments on CUR entrapped in the investigated formulations after dialysis on a Perkin Elmer LS 50 spectrofluorimeter. All fluorescence experiments were carried out at room temperature on solutions with absorbance lower than 0.1 to minimize inner filter effects. Small aliquots of 2 M sodium iodide and 0.1 mM Na_2SO_3 solution or of 1 M MV solution were added to the liposome formulations, previously dialyzed to eliminate the free CUR as described above and diluted to obtain [CUR] 0.75 μM.

The collected data were graphed following the modified Stern-Volmer equation $I_0/(I_0\text{-}I)=1/(f\cdot K\cdot[\text{quencher}])+1/f$ and the parameters K and f were obtained from the linear fitting of the curve.

Evaluation of the antimicrobial activity of liposomal CUR

The antimicrobial activity of CUR included in the different formulations on a Methicillin sensible *Staphylococcus aureus* strain was evaluated as described above (see Chapter 2 section 1.3).

Determination of thermotropic properties of liposomes

Differential scanning calorimetry (DSC) measurements were carried out on 30 µL of MLV. Liposomes (1 mg/10 µL, ≈ 148 mM in total lipids) were prepared in PBS in the presence and in the absence of CUR. Two heating scans were recorded at the rate of 5 °C/min and two subsequent heating scans were recorded at the rate 1 °C/min. Under the experimental conditions, reproducible thermal recordings were obtained. Uncertainty on temperatures is 0.1 °C.

2.2.4 Results and discussion

DLS and zeta potential measurements

The formulations in the presence and in the absence of CUR showed a mean diameter of 100 nm (Table 9). The PDI of the formulations was mainly low except for DPPC liposomes; in this case a second big population around 1 µm, that disappears increasing the time of sonication, was present. As expected the zeta potential was mainly neutral for all the formulations with the exception of liposomes containing EPC, a cationic lipid.

Table 9. Dimensions and potential of investigated liposomal formulations in the absence of CUR. Similar results were obtained in the presence of CUR

Formulation	Hydrodynamic radius (nm) (PDI)	Zeta Potential (mV)
DPPC	110 ± 4, ≈ 1 μm	- 8±3
DPPC/chol 6.7/3.3	170 ± 6, ≈ 900	-11±4
DPPC/EPC 6.7/3.3	133 (0.44)	53±2
DPPC/EPC/chol 6.7/3.3/3.3	117 (0.17)	48±3
DMPC	111 (0.28)	0±2
DMPC/chol 6.7/3.3	162 (0.38)	-6±4
DOPC	122 (0.26)	-5±3
DOPC/chol 6.7/3.3	114 (0.18)	-6±1

Evaluation of E.E. and degradation of CUR

The E.E observed was quite high in all cases and decreases adding chol to the formulations (Table 10). This evidence can be due to the high rigidity and packing that chol confers to the bilayer thus partially hampering the inclusion of CUR. After 4 days about the 10% of entrapped CUR is leaked upon storage. The stability of liposomal CUR was also evaluated: after 3h at pH 7.4 (PBS buffer) no differences were observed whereas at pH 8.6 (borax/boric acid buffer) CUR partially degraded CUR (between 10 and 30%). This result demonstrates that the loading of CUR in liposomes protects the active principle to the degradation besides to increasing its

solubility in water; in fact is reported in literature that CUR normally degrades at neutral pH and more at basic pH.[210,213,214]

Table 10. Entrapment efficiency and residual % of CUR at pH 8.6 after 3h.

Formulation	% E.E. fluorescence	% E.E. HPLC	CUR residual % (pH=8.6 after 3h)
DPPC	87±3	77±5	90±3
DPPC/chol 6.7/3.3	58±2	48±4	71±2
DPPC/EPC 6.7/3.3	78±5	67±5	22±5
DPPC/EPC/chol 3.3/3.3/3.3	48±4	36±2	85±4
DMPC	82±3	75±3	95±3
DMPC/chol 6.7/3.3	62±2	50±6	70±2
DOPC	78±6	75±2	67±6
DOPC/chol 6.7/3.3	72±3	57±5	72±3

The prevention of CUR alkaline degradation when included in lipid bilayer can be attributed to the stabilization of the *bis-keto* tautomer, a limitation of the accessibility of the *keto-enol* moiety to water or OH^- ions or pKa changes promoted by the host environment.[210] The only exception was observed in the presence of EPC: in this

[213] Price, L.C.; Buescher, R.W. Kinetics of Alkaline Degradation of the Food Pigments Curcumin and Curcuminoids. *J. Food Sci.* **1997**, 62, 267-269

[214] D'Archivio, A. A.; Maggi, M. A.; Ruggieri, F. Extraction of Curcuminoids by Using Ethyl Lactate and its Optimisation by Response Surface Methodology. *J. Pharm. Biomed. Anal.* **2018**, 149, 89–95

case at pH 8.6 only the 22% of CUR remains after 3h, probably because in this formulation a less organized packing of the bilayer occurs; this characteristic allows CUR to interact more easily with the bulk solution.

Fluorescence quenching measurements

Fluorescence quenching measurements are reported in Table 11.

Table 11. Fraction *f* of CUR accessible to I^- or MV (used as quenchers) and quenching constant, *K*, obtained by fluorescence quenching experiments of CUR containing liposomal formulations. Reported values correspond to the average values over at least three independent measurements and the errors correspond to the standard deviation among the different measurements (errors in *f* determination are not reported because are < 5%).

Formulation	*f* (I^-)	*K* [M^{-1}] (I^-)	*f* (MV)	*K* [M^{-1}] (MV)
DPPC	0.05	1005±30	0.08	301±28
DPPC/chol	0.22	917±35	0.27	183±43
DPPC/EPC	0.04	4400±115	0.88	10±43
DPPC/EPC/chol	0.22	3757±130	-	-
DMPC	0.07	1205±30	0.22	53±33
DMPC/chol	0.15	920±30	0.42	93±23
DOPC	0.12	242±40	0.20	202±26
DOPC/chol	0.22	310±30	0.65	93±35

To better investigate the location of CUR we used two different collisional quenchers: I^-, that is anionic, spherical and more specific for the lipid bilayer with

respect to MV, that is planar, aromatic and bears two positive charges. Fraction *f* of CUR accessible to the quencher was generally very low for all the formulations, thus CUR can be approached by the quencher at very short distances. This result indicates that CUR is mainly located in the apolar region of the bilayer. In the presence of chol we observed an increase of *f* in all cases that could be caused by the higher rigidity of the membrane with respect to the corresponding formulations devoid of chol. In fact, it is reasonable to hypothesize that a high compaction and a low fluidity of the bilayer can limit the penetration of CUR in the hydrophobic region of the bilayer. In the case of DPPC/EPC liposomes and MV, an anomalous high value of *f* was observed, result that induces to hypothesize a CUR location near the polar headgroups. In the presence of chol *f* could not be obtained because soon after the first addition of MV to liposomes solution the emission peak was shifted to higher values and its intensity increased (Figure 20 bis A). On the other hand, upon the addition of KI to the same sample the expected variation in the emission spectra occurs (Figure 20 bis B) and a low *f* value was obtained, thus indicating that the behavior observed with MV is strictly related to the quencher used. The same trend was observed in all cases using MV, but only after several additions of quencher. As a consequence, the data relative to the measurements in which the concentration of MV was too high were discarded before applying the Stern-Volmer equation. In Figure 20 bis C the fluorescence spectra obtained upon the addition of MV to DPPC/chol liposomes are reported as an example. This evidence indicates that when MV interacts with lipid bilayer it, especially at high concentration, induces a lipid rearrangement that causes a relocation of CUR in a different region of the bilayer with consequent variation of its emission. Obviously this effect is more evident with cationic liposomes than with neutral formulations because of the electrostatic repulsion with the positively charged quencher. It is possible that the same phenomenon, to a lower extent, could have affected the measurements also in the case of the other formulations, especially those containing chol, even if inducing variations not appreciable at naked eye. As a consequence, after the elaboration this phenomenon could bring to a *f* value higher than the real one. This effect seems to be directly dependent on the fluidity of the bilayer of the formulation (low for

DPPC liposomes, intermediate for DMPC liposomes and high for DOPC ones, Table 11). This is not surprising because in the case of a less rigid bilayer the perturbation due to the presence of MV is more effective.

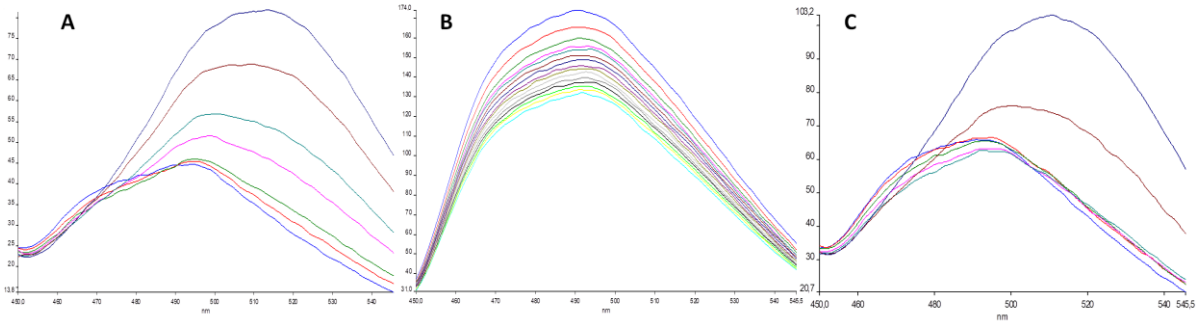

Figure 20 bis. Fluorescence emission spectra obtained upon the addition of (A) MV to DPPC/EPC/chol liposomes, (B) KI to DPPC/EPC/chol liposomes and (C) MV to DPPC/chol liposomes.

Quenching constants *K* were mainly high in all cases with I^-, whereas in the case of MV the values obtained were sensibly lower indicating a less favorable interaction/contact between CUR and the quencher molecule. The highest *K* were observed in the experiments relative to EPC containing liposomes and I^- and were due to positive electrostatic interactions between the cationic liposomes and the anionic quencher and probably also due to the low lipid packing of the bilayer (that make CUR located near the headgroup more accessible) favoring its contact with CUR.

Thermotropic properties of liposomes

Thermodinamic parameters and thermograms of the investigated liposomal formulations are reported respectively in Table 12 and in Figure 21.

Table 12. Thermodynamic parameters of liposomal formulations (MLV) with and without CUR obtained by DSC measurements.

Formulation	pretransition		main transition		
	T (°C)	ΔH_m(kJ/mol)	T(°C)	ΔH_m(kJ/mol)	CU
DMPC	15.1	3.17	24.2	19.1	96
DMPC+CUR	-	-	24.0	21.7	84
DOPC	-	-	-20.7	36.6	-
DOPC+CUR	-	-	-20.0	38.9	-
DPPC	34.8	2.2	41.7	32.1	160
DPPC+CUR	-	-	41.4	31.8	134
DPPC/EPC	-	-	38.9	26.6	157
DPPC/EPC +CUR	-	-	39.2	30.0	122

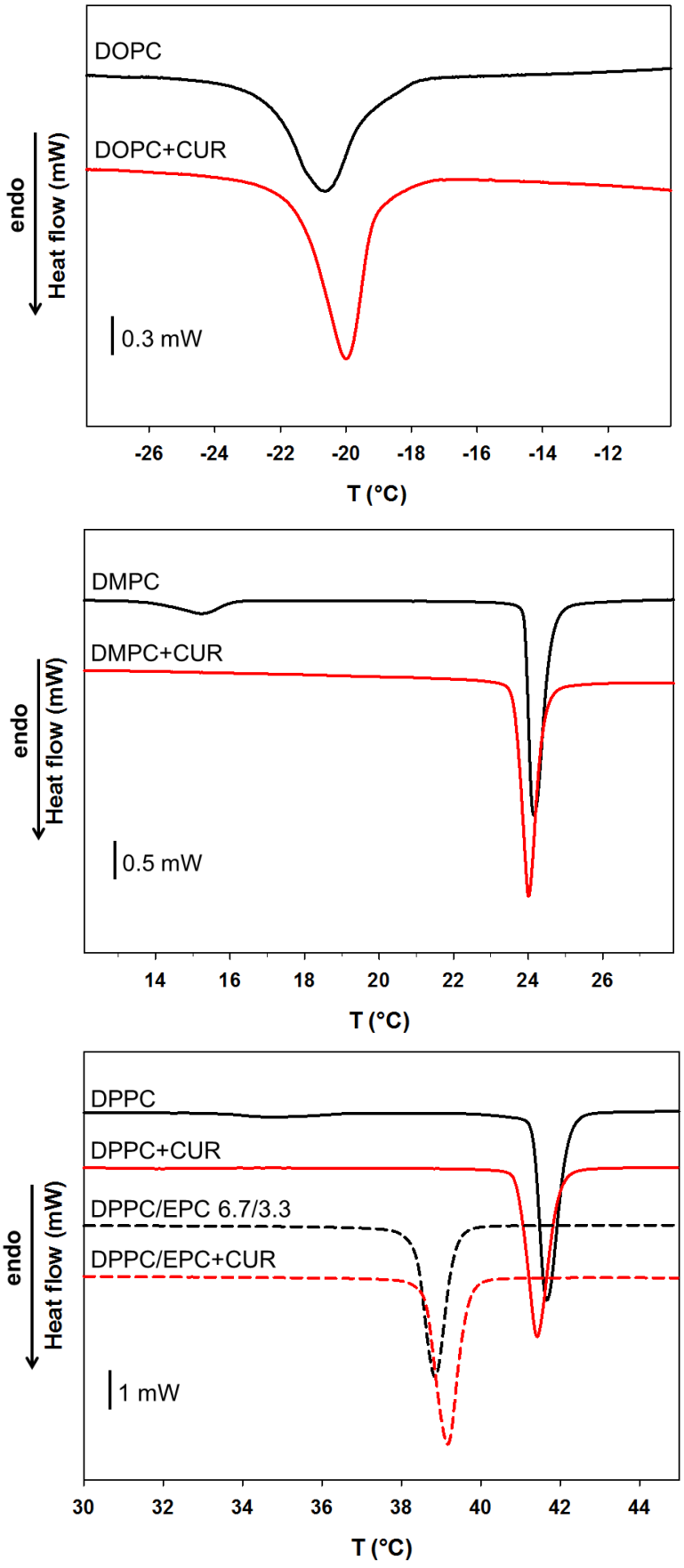

Figure 21. Thermograms of MLVs with and without CUR. Scan rate is 1° C/min.

No big differences, neither changing the composition of the bilayer nor adding CUR, were observed in Tm values: probably CUR components, that are molecules with a flexible structure, can intercalate themselves in the bilayer without disturbing the lipid packing. Considering also the results obtained by quenching experiment, it is reasonable to hypothesize that CUR probably is located near the glycerol scaffold, analogously to chol that is positioned at the lipid–water interface with its steroidal skeleton buried deep in the hydrocarbon region.[215] It's interesting to observe that also in the absence of CUR, the presence of the 33% of EPC lowered the main transition temperature and caused the disappearance of the pretransition. The positive charge of this lipid disturbs the organization of the headgroups region. The addition of CUR caused a disappearance of the pretransition where present. As expected, in all cases the CU relative to the main transition in the presence of CUR decreased; this result can be explained considering that CUR, as suggested by quenching experiments, is mainly located in the apolar region of the bilayer, thus can disturb the cooperativity of the process. Surprisingly, on the other hand the ΔH associated to the transition diminishes in all cases when CUR is included in the bilayer with the exception of DPPC liposomes. Evidently, due to its apolar nature, CUR establishes favorable van der Waals interactions with lipid chains that thus lead to an increase of the enthalpy variation.

Evaluation of the antimicrobial activity of liposomal CUR

Liposomal CUR shows a MIC equal to 7 µg/mL in the range 3.5-14 µg/mL on MSSA only if included in liposomes containing EPC with no significant differences due to the presence or the absence of chol. The same formulations induce a reduction of bacterial growth of about 30% already at a CUR concentration equal to 0.88 µg/mL. On the other hand, all liposomes devoid of CUR (including the cationic ones) did not show any antibacterial activity, like free CUR, at all the concentrations tested. These results put in evidence the synergistic effect of CUR and of cationic liposomes, the only ones able to make CUR effective against bacteria at concentration at which it is ineffective if administered as free drug. Also the low

[215] Marquardt, D.; Kučerka, N.; Wassall, S. R.; Harroun, T. A.; Katsaras, J. Cholesterol's Location in Lipid Bilayers. *Chem. Phys. Lipids*, **2016**, 199, 17-25

lipid packing in the headgroup region of these formulations, as suggested by DSC measurements, together with their positive charge (that favors the interaction with bacterial membrane) plays a role in their efficacy as CUR delivery system.

2.2.5 Conclusions

All the investigated liposomal formulations are able to load and protect CUR from degradation besides increasing its solubility in water. The findings of this study confirm the influence of the structure of liposomes components on the physicochemical features of the aggregates they form and on the location and of a solute included in their bilayer. The differences obtained using I- or MV as quenchers underline that for each system and each physicochemical characterization the choice of the right probe and/or protocol is fundamental in determining the reliability of the obtained data. Our results point out that the rigidity of the bilayer and the charge of the aggregates play a pivotal role in determining liposomes properties and their ability to interact with the biological milieu. The synergistic effect of cationic charge of liposomes and CUR lowers its MIC with respect to the one of free CUR thus enlarging the potential of this natural molecule that displays several pharmacological properties. Moreover, our work put in evidence that the choice of the proper lipid components is fundamental for exalting the pharmacological property of the liposomal drug and for the success of the delivery system.

Chapter 3

Influence of *N*-Oxide moiety on aggregates properties

3.1 Introduction

3.1.1 N-Oxide surfactants

The term *N*-Oxide amine describes all the compounds that bear a *N*-oxide moiety and in which the N atom in the N-O bond is hybridized sp^2 or sp^3. This category can be divided in tertiary *N*-oxide amines, heteroaromatic amines and *N*-oxide enamines (Figure 22).

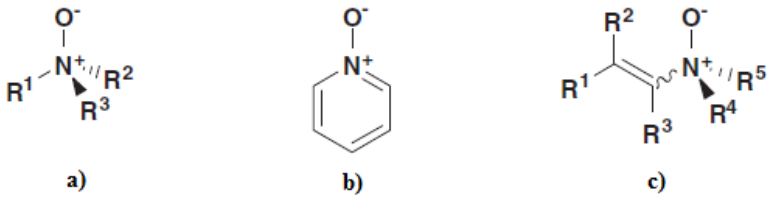

Figure 22. a) General structure of a tertiary *N*-oxide amine, b) pyridine *N*-oxide, a heteroaromatic example, c) general structure of a *N*-oxide enamine.

N-oxide tertiary amines have a chiral center because the presence of the substituents hampers the nitrogen pyramidal inversion and the N-O bond is a dative and not a covalent bond. Moreover, this bond shows one of the highest dipole moments among all organic functional groups;[216] its consequent high polarity confers to the molecule peculiar physicochemical properties:

- ✓ Brönsted basicity,
- ✓ H bond acceptors feature,
- ✓ high hygroscopicity,
- ✓ good water solubility,

[216] Łukomska, M.; Rybarczyk-Pirek, A. J.; Jabłonski, M.; Palusiak, M. The Nature of NO-bonding in *N*-oxide Group. *Phys. Chem. Chem. Phys.*, **2015**, 17, 16375-16387

✓ Lewis basicity and tendency to complex metals.

Moreover *N*-oxide amines are less basic than the corresponding conventional ones. In the presence of acid they form hydroxylammonium salts (pK_a about 4-5)[217] that can be isolated when the starting materials are not stable. *N*-oxide amines can be stabilized thanks to the formation of intermolecular H bonds with the solvent (water,[218] ethanol)[219] and/or intramolecular ones in the presence of functional groups bearing H bond donator moieties (for example OH group in carboxylic acids or alcohols).[220] On the consequence, *N*-oxide amines show a good solubility in water (high polarity of the *N*-oxide bond and formation of H bonds), so are largely used in industrial applications. This feature can also be exploited to control the stereochemistry in the synthesis of proline *N*-oxide derivatives.[220]

In general *N*-oxide based surfactants (N-oxs) show very interesting properties and are involved in a wide variety of industrial applications such as cleaning products (washing-up and laundry detergents), foaming and wetting agents, fabric softeners and thickeners in hair and body care products.[221,222,223] In fact, they are non-ionic (at physiological pH) amphiphilic molecules, environmentally friendly (often they are classified as soft surfactants) and very easy to prepare. Thanks to a number of peculiarities, such as pH-sensitivity, higher emulsifying ability and biodegradability, low irritant action and toxicity, gelating properties,[224] N-oxs are regarded as very interesting molecules that could find application in a range of areas. In research field, *N*-oxide *N,N*-dimetilalkylamines bearing long chains are used as not denaturant zwitterionic surfactants to solubilize proteins or to study the

[217] Bell R. P.; Higginson, W. C. E. The catalyzed Dehydration of Acetaldehyde Hydrate, and the Effect of Structure on the Velocity of Protolytic Reactions. *Pro. Royal Soc.* **1949**, 197, 141-147

[218] Ciganek, E. Reverse Cope eliminations. Pyrrolidine and Piperidine *N*-oxides by Intramolecular Addition of *N,N*-disubstituted Hydroxylamines to Unactivated Double Bonds. *J. Org. Chem.* **1990,** 55, 3007-3009

[219] Bredenkamp, M. W.; Wiechers, A.; Rooyen, P. H. A New Pyrrolizidine Alkaloid *N*-oxide and the Revised Structure of Sceleratine. *Tetrahedron Lett.* **1985**, 26, 5721-5724

[220] O'Neil, I. A.; Miller, N. D.; Peake, J.; Barkley, J. V.; Low, C. M. R.; Kalindjian, S. B. Simple Azetidine *N*-oxides: Synthesis, Structure and Reactivity. *Synlett*, **1993,** 515,1487-1488

[221] Sauer, J.D.; Amine Oxides. Cationic Surfactants in Organic Chemistry. *Surfactant Science Series*, **1990**, 34, 275–295

[222] Vaikunth, S. P. Synthesis of tertiary amine oxides. *US Patent*, **1999**, n. 5, 866,718

[223] Gunstone, F. D.; Padley, F. B. Technology and Applications. *Lipid Technologies and Applications*; **2018**, 265-304

[224] Wang, R.; Li, Y.; Wetting Ability in Aqueous Mixtures of Amine Oxide with Anionic and Nonionic Surfactants. *Tens. Surfact. Deterg.* **2014**, 51(3), 224-228

conformation and the molecular interactions.[225] They can be used as components of bioactive substrate carriers and show antioxidant activity useful for the prevention of cells oxidative damages. These compounds can mime the activity of superoxide dismutase reducing the amount of superoxide anions and carbon radicals.[226] Moreover, it was described that the antioxidant effectiveness of *L*-ascorbic acid (AA), well known for its reducing properties, increases in a dose-dependent manner in the presence of N-ox micelles.[227] Several reports describe the effect of changes in the molecular structure of mono- and di-,[228,229] twin tailed and gemini[230] N-ox on their self-aggregation behavior, their catalytic activity[231,232] and their influence on entrapped solutes.[233] The relation between their molecular structure and the antioxidant activity of these molecules seems to depend mainly on their chain length, their charge and the dimensions of their headgroup and the presence of substituents.

3.2 Aim of the work

As previously explained, the chain length and the presence of a quaternary ammonium moiety, in particular a pyrrolidinium ring, or an *N*-oxide moiety can

---

[225] Lair, V.; Bouguerra, S.; Turmine, M.; Letellier, P. Thermodynamic Study of the Protonation of Dimethyldodecylamine *N*-oxide Micelles in Aqueous Solution at 298 K. Establishment of a Theoretical Relationship Linking Critical Micelle Concentrations and pH. *Langmuir,* **2004,** 20, 8490-8495

[226] Krasowska, A.; Piasecki, A.; Murzyn, A.; Sigler, K. Assaying the Antioxidant and Radical Scavenging Properties of Aliphatic Mono- and Di-*N*-oxides in Superoxide Dismutase-deficient Yeast and in a Chemiluminescence Test. *Folia Microbiol.* **2007,** 52(1) 45-51

[227] Niedziółka, K.; Szymula, M.; Lewin´ska, A.; Wilk, K. A.; Narkiewicz-Michałek, J. Studies of Vitamin C Antioxidative Activity in the *N*-oxide Surfactant Solutions. *Coll. Surf. A: Physicochem. Eng. Asp.* **2012**, 413, 33– 37

[228] Lewińska, A.; Witwicki, M.; Bazylińska, U.; Jezierski, A. Wilk, K. A. Aggregation Behavior of Dicephalic Di-N-Oxide Surfactants in Aqueous Solution: Experimental And Computational Approaches. *Coll. Surf. A Physicochem. Eng. Asp.* **2014**, 442, 34-41

[229] Piasecki, A.; Wójcik, B.; Łuczyński, J.; Piłakowska-Pietras, D.; Witek, S.; Krasowska, A. Bifunctional *N*-Oxides of Alkyldiamidoamines. *J. Surfact. Deterg.* **2009**, 12, 201-207

[230] Bordi, F.; Cerichelli, G.; de Berardinis, N.; Diociaiuti, M.; Giansanti, L.; Mancini, G.; Sennato, S. Synthesis And Physicochemical Characterization of New Twin-Tailed N-Oxide Based Gemini Surfactants. *Langmuir*, **2010**, 26(9), 6177-6173

[231] Katritzky, A. R.; Duell, B. L.; Rasala, D.; Knier, B.; Dupont Durst, H. Synthesis and Catalytic Activity of *N*-Oxide Surfactant Analogues of 4-(Dimethylamino) pyridine. *Langmuir*, **1988**, 4, 1118-1122

[232] Karlovská, J.; Uhríková, D.; Kučerka, N.; Teixeira, J.; Devínsky, F.; Lacko, I.; Balgavý, P. Influence of *N*-dodecyl-*N*,*N*-dimethylamine *N*-Oxide on the Activity Of Sarcoplasmic Reticulum Ca^{2+}-Transporting ATPase Reconstituted Into Diacylphosphatidylcholine Vesicles: Effects of Bilayer Physical Parameters. *Biophys. Chem.* **2006**, 119, 69-77

[233] Piasecki, A.; Piłakowska-Pietras D.; Baran, A.; Krasowska, A. Synthesis and Properties of Surface Chemically Pure Alkylamidoamine-*N*-oxides at the Air/Water Interface. *J. Surfact. Deterg.* **2008**, 11, 187–194

influence the properties of the aggregates they form. As a consequence, also the antioxidant properties of many solutes included or interacting with these aggregates can change. Based on these premises, the aggregation properties of synthetic cationic surfactants derived from *L*-prolinol differing for the length of the alkyl chain (CS **12**, CS **14** and CS **16**) and of their corresponding N-ox (N-ox **12**, N-ox **14** and N-ox **16**, Figure 23) were investigated.

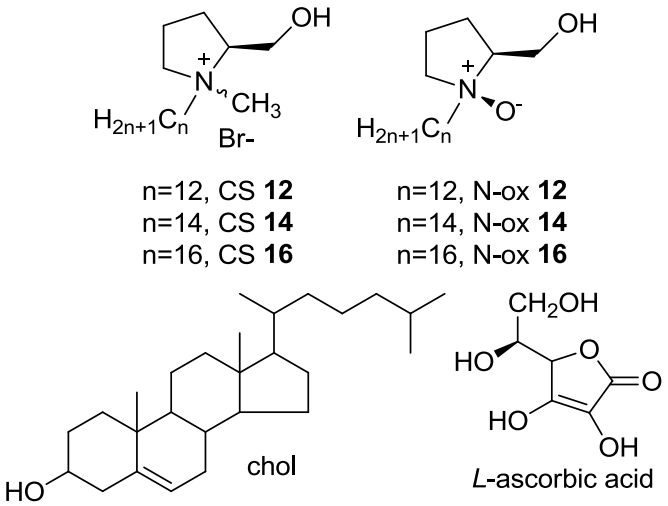

Figure 23. Some of micelle/liposomes/quatsomes components and *L*-ascorbic acid.

In particular, the physicochemical properties of the aggregates that these compounds form alone or formulated as liposomes in mixture with a saturated natural phospholipid, 1,2-dimyristoyl-*sn*-glycero-3-phosphocholine (DMPC), and cholesterol (chol) were studied exploiting two different preparation methodologies, a conventional one, thin film hydration (TFH) and a more recent one, the DELOS-Susp procedure (see Chapter 1, section 3.3) based on the use of compressed CO_2. The methodology used to prepare liposomes can significantly affect their properties, in particular their ability to include solutes, their size and stability:[234,235,236] in general it's preferable to obtain unilamellar liposomes featuring a diameter of about 100-200 nm. Moreover, quatsomes were prepared by DELOS-Susp methodology.

[234] Szoka, F.; Papahadjopoulos. D. Comparative Properties and Methods of Preparation of Lipid Vesicles (Liposomes). *Ann. Rev. Biophys. Bioeng.* **1980**, 9, 467-508

[235] Huang, Z.; Li, X.; Zhang, T.; Song, Y.; She, Z.; Li, J.; Deng, Y. Progress Involving New Techniques for Liposome Preparation. *Asian Journal of Pharmaceutical Sciences,* **2014**, 9(4), 176-182

[236] Allen, T. M.; Cullis, P. R. Liposomal Drug Delivery Systems: from Concept to Clinical Applications. *Adv. Drug Deliv. Rev.* **2013**, 65(1), 36-48

These aggregates are organized in bilayers only containing chol and one of the investigated synthetic surfactants as building blocks and were studied in order to compare their behaviour with liposomes one. (+)-Usnic acid (UA) entrapment efficiency (E.E.) and the effect of its inclusion in the aggregates on its antioxidant activity, an important property often related to the pharmacological activity of many active principle, was also evaluated. The different chemical structure of the monomer could be crucial because it is known that the antioxidant effectiveness is strictly dependent on the microenvironment surrounding the molecule.[237,238] In the case of micelles also the antioxidant capacity of *L*-ascorbic acid (AA, Figure 22) and the influence of the presence of H_2O_2 to catalyse the oxidation were investigated.

3.3 Experimental section

3.3.1 Instrumentation

UV measurements: Cary 50 UV−vis double beam spectrophotometer (Varian) and Cary 5000 UV-Vis-NIR Spectrophotometer (Varian). ^1H and ^{13}C spectra: Bruker 400; δ in ppm relative to the residual solvent peak of $CDCl_3$ at 7.26 and 77.0 ppm for ^1H and ^{13}C, respectively. Conductivity and pH measurements: Amel Model 334-B.

Liposomes by TFH were prepared using a Hielscher UP100-H ultrasonic processor with microtip probe (7 mm). Liposomes by DELOS-Susp were prepared using a DELOS-Susp equipment. For diafiltration we employed a KrosFlo Research IIi TFF System (Spectrum Labs, USA) equipped with mPES Micro Kros filter column (100 kDa MWCO). Dynamic light scattering (DLS) and electrophoretic mobility measurements were performed to infer hydrodynamic diameters and Zeta potential of liposomes by using a Malvern Zetasizer Nano ZS, equipped with a 5 mW He-Ne laser operating at 633 nm.

Cryogenic transmission electronic microscopy images (Cryo-TEM) were acquired with a JEOL TEM microscope (JEOL, Tokyo, Japan) operating at 120kV. Images

[237] Dracha, M.; Narkiewicz-Michałek, J.; Sienkiewicz, A.; Szymula, M.; Bravo-Díaz, C. Antioxidative Properties of Vitamins C and E in Micellar Systems and in Microemulsions. *Colloids Surf. A Physicochem. Eng. Asp.* **2011**, 379, 79-85

[238] Bae, H.; Jayaprakasha, G. K.; Crosby, K.; Jifon, J. L.; Patil, B. S. Influence of Extraction Solvents on Antioxidant Activity and the Content of Bioactive Compounds in Non-pungent Peppers. *Plant. Foods Hum. Nutr.* **2012**, 67(2), 120-128

were recorded on a Gatan 724 CCD camera under low-dose conditions using Digital Micrograph 3.9.2 (Gatan Inc.). The water used was pretreated with the Milli-Q Advantage A10 water purification system (Millipore Ibérica, Madrid, Spain).

3.3.2 Materials

All reagents employed for the synthesis of CS **12**, CS **14**, CS **16** and N-ox **12**, N-ox **14**, N-ox **16** were purchased from Sigma-Aldrich. CS **16** was prepared as previously described (Figure 24).[154] Yields were not optimized. TLC: silica gel 60, F254. All reagents used for the synthesis and solvents were used without further purification.
DMPC, chol, UA, phosphate-buffered saline tablets (PBS, 0.01 M phosphate buffer; 0.0027 M KCl; 0.137 M NaCl; pH 7.4), dialysis tubing cellulose membrane (cut-off = 14,000), CH_3COONa, H_2O_2 and 2,2'-azino-bis(3-ethylbenzothiazoline-6-sulfonic acid) diammonium salt (ABTS) were purchased from Sigma-Aldrich.
Milli-Q water (Millipore Ibérica, Madrid, Spain), ethanol (Teknocroma Sant Cugat del Vallès, Spain) and DMSO (Sigma Aldrich) in high purity were used for all the liposomal preparations by DELOS-Susp. Carbon dioxide (99.9% purity) was purchased from Carburos Metálicos S.A. (Barcelona, Spain).

3.3.3 Methods

*General procedure for the synthesis of compounds **8-10***

The appropriate alkyl bromide **5-7** (10 mmol) and *L*-prolinol (5 mmol) was dissolved in 10 mL of acetone. The solution was kept under stirring at 60 °C with reflux condenser overnight. Upon cooling, a white solid precipitated, and was subsequently washed with acetone (10 mL) and diethyl ether (20 mL). The recovered material was dissolved in EtOH and Na_2CO_3 was added until the disappearance of bubbling due to CO_2 formation. The excess of Na_2CO_3 was filtered off, the solvent was removed under reduced pressure and the product was crystallized from acetone. Compound **8**. White solid. Yield: 57%. ^{1}H-NMR ($CDCl_3$): δ= 3.84 (dd, 1H, C<u>H$_2$</u>OH); 3.49 (dd, 1H, C<u>H$_2$</u>OH); 2.88-2.53 (m, 6H, C<u>H$_2$</u>N); 1.73-1.42 (m, 6H, C<u>H$_2$</u>CH$_2$N); 1.37-1.31 (m, 18H); 0.99 (t, 3H, CH_3) 0.67 (s, 1H, OH). ^{13}C-NMR ($CDCl_3$): δ= 64.57; 61.83; 54.95; 53.23; 31.65; 29.06; 28.96; 28.90; 27.90; 27.55; 24.15; 22.94; 14.02. Compound **9**. White solid. Yield: 58%. ^{1}H-NMR ($CDCl_3$): δ= 3.84 (dd,

1H, C$\underline{H_2}$OH); 3.49 (dd, 1H, C$\underline{H_2}$OH); 2.88-2.53 (m, 6H, C$\underline{H_2}$N); 1.73-1.42 (m, 6H, C$\underline{H_2}$CH$_2$N); 1.37-1.31 (m, 20H); 0.99 (t, 3H, CH$_3$); 0.67 (s, 1H, OH). ^{13}C-NMR ($CDCl_3$): δ= 64.57; 61.83; 54.95; 53.23; 31.65; 29.06; 28.96; 28.90; 27.90; 27.55; 24.15; 22.94; 14.02. Compound **10**. White solid. Yield: 56%. ^{1}H-NMR ($CDCl_3$): δ= 3.84 (dd, 1H, C$\underline{H_2}$OH); 3.49 (dd, 1H, C$\underline{H_2}$OH); 2.88-2.53 (m, 6H, C$\underline{H_2}$N); 1.73-1.42 (m, 6H, C$\underline{H_2}$CH$_2$N); 1.37-1.31 (m, 22H); 0.99 (t, 3H, CH$_3$); 0.67 (s, 1H, OH). ^{13}C-NMR ($CDCl_3$): δ= 64.57; 61.83; 54.95; 53.23; 31.65; 29.06; 28.96; 28.90; 27.90; 27.55; 24.15; 22.94; 14.02.

*General procedure for the synthesis of CS **12** and CS **14**.*

CS **12** and CS **14** were obtained by quaternisation of 1 mmol of the appropriate *L*-prolinol derivative **8-9** with 1 mL of CH_3I in methanol (20 mL) in the presence of 1 g $NaHCO_3$ at room temperature till complete conversion of the amine, generally 24 hours. After filtration, the reaction mixture was evaporated to dryness and washed several times with cold diethyl ether until compounds were obtained as white solids. To exchange the counterion from I^- to Br^-, a saturated NaBr solution in MeOH was added and left under stirring at room temperature for 24 h; the solution was then evaporated to give CS **12** and CS **14.** The chlorine water assay was used to confirm the completeness of counterion exchange: 10 mg of CS **12** or CS **14** were added to 3 mL aqueous solution of $AgNO_3$ 0.25M and HNO_3 0.25 M. The solution was centrifuged and the precipitate was treated with chlorine water (obtained from HCl and $KClO_3$). If iodide is present, even in traces, I_2 is formed by oxidation and it confers a violet color to the organic layer after extraction of the aqueous phase with chloroform. Compound CS **12**. White solid. Yield: 60%. ^{1}H-NMR ($CDCl_3$): δ= 4.13 (dd, 1H, C$\underline{H_2}$OH); 3.89 (dd, 1H, C$\underline{H_2}$OH); 3.48 (m, 2H, NC$\underline{H_2}$CH$_2$OH); 3.27-3.22 (m, 4H, C$\underline{H_2}$N); 3.30 (t, 3H, C$\underline{H_3}$N); 1.86-1.54 (m, 6H, C$\underline{H_2}$CH$_2$N); 1.37-1.29 (m, 18H); 0.99 (t, 3H, CH$_3$); 0.83 (s, 1H, OH). ^{13}C-NMR ($CDCl_3$): δ= 63.67; 63.34; 60.61; 47.97; 31.65; 29.04; 28.96; 27.81; 27.05; 23.34; 23.21; 22.94; 14.02. Compound CS **14**. White solid. Yield: 62% ^{1}H-NMR ($CDCl_3$): δ= 4.13 (dd, 1H, C$\underline{H_2}$OH); 3.89 (dd, 1H, C$\underline{H_2}$OH); 3.48 (m, 2H, NC$\underline{H_2}$CH$_2$OH); 3.27-3.22 (m, 4H, C$\underline{H_2}$N); 3.30 (t, 3H, C$\underline{H_3}$N); 1.86-1.54 (m, 6H, C$\underline{H_2}$CH$_2$N); 1.37-1.29 (m, 20H); 0.99 (t, 3H, CH$_3$); 0.83 (s, 1H, OH). ^{13}C-NMR

($CDCl_3$): δ= 63.67; 63.34; 60.61; 47.97; 31.65; 29.04; 28.96; 27.81; 27.05; 23.34; 23.21; 22.94; 14.02.

*General procedure for the synthesis of N-ox **12**, N-ox **14** and N-ox **16**.*

The appropriate *L*-prolinol derivative **8-10** (1.5 mmol) was dissolved in absolute EtOH (0.5 mL), then 330 µL H_2O_2 (40% m/v, 3.9 mmol) were added dropwise. The solution was kept at 50 °C under stirring for 4 hours. The reaction was cooled and a small amount of MnO_2 was added to quench the excess of H_2O_2. Excess MnO_2 was removed by filtration, washed with 20 mL of ethanol and the solvent removed under reduced pressure. The residue was dissolved in 15 mL diethyl ether and the solvent was removed under reduced pressure three times giving N-ox **12**, N-ox **14** and N-ox **16.** Compound N-ox **12**. White solid. Yield: 70%. ^{1}H-NMR ($CDCl_3$): δ= 4.13 (dd, 1H, C$\underline{H_2}$OH); 3.86 (dd, 1H, C$\underline{H_2}$OH); 3.48 (m, 2H, NC$\underline{H_2}CH_2$OH); 3.27-3.22 (m, 4H, C$\underline{H_2}$N); 1.86-1.54 (m, 6H, C$\underline{H_2}CH_2$N); 1.37-1.30 (m, 18H); 0.99 (t, 3H, CH_3); 0.81 (s, 1H, OH). ^{13}C-NMR ($CDCl_3$): δ= 69.43; 66.90; 60.03; 31.65; 29.06; 28.96; 27.81; 27.50; 23.58; 23.09; 22.94; 14.02. Compound N-ox **14**. White solid. Yield: 73%. ^{1}H-NMR ($CDCl_3$): δ= 4.13 (dd, 1H, C$\underline{H_2}$OH); 3.86 (dd, 1H, C$\underline{H_2}$OH); 3.48 (m, 2H, NC$\underline{H_2}CH_2$OH); 3.27-3.22 (m, 4H, C$\underline{H_2}$N); 1.86-1.54 (m, 6H, C$\underline{H_2}CH_2$N); 1.37-1.30 (m, 20H); 0.99 (t, 3H, CH_3); 0.81 (s, 1H, OH). δ= 69.43; 66.90; 60.03; 31.65; 29.06; 28.96; 27.81; 27.50; 23.58; 23.09; 22.94; 14.02. Compound N-ox **16**. White solid. Yield: 68%. ^{1}H-NMR ($CDCl_3$): δ= 4.13 (dd, 1H, C$\underline{H_2}$OH); 3.86 (dd, 1H, C$\underline{H_2}$OH); 3.48 (m, 2H, NC$\underline{H_2}CH_2$OH); 3.27-3.22 (m, 4H, C$\underline{H_2}$N); 1.86-1.54 (m, 6H, C$\underline{H_2}CH_2$N); 1.37-1.30 (m, 22H); 0.99 (t, 3H, CH_3); 0.81 (s, 1H, OH). δ= 69.43; 66.90; 60.03; 31.65; 29.06; 28.96; 27.81; 27.50; 23.58; 23.09; 22.94; 14.02.

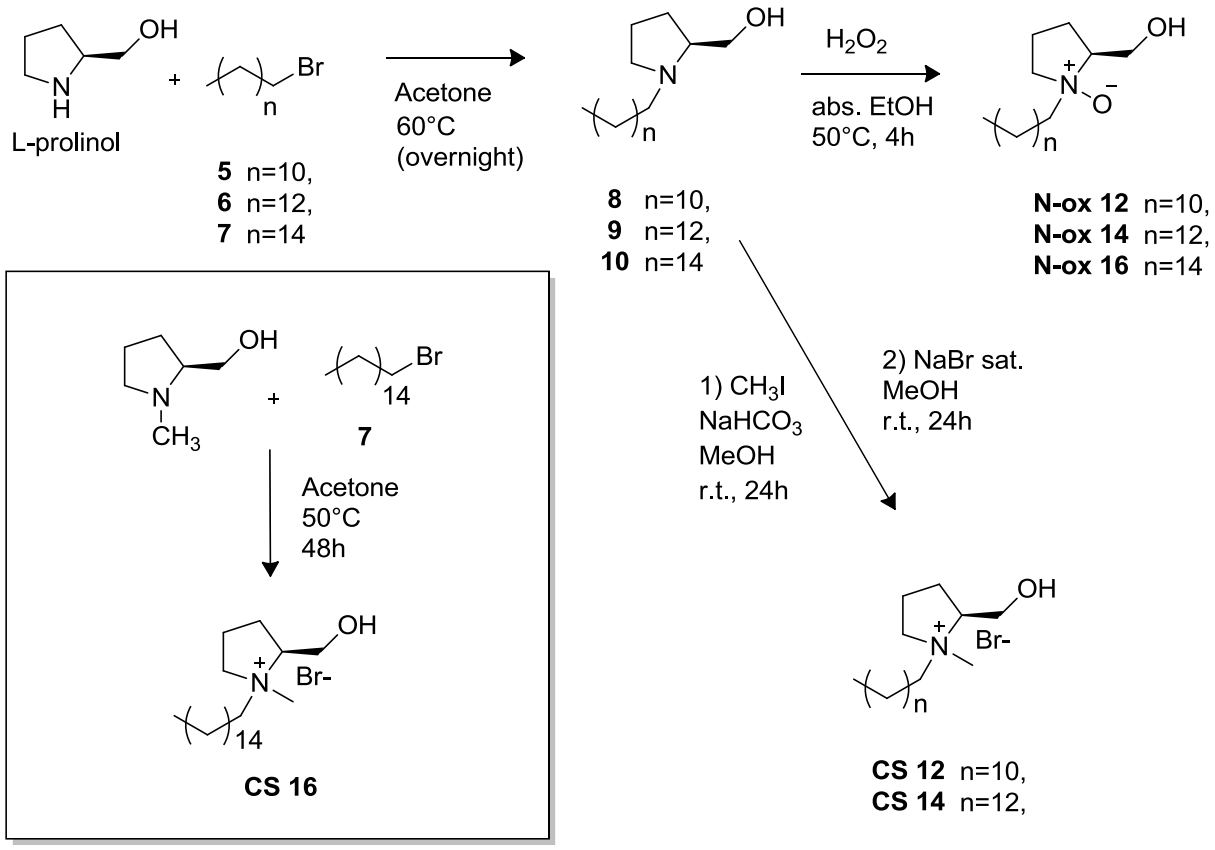

Figure 24. General procedure for the synthesis of *L*- prolinol derivatives CS **12-14-16** and N-ox **12-14-16.**

Determination of L-prolinol derivatives critical micellar concentration (cmc) through conductimetric measurements and evaluation of Krafft temperature.

6 mL of distilled water were put in a test tube and initial conductivity was evaluated; small amounts of surfactant dissolved in water were added to the solution under stirring in order to obtain concentrations between 10^{-7} M and 10^{-3} M measuring the conductivity after each addition. Krafft temperature was evaluated keeping at 4 °C overnight an aqueous solution of surfactant at a concentration higher than *cmc* value.

*Determination of surfactants N-ox **12-14-16** pK_a.*

The pK_a of each N-ox was evaluated titrating it with HCl and exploiting the Gran plot. In a test tube 9 mL of distilled water and surfactant (final concentration equal to 3 *cmc* values) were put and a NaOH water solution ($1.35 \cdot 10^{-3}$ M) was added

slowly until pH=10. Small aliquots of a HCl 10^{-3} M water solution were added and the pH after stirring was measured every time well above the equivalent point. The collected data were used to construct the Gran plot according to the equation:

$$10^{pH} \cdot Va = K_a^{-1}(Ve\text{-}Va)$$

where Va is the total HCl volume added, Ve is the HCl volume added at the equivalent point and K_a is the acidic constant of the analysed substance.

AA degradation in water with or without L-prolinol derivatives micelles

In a cuvette 20 µL of AA $7.8 \cdot 10^{-3}$ M in water were added to 2500 µL of water; in case of a test with N-ox, this was present at a final concentration 20-fold above *cmc*. The decrease in time of the intensity of the AA absorbance peak at 265 nm in water was evaluated for 1 hour.

AA and UA degradation in the presence of H_2O_2 with or without L-prolinol derivatives micelles

In a cuvette, 20 µL of AA $7.8 \cdot 10^{-3}$ M in water or 2.5 µL of UA $3.75 \cdot 10^{-2}$ M in DMSO and a proper amount of H_2O_2 (mol H_2O_2/mol AA or UA 10/1) were added to 2500 µL of water containing or not each *L*-prolinol derivative at a final concentration $1.4 \cdot 10^{-4}$ M for N-ox (well above their *cmc*), 2 *cmc* values for CS and $5 \cdot 10^{-2}$M for CS **14** and CS **16**. The variation of the peaks at 265 nm for AA and at 290 nm and 330 nm for UA was followed over 30 minutes; the experiment was performed at pH 7.4 for AA and at pH 10.9 for UA.

Liposomes preparation by TFH

Lipid films were prepared on the inside wall of a round-bottom flask by evaporation of solutions containing the proper amount of DMPC, cholesterol one *L*-prolinol derivatives (molar ratio: 6/3/1) dissolved in $CHCl_3$. The obtained films were stored overnight under reduced pressure (0.4 mbar), then PBS was added to obtain a 1 mM lipid dispersion. The solutions were heated at 50°C and vortex-mixed, then the suspensions were sonicated for 4 minutes at 72 W (cycles: 0.5 s) under cooling condition of an ice-water bath.

Liposomes/ quatsomes preparation by DELOS-Susp methodology

Mixed liposomes were prepared by DELOS-Susp (*depressurization of an expanded liquid organic solution-suspension*), a compressed fluids (CFs) based method. Chol (3 mg for liposomes, 4.87 mg for quatsomes) and DMPC (10 mg for liposomes, no present in quatsomes) were first dissolved in 1.2 mL of EtOH at working temperature T_w (T_w=38 °C). The solution was then added to a high-pressure vessel (V=7.3 mL) at atmospheric pressure and T_w. After 20 minutes of equilibration, the vessel was pressurized with CO_2 at the working pressure P_w (P_w=11.5 MPa) in order to obtain an expanded liquid EtOH solution. The reactor was kept at the working condition for 1 h in order to homogenize the system. The organic solution was then depressurized over 24 mL of PBS (water for quatsomes, warmed at T_w), containing or not around 0.5 mg for liposomes and around 5 mg for quatsomes of one of the CS **12-16** or N-ox **12-16** (molar ratio DMPC/chol/CS(N-ox) 6/3/1 for liposomes; chol/CS(N-ox) 5/5 for quatsomes). N_2 at 11.5 MPa was added to the vessel during the depressurization in order to maintain constant P_w inside. Aggregates were purified by diafiltration or by dialysis exchanging 4 times the external medium PBS (water for quatsomes) solution (25 fold the liposome dispersion volume) in an hour in order to remove ethanol.

Inclusion of UA in the aggregates and evaluation of E.E.

By incubation: a small amount of UA dissolved in DMSO 37.5 mM was added to preformed aggregates both prepared by TFH and by DELOS-Susp (molar ratio UA/lipids 1/20) and heated at 40 °C for 1 hour. They were purified by diafiltration or by dialysis to remove, besides ethanol, DMSO and unentrapped UA.

In the reactor: UA was entrapped also adding directly it in the reactor: chol and DMPC were first dissolved in 1.15 mL of EtOH at working temperature T_w whereas UA was dissolved in 50 μL of DMSO, heated at T_w and then added dropwise to the ethanol solution. The rest of the procedure was the same described above for liposomes/quatsomes without UA. The vessel was equipped with a gas filter, in order to prevent any unsolved compounds present in the CO_2-expanded solution to

reach the aqueous solution of the surfactant. Aggregates were purified by diafiltration or by dialysis to remove, besides ethanol, DMSO and unentrapped UA. The E.E. of UA was evaluated by UV measurements at 290 nm of solutions composed of 1.5 mL of methanol and 1.5 mL of the aggregate suspension before and after removal of unentrapped UA by dialysis or diafiltration.

DLS and Zeta potential measurements

DLS and electrophoretic mobility measurements were carried out at 25°C as explained above (see Chapter 2 section 1.3) on the samples without dilution directly just after their preparation and after 1 week. In the latter case measurements were carried out before and after diafiltration or dialysis. The stability of each formulation was checked over time (up to 6 months).

Preparation of $ABTS^{\cdot+}$ reagent solution

Four aqueous solutions were prepared as reported in literature:[239] (A) CH_3COONa 0.4 M and NaCl 150 mM; (B) CH_3COONa 30 mM and NaCl 150 mM; (C) glacial acetic acid 0.4 M and NaCl 150 mM; (D) glacial acetic acid 30 mM and NaCl 150 mM. An acetate buffer at pH 5.8 was obtained mixing 235 mL of A solution and 15 mL of C solution; an acetate buffer at pH 3.6 was obtained mixing 18.75 mL of B solution and 231.25 mL of D solution. A solution at pH 5.5, was prepared by mixing 28 mL of the buffer at pH 5.8 and 250 mL of the buffer at pH 3.6. An $ABTS^{\cdot+}$ solution 10 mM was prepared solubilizing 0.2745 g of ABTS diammonium salt in 50 mL acetate buffer at pH 3.6: the radical cation was generated when 14 µL of H_2O_2 35% (w/v, final concentration 2 mM) were added and left stirring in the dark for one hour and stored in the dark at 4°C.

Evaluation of antioxidant activity of free or loaded UA by $ABTS^{\cdot+}$ methodology

25 µL of $ABTS^{\cdot+}$ reagent solution were rapidly added to 2450 µL of acetate buffer at pH 5.5 prepared as described above containing a proper amount of dialysed liposomes/quatsomes, depending on the E.E. of each system, and PBS (water for

[239] Erel, O. A Novel Automated Direct Measurement Method for Total Antioxidant Capacity Using a New Generation, More Stable ABTS Radical Cation. *Clin. Biochem.* **2004**, 37(4), 277-285

quatsomes; total PBS or water volume 250 μL, final concentration in cuvette of UA: $1.38 \cdot 10^{-6}$ M and of $ABTS^{\cdot+}$ $9.17 \cdot 10^{-5}$ M). We followed the variation of the maximal absorbance at 417 nm over 60 minutes. All the measurements were repeated at least 3 times and then averaged. The temporal evolution of the absorption at 417 nm was then fitted to obtain the time constants that describe the degradation rate of $ABTS^{\cdot+}$. $ABTS^{\cdot+}$ itself showed an inherent decay of the absorbance that could be properly fitted with a simple exponential decay ($y= y_0+A_{ABTS} \cdot \exp(-t/\tau_{ABTS})$), with a time constant of τ_{ABTS} = 28.2 min for liposomes and τ_{ABTS} = 34.4 min for quatsomes. All preparations containing UA, however, show a decay by two processes and cannot be fitted with a simple exponential decay. Therefore, these curves were fitted according to the following equation

$$y= y_0+A_{UA} \cdot \exp(-t/\tau_{UA})+A_{ABTS} \cdot \exp(-t/\tau_{ABTS})$$

and fixing the parameter τ_{ABTS} = 28.2 min for liposomes and τ_{ABTS} = 34.4 min for quatsomes to obtain the values of the time constant τ_{UA}.

The relative change in absorbance, A_{UA}/A_{tot}, was calculated with $A_{tot} = y\ (t = 0) - y_0$.

Cryo-TEM measurements

Aggregates morphology was studied by cryo-TEM measurements. The samples were prepared in a controlled environment vitrification system (CEVS) (Leica EM-CPC, Leica) in a climate chamber at 23-25 °C keeping the relative humidity close to saturation to avoid evaporation of volatiles from the sample during its preparation. 5 μL of liposomes solution were placed on a carbon-coated holey film supported by a copper standard TEM grid. After about 30 s, the grid was gently blotted with a double layer of filter paper to obtain a thin film (20-400 nm) on the grid before it was plunged into liquid ethane at its freezing temperature (-180 °C) and transferred into liquid nitrogen (-196 °C). The vitrified specimens were stored in liquid nitrogen and transferred to a microscope using a cryotransfer and its workstation (Gatan 626 DH, Gatan). The working temperature was kept below -175 °C, and the acceleration voltage was 200 kV. Images of the nanovesicles in amorphous ice over holes were recorded digitally with a slow-scan camera (Gatan 694 CCD, Gatan) under low-dose conditions using the Digital Micrograph 3.9.2. software package.14 The morphology

of the samples was also examined using an optical microscope (Olympus BX51, Olympus, U.K.) by transmitted and polarized light.

Evaluation of the antimicrobial/antifungal activity of quatsomes

The antimicrobial activity of quatsomes devoid of UA was evaluated as described above (see Chapter 2 section 1.3) on a Methicillin resistant *Staphylococcus aureus* (ATCC43300), on an *Escherichia coli* (ATCC25922) bacterial strains and on a *Candida Albicans* fungal strain.

3.4 Results and discussion

3.4.1 Aggregation properties

Chemistry

CS **12-14** and N-ox **12-16** were obtained by alkylation of secondary amine of *L*-prolinol with the corresponding *n*-bromoalcane to give the intermediate products **8-10**. These compounds were reacted with CH_3I to alkylate the nitrogen; the iodide ammonium products underwent an ion exchange by dissolving the iodide ammonium salt in a saturated NaBr methanol solution to yield CSs **12-14**. The precipitation of the surfactant counterions as silver salt by addition of an $AgNO_3$ solution established the completeness of the counterion exchange: the absence of iodide was confirmed by the addition of chlorine water to the obtained salt after an extraction with chloroform. Precipitation of counterions was carried out to avoid the perturbation of the oxidation assay by the surfactant alkyl chain. CS **16** was obtained by alkylation of the *N*-methyl-*L*-prolinol with the corresponding *n*-bromoalcane. N-ox **12-16** were obtained by oxidation of the corresponding tertiary amine using aqueous hydrogen peroxide. While in case of CSs **12-14** a racemic mixture was obtained, only a single diastereoisomer with the amine oxide *syn* to the hydroxyl side chain was formed in case of N-ox **12-16**. This peculiar behavior is due to the stabilization of the product by intramolecular hydrogen bonding between the

hydrogen of the hydroxyl group and oxygen of N-oxide moiety that brings to the formation of a favored six-member ring.[240]

Determination of cmc and Krafft T of L-prolinol derivatives

The *cmc* of *L*-prolinol derivatives was evaluated by plotting the conductivity *versus* the concentration of each surfactant; the intersection point between the two linear trends described by the experimental values represents the *cmc*. The results are reported in Table 13.

Table 13. *cmc* values of *L*-prolinol derivatives.

Surfactant	*cmc* (M)
CS **12**	$(2.3 \pm 0.3) \cdot 10^{-2}$
CS **14**	$(2.6 \pm 0.4) \cdot 10^{-3}$
CS **16**	$(2.5 \pm 0.2) \cdot 10^{-4}$
N-ox **12**	$(1.4 \pm 0.3) \cdot 10^{-5}$
N-ox **14**	$(5.8 \pm 0.4) \cdot 10^{-6}$
N-ox **16**	$(1.5 \pm 0.5) \cdot 10^{-6}$

As expected *cmc* value decreases as a function of the chain length of the surfactant in each series and it is lower for N-oxs with respect to CSs because the lower repulsions between the polar zwitterionic headgroups promote the aggregation at lower monomer concentration. Krafft temperatures were also evaluated; for all surfactants they were lower than 4°C due to the absence of a precipitate after storage in these conditions.

[240] O'Neil, I. A.; Potter, A. J. Simple Azetidine *N*-Oxides: Synthesis, Structure and Reactivity. *Chem. Commun.* **1998**, 14, 1487-1488

*Determination of N-ox **12**, **14** and **16** pK_a*

In water N-oxs are present in either the protonated or the deprotonated form because of the acid-base equilibrium; this phenomenon can strongly influence the properties of aggregates of pH-sensitive surfactants. The apparent pK_a of N-oxs, estimated using the Gran plot after the equivalent point, were all similar, as expected, and equal to about 5.4. Despite these values were obtained in aggregative conditions (titrations were carried out at concentrations above *cmc*), they are in good agreement with pK_a values reported in literature for *N*-oxide group,[241,242] suggesting that aggregation does not influence the protonation of the oxygen in the investigated N-ox, in contrast with the general observation for the nitrogen of tertiary amines.[243,244,245]

3.4.2 Micelles

In this section the investigation on the aggregation properties of synthetic cationic surfactants (CSs) **1-3** derived from *L*-prolinol differing for the length of the alkyl chain, and their corresponding N-ox **4-6** (Figure 24) is reported. Moreover, the antioxidant activity of two natural compounds, (+)-usnic acid (UA) and AA, was evaluated with respect to *L*-prolinol derivatives micelles in aqueous solution, and H_2O_2 (in the case of UA) to catalyze the oxidation. AA is a hydrophilic molecule that easily undergoes a two-electron oxidation reaction under aerobic conditions. UA is a secondary metabolite of many lichens with antioxidant properties[246,247] that is high lipophilic even in its deprotonated forms thanks to the possibility to stabilize the negative charge on the β-triketone groups by resonance.[79] The aim of this

[241] Búcsi, A.; Karlovská, J.; Chovan, M.; Devínsky, F.; Uhríková, D. Determination of pKa of *N*-alkyl-*N*,*N*-dimethylamine-*N*-oxides Using ^{1}H NMR and ^{13}C NMR Spectroscopy. *Chem. Pap.* **2014**, 68, 842–846

[242] Huláková, S.; Gallová, J.; Devínsky, F. Cholesterol Protects Phosphatidylcholine Liposomes from *N*,*N*-dimethyl-1-dodecanamine *N*-oxide Influence. *Acta Chim. Slov.* **2015**, 62, 420–427

[243] Mezei, A.; Pérez, L.; Pinazo, A.; Comelles, F.; Infante, M. R.; Pons, R. Self-assembly of pH-sensitive Cationic Lysine Based Surfactants. *Langmuir*, **2012**, 28, 16761-16771

[244] Colomer, A.; Pinazo, A.; Manresa, M. A.; Vinardell, M. P.; Mitjans, M.; Infante, M. R.; Pérez, L. Cationic Surfactants Derived from Lysine: Effects of Their Structure and Charge Type on Antimicrobial and Hemolytic Activities. *J. Med. Chem.* **2011**, 54, 989–1002

[245] Giansanti, L.; Mauceri, A.; Galantini, L.; Altieri, B.; Piozzi, A.; Mancini, G. Glucosylated pH-Sensitive Liposomes for Potential Drug Delivery to Tumor Tissue. *Chem. Phys. Lip.* **2016**, 200, 113-119

[246] Luzina, O.A.; Salakhutdinov, N. F. Usnic Acid and its Derivatives for Pharmaceutical Use: a Patent Review (2000-2017). *Expert Opin. Ther. Pat.* **2018**, 28, 477–491

[247] Suwalsky, M.; Jemiola-Rzeminska, M.; Astudillo, C.; Gallardo, M. J.; Staforelli, J. P.; Villena, F.; Strzalka, K. An in Vitro Study on the Antioxidant capacity of Usnic Acid on Human Erythrocytes and Molecular Models of its Membrane. *Biochim. Biophys. Acta*, **2015**, 1848 (11 Part A), 2829–2838

investigation is to study the effect of the presence of a *N*-oxide or a quaternary ammonium as polar headgroup and of the length of the alkyl chain on micelle properties and on the antioxidant activity of natural substances with different water solubility.

AA degradation with or without L-prolinol micelles

The degradation of AA in water was investigated both in presence and in absence of micelles of N-oxs and CSs. The decrease of the absorbance intensity at λ_{max} of the reduced form of AA (265 nm) was followed to evaluate the influence of the different aggregates on the rate of oxidation. It has to be considered that, while oxygen (the oxidant) may enter the micelles,[248] whereas AA, more hydrophilic, is excluded from micelles hydrophobic core but can interact with the polar headgroup of the surfactant.

The degradation process was faster in the presence of N-ox micelles, in particular in the case of N-ox **14**, whereas the variation observed carrying out the same experiment in the presence of micelles of CSs was neglectable as in the case of AA alone (black trace reported in Figure 25 as an example). Our results show that N-ox moiety seems to enhance AA oxidation, thus exalting its antioxidant capacity, in good agreement with literature report.[229] The fact that in the case of CSs this effect is not observed can be explained considering that the rate of AA oxidation is inversely proportional to the polarity of the surrounding media;[237] based on these premises, being the zwitterionic N-oxide group less polar than a charged quaternary ammonium and being AA located in the headgroup region, it is reasonable to speculate that in the case of N-ox micelles AA oxidation is favoured. Moreover, it is reasonable to hypothesize that also water penetration in N-ox or CS micelles is different, with consequences on the polarity of the interfacial region of the aggregates and, in turn, on AA oxidation. The linearity of the obtained curve indicates that AA oxidation occurs at constant rate, *i.e.* the reaction is of zero order with respect to AA (thus the oxidation rate is independent from AA concentration).

[248] Geiger, M. W.; Turro, N. J. Pyrene Fluorescence Lifetime as a Probe for Oxygen Penetration of Micelles. *Photochemistry and Photobiology*, **1975**, 22(6), 273-276

This behaviour is typical of heterogeneous reactions at an interface such as micelles surface. [249]

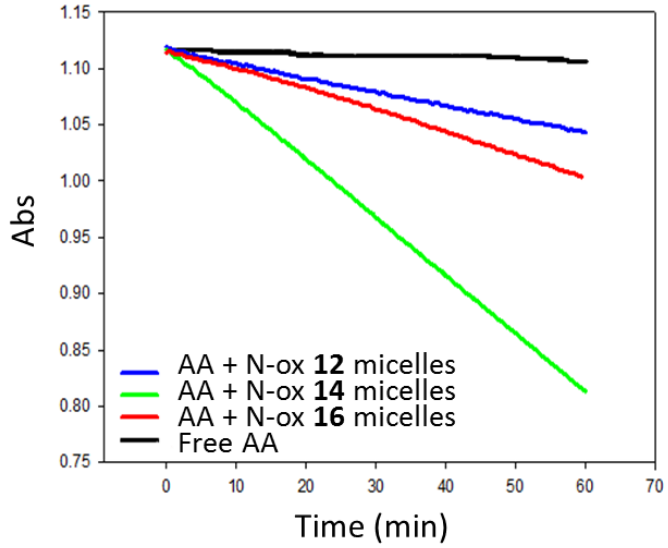

Figure 25. Kinetic measurements of AA degradation at 265 nm in pure water in the presence of N-ox micelles.

The same experiments were repeated in the presence of an excess H_2O_2 to accelerate the oxidation process: obviously AA oxidation was faster with respect to the uncatalyzed reaction and was complete within 30 minutes. In this case as well, in presence of N-ox micelles the process was accelerated especially in the case of N-ox **14** (Figure 26A) whereas CS micelles did not affect AA oxidation with the exception of CS **12** (Figure 26B). This anomalous result could be rationalized considering *cmc* values (Table 13). In fact, in the case of N-ox the experiments were carried out well above their *cmc*. On the other hand, in the case of CS, the experiments were carried out only at 2 *cmc* of each compound because of their higher *cmc* values. As a consequence, being **1** the surfactant that features the highest *cmc*, a very high amount of it was present in the cuvette and this peculiar condition could influence the result obtained. To verify this hypothesis, we investigated the kinetic at 265 nm in presence of surfactants CS **14** and CS **16** at a concentration equal to the experiment performed with micelles CS **12**, *i.e.*: $5 \cdot 10^{-2}$ M; the rate of the reaction slightly increased at increasing concentration both of CS **14** and CS **16**. In

[249] Weitbrecht, N.; Kratzat, M.; Santoso, S.; Schomacker, R. Reaction Kinetics of Rhodium Catalysed Hydrogenations in Micellar Solutions. *Catal. Today*, **2003**, 79–80, 401-408

Figure 26C shows, as an example, the comparison of the results obtained for micelles CS **16** at two different concentrations. In the case of N-ox micelles, the increase of surfactant concentration does not affect at all the kinetic of the process (data not shown). These results indicate that this parameter can influence the investigated phenomenon and that at high concentrations the behaviour of CS micelles tends to that of N-ox ones.

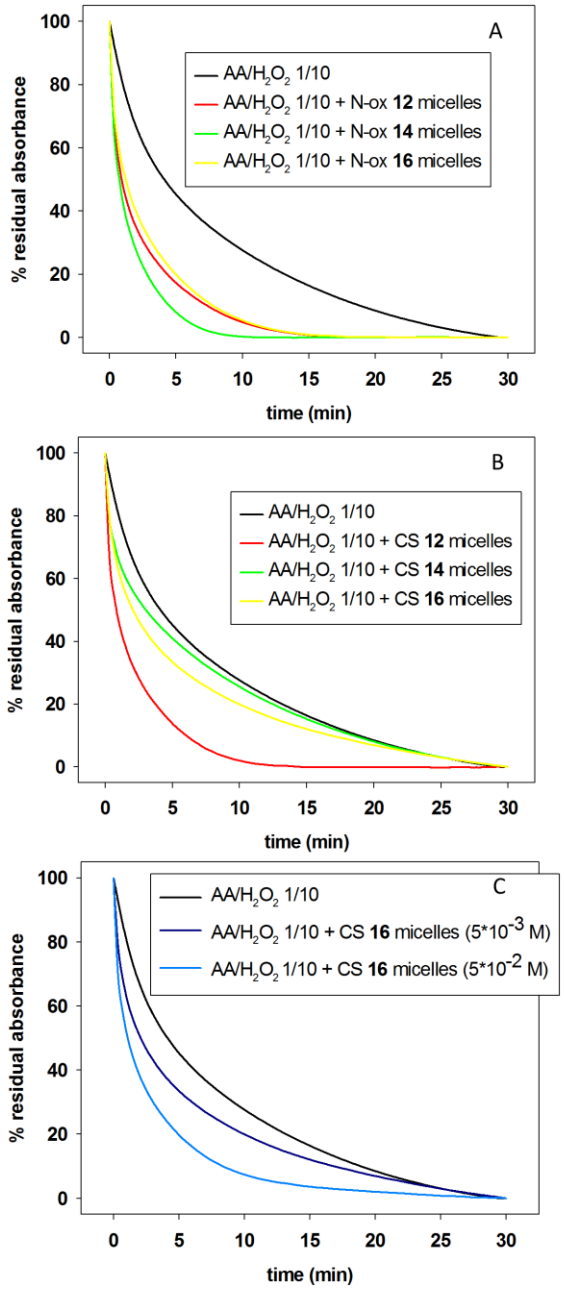

Figure 26. Kinetic measurements (reported as percentage) of AA degradation by H_2O_2 at 265 nm in pure water A) in the presence of N-ox micelles, B) in the presence of CS micelles, C) in the presence of micelles formed by CS **16** at different concentrations.

UA degradation in the presence of H_2O_2 with or without L-prolinol micelles

UV spectra of UA at various pH are reported in Figure 27. It can be clearly observed that at basic (10.9), neutral (7.4) or slightly acidic (5) pH, at which the enolic OH in position 3 (the most acidic, pK_a 4.4)[86] is deprotonated, a predominant peak at about 300 nm is present whereas at acidic pH, where all the hydroxyl functionalities are protonated, a second peak appears at about 400 nm. This behaviour is due to complex tautomeric equilibria of UA in solution that bring to the coexistence of species with different degree of protonation whose relative abundance is strictly dependent on the pH of the solution and on the polarity of the medium. The variations in signal intensities could be linked to the different interaction of the species present in solution with the solvent.

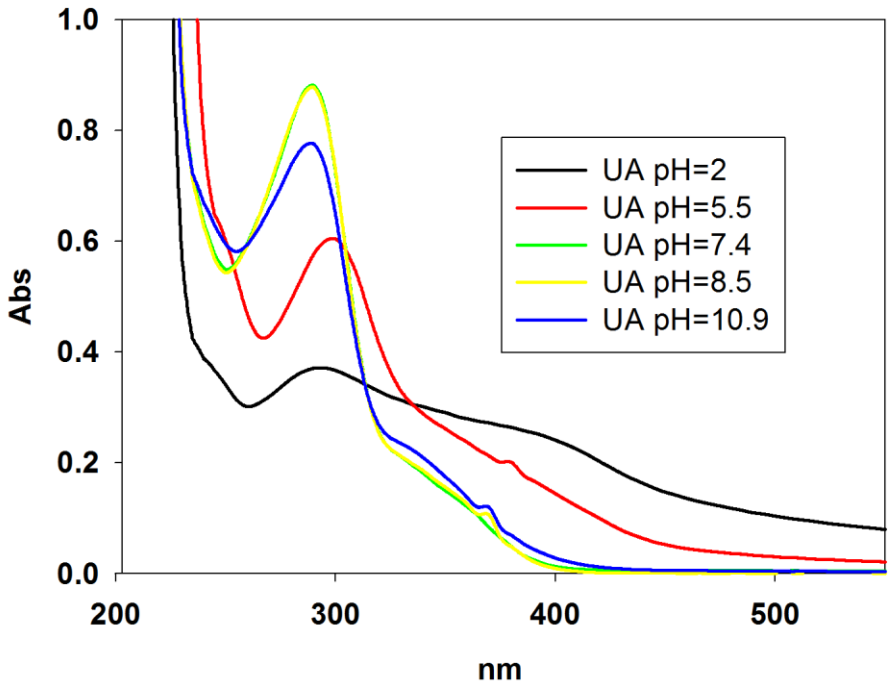

Figure 27. UV spectra of UA in water at various pH.

Oxidation of UA in water at any pH investigated can be followed by UV measurements only if promoted by H_2O_2 (in Figure 28 is reported an example). At

pH 2 precipitation occurred with or without H_2O_2. At pH 10.9 the most evident variation of UV spectra of UA after 1 h was observed; it was, therefore, chosen to carry out the experiments in the presence of micelles under this condition. Soon after the addition of H_2O_2 the peak at 290 nm increased, but after 1 h it almost disappeared and the peak at 330 nm slightly increased (Figure 28A). On the other hand, at lower pH after 1h the variations are negligible (pH 7.4 is reported as an example in Figure 28B). This difference is reasonable due to the fact that the nature and the amount of oxidizable species present in solution vary as a consequence of pH: for example, the extent of water solvation of the deprotonated forms of UA *via* hydrogen bonding (that stabilizes them) increases as a function of pH. In the same way, also the oxidized species can be more or less stabilized at different pH. In general, the oxidation of the phenolic hydroxyl of UA is strongly affected by the environmental conditions.[250] Obviously, the extent of the oxidation also affects the kinetic of the interconversion of the tautomeric forms that is proportionally hindered.

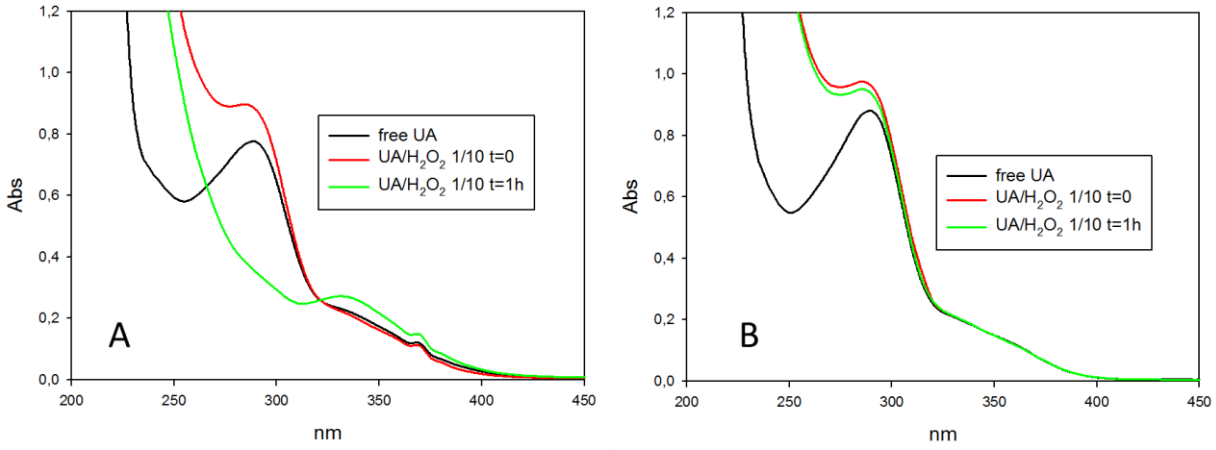

Figure 28. Comparison of UV spectra in water at pH 10.9 (A) and 7.4 (B).

UA absorbance did not change at pH 10.9 in the presence of N-ox micelles (in Figure 28A is reported an example). Adding H_2O_2 to the same solution (and in the same experimental conditions used with AA), similar variations to those observed with free UA at the same pH after 1 hour appeared in the UV spectrum (suggesting that

[250] Iorgulescu, E. E.; Varzaru, E.; Bala, D.; Mihailciuc, C. Electrochemical Study of the Oxidation of Usnic Acid in Different Organic Solvents. *Rev. Roum. Chim.* **2012**, 57, 699-705

the same oxidation process occurred) without showing any dependence on the chain length of the surfactant. We reported as an example the results obtained in the case of N-ox **14** in Figure 29A.

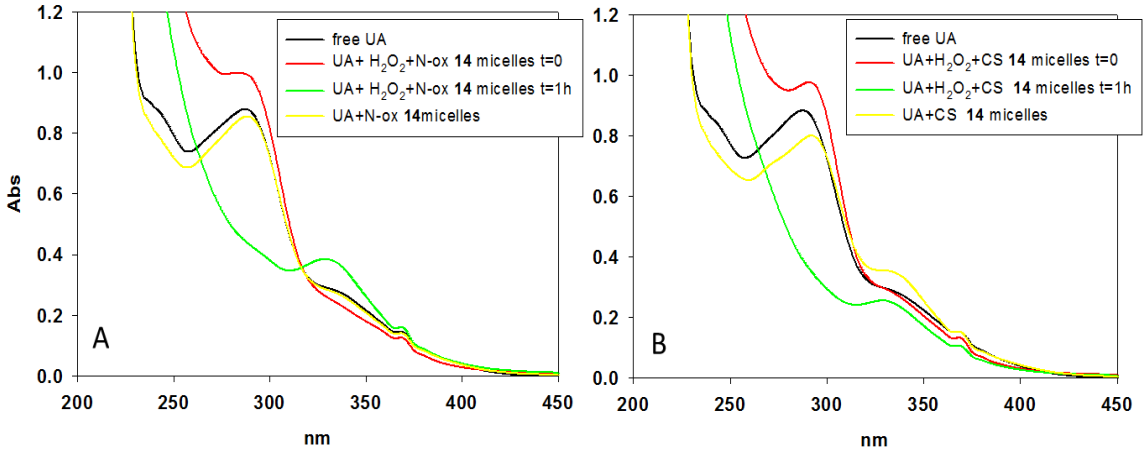

Figure 29. Spectra of free UA (black trace) and of UA A) in the presence of N-ox micelles or B) in the presence of CS micelles at pH=10.9 without H_2O_2 (yellow trace), soon after the addition of H_2O_2 (red trace) and 1 hour after the addition of H_2O_2 (green trace).

We followed the variation over time of the peak at 290 nm and 330 nm in the presence of N-ox micelles; a slight increase of the rate of disappearance of the peak at 290 nm with respect to UA was registered, especially with **4** (Figure 30A). The height of the peak at 330 nm varied over time, to an extent depending on the length of the alkyl chain (Figure 30B), indicating that a transient species was formed during the oxidation.

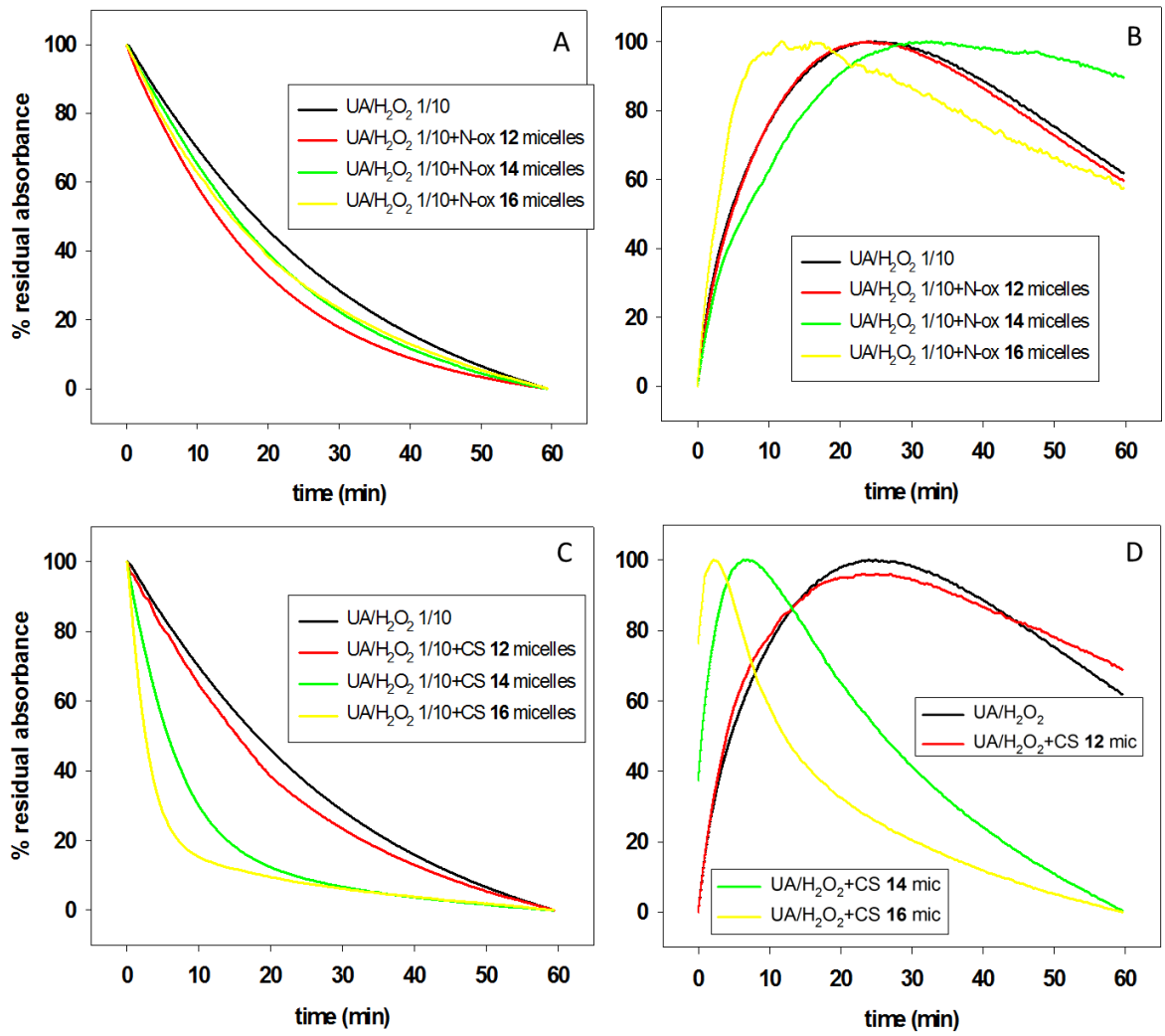

Figure 30. Kinetic measurements (reported as percentage) of the peak in the presence of N-ox micelles at A) 290 nm or B) 330 nm or in the presence of CS micelles at C) 290 nm or D) 330 nm of UA degradation by H_2O_2.

The dependence of the appearance of the peak at 330 nm on the structure of the surfactant could be due to the predominance of one of the tautomeric species that are in dynamic equilibrium;[250] it is possible that the rapid interconversion of the tautomeric forms is, to some degree, hindered with the inclusion of UA in micelles, phenomenon that can affect the different equilibria involved in oxidation process. As a consequence, also the rate of formation and the nature of the species obtained by oxidation can be influenced to an extent strictly related to the surfactants molecular structure. It needs to be considered that the different partitioning of the compound inside the aggregates can play a pivotal role in the antioxidant

effectiveness rates;[251,252,253,254] in the investigated systems the location and the amount of UA in micelles could vary because of the different chain length of the surfactant, characteristic that also affect the degree of hydration, the water penetration and the inner polarity.[255,256,257] It follows that the oxidation process, sensitive to the polarity of UA microenvironment, could also be perturbed. Moreover, the solubility in micelles of relatively polar molecules such as UA in its deprotonated form increases in the case of surfactants with longer alkyl chains thanks to additional ion-dipole solute-surfactant interactions.[258]

Analogue experiments in the presence of CSs were carried out and a different behaviour with CS **14** or CS **16** compared to N-ox ones was observed; upon addition of a CS to a solution of UA at pH 10.9 the peak at 330 nm increased (Figure 29B) and the peak at 290 nm decreased, whereas in the case of the corresponding N-ox no variations were observed in the UV spectrum of UA (Figure 29A). This evidence suggests that also in this case UA is located in a different region of the aggregates. Another aspect that could affect the location of the solute and, in turn, the polarity of its microenvironment is the presence of a strong hydrogen bond between the hydroxyl group and the *N*-oxide moiety:[240] this interaction blocks the pendant arm linked to the OH in a folded conformation hampering its free rotation as in the case of CSs. Soon after the addition of the peroxide the peak at 330 nm diminished for CS **14** and CS **16**, whereas the peak at 290 nm increased. After 1 h the peak at 330 nm was again observable whereas the peak at 290 nm completely disappeared for CS **14** and CS **16** whereas for CS **12** was still present, in analogy with N-ox micelles. These results confirm the crucial role of the surfactant chain length that in this case is even

[251] Richards, M. P.; Chaiyasit, W.; Mc Clemments, J.; Decker, E. J. Ability of Surfactant Micelles to Alter the Partitioning of Phenolic Antioxidants in Oil-in-water Emulsions. *Agric. Chem. Food,* **2002**, 50, 1254-1259

[252] Frankel, E. N. Interfacial Lipid Oxidation and Antioxidation. *J. Oleo Sci.* **2001**, 50, 387-391

[253] Mc Clemments, D. J.; Decker, E. A. Lipid Oxidation in Oil-in-water Emulsions: Impact of Molecular Environment on Chemical Reactions in Heterogeneous Food Systems. *J. Food Sci.* **2000**, 65, 1270-1272

[254] Costas-Costas, U.; Bravo-Díaz, C.; González-Romero, E. Micellar Effects on the Reaction Between an Arenediazonium Salt and 6-O-Octanoyl-*L*-ascorbic Acid. Kinetics and Mechanism of the Reaction. *Langmuir,* **2004,** 20, 1631-1638

[255] Long, J. A.; Rankin, B. M.; Ben-Amotz, D. Micelle Structure and Hydrophobic Hydration. *J. Am. Chem. Soc.* **2015**, 137(33), 10809-10815

[256] Menger, F. M. The Structure of Micelles. *Acc. Chem. Res.* **1979**, 12(4), 111–117

[257] Sato, T.; Saito, Y.; Anazawa, I. Micellar Structure and Micellar Inner Polarity of Octaethylene Glycol *n*-alkyl Ethers. *J. Chem. Soc., Faraday Trans. 1*, **1988**, 84, 275-279

[258] Vinarov, Z.; Katev, V.; Radeva, D.; Tcholakova S.; Denkov, N. D. Micellar Solubilization of Poorly Water-soluble Drugs: Effect of Surfactant and Solubilizate Molecular Structure. *Drug Development and Industrial Pharmacy*, **2017**, DOI: 10.1080/03639045.2017.1408642

determinant to invert the trend in the interaction with the solute: the behaviour of CS **12**, the CS with the shortest chain, is more similar to the one of zwitterionic N-ox -in particular of N-ox **12**- rather than the other cationic analogues. This complex behaviour is determined by possible and probable tautomeric balance, by the polarity of UA environment, the polarizability of the antioxidant and the formation of hydrogen bonds in micelles. It seems that UA is more easily oxidized in the more polar environment formed by cationic micelles with respect to N-ox ones, suggesting that the higher the polarity of the medium, the easier the oxidation process is, as reported in literature, because of an increased stabilization of polar oxidized products (that cannot delocalize the charge on the aromatic structure as reagents can).[79]

From the observation of the kinetic of UA oxidation at 290 nm (Figure 30C) and 330 nm (Figure 30D), the process is faster in presence of CS **14** and, more markedly, of CS **16** (that features the longest chain), more than with the corresponding N-ox or without micelles; in the case of N-ox, after one hour it was observed mainly the appearance of the peak at 330 nm (thus the transient species related to its presence are still in solution), whereas with the corresponding cationic compounds its disappearance could be followed more extensively. A different behaviour was showed by the surfactant CS **12**: the observed kinetic was similar to the one of the N-ox surfactants (even at 330 nm). In analogy to the case of AA, it was verified the effect of concentration of surfactants on the oxidation process of UA, by comparing the kinetic at 290 nm in presence of CS **16** at two different concentrations, *i.e.* around and well above its *cmc* (Figure 31). Increasing the concentration of CS **16**, the rate of the reaction decreased approaching the UA behaviour observed in the presence N-ox surfactants micelles. Also, in the presence of AA the similarity of behaviour between micelles of CS **12** and of N-ox increases as a function of surfactant concentration. This result indicates that the nature and the number of micelles in solution affected the kinetic of the oxidation process of anionic antioxidant compounds.

Comparing AA to UA the effect of the presence of cationic or N-ox surfactants was opposite. A possible explanation could be the different dimensions and charge

densities of the antioxidants. In fact, in the case of UA, bigger than AA, the negative charge is delocalized on the aromatic structure,[79] whereas in the case of AA the charge is more localized. Both these features can influence either the localization of the antioxidant in/nearby the micelles and its reactivity; if the interaction between the anionic antioxidant and the cationic headgroups is too strong the formation of a ion-pair can reduce its reactivity by decreasing its availability to react with the oxidant (oxygen or H_2O_2). Moreover, also the ease of access of the antioxidant in the different micelles can vary in the case of cationic or zwitterionic micelles and in the case of oxygen or H_2O_2 as oxidant species. If the antioxidant compound can penetrate too deeply in the aggregates, the oxidant species cannot be able to react with it. In both cases the longer the alkyl chain, the faster the process. In general, polar solutes that can form hydrogen bond are scarcely internalized in micellar cores and are preferentially located at micellar interface (that is often considered an "alcohol-like" medium);[259] in particular, AA and UA (almost fully deprotonated at basic pH 10.9) should be with the O···H bonds aligned tangentially to water-micelles interface or with the hydrogen atoms pointing at the bulk.[260] However, considering the high lipophilicity of UA even in its anionic form, it will be positioned more deeply in the internal core (more hydrophobic and less solvated) with respect to AA; such a difference in the microenvironment influence the oxidation process even because can bring to separation or concentration of the reactant species.

[259] Sepulveda, L.; Lissi, E.; Quina, F. Interactions of Neutral Molecules with Ionic Micelles. *Adv. Colloid interface Sci.* **1986**, 25, 1-57

[260] Quina, F. H.; Alonso, E. O.; Farah, J. P. S. Incorporation of Nonionic Solutes into Aqueous Micelles: a Linear Solvation Free Energy Relationship Analysis. *J. Phys. Chem.* **1995**, 99, 11708-11714

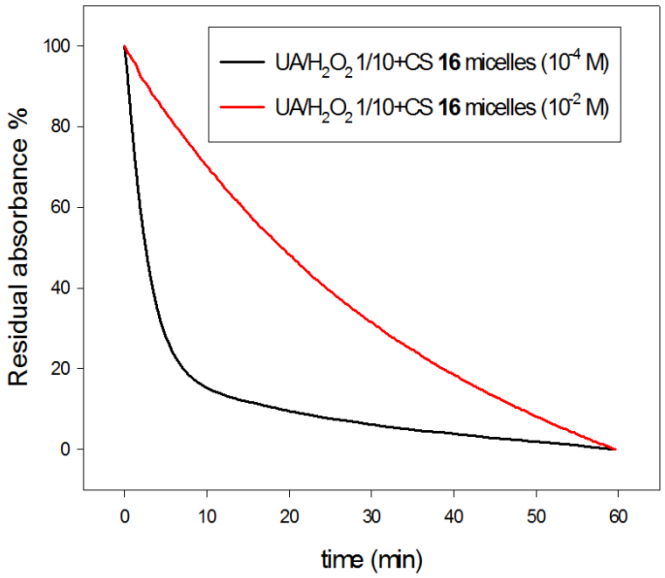

Figure 31. Comparison of kinetic measurements of UA degradation by H_2O_2 in the presence of micelles of CS **16** at different concentrations (290 nm).

3.4.3 Vesicles preparation

TFH

Conventional techniques for liposomes preparation include TFH, reverse phase evaporation, injection of lipids dissolved in a proper organic solvent into the aqueous phase and are often associated to sonication, homogenization or high pressure membrane extrusion for size reduction.[261] Sonication is perhaps the most extensively used method for the preparation of SUV.[262] The main disadvantages of this method are very low internal volume/encapsulation efficacy, possible degradation of phospholipids and or solute , metal pollution from probe tip and presence of MLV along with SUV.[263]

MLVs obtained by TFH can be sonicated either with a bath type sonicator or a probe sonicator:

- probe sonication. The tip of a sonicator is directly engrossed into the liposome dispersion. The energy input into lipid dispersion is very high in this method. The coupling of energy at the tip results in local hotness; therefore, the vessel must be

[261] Patil, Y. P.; Jadhav, S. Novel Methods for Liposome Preparation. *Chem. Phys. Lipids,* **2014**, 177, 8–18

[262] Akbarzadeh, A.; Rezaei-Sadabady, R.; Davaran, S.; Joo, S. W.; Zarghami, N.; Hanifehpour , Y.; Samiei, M.; Kouhi, M.; Nejati-Koshk, K. Liposome: Classification, Preparation, and Applications. *Nanoscale Research Letters* **2013**, 8, 102, 1-12

[263] Riaz, M., Liposome Preparation Method. *J. Pharm. Sci.* **1996**, 9(1), 65–77

engrossed into a water/ice bath. Throughout the sonication up to 1 h, more than 5% of the lipids can be de-esterified. Also, with the probe sonicator, titanium will slough off and pollute the solution.

- bath sonication. The liposome dispersion in a cylinder is placed into a bath sonicator. Controlling the temperature of the lipid dispersion is usually easier in this method, in contrast to sonication by dispersal directly using the tip. The material being sonicated can be protected in a sterile vessel, dissimilar the probe units, or under an inert atmosphere.[264]

DELOS-Susp liposomes

Despite the numerous liposomes advantages, their use in pharmaceutics is hampered by their relative low long-term stability because they tend to aggregate with consequent loss of structural homogeneity and leakage of their payload upon storage.[262,265,266,267] More recently, different methodologies that bring to liposomes formation mainly based on microfluidics[268] or compressed fluids[269] have been developed. Among the latter ones, DELOS-Susp methodology allows to prepare monomodal unilamellar liposomes (even using micelle-forming lipids) more homogeneous and stable with respect to conventional preparation methods[270] This technique is based on the depressurization of cholesterol (chol) dissolved into CO_2-expanded ethanol (or another organic solvent miscible with CO_2) into an aqueous solution containing the charged lipids that will form the bilayer together with chol (Figure 32).

[264] Kataria, S.; Sandhu, P.; Bilandi, A.; Akanksha, M.; Kapoor, B.; Seth, G. L.; Bihani, S. D. Stealth Liposomes: a Review. *ijrap*, **2011**, 2(5), 1534–1538

[265] Crommelin, D. J. A.; Fransen, G. J.; Salemink, P. J. M. Stability of Liposomes on Storage. *Targeting of Drugs With Synthetic Systems,* **1986**, 113.

[266] Grit, M.; Crommelin, D. J. A. Chemical Stability of Liposomes: Implications for Their Physical Stability. *Chem. Phys. Lipids,* **1993**, 64(1–3), 3-18

[267] Du Plessis, J.; Ramachandran, C.; Weiner, N.; Müller, D. G. The Influence of Lipid Composition and Lamellarity of Liposomes on the Physical Stability of Liposomes Upon Storage. *Int. J. Pharm.* **1996**, 127(2), 273-278

[268] Carugo, D.; Bottaro, E.; Owen, J.; Stride, E.; Nastruzzi, C. Liposome Production by Microfluidics: Potential and Limiting Factors. *Sci. Rep.* **2016**, 6, 25876

[269] Grimaldi, N.; Andrade, F.; Segovia, N.; Ferrer-Tasies, L.; Sala, S.; Veciana, J.; Ventosa, N. Lipid-based Nanovesicles for Nanomedicine. *Chem. Soc. Rev.* **2016**, 45, 6520-6545

[270] Meure, L. A.; Foster, N. R.; Dehghani, F. Conventional and Dense Gas Techniques for the Production of Liposomes: a Review. *AAPS Pharm. Sci. Tech.* **2008**, 9(3), 798-809

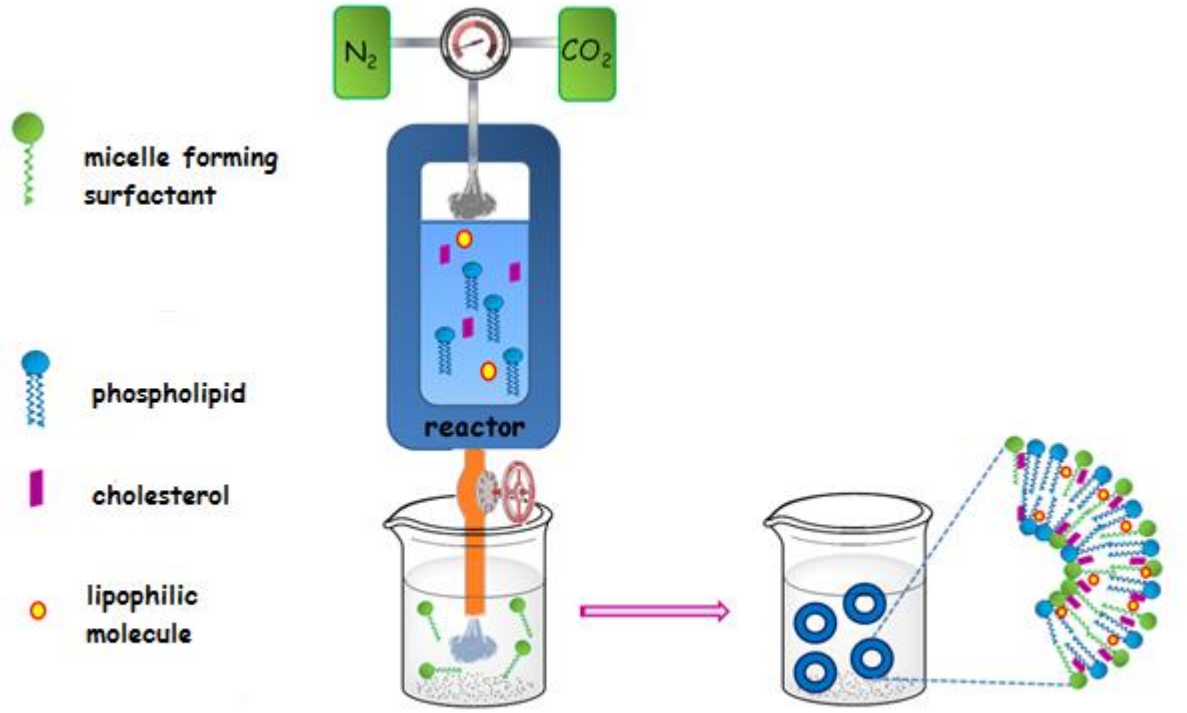

Figure 32. Schematic representation of DELOS-Susp procedure.

If phospholipids are also present in the formulation they can be dissolved together with chol in the organic phase. Thanks to this one-step procedure is it possible to avoid problems of low reproducibility and scarce control of particle dimensions and size distribution frequently occurring with other solvent-based processes. These disadvantages can be overcome with DELOS-Susp process because the propagation of CO_2 as co-solvent in its supercritical state is more quick and uniform than other solvent-based methods.[77] By the use of compressed fluids it is possible to have the control over some characteristics of the aggregates such as dimensions, homogeneity, stability and morphology, difficult to achieve by conventional liposomes preparation methodologies. Moreover, DELOS-Susp is a scalable methodology that respects the dictates of green chemistry process and allows working in sterile conditions.

Quatsomes

Quatsomes are vesicles formed by the self-assembly of sterols, basically chol, and surfactants bearing quaternary-ammonium moiety, even if these components alone in aqueous solutions form crystals and micelles, respectively. These systems have a great potential because feature properties similar to liposomes ones, but they allow to overcome loss of stability and aggregation over time mainly showed by liposomes. In fact, quatsomes are very stable and homogeneous for lamellarity and size, parameters that do not change with temperature or dilution.[77,78] They can be prepared exploiting protocols based mainly on the use of supercritical fluids.[269] As a consequence of their unique characteristics, they can be used in a wide variety of application fields, like nanomedicine[271] or cosmetic and pharmaceutical.[272,273,274,275 276,277,278] For example, it's known that some of these nanovesicles enhance specific bioactivity of proteins and protect them against premature degradation in topical pharmaceutical formulations.[279] In literature is reported an higher antibacterial activity of cetylpyridinium chloride quatsomes on *Staphylococcus aureus* biofilm with respect to micelles of the same surfactant.[280]

[271] Elizondo, E.; Veciana, J.; Ventosa, N. Nanostructuring Molecular Materials as Particles and Vesicles for Drug Delivery, Using Compressed and Supercritical Fluids. *Nanomedicine*, **2012**, 7(9), 1391–1408

[272] Gregoriadis, G. Carrier Potential of Liposomes in Biology and Medicine. *New Engl. J. Med.* **1976**, 295(13), 704−710

[273] Gregoriadis, G. Engineering Liposomes for Drug Delivery: Progress and Problems. *Trends Biotechnol.* **1995**, 13(12), 527−537

[274] Lian, T.; Ho, R. J. Y. Trends and Developments in Liposome Drug Delivery Systems. *J. Pharm. Sci.* **2001**, 90(6), 667−680

[275] Malam, Y.; Loizidou, M.; Seifalian, A. M. Liposomes and Nanoparticles: Nanosized Vehicles for Drug Delivery in Cancer. *Trends Pharmacol. Sci.* **2009**, 30(11), 592−599

[276] Sawant, R. R.; Torchilin, V. P. Liposomes as 'Smart' Pharmaceutical Nanocarriers. *Soft Matter*, **2010**, 6(17), 4026−4044

[277] Whitesides, G. M.; Grzybowski, B. Self-assembly at All Scales. *Science*, **2002**, 295 (5564), 2418−2421

[278] Guida, V. Thermodynamics and Kinetics of Vesicles Frmation Processes. *Adv. Colloid Interface Sci.* **2010**, 161(1−2), 77−88

[279] Ventosa, N.; Cabrera, I.; Veciana, J.; Santana, H.; Martinez, E.; Berlanga, J. A. Vesicles Comprising Epidermal Growth Factor and Compositions That Contain Them. *Cuban Patent Appl.* **2012**, CU2012-0112

[280] Thomas, N.; Dong, D.; Richter, K.; Ramezanpour, M.; Vreugde, S.; Thierry, B.; Wormald P.; Prestidge, C. A. Quatsomes for the Treatment of *Staphylococcus aureus* Biofilm. *J. Mater. Chem. B*, **2015**, 3, 2770-2777

3.4.4 DLS and Zeta potential of the aggregates

TFH

Size and stability of liposomes were evaluated by DLS measurements soon after liposomes preparation and over time. Freshly prepared, all formulations, both in presence or in the absence of UA, showed a bimodal distribution of the diameters with a main peak around 100 nm and a minor population (less than 10% in intensity weighted distribution) with dimensions ranging from 300 nm to 600 nm. This is not surprising because it is known from literature that usually a small population of large vesicles is still present in solution after sonication.[162,281]

As expected, liposomes dimensions did not show any dependence on the molecular structure of the minority component: soon after their preparation, both in presence or in the absence of UA, liposomes showed dimensions around 100 nm as reported in Table 14. In all cases only a slight increase of liposomes dimensions (about 10%) was observed after UA loading, as observed in other cases after UA inclusion.[124]

Table 14. D_H of the investigated formulations in the presence or in the absence of UA. Reported D_H values correspond to the average values over 3 measurements and are obtained from intensity weighted distributions. PDI is lower than 0.2.

Formulation	Without UA (nm)	With UA (nm)
DMPC/chol	92±3	110±4
DMPC/chol/CS **12**	90±5	122±6
DMPC/chol/CS **14**	84±3	114±3
DMPC/chol/CS **16**	75±2	87±2
DMPC/chol/N-ox **12**	80±6	106±4
DMPC/chol/N-ox **14**	85±2	96±4
DMPC/chol/N-ox **16**	92±4	100±5

[281] Zasadzinski, J. A. N. Transmission Electron Microscopy Observations of Sonication-induced Changes in Liposome Structure. *Biophys. J.* **1986**, 49, 1119-1130

All the samples tended to aggregate over time suggesting a low stability of these systems: in two weeks the dimensions of each population tended to increase and the largest population became the most abundant with a diameter of about 1 μm. Only in the presence of N-ox **12** precipitate was observed after one week.
Zeta potential values are reported in Table 15.

Table 15. Zeta potential of the investigated formulations in the presence or in the absence of UA in PBS or in water (data in brackets). All values reported were obtained by the average of 3 consecutive measurements of the same samples.

Formulation	Without UA (mV)	With UA (mV)
DMPC/chol	-2±3 (-2±2)	-4±2 (-5±2)
DMPC/chol/CS **12**	24±4 (44±8)	17±4 (37±8)
DMPC/chol/CS **14**	27±6 (47±13)	22±5 (42±10)
DMPC/chol/CS **16**	33±4 (52±6)	15±3 (35±7)
DMPC/chol/N-ox **12**	4±2 (4±7)	1±2 (1±6)
DMPC/chol/N-ox **14**	28±4 (43±7)	17±6 (37±8)
DMPC/chol/N-ox **16**	19±4 (29±6)	18±5 (28±5)

As expected, we observed a potential around zero for DMPC/chol liposomes and a positive one for DMPC/CS liposomes. Surprisingly, in N-ox containing liposomes, even if they are zwitterionic as DMPC, potentials were positive and quite high, with the exception of liposomes formulated with N-ox **12**. The low potential

observed in the latter case could explain the fact that this formulation showed the lowest stability. The highest zeta potential (similar to cationic liposomes) for N-ox containing liposomes was observed in the case of liposomes formulated with N-ox **14**. The variability in zeta potential values of N-ox containing liposomes demonstrates as the subtle hydrophobic/hydrophilic balance in surfactant structure can significantly influence their properties and confirms that chain length can play a crucial role in determining liposomes properties,[282,283,284] in analogy with what observed for micelles of pure synthetic surfactants.[156] The unexpected zeta potential of DMPC/chol/N-ox liposomes could result from the location at the same side of the pyrrolidinium ring of both the hydrophilic *N*-oxide and hydroxyl moieties. This characteristic could induce a folding of the pyrrolidinium ring that entails the exposure of these two polar moieties to the bulk (Figure 33), as hypothesized in the case of other pyrrolidinium based surfactants.[285] The presence of the strong intramolecular hydrogen bond between the polar *N*-oxide and the hydroxyl groups are favoured by the proximity due to the pyrrolidinium ring and typically observed in *N*-oxide derivatives of *L*-proline,[240] could stabilize this folded conformation. This peculiar topology could cause a variation of lipid bilayer organization and of charge exposure and/or hydration and/or counterion association with a logical consequent influence on the potential of the aggregates in which they are included.

[282] Nagarajan, R. Molecular Packing Parameter and Surfactant Self-Assembly: The Neglected Role of the Surfactant Tail. *Lanmguir*, **2002**, *18*, 31-38

[283] Svenson, S. Controlling Surfactant Self-assembly. *Curr. Opin. Colloid Interface Sci.* **2004**, 9(3-4), 201-212

[284] Jurašin, D.; Habuš, I.; Filipović-Vinceković, N. Role of the Alkyl Chain Number and Headgroups Location on Surfactants Self-assembly in Aqueous Solutions. *Coll. Surf. A Phys. Eng. Asp.* **2010**, 368(1-3), 119-128

[285] Bartoloni , A.; Bombelli, C.; Borocci, S.; Bonicelli, M. G.; Galantini, L.; Giansanti, L.; Ierino, M.; Mancini, G.; Muschietti, A.; Sperduto, C. Synthesis and Physicochemical Characterization of Pyrrolidinium Based Surfactants. *J. Colloid Interface Sci.* **2013**, 392, 297-303

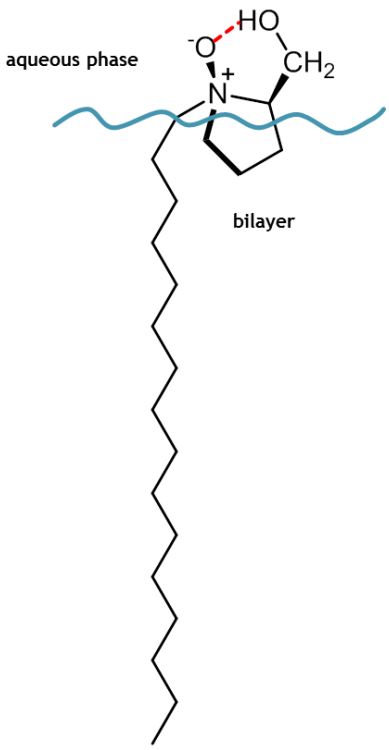

Figure 33. Possible topology of the pyrrolidinium ring of the N-ox in lipid bilayer.

Another aspect that could contribute to explain this anomalous result could be that the high concentration of the sodium cation (abundant in the buffer) in the region of the polar headgroups and its strong interaction with the carbonyl region of the phospholipid membrane.[286] It is reasonable to hypothesize that Na^+ also interact electrostatically with the oxygen of the *N*-oxide moiety, thus partially shielding its negative charge and bringing to a higher potential than the expected one. To verify the veracity of this hypothesis we carried out the same measurement in water. It is evident that the same trend in PBS and in water was observed, thus demonstrating that this explanation is not realistic.

The presence of UA caused a decrease of the zeta potential in the case of DMPC/CS liposomes and of DMPC/N-ox **14** liposomes. This shielding effect (UA is partially deprotonated in the experimental conditions) indicates that in these formulations it is located in the polar headgroup region, in good agreement with what observed in glucosylated cationic liposomes.[124] The fact that UA can penetrate the bilayer (even if not deeply) being negatively charged is not surprising considering that also its

[286] Gurtovenko A. A. Charge Transport in Self-organized π-Stacks of *p*-Phenylene Vinylene Oligomers. *J. Phys. Chem. B*, **2005**, 109(39), 18267-18274

deprotonated form is highly lipophilic because it can delocalize the charge on the aromatic rings.[250] The fact that the inclusion of UA in DMPC/N-ox **12** and DMPC/N-ox **16** liposomes does not interfere with zeta potential values indicates that UA is located in a deeper region of the bilayer, confirming once more that either the nature of the headgroup and chain length can control liposomes properties.

DELOS-Susp liposomes

Dimensions and polydispersity of liposomes prepared by DELOS-Susp were determined by DLS measurements one week after their preparation to allow the rearrangements of bilayer components, according to the common protocol. All formulations showed a monomodal distribution with a hydrodynamic diameter D_H centered at around 100 nm (in the intensity weighted distributions), independently of the synthetic surfactant or the presence of UA (Table 16). Only the formulation DMPC/chol/N-ox **12** showed low reproducibility with the presence of larger aggregates and a high polydispersity index (PDI≈0.6). Moreover, liposomes formulated with mere DMPC and chol were polydisperse (PDI≈0.8) and very large (D_H≈1 μm), evidencing the crucial role of the synthetic micelle-forming surfactant in the liposome formation with this methodology. In contrast to DELOS-Susp, liposomes obtained by THF did not show any major differences in size for the different membrane compositions.[163]

Vesicle size and polydispersity remained unchanged after dialysis. On the other hand, after diafiltration liposomes generally maintained their dimensions, except those containing CS **12** and N-ox **12** (with or without UA). In the latter cases we observed the presence of a second large size population, leading to an increase of the PDI of up to 0.35, and the tendency to precipitate over time. This phenomenon might be related to the pressure applied to the vesicles during diafiltration, which may lead to the expulsion of the less hydrophobic surfactants (*i.e.* those with shorter chain lengths) from the vesicle membrane.

Table 16. D_H and PDI (reported in bracket) of mixed liposomes containing or not UA 1 week after their preparation and prior to diafiltration or dialysis.

Formulation (molar ratio 6/3/1)	Without UA (nm)	With UA in the reactor (nm)	With incubated UA (nm)
DMPC/chol	≈1000 (0.8)	-	-
DMPC/chol/CS **12**	123±5 (0.24)	109±2 (0.25)	126±5 8 (0.24)
DMPC/chol/CS **14**	122±4 (0.21)	99±4 (0.20)	131±4 (0.19)
DMPC/chol/CS **16**	119±6 (0.17)	131±5 (0.15)	128±3 (0.16)
DMPC/chol/N-ox **12**	112±3 (0.25)	197±6 (0.26)	123±2 (0.23)
DMPC/chol/N-ox **14**	135±2 (0.20)	126±2 (0.18)	146±5 (0.21)
DMPC/chol/N-ox **16**	124±5 (0.16)	125±3 (0.15)	131±6 (0.16)

Reported D_H values correspond to the average values over at least three independent measurements, and the errors correspond to the standard deviation among the different measurements.

Moreover, is reported in literature that the presence of N-ox surfactants bearing a C12 chain can break down or destabilize (at low concentrations) the liposomes structure (sometimes the formation of pores is observed).[287,288] Also the vesicle stability over time is dependent on the surfactant chain length: while formulations containing CS **14,** CS **16,** N-ox **14** and N-ox **16** showed no changes in dimension after 6 months and a good homogeneity, vesicles containing CS **12** and N-ox **12** became bigger (D_H≈200 nm) even if they were not treated by diafiltration. Cryo-TEM measurements confirm these observations (Figure 34): while DMPC/chol/CS **12** liposomes one week after the preparation show a homogeneous morphology (Figure 34A), the appearance of large and elongated aggregates is clearly observable after diafiltration (Figure 34B). On the other hand, DMPC/chol/CS **14** liposome morphology is not affected by the diafiltration process (Figure 34C and D).

[287] Huláková, S.; Fulier, B.; Gallová, J.; Balgavý, P. Effect of *N*-dodecyl-*N*,*N*-dimethylamine *N*-oxide on Unilamellar Liposomes *Acta Fac. Pharm. Univ. Comen.* **2013**, 2, 7–13

[288] Karlovská, J.; Lohner , K.; Degovics, G.; Lacko , I.; Dev´ınsky, F.; Balgavý, P. Effects of Non-ionic Surfactants *N*-alkyl-*N*,*N*-dimethylamine-*N*-oxides on the Structure of a Phospholipid Bilayer: Small-angle X-ray Diffraction Study. *Chem. Phys. Lipids*, **2004**, 129, 31–41

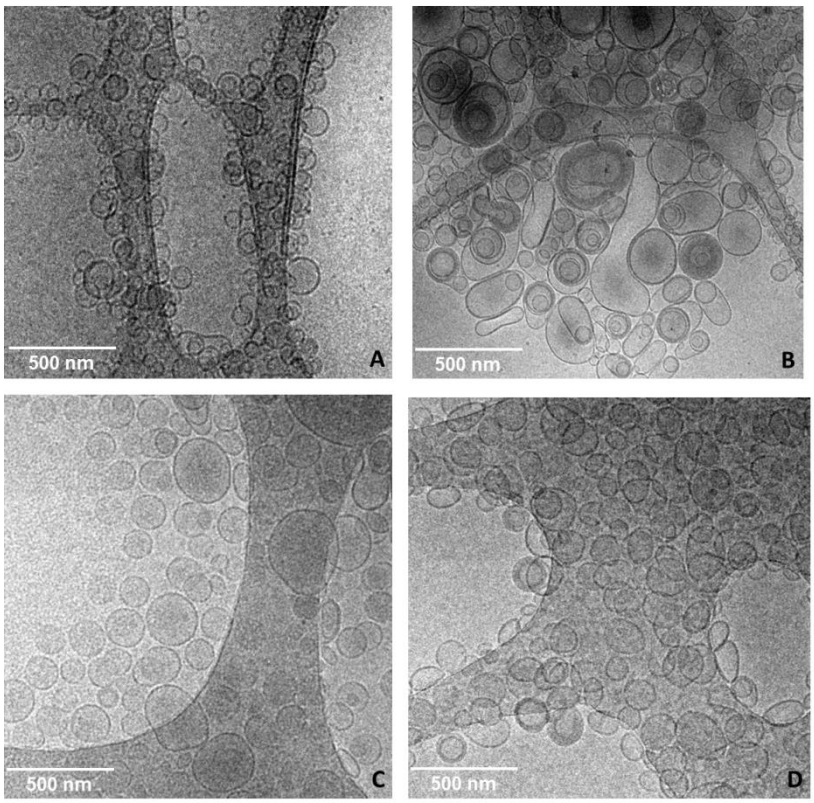

Figure 34. Cryo-TEM images of DMPC/chol/CS **12** one week after their preparation (A) before and (B) after diafiltration and of DMPC/chol/CS **14** one week after their preparation (C) before and (D) after diafiltration.

Considering that all the formulations prepared by TFH tended to aggregate over time,[163] our data confirm that the use of compressed CO_2 allows to achieve more homogeneous, stable and ordered bilayers with respect to TFH, especially in the presence of surfactants bearing longer chains. In fact, compressed fluids fuse the gas-like mass transfer with the liquid-like solvent properties. These features, together with pressure-tunability, grant the production of high-quality vesicles in a one-step process, because pressure variations propagate fast (at the speed of sound) and homogeneously across the solvent, leading to uniform modifications of the fluid density. This obviates the necessity of further modifications required in conventional methods.[269]

Zeta potential values of the investigated mixed liposomes are reported in Table 17. They were in the range of 15-30 mV, even in the presence of N-ox. Only the formulation containing N-ox **12** showed a very low zeta potential, which was similarly observed for liposomes prepared by TFH.[163] The high zeta potential of

zwitterionic formulations (similar to cationic liposomes) containing N-ox could be ascribed to the same reasons mentioned above for TFH liposomes.

The presence of UA in the liposomal formulations caused a decrease of the potential in all cases, likely due to its position in the headgroup area of the membrane surface, result similar to the one observed by TFH.

Table 17. Zeta potential of the investigated liposome formulations in the presence or absence of UA in PBS. Measurements were performed 1 week after liposome preparation.

Formulation (molar ratio 6/3/1)	Without UA (mV)	With UA in reactor (mV)	With incubated UA (mV)
DMPC/chol	-3±2	-	-
DMPC/chol/CS **12**	14±3	12±3	11±3
DMPC/chol/CS **14**	26±5	17±2	18±5
DMPC/chol/CS **16**	27±1	13±4	14±3
DMPC/chol/N-ox **12**	4±2	0±3	1±1
DMPC/chol/N-ox **14**	29±4	15±2	14±4
DMPC/chol/N-ox **16**	21±3	17±3	15±2

The reported values are the average ± standard deviation of 3 independent measurements.

Quatsomes

Dimensions and polydispersity of quatsomes were measured soon after their preparation, after one week (Table 18) and over time as done for DELOS-Susp liposomes.

Table 18. D_H and PDI (reported in bracket) of quatsomes containing or not UA not dialysed. Reported D_H values correspond to the average values over at least three independent measurements. Reported errors correspond to mean of the standard deviation obtained by each independent measurement.

Formulation (5/5)	Without UA (nm)	With UA in the reactor (nm)	With incubated UA (nm)
chol/CS **12**	99±3 (0.17)	110±3 (0.19)	120±2 (0.15)
chol/CS **14**	79±4 (0.19)	82±4 (0.24)	112±1 (0.16)
chol/CS **16**	63±2 (0.23)	55±2 (0.18)	51±3 (0.23)
chol/N-ox **12**	≈1000 (0.63)	≈1000 (0.54)	≈1000 (0.56)
chol/N-ox **14**	83±2 (0.16)	80±2 (0.18)	109±3 (0.12)
chol/N-ox **16**	80±4 (0.23)	191±4 (0.31)	180±4 (0.38)

After one week and in the absence of UA all the samples were monomodal and homogenous and their size was about 70 nm except in the presence of CS **12** (about 100 nm) and N-ox **12** (polidispersed sample, dimensions around 1 μm). The last sample was monodispersed and showed a size of 100 nm soon after the preparation like all the other formulations. After 4 months all the samples remain homogeneous and monodispersed even if their dimensions mostly increased about 30-40 nm except for the formulations containing C16 surfactants.

In the presence of UA both added in the reactor or incubated no differences were observed; only with N-ox **16** we observed liposomes dimensions about 200 nm. Also in this case, after 4 months the dimensions mostly increased of about 50 nm except for the formulations containing CS **16** and N-ox **16**.

The dialysis (performed one week after the preparation) did not affect the sample dimensions except in the presence of CS **12** that showed an increase of the dimensions and of the PDI value together with precipitation one week after dialysis.

Z-potential one week after the preparation were positive and quite high, as expected, for all the samples in the absence of UA with the exception of the formulation containing N-ox **12** (Table 19); these aggregates featured a positive potential around 50 mV soon after the preparation (similarly to CS 12 containing

quatsomes) that turned on negative after one week, thus confirming the low stability of this sample.

Table 19. Zeta potential of the investigated quatsomes with and without UA in water. All values reported were obtained by the average of 3 consecutive measurements of the same samples.

Formulation (5/5)	Without UA (mV)	UA in the reactor (mV)	incubated UA (mV)
chol/CS **12**	+49±2	+55±2	+51±1
chol/CS **14**	+78±3	+73±3	+73±1
chol/CS **16**	+90±1	+86±1	+91±6
chol/N-ox **12**	-40±2	-35±2	-38±2
chol/N-ox **14**	+73±2	+69±2	+65±3
chol/N-ox **16**	+69±3	+81±3	+83±1

In the presence of UA both by incubation and added in the reactor no variations occurred differently from what observed with the analogue liposomes: the high amount of synthetic surfactant (50%) probably in quatsomes masks the effect of the presence of UA. Moreover, the absence of the phospholipid that bears two long chains could make the bilayer slacker with respect to liposomes, allowing UA to deeper penetrate in the hydrophobic region.

All the samples mainly showed a slight decrease (about ten mV) of the potential over time, more prominent (30 mV) in the presence of CS **12**, thus indicating that, despite not as much as the corresponding N-ox **12**, also this surfactant with short chain forms aggregates less stable than the longer ones. Also performing dialysis one week after the preparation we observed a similar decrease of the potential for the sample containing CS **12**, thus confirming the low stability of the formulation.

3.4.5 UA entrapment in the aggregates

TFH

UA was added to preformed liposomes by incubation even if this molecule is a weak acidic compound that could be entrapped exploiting an active loading methodology based on a pH gradient. We used passive loading because we previously demonstrated that the highest E.E. was observed applying this technique (see Chapter 2 section 1.4). The E.E. values of UA in the investigated formulations are reported in Table 20. In all cases similar E.E. values ranging around 50-60% were observed. The fact that DMPC/chol liposomes showed the highest E.E. could be due to their higher bilayer compaction with respect to the other formulations: in fact, these synthetic surfactants, featuring a very different molecular structure with respect to DMPC, could reduce lipid packing (especially in the case of folding of the pyrrolidinium ring), thus lowering the ability of the liposomes membrane to retain the UA molecule.

Table 20. E.E. of UA in the investigated formulations obtained by incubation. The reported values are the average of 3 independent measurements and the errors correspond to standard error of the mean.

Formulation (6/3/1)	E.E. %
DMPC/chol	77±2
DMPC/chol/CS **12**	52±4
DMPC/chol/CS **14**	56±2
DMPC/chol/CS **16**	58±3
DMPC/chol/N-ox **12**	52±2
DMPC/chol/N-ox **14**	55±4
DMPC/chol/N-ox **16**	66±5

DELOS-Susp liposomes

E.E. of UA in the mixed liposomes prepared by DELOS-Susp are reported in Table 21. We studied the impact of adding UA during or after liposome preparation, as

well as the differences due to the technique employed for separating free from entrapped UA (diafiltration *vs* dialysis). Results showed that in general higher E.E. values were obtained when dialysis was employed for removing unentrapped UA (besides DMSO and ethanol), likely because it is performed without applying pressure to the sample, in contrast to the diafiltration process, where the applied pressure may lead to the loss of UA. In particular applying diafiltration, the E.E. was higher if UA was added during liposome preparation than when added to preformed vesicles by incubation. Moreover, in most cases the highest E.E. was observed with liposomes containing the longest surfactants. Probably in these formulations UA is more strongly retained because of the high lipid packing due to more efficient van der Waals interactions. The removal of unentrapped UA by dialysis also leads to higher E.E. if UA was added during the formation process than afterwards (with the exception of liposomes containing CS **12** and CS **14**). In particular, the increase is considerable when vesicles contain N-ox **12** and N-ox **14**. In general, E.E. values were in good agreement with those observed for liposomes prepared by TFH (UA added by incubation, E.E. determined after dialysis). Taken together, these results put in evidence that the E.E. of a solute in the bilayer is influenced by the lipid molecular structure and the encapsulation procedure, but also by the methodology used for its evaluation, reflecting the complex equilibrium among several factors such as the aggregates potential, hydrophilicity/hydrophobicity of the solute, lipid packing and homogeneity

Table 21. Encapsulation efficiency (%) of UA in the investigated formulations.

Formulation (6/3/1)	diafiltration		dialysis	
	E.E. UA in the reactor	E.E. UA incubated	E.E. UA in the reactor	E.E. UA incubated
DMPC/chol/CS **12**	43±3	21±4	49±3	64±3
DMPC/chol/CS **14**	42±4	23±2	69±5	60±4
DMPC/chol/CS **16**	42±4	30±3	54±1	70±3
DMPC/chol/N-ox **12**	28±2	19±2	80±2	38±5
DMPC/chol/N-ox **14**	36±3	14±2	81±4	61±3
DMPC/chol/N-ox **16**	42±5	36±3	60±3	50±2

The reported values are the average of 3 independent measurements and the errors correspond to the standard deviation.

Quatsomes

E.E. of UA in the quatsomes are reported in Table 22. All the formulations showed very high E.E., indicating good permeability of the bilayer. The only exception was the sample containing CS **12** in which UA was included by incubation: in this case the percentage was around 50%. The same formulation showed a different behavior over time and if subjected to dialysis with respect to all the other samples. Moreover, the fact that a low percentage is observed only by incubation of UA suggests a different location of this molecule in the bilayer or a lower permeability changing the methodology of preparation.

An interesting result is that the formulation containing N-ox **12** showed a high E.E. (both adding UA in the reactor or by incubation) even if the Z-potential in the last case was negative.

Table 22. E.E. (percentage) of UA loaded in the investigated quatsomes.

Formulation (5/5)	E.E. of UA in the reactor	E.E. of incubated UA
chol/CS **12**	45±4	99±2
chol/CS **14**	80±3	100±5
chol/CS **16**	96±5	89±3
chol/N-ox **12**	100±4	92±1
chol/N-ox **14**	100±2	100±3
chol/N-ox **16**	98±3	91±2

3.4.6 Antioxidant activity of UA

Several biological properties of UA, such as gastroprotective,[114] cardiovascular[289] and cytoprotective,[114,290] immunoestimulatory,[291] antimicrobial,[292] anti-inflammatory [293] and anticarcinogenic activities[294,295,296] are strictly related to its antioxidant action

[289] Behera, B. C.; Mahadik, N.; Morey, M. Antioxidative and Cardiovascular-protective Activities of Metabolite Usnic Acid and Psoromic Acid Produced by Lichen Species *Usnea Complanata* Under Submerged Fermentation. *Pharm. Biol.* **2012**, 50, 968–979

[290] De Paz, G. A.; Raggio, J.; Gómez-Serranillos, M. P.; Palomino, O. M.; González-Burgos, E.; Carretero, M. E.; Crespo, A. HPLC Isolation of Antioxidant Constituents from *Xanthoparmelia*. *J. Pharm. Biomed. Anal.* **2010**, 53, 165–171

[291] Santos, L. C.; Honda, N. K.; Carlos, I. Z.; Vilegas, W. Intermediate Reactive Oxygen and Nitrogen from Macrophages Induced by Brazilian Lichens. *Fitoterapia*, **2004**, 75, 473–479

[292] Ranković, B.; Kosanić, M.; Stanojković, T.; Vasiljević, P.; Manojlović, N. Biological Activities of *Toninia candida* and *Usnea Barbata* Together with Their Norstictic Acid and Usnic Acid Constituents. *Int. J. Mol. Sci.* **2012**, 13, 14707–14722

[293] Jin, J.Q.; Li, C.Q.; He, L.C. Down-regulatory Effect of Usnic Acid on Nuclear Factor-kappaB-dependent Tumor Necrosis Factor-alpha and Inducible Nitric Oxide Synthase Expression in Lipopolysaccharide-stimulated Macrophages RAW 264.7. *Phytother. Res.* **2008**, 22, 1605–1609

[294] Brisdelli, F.; Perilli, M.; Sellitri, D.; Piovano, M.; Garbarino, J. A.; Nicoletti, M.; Bozzi, A.; Amicosante, G.; Celenza, G. Cytotoxic Activity and Antioxidant Aapacity of Purified Lichen Metabolites: an *in Vitro* Study. *Phytother. Res.* **2013**, 27, 431–437

[295] Marante, F. J. T.; Castellano, A. G.; Rosas, F. E.; Aguiar, J. Q.; Barrera, J. J. B. Identification and Quantitation of Allelochemicals from the Lichen *Lethariella canariensis*: Phytotoxicity and Antioxidative Activity. *Chem. Ecol.* **2003**, 29, 2049–2071

in reducing oxidative damage.[289,295 ,297,298] According to Odabasoglu *et al.*,[114] UA (25, 50, 100, and 200 mg/kg) exerted gastroprotective effects on indomethacin-induced gastric ulcers in rats by reducing oxidative damage. UA also promoted the increase of superoxide dismutase activity, glutathione peroxidase activity, total glutathione and constitutive nitric oxide synthase activities, and through the reduction of catalase, glutathione reductase, lipid peroxidation, inducible nitric oxide synthase and myeloperoxidase activities. Behera, Mahadik, and Morey,[299] studying the cardiovascular protective activity of UA (0.005–0.2 mg/mL), observed moderate to strong antioxidant activity, in a concentration-dependent manner, in the free radical scavenging assay, nitric oxide radical scavenging assay and lipid peroxidation assay (LPO). Strong scavenging activity was likewise verified by Ranković *et al.*[292] in the 2,2-diphenyl-1-picrylhydrazyl (DPPH) reducing power and supraregional assay service (SAS). In this same study, a very strong antimicrobial activity was also detected against bacteria and fungi (*B. mycoides*, *B. subtilis*, *E. coli*, *K. pneumonia*, *S. aureus*, *A. flavus*, *A. fumigatus*, *C. albicans*, *P. purpurescens*, *P. verrucosum*) in the MIC assay. Jin, Li and He,[293] studying the molecular mechanisms responsible for the anti-inflammatory effects of UA (1, 2.5, 5, 10, and 20 μM), showed that this compound presented a dose-dependent inhibitory effect on lipopolysaccharide induced tumor necrosis factor–α and nitric oxide (NO) production in macrophages RAW 264.7. This effect could be associated with decreased synthesis of TNF-α mRNA and inducible nitric oxide synthase protein.[293] Strong cytotoxic action of UA (25–100 μM) was demonstrated in the 3-[4,5-dimethylthiazol-2-yl]- 2,5 diphenyltetrazolium bromide assay, against several human cancer cell lines such as FemX (melanoma), LS174 (colon carcinoma),[292] MCF-7 (breast adenocarcinoma), HeLa (cervix adenocarcinoma), HCT-116 (colon carcinoma),[294] U937 (monocytic leukemia), HL-60 (monocytic leukemia),[295] A2780 (ovarian carcinoma), SK-BR-3 (breast

[296] Bačkorová, M.; Bačkor, M.; Mikeš, J.; Jendželovský, R.; Fedoročko, P. Variable Responses of Different Human Cancer Cells to the Lichen Compounds Parietin, Atranorin, Usnic Acid and Gyrophoric Acid. *Toxicol. In Vitro,* **2011**, 25, 37–44

[297] Polat, Z.; Aydin, E.; Türkez, H.; Aslan, A. *In Vitro* Risk Assessment of Usnic Acid Compound. *Toxicol. Ind. Health,* **2013**, doi:10.1177/0748233713504811

[298] Rabelo, T. K.; Zeidán-Chuliá, F.; Vasques, L. M.; Dos Santos, J. P.; Da Rocha, R. F.; Pasquali, M. A.; Rybarczyk-Filho, J. L.; Araújo, A. A.; Moreira, J. C.; Gelain, D. P. Redox Characterization of Usnic Acid and its Cytotoxic Effect on Human Neuron-like Cells (SH-SY5Y). *Toxicol. In Vitro,* **2012**, 26, 304–314

[299] Dévéhat, F.; Tomasi, S.; Elix, J.A.; Bernard, A.; Rouaud, I.; Uriac, P.; Boustie, J. Stictic Acid Derivatives from the Lichen *Usnea articulata* and Their Antioxidant Activities. *J. Nat. Prod.* **2007**, 70, 1218–1220

adenocarcinoma), HT-29 (colon adenocarcinoma), HCT-116 p53−/− (colon carcinoma p53-null subline) and Jurkat (T cells lymphocyte leukaemia).[296] This action can be determined by pro-apoptotic activity, supported by the suppression of viability and cell proliferation, that correlated more strongly with an increased number of floating cells. Moreover, cell cycle distribution can present a variation, revealing an accumulation of cells in S-phase.[296] Nevertheless, Ranković *et al.*,[292] observed pro-apoptotic effects correlated with an increase in the number of cells in the sub-G1 phase, while the percentage of cells in the S-phase and G2/M phase remained unchanged compared to the controls, supporting a G1 phase arrest mechanism. These results provide scientific data supporting potential use of UA in the treatment of several types of cancer. On the other hand, protective effects were found by De Paz *et al.*[290] against hydrogen peroxide-induced damage in U373 MG cells (human glioblastoma astrocytoma). UA showed a strong antioxidant capacity in the oxygen radical absorbance capacity assay, indicating significantly reduced radical oxygen species (ROS) production. These data indicate that UA (5–50 μg/mL) could act as an antioxidant agent against neurodegenerative disorders associated with oxidative damage, such as Alzheimer's and Parkinson's disease. In a study by Santos *et al.*,[291] usnic acid induced the greatest release of NO in peritoneal macrophages, promoting an immunostimulatory effect. Polat *et al.*,[289] assessing the genotoxic and antioxidant effects of UA in human blood cells, observed that UA did not induce mutagenic effects on human lymphocytes, and increased total antioxidant capacity (TAC) at low doses (1 and 5 μg/mL) and in total oxidative status, at a high dose (200 μg/mL). However, at this high dose, UA significantly decreased TAC levels. Conversely, no antioxidant action of UA was observed by Dévéhat *et al.*[299] and Thadhani *et al.*[300] on the DPPH assay. The radical-scavenging effect of antioxidants on DPPH is a simple and reliable method to quantify the hydrogen donating potency of chemicals. Since no activity of UA was observed in the DPPH, it does not seem to have labile hydrogen atoms. As for the contradictory data in the LPO assay, the different concentrations utilized could have influenced the test results. Furthermore, in a study conducted by Rabelo *et al.*,[297] who tested the

[300] Thadhani, V. M.; Choudhary, M. I.; Ali, S.; Omar, I.; Siddique, H.; Karunaratne, V. Antioxidant Activity of Some Lichen Metabolites. *Nat. Prod. Res.* **2011**, 25, 1827–1837

UA redox properties against different reactive species (RS) generated in vitro, and evaluated its action on SH-SY5Y neuronal-like cells upon H_2O_2 exposure, it was observed that UA could display significant antioxidant properties in the total antioxidant potential / total antioxidant reactivity and OH radical scavenging activity tests. It also induced cell detachment and loss of viability of SH-SY5Y cells at higher concentrations (20 μg/mL) alone or in the presence of H_2O_2 or 1% of fetal bovine serum, related to the increase of intracellular ROS, inducing an oxidative stress scenario, potentiated in the presence of H_2O_2. The pro-oxidant properties in biological systems might be responsible for the potential neurotoxicological effects of UA. The heterocyclic structure composed by conjugated dienes and polar OH groups of UA suggests that this molecule is able to act as a redox-active agent, thus interacting with different RS as observed in some *in vitro* assays by the works described above. Nonetheless, the results observed in different biological experiments indicate that UA may exert either pro-oxidant or antioxidant effects in different cell types and tissues, thus other mechanisms such as modulation of antioxidant enzymes and cell detoxification systems must be further investigated to address the mechanism of its redox actions. Also, UA may influence the polarity of the inner mitochondrial membrane,[301] which may be reflected in changes in basal RS production to varying degrees in different cell types. As the profile of mitochondria expression and activity varies according the cell type, the effect of UA on mitochondrial integrity and activity should be further investigated in the different cell models studied.

3.4.7 Evaluation of antioxidant activity of free or loaded UA by $ABTS^{\cdot+}$ methodology

TFH

The antioxidant activity of UA entrapped in liposomes was evaluated according to a procedure described in the literature by using $ABTS^{\cdot+}$,[239] which is reduced (with a consequent fading of the solution from green to transparent) at a rate that depends

[301]Bessadottir, M.; Egilsson, M.; Einarsdottir, E.; Magnusdottir, I. H.; Ogmundsdottir, M. H.; Omarsdottir, S.; Ogmundsdottir, H. M. Proton-shuttling Lichen Compound Usnic Acid Affects Mitochondrial and Lysosomal Function in Cancer Cells. *PLoS One*, **2012**, 7, 51296.

on the antioxidant effectiveness of the system. The degradation of $ABTS^{\bullet+}$ as a function of time was followed by monitoring the absorbance at 417 nm in the presence or in the absence of UA entrapped in liposomes or free UA (Figure 35A). The acetate buffer also contains NaCl 150 mM to avoid liposomes rupture due to osmotic shock because for their preparation we used PBS 150 mM. The UV measurements were performed at pH 5.5 in order to obtain a low (but valuable) free $ABTS^{\bullet+}$ degradation rate (red dashed line).

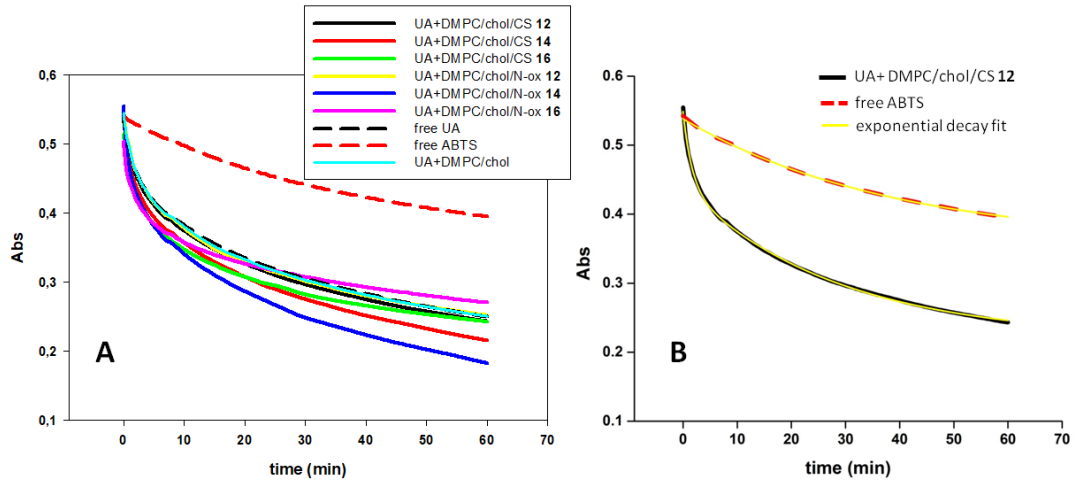

Figure 35. (A) Kinetic measurements of $ABTS^{\bullet+}$ degradation determined by monitoring the absorbance at 417 nm in the presence or in the absence of free or liposomal UA. The reported curves are the average of at least 3 independent measurements. (B) Fit (yellow traces) to the absorbance curves in the absence (red dashed trace) or in the presence of UA entrapped in DMPC/chol/CS **12** liposomes (black trace) reported as an example.

The degradation of $ABTS^{\bullet+}$ itself leads to a simple exponential decay ($y = y_0 + A_{ABTS} \cdot \exp(-t/\tau_{ABTS})$), while all samples containing UA show two processes ($y = y_0 + A_{UA} \cdot \exp(-t/\tau_{UA}) + A_{ABTS} \cdot \exp(-t/\tau_{ABTS})$.

As expected, the presence of free UA (black dashed trace) strongly increases the degradation rate of $ABTS^{\bullet+}$ due to the well-known antioxidant properties of UA. [246,247] When UA was formulated in liposomes containing the surfactants bearing the alkyl chain with 14 carbons, mostly N-ox **14**, the antioxidant activity was increased significantly. On the other hand, if UA is included in liposomes containing CS **16** or N-ox **16**, after an initial burst common to the other samples, its antioxidant activity is slightly slowed down, and in the case of DMPC/chol and DMPC/chol/CS **12**(N-ox **12**) liposomes the antioxidant activity is comparable to that of free UA.

Our data indicates that the length of the chain has a greater impact on the antioxidant efficacy of liposomal UA than the charge of the polar headgroup. This influence of the chain length could be ascribed to a different accessibility of $ABTS^{\cdot+}$ to UA and/or to a different location of UA in the bilayer. These results could also be partially explained considering that both DMPC (the major liposomes component) and the surfactants CS **14** and N-ox **14** bear chains of 14 methylenes. The mismatch in chain length liposomes components that occur in the other cases can affect lipid organization[167] and/or the exposure of the charged polar headgroups,[125,302,303] confirming the influence of this feature, and in general of monomer chain length, on liposome properties. The differences of zeta potential values of N-ox containing liposomes indicate that the polarity of the microenvironment of the headgroup region can vary among the different formulations. As reported in literature, the antioxidant effectiveness is strictly dependent on the microenvironment.[238,250] In particular, the fact that in the case of UA the oxidation rate increases as a function of the polarity of the medium[250] could contribute to the highest antioxidant activity of UA observed in DMPC/chol/N-ox **14** liposomes. It is interesting that in the case of micelles of pure synthetic surfactants the nature of the polar headgroup rather than chain length seems to play a major role in affecting the antioxidant activity of UA, indicating the complex crucial effect of the incorporating aggregates.[239] To deepen our understanding of the investigated process, kinetics curves were fitted with an exponential decay by two processes (equation reported in the experimental section), related to the spontaneous degradation of free $ABTS^{\cdot+}$ and the reaction between $ABTS^{\cdot+}$ and our systems containing UA. The time constant τ_{ABTS} was determined by fitting the temporal evolution of the absorption of free $ABTS^{\cdot+}$ with a simple exponential decay ($y = y_0+A_{ABTS}\cdot\exp(-t/\tau_{ABTS})$).

This analysis allows exploring more in the detail the initial phases of the oxidation process in which most part of the oxidation occurs. The fit to the data of free $ABTS^{\cdot+}$ and of UA entrapped in DMPC/chol/CS **12** liposomes are reported as an example in Figure 35B and the obtained τ_{UA} values are shown in Figure 36.

[302] Goodwin, G. C.; Hammond, K.; Lyle, I. G.; Jones, M. N.; Lectin-mediated Agglutination of Liposomes Containing Glycophorin Effects of Acyl Chain Length. *Biochim. Biophys. Acta*, **1982**, 689, 80–88

[303] Yun, H.; Choi, Y. W.; Kim, N. J.; Sohn, D. Physicochemical Properties of Phosphatidylcholine (PC) Monolayers with Different Alkyl Chains, at the Air/Water Interface. *Bull. Korean Chem. Soc.* **2003**, 24(3) 377-383

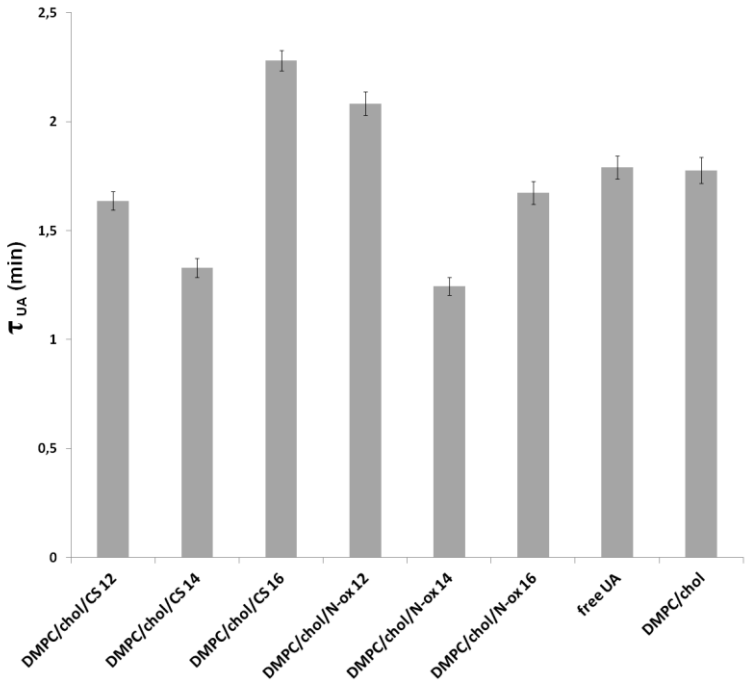

Figure 36. Comparison of τ_{UA} relative to of $ABTS^{\bullet+}$ degradation curve in the presence of free UA or liposomal UA. The reported errors correspond to the standard error obtained from the fit.

In agreement with the results obtained by kinetic curves, the fastest initial catalytic effect was obtained using liposomes containing CS **14** and N-ox **14** (the time constant τ_{UA} is reduced of ≈ 30% compared with free UA). On the other hand, the slowest oxidation occurred with liposomes including CS **16**. As previously mentioned, it is possible that in this case UA is less accessible and then less disposable to react with $ABTS^{\bullet+}$. Also in the case of DMPC/chol/N-ox **12** a slow reaction rate was observed, but reasonably this result can be ascribed to the low potential that reduces the electrostatic interactions with anionic UA. The analysis of the amplitude of the curves puts in evidence that liposomal UA contributes to $ABTS^{\bullet+}$ reduction at ≈ 30% in all cases similarly to what observed with free UA (Figure 38, right).

DELOS-Susp liposomes

In the same way the antioxidant activity of UA loaded in liposomes prepared by DELOS-Susp was investigated. As expected, the slow degradation rate of the free

radical cation was enhanced by the presence of the free UA. On the other hand, when UA was loaded in liposomes (both added during and after liposome formation) all curves were similar to the one obtained with the free radical cation alone in solution, independently from the liposome composition (Figure 37).

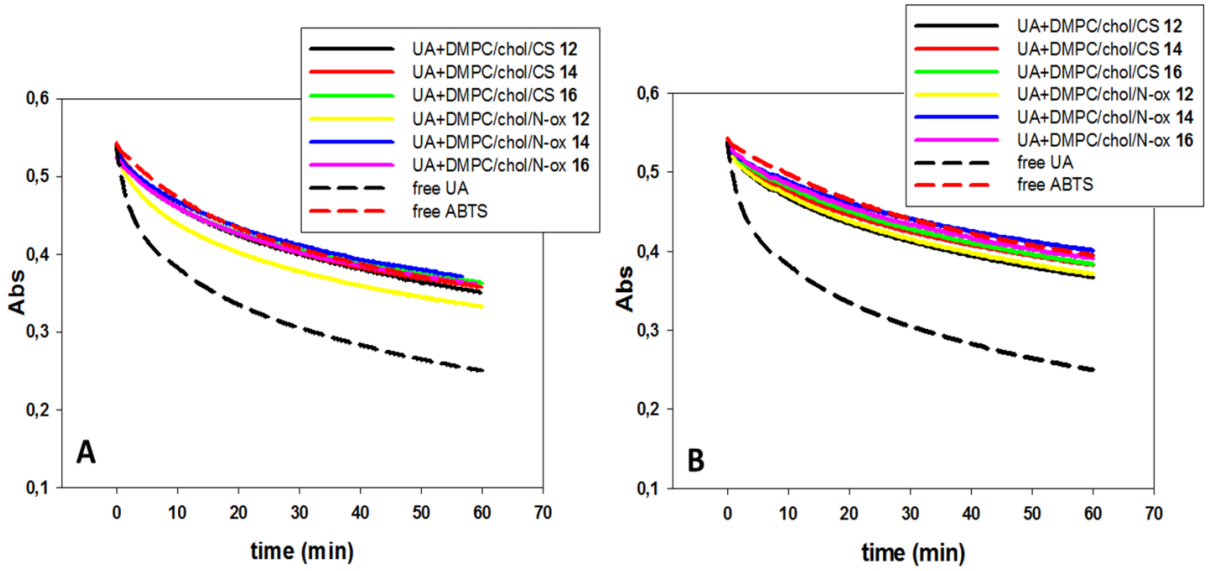

Figure 37. Kinetic measurements of $ABTS^{\bullet+}$ degradation at 417 nm in the presence or in the absence of free or liposomal UA (A) added in the reactor or (B) incubated with preformed liposomes.

For a more quantitative analysis of the antioxidant activity, it must be considered that two simultaneous processes occur, namely the degradation of free $ABTS^{\bullet+}$ and its reaction with UA, each with a characteristic time constant, as mentioned above. The obtained contribution of UA to the reduction of $ABTS^{\bullet+}$ (*i.e.* the relative change in absorbance, A_{UA}/A_{tot}) and the time constant τ_{UA} are reported in Figure 38, together with the values obtained for UA included in liposomes prepared by TFH. Compared to free UA and UA included in liposomes prepared by TFH, UA included in liposomes prepared by DELOS contributes significantly less to the reduction of $ABTS^{\bullet+}$, independently of the inclusion procedure of UA and the molecular structure of the liposome components. Thus, $ABTS^{\bullet+}$ interacts only marginally with UA when included in liposomes prepared by DELOS, and liposomal UA cannot exert its antioxidant action, differently from UA loaded in the same formulations prepared by TFH. It is reasonable to hypothesize that the homogeneous liposomes prepared using DELOS-Susp methodology are

characterized by a very high compaction of the bilayer (consistent with the high stability observed). As a consequence, it is possible that $ABTS^{\cdot+}$ cannot penetrate in the bilayer to reach UA. This aspect confirms that liposomes of identical composition can show different characteristics as a function of the methodology used for their preparation.

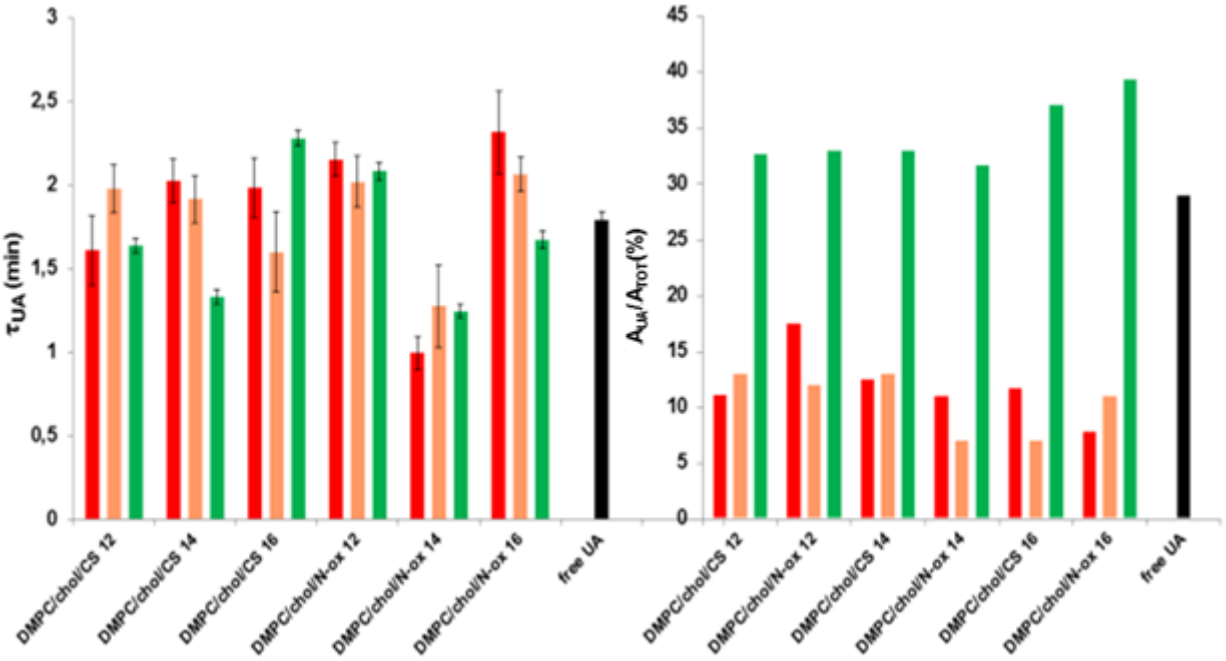

Figure 38. Characteristic time constant τ_{UA} (left) and total contribution (right) of UA to the degradation of $ABTS^{\cdot+}$. Comparison of free UA (black bar) with UA added to liposomes prepared by DELOS-Susp after vesicle preparation (orange bars), during vesicle preparation (red bars) or added to liposomes prepared by TFH after vesicle preparation (green bars). Standard errors of τ_{UA} shown in the graph are obtained from the fit. For A_{UA}/A_{tot} (%) standard errors are smaller than 1%.

Once UA gets to interact with $ABTS^{\cdot+}$, the rate of reduction (related to the time constant τ_{UA}) does not show significant differences between adding UA during or after liposome preparation. Regarding differences in liposome composition, only liposomes containing N-ox **14** consistently show a significantly higher reduction rate, independently of the preparation process. On the other hand, the slowest reduction occurred with liposomes containing N-ox **16** and not CS **16** like for TFH. These differences confirm that also the reduction process can be affected by the liposome preparation methodology.

Quatsomes

Also in the case of quatsomes, the antioxidant activity of loaded UA (both by incubation and adding it in the reactor) was evaluated following the degradation of $ABTS^{\bullet+}$ over time (Figure 39).

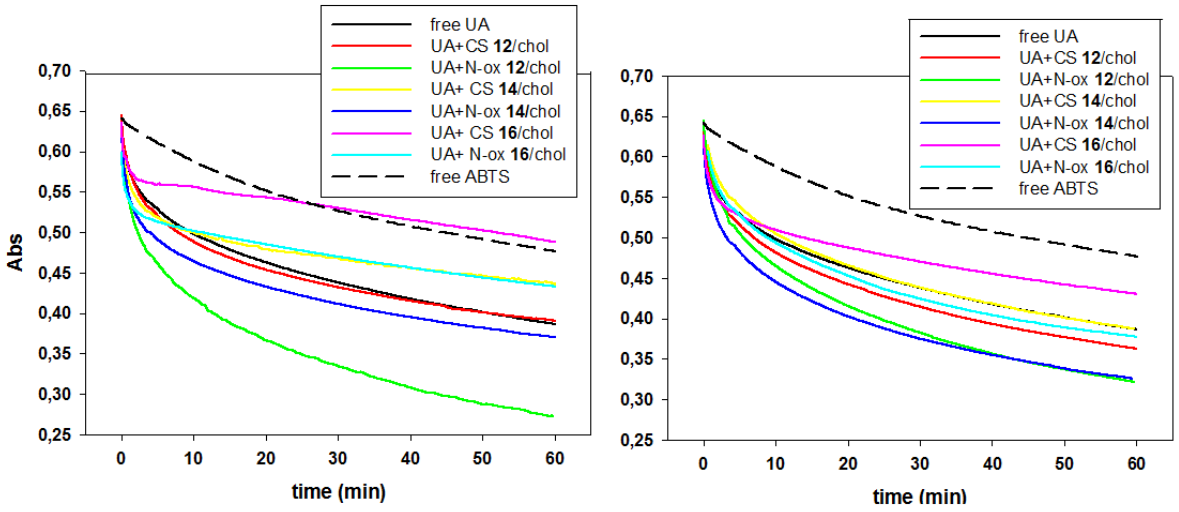

Figure 39. Kinetic measurements of $ABTS^{\bullet+}$ degradation at 417 nm in the presence or in the absence of free or quatsomal UA incubated (left) with preformed quatsomes or added in the reactor (right).

In general, we observed that at the same chain length N-oxs increase UA antioxidant activity more than the corresponding CSs. It's important to consider that in these samples the synthetic surfactant is present at the 50% together with chol in the absence of natural phospholipid (unlike analogue liposomes): probably in this case the major role is played by the charge of the polar headgroup. The best results were obtained in the presence of the shorter chain lengths, in particular with N-ox **12** and **14**. The same trend was observed both by incubation and adding UA in the reactor (Figure 39, left and right respectively) but by incubation the increase in the $ABTS^{\bullet+}$ degradation rate due to the presence of N-ox **12** was more evident, suggesting a different arrangement and/or compaction of the bilayer changing the procedure of UA loading. For the samples containing C16 chains the trend was respected but complex phenomenona occurred. In fact, to better understand these aspects we also fitted all the curves, as done for liposomes, with an exponential decay by two processes considering that one of them is the spontaneous degradation of free $ABTS^{\bullet+}$ too. In general, we observed that in water the rate of the $ABTS^{\bullet+}$ degradation without UA is 34.4 min, differing from what observed before in

PBS (28.2 min), suggesting that probably the presence of salts can strongly influence the oxidation reaction.[304] In particular, in the presence of C16 chains, especially for incubated samples, it's possible to fit the curves with a third order exponential decay suggesting the co-presence of other unexpected processes.

The time constants $\tau_{UA,}$ reported in Figure 40, showed (where it was possible to calculate them) that mainly the degradation process in the presence of quatsomes was very fast during the first minutes and after became slower than before (maintaining the differences observed in the curves). As observed in the case of liposomes prepared by TFH, UA contributes for about 30-40% to the process (Figure 40), especially for incubated samples.

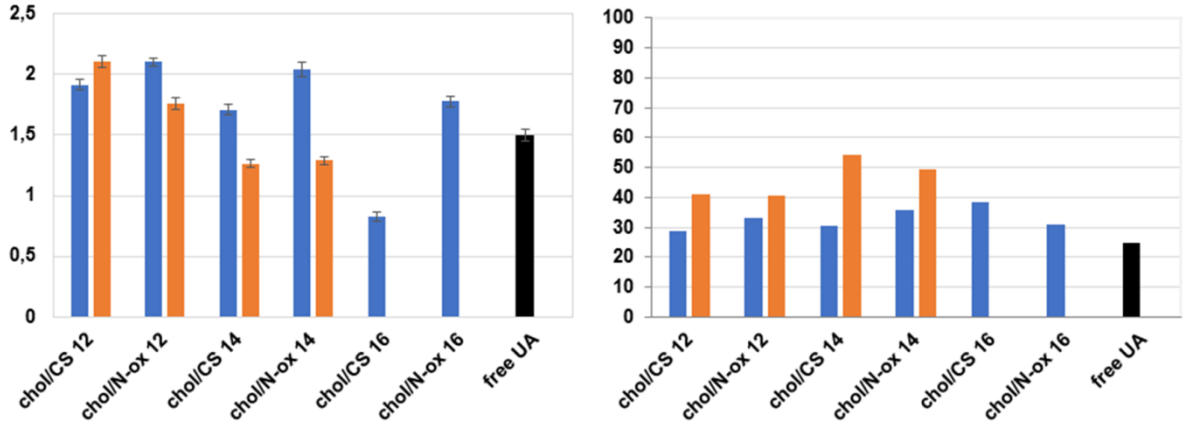

Figure 40. Characteristic time constant τ_{UA} (left) and total contribution (right) of UA to the degradation of $ABTS^{\cdot+}$.Comparison of free UA (black bar) with UA added to quatsomes after vesicle preparation (orange bars) or during vesicle preparation (blue bars). Standard errors of τ_{UA} shown in the graph are obtained from the fit. For A_{UA}/A_{tot} (%) standard errors are smaller than 1%.

3.4.8 Evaluation of the antimicrobial/antifungal activity of quatsomes

The antibacterial activity of quatsomal formulations devoid of UA (except chol/N-ox **12** that was polidispersed) was evaluated on Methicillin resistant *Staphylococcus aureus (Gram +)*, on *Escherichia Coli (Gram -)* bacterial strains and on a *Candida*

[304] Budilarto, E. S.; Kamal-Eldin, A. The Supramolecular Chemistry of Lipid Oxidation and on *Escherichia Coli* Antioxidation in Bulk Oils. *Eur. J. Lipid Sci. Technol.* **2015**, 117(8), 1095–1137

Albicans fungal strain. On *Staphylococcus aureus* formulations containing CS **12**, CS **16** and N-ox **16** showed **a** minimum inhibitory concentration (MIC) about 10^{-4} M whereas samples containing CS **14** and N-ox **14** showed a MIC about 10^{-5} M. On *Escherichia Coli* in the presence of surfactants bearing C14 or C16 chains the observed MIC was about 10^{-4} M whereas the formulation chol/CS **12** was not active at similar concentrations. On *Candida Albicans* we did not observe any effect due to the presence of the investigated formulations except in the case of chol/CS **16** where a small growth reduction was observed. Further investigations on analogue formulations containing UA are in progress to evaluate an eventual synergistic effect.

3.5 Conclusions

The effect of charge and chain length of structurally related N-oxs and CSs on their aggregation and physicochemical properties were fully investigated. In particular, a neat dependence of antioxidant efficacy on the surfactant chain length, charge and of the lipophilicity of the solute was observed. In the case of *L*-prolinol derivatives micelles these differences can be explained by taking into consideration the effects of the polarity of the microenvironment of the antioxidant, on its polarizability and its location in the aggregates, on the pH of the solution and, in the case of UA, also on the coexistence of different tautomeric species in dynamic balance. As a whole, the micellar effects on the reaction can be interpreted in terms of subtle and complex equilibria among repulsive and attractive interactions between molecules (surfactants and antioxidant).

Also mixed liposomes containing DMPC, chol and one among the synthetic CSs or their corresponding N-Ox were investigated with respect to their physicochemical properties and their ability of influencing the antioxidant effectiveness of UA. Our investigation points out that, more than the charge *or* the chain length, the *combination* of both these parameters is fundamental. In particular, a synergistic effect between C14 chain length and the *N*-oxide moiety -less relevant with the cationic analogue- confirm the potentiality of N-ox in enhancing the antioxidant

properties of the included solute when liposomes are prepared by TFH.[163] Our results also confirm that even subtle variations of molecular structure of liposomes components can palpably affect their physicochemical properties. As a consequence, even considering an analogous series-based scaffold, it is possible to modulate the properties of the aggregates they form or in which they are included to optimize them for specific application areas by changing the length of the hydrophobic chains or functionalizing the hydrophilic moiety. Some of these investigated formulations show a good potentiality as UA delivery systems, despite their relatively low stability. On the other hand, if liposomes were prepared by DELOS-Susp we observed long-lasting stability and high homogeneity, differently from what was observed using TFH, and that, besides the preparation technique, also the procedure used to remove the unentrapped solute (hydrophobic UA in this case) can affect liposome properties such as E.E. or stability. Moreover, from our analysis the picture of a high compaction of the bilayer of liposomes prepared with DELOS-Susp clearly emerges, likely contributing to their noticeable stability.

A similar stability but a lower lipid compaction were observed investigating the corresponding quatsomes. The differences observed with respect to liposomes prepared with the same methodology put in evidence that, despite similar vesicular organization, stability and homogeneity, lipid packing, and consequently the ability to interact with a solute, are different.

Chapter 4

Polydiacetylenic liposomes

4.1 Introduction

The development of fluorescent and colorimetric sensors for the efficient detection of chemically, biologically and environmentally important molecules has attracted continuous attention in the past years.[305,306,307] Compared to small molecule-based[308,309,310] and nanoparticle-based[311,312] sensors, conjugated polymer-based sensors have several advantages, such as enhanced binding efficiency, amplified signal output, improved stability, easy fabrication into devices, *etc.*[313,314] Polydiacetylenes, (PDAs) a unique class of conjugated polymeric materials that combines highly ordered backbones with customizable side chains, have been extensively studied ever since the first preparation by Wegner in 1969.[315] PDAs are usually prepared from the 1,4-addition of diacetylene monomers initiated by ultraviolet (UV) or γ light irradiation, which generates the polymeric backbone with

[305] Jung, H. S.; Chen, X.; Kim, J. S.; Yoon, J. Recent Progress Inluminescent and Colorimetric Chemosensors for Detection of Thiols. *Chem. Soc. Rev.* **2013**, 42, 6019−6031

[306] Zhou, Y.; Xu, Z.; Yoon, J. Fluorescent and Colorimetric Chemosensors for Detection of Nucleotides, FAD and NADH: Highlighted Research During 2004−2010. *Chem. Soc. Rev.* **2011**, 40, 2222−2235

[307] Kim, H. N.; Ren, W. X.; Kim, J. S.; Yoon, J. Fluorescent and Colorimetric Sensors for Detection of Lead, Cadmium, and Mercury Ions. *Chem. Soc. Rev.* **2012**, 41, 3210−3244

[308] Peng, Y.; Zhang, A. J.; Dong, M.; Wang, Y. W. A Colorimetric and Fluorescent Chemosensor for The Detection of an Explosive–2,4,6-trinitrophenol (TNP). *Chem. Commun.* **2011**, 47, 4505−4507

[309] Guo, Z.; Song, N. R.; Moon, J. H.; Kim, M.; Jun, E. J.; Choi, J.; Lee, J. Y.; Bielawski, C. W.; Sessler, J. L.; Yoon, J. A Benzobisimidazolium-based Fluorescent and Colorimetric Chemosensor for CO_2. *J. Am. Chem. Soc.* **2012**, 134, 17846−17849

[310] Yang, Y. K.; Tae, J. Acridinium Salt Based Fluorescent and Colorimetric Chemosensor for the Detection of Cyanide in Water. *Org. Lett.* **2006**, 8, 5721−5723

[311] Aldewachi, H.; Chalati, T.; Woodroofe, M. N.; Bricklebank, N.; Sharrack, B.; Gardiner, P. Gold Nanoparticle-based Colorimetric Biosensors. *Nanoscale*, **2018**, 10, 18−33

[312] Bigdeli, A.; Ghasemi, F.; Golmohammadi, H.; Abbasi-Moayed, S.; Nejad, M. A. F.; Fahimi-Kashani, N.; Jafarinejad, S.; Shahrajabian, M.; Hormozi-Nezhad, M. R. Nanoparticle-based Optical Sensor Arrays. *Nanoscale*, **2017**, 9, 16546−16563

[313] Kim, H. N.; Guo, Z.; Zhu, W.; Yoon, J.; Tian, H. Recent Progress on Polymer-based Fluorescent and Colorimetric Chemosensors. *Chem. Soc. Rev.* **2011**, 40, 79−93

[314] Li, C.; Numata, M.; Takeuchi, M.; Shinkai, S. A Sensitive Colorimetric and Fluorescent Probe Based on a Polythiophene Derivative for the Detection of ATP. *Angew. Chem.* **2005**, 44, 6371−6374

[315] Wegner, G. Topochemische Reaktionen von Monomeren mit Konjug Ierten Dreifachbindungen. *Z. Naturforsch. B. J. Chem. Sci.* **1969**, 24, 824−832

alternating C=C and C≡C bonds (*ene-yne*, Figure 41). The ease of their preparation ensures the purity of the resulting polymer and is simpler than the synthesis of most of the covalent polymers that occur *via* chemical reactions at high temperatures, chemical initiators, catalysts, or heating. The precondition for the successful topochemical polymerization of diacetylenes is that they must be self-assembled to meet specific geometrical parameters. An optimal packing orientation of the diacetylene units is required to promote propagation of the liner chain through the ordered phase. Polymerization of diacetylenes stabilizes the physical structure, enhances the thermal stability and reinforces the mechanical stability of the system.[316]

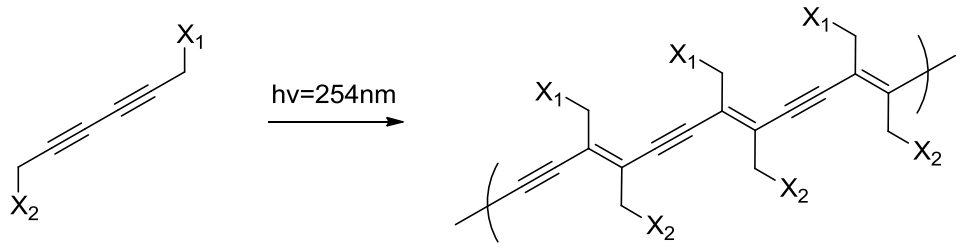

Figure 41. Schematic representation of diacetylenes polymerized by UV irradiation.

The most meritorious aspect of PDAs is their unique optical feature, originating from the existence of extensively delocalized π-electron networks and conformational restrictions along the main backbone. It has been shown that in most cases, PDAs show an absorption peak at ~640 nm due to electron delocalization within the conjugated backbone, which appears visually as an intense blue color. Upon interaction with external stimuli, the main absorption peak shifts hypsochromically to ~540 nm and exhibits a red color, which can be easily detected by the naked eye. The detailed mechanism for the color transition remains to be fully elucidated. It is usually presumed that the conformational change of the polymer backbone from planar to nonplanar upon stimulation contributes to the

[316] Sheth, S. R.; Leckband, D. E. Direct Force Measurements of Polymerization-dependent Changes in the Properties of Diacetylene Films. *Langmuir*, **1997**, 13, 5652−5662

blue-shift in the spectra.[317,318] In addition, the blue phase PDAs are not fluorescent, while in the red phase, a red fluorescence with negligible bleaching is usually observed. This is suggested to be the result of an energy shift in the lowest excited state from the blue phase to the red phase. Therefore, a PDA-based system has dual-signal outputs when it is being used as a sensing platform. It is widely accepted that the alkyl chain length, the position of the butadiyne moiety in the molecule, and the polar head have a pronounced impact on self-assembly behaviors of diacetylenes[319,320] and the optical properties of PDAs, *i.e.*, the blue-to-red colorimetric transition along with an enhancement of fluorescence upon interaction with various *stimuli*.[321,322] Ever since the first report involving a sialic acid-modified PDA as a selective sensor for influenza virus presented by Charych et al. in 1993,[323] PDA-based sensors have attracted the attention of scientists, yielding in a variety of reports PDAs as chemo/biosensing materials based on their colorimetric and fluorescent transition. To date, the stimuli that are able to induce the optical transition of PDAs come in numerous forms, such as solvents (solvatochromism),[324] heat (thermochromism),[325] mechanical stress (mechanochromism),[326] light (photochromism),[327] pH,[328,329] metal ions,[330,331] anions,[332] surfactants,[333,334]

[317] Carpick, R. W.; Sasaki, D. Y.; Marcus, M. S.; Eriksson, M. A.; Burns, A. R. Polydiacetylene Films: a Review of Recent Investigations into Chromogenic Transitions and Nanomechanical Properties. *J. Phys. Condens. Matter,* **2004**, 16, 679−697

[318] Jelinek, R.; Ritenberg, M. Polydiacetylenes − Recent Molecular Advances and Applications. *RSC Adv.* **2013**, 3, 21192−21201

[319] Menzel, H.; Horstmann, S.; Mowery, M. D.; Cai, M.; Evans, C. E. Diacetylene Polymerization in Self-assembled Monolayers: Influence of the Odd/Even Nature of the Methylene Ppacer. *Polymer*, **2000**, 41, 8113−8119

[320] Aoki, K.; Kudo, M.; Tamaoki, N. Novel Odd/Even Effect of Alkylene Chain Length on the Photopolymerizability of Organogelators. *Org. Lett.* **2004**, 6, 4009−4012

[321] Charoenthai, N.; Pattanatornchai, T.; Wacharasindhu, S.; Sukwattanasinitt, M.; Traiphol, R. Roles of Headgroup Architecture and Side Chain Length on Colorimetric Response of Polydiacetylene Vesicles to Temperature, Ethanol and pH. *J. Colloid Interface Sci.* **2011**, 360, 565−573

[322] Khanantong, C.; Charoenthai, N.; Phuangkaew, T.; Kielar, F.; Traiphol, N.; Traiphol, R. Phase Transition, Structure and Color Transition Behaviors of Monocarboxylic Diacetylene and Polydiacetylene Assemblies: the Opposite Effects of Alkyl Chain Length. *Colloids Surf. A,* **2018**, 553, 337−348

[323] Charych, D.; Nagy, J.; Spevak, W.; Bednarski, M. Direct Colorimetric Detection of a Receptor-ligand Interaction by a Polymerized Bilayer Assembly. *Science*, **1993**, 261, 585−588

[324] Chance, R. R. Chromism in Polydiacetylene Solutions and Crystals. *Macromolecules*, **1980**, 13, 396−398

[325] Chance, R. R.; Baughman, R. H.; Muller, H.; Eckhardt, C. J. Thermochromism in a Polydiacetylene Crystal. *J. Chem. Phys.* **1977**, 67, 3616−3618

[326] Nallicheri, R. A.; Rubner, M. F. Investigations of the Mechanochromic Behavior of Poly(urethane-diacetylene) Segmented Copolymers. *Macromolecules,* **1991**, 24, 517−525

[327] Chen, X.; Hong, L.; You, X.; Wang, Y.; Zou, G.; Su, W.; Zhang, Q. Photo-controlled Molecular Recognition of Alpha Cyclodextrin with Azobenzene Containing Polydiacetylene Vesicles. *Chem. Commun.* **2009**, 1356−1358

microorganisms,[335,336,337] and biomolecules[338,339,340,341,342,343,344] which have greatly broadened the applications of PDAs as versatile sensing materials in various fields. Even though the exact mechanism of the optical transition of PDAs induced by external stimuli remains debatable, it is widely accepted that the pendant side chains of PDAs play a significant role in the optical transition. Specifically, the interactions between the side chains themselves as well as the interaction between functional groups (headgroups) on the side chains and the stimuli prominently influence the overall conformation of the polymer chain, thus leading to the optical change. The interaction between the side chains can be manipulated by adjusting their integral topological structure, including the length of the alkyl chain, the position of the butadiyne group, and the type of headgroup, which is crucial for

---

328 Song, J.; Cheng, Q.; Kopta, S.; Stevens, R. C. Modulating Artificial Membrane Morphology: pH-induced Chromatic Transition and Nanostructural Transformation of a Bola Amphiphilic Conjugated Polymer from Blue Helical Ribbons to Red Nanofibers. *J. Am. Chem. Soc.* **2001**, 123, 3205−3213

329 Kew, S. J.; Hall, E. A. pH Response of Carboxy-terminated Colorimetric Polydiacetylene Vesicles. *Anal. Chem.* **2006**, 78, 2231−2238

330 Lee, J.; Jun, H.; Kim, J. Polydiacetylene-liposome Microarrays for Selective and Sensitive Mercury(II) Detection. *Adv. Mater.* **2009**, 21, 3674−3677

331 Jose, D. A.; Konig, B. Polydiacetylene Vesicles Functionalized with *N*-heterocyclic Ligands for Metal Cation Binding. *Org. Biomol. Chem.* **2010**, 8, 655−662

332 Xia, H.; Li, J.; Zou, G.; Zhang, Q.; Jia, C. A highly Sensitive and Reusable Cyanide Anion Sensor Based on Spiropyran Functionalized Polydiacetylene Vesicular Receptors. *J. Mater. Chem. A*, **2013**, 1, 10713−10719

333 Thongmalai, W.; Eaidkong, T.; Ampornpun, S.; Mungkarndee, R.; Tumcharern, G.; Sukwattanasinitt, M.; Wacharasindhu, S. Polydiacetylenes Carrying Amino Groups for Colorimetric Detection and Identification of Anionic Surfactants. *J. Mater. Chem.* **2011**, 21, 16391−16397

334 Lee, S.; Lee, K. M.; Lee, M.; Yoon, J. Polydiacetylenes Bearing Boronic Acid Groups as Colorimetric and Fluorescence Sensors for Cationic Surfactants. *ACS Appl. Mater. Interfaces*, **2013**, 5, 4521−4526

335 Pindzola, B. A.; Nguyen, A. T.; Reppy, M. A. Antibody Functionalized Polydiacetylene Coatings on Nanoporous Membranes for Microorganism Detection. *Chem. Commun.* **2006**, 3, 906−908

336 Park, C. K.; Kang, C. D.; Sim, S. J. Non-labeled Detection of Waterborne Pathogen *Cryptosporidium Parvum* Using a Polydiacetylene-based Fluorescence Chip. *Biotechnol. J.* **2008**, 3, 687−693

337 Park, C. H.; Kim, J. P.; Lee, S. W.; Jeon, N. L.; Yoo, P. J.; Sim, S. J. A Direct, Multiplex Biosensor Platform for Pathogen Detection Based on Cross-linked Polydiacetylene (PDA) Supramolecules. *Adv. Funct. Mater.* **2009**, 19, 3703−3710

338 Jung, Y. K.; Kim, T. W.; Park, H. G.; Soh, H. T. Specific Colorimetric Detection of Proteins Using Bidentate Aptamer- conjugated Polydiacetylene (PDA) Liposomes. *Adv. Funct. Mater.* **2010**, 20, 3092−3097

339 Seo, D.; Kim, J. Effect of the Molecular Size of Analytes on Polydiacetylene Chromism. *Adv. Funct. Mater.* **2010**, 20, 1397−1403

340 Kang, D. H.; Jung, H. S.; Ahn, N.; Lee, J.; Seo, S.; Suh, K. Y.; Kim, J.; Kim, K. Biomimetic Detection of Aminoglycosidic Antibiotics Using Polydiacetylene-phospholipids Supramolecules. *Chem. Commun.* **2012**, 48, 5313−5315

341 Kwon, I. K.; Song, M. S.; Won, S. H.; Choi, S. P.; Kim, M.; Sim, S. J. Signal Amplification by Magnetic Force on Polydiacetylene Supramolecules for Setection of Prostate Cancer. *Small*, **2012**, 8, 209− 213

342 Zhou, G.; Wang, F.; Wang, H.; Kambam, S.; Chen, X. Colorimetric and Fluorometric Detection of Neomycin Based on Conjugated Polydiacetylene Supramolecules. *Macromol. Rapid Commun.* **2013**, 34, 944−948

343 Cho, Y.-S.; Ahn, K. H. Molecular Interactions Between Charged Macromolecules: Colorimetric Detection and Quantification of Heparin with a Polydiacetylene Liposome. *J. Mater. Chem. B*, **2013**, 1, 1182− 1189

344 Jeon, H.; Lee, S.; Li, Y.; Park, S.; Yoon, J. Conjugated Polydiacetylenes Bearing Quaternary Ammonium Groups as a Dual Colorimetric and Fluorescent Sensor for ATP. *J. Mater. Chem.* **2012**, 22, 3795−3799

sensing stimuli from the ambient environment, such as temperature and mechanical stress instead of a specific analyte. This can be considered as "intramolecular" modification. The interactions between the headgroups and the stimuli are much more versatile. Using a "lock and key" strategy, modifying the headgroups of PDAs that can exclusively interact with the target analytes is plausible, depending on their properties and whether the interaction is a metal−ligand coordination, a biorecognition, or a chemical reaction. This case is considered as "intermolecular" modification. The functions of a material are determined not only by the compositions but also by the way the components are arranged, namely, in which form the material is presented. PDA materials have been structured in various forms, such as Langmuir−Blodgett (LB)[345,346,347] and Langmuir−Schaefer (LS) films,[348,349] nanoparticles in aqueous solution,[350,351] and solid matrices,[352,353,354] depending on the chemo-physical features of the diacetylene monomers and the environment in which the PDAs are intended to be used. Moreover, the topological structures of diacetylenes significantly affect their self-assembly, which in a way determines the final optical properties of PDAs. The ultrathin LB and LS films are intriguing because the molecular orientation can be controlled, and they can be potentially used as colorimetric sensing surfaces in micro- and nanodevices as well as for fundamental studies using surface-sensitive probes, including scanning probe

[345] Xu, Y.; Li, J.; Hu, W.; Zou, G.; Zhang, Q. Thermochromism and Supramolecular Chirality of the Coumarin-substituted Polydiacetylene LB Films. *J. Colloid Interface Sci.* **2013**, 400, 116−122

[346] Zhu, Y.; Xu, Y.; Zou, G.; Zhang, Q. Chirality Transfer and Modulation in LB Films Derived from the Diacetylene/Melamine Hydrogen-bonded Complex. *Chirality*, **2015**, 27, 492−499

[347] Araghi, H. Y.; Paige, M. F. Insight into Diacetylene Photopolymerization in Langmuir-Blodgett Films Using Simultaneous AFM and Fluorescence Microscopy Imaging. *Surf. Interface Anal.* **2017**, 49, 1108−1114

[348] Ahn, D. J.; Chae, E. H.; Lee, G. S.; Shim, H. Y.; Chang, T. E.; Ahn, K. D.; Kim, J. M. Colorimetric Reversibility of Polydiacetylene Supramolecules Having Enhanced Hydrogen-bonding Under Thermal and pH Stimuli. *J. Am. Chem. Soc.* **2003**, 125, 8976−8977

[349] Alekseev, A.; Ihalainen, P.; Ivanov, A.; Domnin, I.; Rosqvist, E.; Lemmetyinen, H.; Vuorimaa-Laukkanen, E.; Peltonen, J.; Vyaz'min, S. Stable Blue Phase Polymeric Langmuir-Schaefer Films Based on Unsymmetrical Hydroxyalkadiynyl *N*-arylcarbamate Derivatives. *Thin Solid Films,* **2018**, 645, 108−118

[350] Chu, B.; Xu, R. Chromatic Transition of Polydiacetylene in Solution. *Acc. Chem. Res.* **1991**, 24, 384−389

[351] Okada, S.; Peng, S.; Spevak, W.; Charych, D. Color and Chromism of Polydiacetylene Vesicles. *Acc. Chem. Res.* **1998**, 31, 229−239

[352] Itoh, T.; Shichi, T.; Yui, T.; Takahashi, H.; Inui, Y.; Takagi, K. Reversible Color Changes in Lamella Hybrids of Poly-(diacetylenecarboxylates) Incorporated in Layered Double Hydroxide Nanosheets. *J. Phys. Chem. B*, **2005**, 109, 3199−3206

[353] Meir, D.; Silbert, L.; Volinsky, R.; Kolusheva, S.; Weiser, I.; Jelinek, R. Colorimetric/Fluorescent Bacterial Sensing by Agarose Embedded Lipid/Polydiacetylene Films. *J. Appl. Microbiol.* **2008**, 104, 787−795

[354] Kauffman, J. S.; Ellerbrock, B. M.; Stevens, K. A.; Brown, P. J.; Pennington, W. T.; Hanks, T. W. Preparation, Characterization, and Sensing Behavior of Polydiacetylene Liposomes Embedded in Alginate Fibers. *ACS Appl. Mater. Interfaces*, **2009**, 1, 1287−1291

microscopy. Such materials can show relatively poor sensitivity and stability, thus, to improve the sensing performance, PDAs can be prepared or incorporated into a host matrix, such as paper, hydrogels, microbeads, membranes, *etc*., to form composites. The ambient matrix has a significant influence on the optical and sensing properties of PDAs. In addition, the embedding could also give access to PDA sensors in the solid state, which show several advantages over their solution-based counterparts, such as easy handling, enhanced stability, and good portability. The most widely investigated form of PDA materials, however, is presented as self-assembled nanoparticles in aqueous solution, mostly liposomes.[355]

4.1.1 Applications

The fusion of multiple disciplines, such as chemistry, biology, and engineering, has opened new potential applications in numerous fields for PDAs such as carriers for catalysts,[356,357,358] drugs,[359,360,361] siRNA,[362] cells,[363] and genes[364,365] and as components in cell imaging,[366,367] tumor targeting,[368,369] solar cells,[370,371,372] gas

---

[355] Qian, X.; Städler, B. Recent Developments in Polydiacetylene-based Sensors, DOI: 10.1021/acs.chemmater.8b05185

[356] Clarisse, D.; Prakash, P.; Geertsen, V.; Miserque, F.; Gravel, E.; Doris, E. Aqueous 1,3-dipolar Cycloadditions Promoted by Copper Nanoparticles in Polydiacetylene Micelles. *Green Chem.* **2017**, 19, 3112−3115

[357] Villemin, E.; Gravel, E.; Jawale, D. V.; Prakash, P.; Namboothiri, I. N. N.; Doris, E. Polydiacetylene Nanotubes in Heterogeneous Catalysis: Application to the Gold-mediated Oxidation of Silanes. *Macromol. Chem. Phys.* **2015**, 216, 2398−2403

[358] Geng, Q.; Du, J. Reduction of 4-Nitrophenol Catalyzed by Silver Nanoparticles Supported on Polymer Micelles and Vesicles. *RSC Adv.* **2014**, 4, 16425−16428

[359] Li, L.; An, X.; Yan, X. Folate-polydiacetylene-liposome for Tumor Targeted Drug Delivery and Fluorescent Tracing. *Colloids Surf. B,* **2015**, 134, 235−239

[360] Yao, D.; Li, S.; Zhu, X.; Wu, J.; Tian, H. Tumor-cell Targeting Polydiacetylene Micelles Encapsulated with an Antitumor Drug for the Treatment of Ovarian Cancer. *Chem. Commun.* **2017**, 53, 1233−1236

[361] Fang, J. H.; Chiu, T. L.; Huang, W. C.; Lai, Y. H.; Hu, S. H.; Chen, Y. Y.; Chen, S. Y. Dual-targeting Lactoferrin-Conjugated Polymerized Magnetic Polydiacetylene-assembled Nanocarriers with Self-responsive Fluorescence/Magnetic Resonance Imaging for *in Vivo* Brain Tumor Therapy. *Adv. Healthcare Mater.* **2016**, 5, 688−695

[362] Ripoll, M.; Neuberg, P.; Kichler, A.; Tounsi, N.; Wagner, A.; Remy, J. S. pH-responsive Nanometric Polydiacetylenic Micelles Allow for Efficient Intracellular siRNA Delivery. *ACS Appl. Mater. Interfaces*, **2016**, 8, 30665−30670

[363] Neuberg, P.; Perino, A.; Morin-Picardat, E.; Anton, N.; Darwich, Z.; Weltin, D.; Mely, Y.; Klymchenko, A. S.; Remy, J. S.; Wagner, A. Photopolymerized Micelles of Diacetylene Amphiphile: Physical Characterization and Cell Delivery Properties. *Chem. Commun.* **2015**, 51, 11595−11598

[364] Morin, E.; Nothisen, M.; Wagner, A.; Remy, J. S. Cationic Polydiacetylene Micelles for Gene Delivery. *Bioconjugate Chem.* **2011**, 22, 1916−1923

[365] Ma, B.; Zhang, S.; Jiang, H.; Zhao, B.; Lv, H. Lipoplex Morphologies and Their Influences on Transfection Efficiency in Gene Delivery. *J. Controlled Release*, **2007**, 123, 184−194

[366] Jiang, H.; Hu, X. Y.; Schlesiger, S.; Li, M.; Zellermann, E.; Knauer, S. K.; Schmuck, C. Morphology-dependent Cell Imaging by Using a Self-assembled Diacetylene Peptide Amphiphile. *Angew. Chem.* **2017**, 56, 14526−14530

[367] Jung, Y. K.; Woo, M. A.; Soh, H. T.; Park, H. G. Aptamer-based Cell Imaging Reagents Capable of Fluorescence Switching. *Chem. Commun.* **2014**, 50, 12329−12332

sorption, [373,374] organic field effect transistors,[375,376] actuators,[377] supercapacitors,[378] and polymer stabilizers[379] because of their unique structural and physical features. Various target analytes can be detected by PDAs[380] included in different support such as one-dimensional fiber or polymer matrix.[381] The applications of PDAs are in a way determined by the molecular structure of the diacetylene monomers, but it is also greatly affected by the matrix in which they are embedded.

Affinochromism

As mentioned above, the disturbance of the backbone of PDAs leads to a chromatic change and the interactions between the headgroups and the analytes significantly affect the overall conformation of the polymer backbone. Therefore, manipulating the affinity behavior between them is the primary way to allow the detection of a certain analyte. The affinity can be a noncovalent interaction or biomolecular

---

[368] Haridas, V.; Sadanandan, S.; Collart-Dutilleul, P. Y.; Gronthos, S.; Voelcker, N. H. Lysine-appended Polydiacetylene Scaffolds for Human Mesenchymal Stem Cells. *Biomacromolecules*, **2014**, 15, 582− 590

[369] Theodorou, I.; Anilkumar, P.; Lelandais, B.; Clarisse, D.; Doerflinger, A.; Gravel, E.; Duconge, F.; Doris, E. Stable and Compact Zwitterionic Polydiacetylene Micelles with Tumor-targeting Properties. *Chem. Commun.* **2015**, 51, 14937−14940

[370] Desta, M. A.; Liao, C. W.; Sun, S. S. A General Strategy to Enhance the Performance of Dye-sensitized Solar Cells by Incorporating a Light-harvesting Dye with a Hydrophobic Polydiacetylene Electrolyte-blocking Layer. *Chem. Asian J.* **2017**, 12, 690−697

[371] Pootrakulchote, N.; Reanprayoon, C.; Gasiorowski, J.; Sariciftci, N. S.; Thamyongkit, P. A Polydiacetylene-nested Porphyrin Conjugate for Dye-sensitized Solar Cells. *New J. Chem.* **2015**, 39, 9228−9233

[372] Reanprayoon, C.; Gasiorowski, J.; Sukwattanasinitt, M.; Sariciftci, N. S.; Thamyongkit, P. Polydiacetylene-nested Porphyrin as a Potential Light Harvesting Component in Bulk Heterojunction Solar Cells. *RSC Adv.* **2014**, 4, 3045−3050

[373] Bhowmik, S.; Konda, M.; Das, A. K. Light Induced Construction of Porous Covalent Organic Polymeric Networks for Significant Enhancement of CO_2 Gas Sorption. *RSC Adv.* **2017**, 7, 47695−47703

[374] Bhowmik, S.; Jadhav, R. G.; Das, A. K. Nanoporous Conducting Covalent Organic Polymer (COP) Nanostructures as Metal-Free High Performance Visible-Light Photocatalyst for Water Treatment and Enhanced CO_2 Capture. *J. Phys. Chem. C,* **2018**, 122, 274−284

[375] Nishide, J.; Oyamada, T.; Akiyama, S.; Sasabe, H.; Adachi, C. High Field-effect Mobility in an Organic Thin-Film Transistor with a Solid-state Polymerized Polydiacetylene Film as an Active Layer. *Adv. Mater.* **2006**, 18, 3120−3124

[376] Cho, S.; Han, G.; Kim, K.; Sung, M. M. High-performance Two Dimensional Polydiacetylene with a Hybrid Inorganic-organic Structure. *Angew. Chem.* **2011**, 50, 2742−2746

[377] Liang, J.; Huang, L.; Li, N.; Huang, Y.; Wu, Y.; Fang, S.; Oh, J.; Kozlov, M.; Ma, Y.; Li, F.; Baughman, R.; Chen, Y. Electromechanical Actuator with Controllable Motion, Fast Response Rate, and High Frequency Resonance Based on Graphene and Polydiacetylene. *ACS Nano*, **2012**, 6, 4508−4519

[378] Ulaganathan, M.; Hansen, R. V.; Drayton, N.; Hingorani, H.; Kutty, R. G.; Joshi, H.; Sreejith, S.; Liu, Z.; Yang, J.; Zhao, Y. Photopolymerization of Diacetylene on Aligned Multiwall Carbon Nanotube Microfibers for High-performance Energy Devices. *ACS Appl. Mater. Interfaces*, **2016**, 8, 32643−32648

[379] Choi, Y. K.; Kim, H. J.; Kim, S. R.; Cho, Y. M.; Ahn, D. J. Enhanced Thermal Stability of Polyaniline with Polymerizable Dopants. *Macromolecules,* **2017**, 50, 3164−3170

[380] Lee, S.; Kim, J. Y.; Chen, X.; Yoon, J. Recent Progress in Stimuli-induced Polydiacetylenes for Sensing Temperature, Chemical and Biological Targets. *Chem. Commun.* **2016**, 52, 9178−9196

[381] Chen, X.; Zhou, G.; Peng, X.; Yoon, J. Biosensors and Chemosensors Based on the Optical Responses of Polydiacetylenes. *Chem. Soc. Rev.* **2012**, 41, 4610−4630

recognition. Affinochromism has been one of the most widely explored properties of PDAs because it can be customized for a specific target analyte. Depending on the chemical or biological activity of the analyte, the headgroups of PDAs can be tailor-made to fulfill the detection of the specific analyte with high selectivity. Most of the PDA-based sensors can be included in this group. However, sometimes the analyte-active group does not necessarily have to be covalently grafted onto the diacetylene monomers. It could also be inserted into the diacetylenes and co-assembles with them to form the PDA-based sensor.[382,383,384] In fact, such a physical doping method offers several advantages over the chemical attachment method, such as the absence of a chemical synthesis and the minimal interruption of the organization and self-assembly of the diacetylene monomers. The affinochromism sensors can be classified on the basis of the form in which they were constructed, namely, in solution, in solid substrates (for example paper), or in other forms (such as hydrogels, membranes, microbeads). The form has a significant influence on the sensing properties of PDA-based sensors.

Solvatochromism

PDAs undergo colorimetric and fluorescent changes that are dependent on the polarity of solvents, which is usually nonspecific and irreversible. The optical transition is intimately related to a corresponding conformational switch in PDAs upon interaction with different solvents. As an alternative to conventional methods like gas chromatography-mass spectrometry, the solvatochromism of PDAs makes them potential sensors for differentiating solvents visually while circumventing shortcomings such as the need for well-trained experts and expensive equipment as well as the lack of an immediate response. Undoubtedly, the colorimetric differentiation of solvents with similar polarities can be extremely challenging using a single-component sensor because the sensor inevitably exhibits broad overlaps in

[382] Kang, D. H.; Jung, H. S.; Ahn, N.; Yang, S. M.; Seo, S.; Suh, K. Y.; Chang, P. S.; Jeon, N. L.; Kim, J.; Kim, K. Janus-compartmental Alginate Microbeads Having Polydiacetylene Liposomes and Magnetic Nanoparticles for Visual Lead(II) Detection. *ACS Appl. Mater. Interfaces*, **2014**, 6, 10631−10637

[383] De Oliveira, T. V.; Soares, N. D. F. F.; de Andrade, N. J.; Silva, D. J.; Medeiros, E. A.; Badaro, A. T. Application of PCDA/SPH/ CHO/Lysine Vesicles to Detect Pathogenic Bacteria in Chicken. *Food Chem.* **2015**, 172, 428−432

[384] Ma, X.; Sheng, Z.; Jiang, L. Sensitive Naked-eye Detection of Hg^{2+} Based on the Aggregation and Filtration of Thymine Functionalized Vesicles Caused by Selective Interaction Between Thymine and Hg^{2+}. *Analyst*, **2014**, 139, 3365−3368

the absorption and emission bands in different solvents. As far as we know, only a few reported PDAs showed a specific color transition to a specific solvent.[385,386] To overcome the no specificity, Lee *et al.* developed a protective layer method that enabled the visual differentiation of dichloromethane from chloroform.[387] However, for this strategy, specific polymers are needed to prevent PDAs from interacting directly with certain solvents, which could again be a challenge and hinders their wide application. Alternatively, the use of sensor arrays consisting of a group of solvatochromic molecules to build a "fingerprint" of each solvent is considered. PDAs are widely exploited in this context due to their relatively simple chemical modification, giving access to a large structural diversity of diacetylenes as the precursors.[388,389,390]

Thermochromism

When the ambient temperature varies in a certain range, PDAs with thermochromism undergo colorimetric transitions, usually from blue to red as the temperature increases gradually. Thermochromism is likely the most exhaustively investigated chromatic effect of PDAs ever since the first report in 1976.[391] These studies not only facilitated the fundamental understanding of the color transition, but also made the development of temperature sensitive materials possible. Numerous studies have revealed that the molecular structures of diacetylenes,[321,392,393,394,395] together with the matrices in which PDAs are

[385] Park, D. H.; Kim, B.; Kim, J. M. A Tetrahydrofuran-selective Optical Solvent Sensor Based on Solvatochromic Polydiacetylene. *Bull. Korean Chem. Soc.* **2016**, 37, 793−794

[386] Wang, X.; Sun, X.; Hu, P. A.; Zhang, J.; Wang, L.; Feng, W.; Lei, S.; Yang, B.; Cao, W. Colorimetric Sensor Based on Self- assembled Polydiacetylene/Graphene-stacked Composite Film for Vapor-phase Volatile Organic Compounds. *Adv. Funct. Mater.* **2013**, 23, 6044−6050

[387] Lee, J.; Chang, H. T.; An, H.; Ahn, S.; Shim, J.; Kim, J. M. A Protective Layer Approach to Solvatochromic Sensors. *Nat. Commun.* **2013**, 4, 2461-2463

[388] Yoon, J.; Chae, S. K.; Kim, J. M. Colorimetric Sensors for Volatile Organic Compounds (VOCs) Based on Conjugated Polymer Embedded Electrospun Fibers. *J. Am. Chem. Soc.* **2007**, 129, 3038− 3039

[389] Jiang, H.; Wang, Y.; Ye, Q.; Zou, G.; Su, W.; Zhang, Q. Polydiacetylene-based Colorimetric Sensor Microarray for Volatile Organic Compounds. *Sens. Actuators B,* **2010**, 143, 789−794

[390] Eaidkong, T.; Mungkarndee, R.; Phollookin, C.; Tumcharern, G.; Sukwattanasinitt, M.; Wacharasindhu, S. Polydiacetylene Paper Based Colorimetric Sensor Array for Vapor Phase Detection and Identification of Volatile Organic Compounds. *J. Mater. Chem.* **2012**, 22, 5970−5977

[391] Exarhos, G. J.; Risen, W. M.; Baughman, R. H. Resonance Raman Study of the Thermochromic Phase Transition of a Polydiacetylene. *J. Am. Chem. Soc.* **1976**, 98, 481−487

[392] Yu, L.; Hsu, S. L. A Spectroscopic Analysis of the Role of Side Chains in Controlling Thermochromic Transitions in Polydiacetylenes. *Macromolecules*, **2012**, 45, 420−429

embedded,[396,397] have a significant influence on the thermochromic behaviors of PDAs. PDAs with different color transition temperatures could be obtained by carefully manipulating these two parameters. The most intriguing characteristic of the thermochromism of PDAs is the reversibility within a certain temperature range. This is in stark contrast to other stimulus-triggered chromism of PDAs, most of which is typically irreversible. Studies have revealed that the reversible thermochromic behaviors of PDAs are largely dependent on the intramolecular noncovalent interactions, *i.e*. hydrogen bonds, π−π stacking, van der Waals force, *etc*.[348,393,398,399,400,401,402] In general terms, the stronger the interactions, the better the thermochromic properties of PDAs *i.e*. reversibility in a wider temperature range. The thermochromic reversibility of PDAs has been achieved by strengthening the intramolecular interactions. For example, Guo *et al*. prepared a peptide-decorated PDA with multiple hydrogen bonding sites that has shown reversible thermochromism at temperatures of ≤200 °C.[403] The transition took place even when the heating rate was 5000 K/s. This remarkable thermochromism was attributed to the hierarchically assembled structure promoted by the multiple hydrogen bonds among the peptide segments. As alternatives for obtaining reversible

---

[393] Tanioku, C.; Matsukawa, K.; Matsumoto, A. Thermochromism and Structural Change in Polydiacetylenes Including Carboxy and 4-Carboxyphenyl Groups as the Intermolecular Hydrogen Bond Linkages in the Side Chain. *ACS Appl. Mater. Interfaces,* **2013**, 5, 940−948

[394] Park, I. S.; Park, H. J.; Jeong, W.; Nam, J.; Kang, Y.; Shin, K.; Chung, H.; Kim, J.-M. Low Temperature Thermochromic Polydiacetylenes: Design, Colorimetric Properties, and Nanofiber Formation. *Macromolecules,* **2016**, 49, 1270−1278

[395] Han, N.; Woo, H. J.; Kim, S. E.; Jung, S.; Shin, M. J.; Kim, M.; Shin, J. S. Systemized Organic Functional Group Controls in Polydiacetylenes and Their Effects on Color Changes. *J. Appl. Polym. Sci.* **2017**, 134, 45011

[396] Lu, J.; Zhou, J.; Li, J. Tuned Chromic Process for Polydiacetylenes Vesicles: the Influence of Polymer Matrices. *Soft Matter*, **2011**, 7, 6529−6531

[397] Lee, S.; Lee, J.; Kim, H. N.; Kim, M. H.; Yoon, J. Thermally Reversible Polydiacetylenes Derived from Ethylene Oxide-containing Bisdiacetylenes. *Sens. Actuators B*, **2012**, 173, 419−425

[398] Hu, W.; Hao, J.; Li, J.; Zou, G.; Zhang, Q. Novel Chromatic Transitions of Azobenzene-functionalized Polydiacetylene Aggregates in 1,2-Dichlorobenzene Solution. *Macromol. Chem. Phys.* **2012**, 213, 2582−2589

[399] Park, S. H.; Roh, J.; Ahn, D. J. Optimal Photoluminescence Achieved by Control of Photopolymerization for Diacetylene Derivatives that Induce Reversible, Partially Reversible, and Irreversible Responses. *Macromol. Res.* **2017**, 25, 960−962

[400] Huo, J.; Hu, Z.; He, G.; Hong, X.; Yang, Z.; Luo, S.; Ye, X.; Li, Y.; Zhang, Y.; Zhang, M.; Chen, H.; Fan, T.; Zhang, Y.; Xiong, B.; Wang, Z.; Zhu, Z.; Chen, D. High Temperature Thermochromic Polydiacetylenes: Design and Colorimetric Properties. *Appl. Surf. Sci.* **2017**, 423, 951−956

[401] Dong, W.; Lin, G.; Wang, H.; Lu, W. New Dendritic Polydiacetylene Sensor with Good Reversible Thermochromic Ability in Aqueous Solution and Solid Film. *ACS Appl. Mater. Interfaces*, **2017**, 9, 11918−11923

[402] Niu, R.; Meng, X.-l.; Yang, D.-d.; Chang, Y.; Zha, F. Preparation of Reversible Thermochromism Supramolecules of 4- Aminophenol-modified Polydiacetylene. **Arab. J. Sci. Eng. 2015**, 40, 2867−2872

[403] Guo, H.; Zhang, J.; Porter, D.; Peng, H.; Loẅik, D. W. P. M.; Wang, Y.; Zhang, Z.; Chen, X.; Shao, Z. Ultrafast and Reversible Thermochromism of a Conjugated Polymer Material Based on the Assembly of Peptide Amphiphiles. *Chem. Sci.* **2014**, 5, 4189−4195

thermochromism from a molecular level, intercalation with polymers,[404,405,406] organic amines,[407,408] layered double hydroxide nanosheets,[352] and metal ions[409,410,411,412,413] to form layered nanocomposites or co-assembly with small molecule[414] was successfully employed. On the basis of the thermochromism of PDAs, various novel temperature-sensitive materials were fabricated. Inspired by natural nacres, which have outstanding mechanical properties derived from their layered structure and synergistic interfacial interactions, a PDA-embedded artificial nacre integrating mechanical robustness with thermochromism was fabricated.[415]

Mechanochromism

An alternative sensing mechanism considers the application of mechanical stress to induce the color transition of PDAs.[416,417,418] When a proper amount of mechanical stretching energy is delivered to the PDA backbone, the disruption of the π-orbitals

[404] Kamphan, A.; Traiphol, N.; Traiphol, R. Versatile Route to Prepare Reversible Thermochromic Polydiacetylene Nanocomposite Using Low Molecular Weight Poly(vinylpyrrolidone). *Colloids Surf. A,* **2016**, 497, 370−377

[405] Kamphan, A.; Khanantong, C.; Traiphol, N.; Traiphol, R. Structural-thermochromic Relationship of Polydiacetylene (PDA)/Polyvinylpyrrolidone (PVP) Nanocomposites: Effects of PDA Side Chain Length and PVP Molecular Weight. *J. Ind. Eng. Chem.* **2017**, 46, 130−138

[406] Gu, Y.; Cao, W.; Zhu, L.; Chen, D.; Jiang, M. Polymer Mortar Assisted Self-assembly of Nanocrystalline Polydiacetylene Bricks Showing Reversible Thermochromism. *Macromolecules*, **2008**, 41, 2299−2303

[407] Oaki, Y.; Ishijima, Y.; Imai, H. Emergence of Temperature Dependent and Reversible Color-changing Properties by the Stabilization of Layered Polydiacetylene Through Intercalation. *Polym. J.* **2018**, 50, 319−326

[408] Shimogaki, T.; Matsumoto, A. Structural and Chromatic Changes of Host Polydiacetylene Crystals During Intercalation with Guest Alkylamines. *Macromolecules*, **2011**, 44, 3323−3327

[409] Chanakul, A.; Traiphol, N.; Traiphol, R. Controlling the Reversible Thermochromism of Polydiacetylene/Zinc Oxide Nanocomposites by Varying Alkyl Chain Length. *J. Colloid Interface Sci.* **2013**, 389, 106−114

[410] Traiphol, N.; Chanakul, A.; Kamphan, A.; Traiphol, R. Role of Zn^{2+} Ion on the Formation of Reversible Thermochromic Polydiacetylene/Zinc Oxide Nanocomposites. *Thin Solid Films,* **2017**, 622, 122− 129

[411] Okaniwa, M.; Oaki, Y.; Kaneko, S.; Ishida, K.; Maki, H.; Imai, H. Advanced Biomimetic Approach for Crystal Growth in Nonaqueous Media: Morphology and Orientation Control of Pentacosadiynoic Acid and Applications. *Chem. Mater.* **2015**, 27, 2627−2632

[412] Wu, A.; Beck, C.; Ying, Y.; Federici, J.; Iqbal, Z. Thermochromism in Polydiacetylene−ZnO Nanocomposites. *J. Phys. Chem. C*, **2013**, 19593−19600

[413] Yao, Y.; Fu, K.; Huang, X.; Chen, D. Polydiacetylene-Tb^{3+} Nanosheets of Which Both the Color and the Fluorescence Can Be Reversibly Switched Between Two Colors. *Chin. J. Chem.* **2017**, 35, 1678−1686

[414] Guo, J.; Fu, K.; Zhang, Z.; Yang, L.; Huang, Y.-C.; Huang, C.- I.; Zhu, L.; Chen, D. Reversible Thermochromism via Hydrogen Bonded Cocrystals of Polydiacetylene and Melamine. *Polymer*, **2016**, 105, 440−448

[415] Peng, J.; Cheng, Y.; Tomsia, A. P.; Jiang, L.; Cheng, Q. Thermochromic Artificial Nacre Based on Montmorillonite. *ACS Appl. Mater. Interfaces,* **2017**, 9, 24993−24998

[416] Tomioka, Y.; Tanaka, N.; Imazeki, S. Surface-pressure Induced Reversible Color Change of a Polydiacetylene Monolayer at a Gas-water Interface. *J. Chem. Phys.* **1989**, 91, 5694−5700

[417] Carpick, R. W.; Sasaki, D. Y.; Burns, A. R. First Observation of Mechanochromism at the Nanometer Scale. *Langmuir*, **2000**, 16, 1270−1278

[418] Feng, H.; Lu, J.; Li, J.; Tsow, F.; Forzani, E.; Tao, N. Hybrid Mechanoresponsive Polymer Wires Under Force Activation. *Adv. Mater.* **2013**, 25, 1729−1733

takes place to induce a colorimetric transition. Such a mechanical stress induced phenomenon is rather useful for sensing. Specifically, it is possible to detect a certain analyte, which does not interact directly with PDAs but induces a mechanical change in the matrices in which PDAs are encapsulated. Once the matrices are disrupted by the analyte mechanically, the mechanical stretching energy is delivered to the PDA backbone, which leads to the color change. This sensing mechanism is particularly useful for analytes that are chemically or biologically inert and difficult to detect, for example, saturated aliphatic hydrocarbons, whose colorimetric differentiation remains challenging because of the nonpolar nature and deficiency of functional groups that can interact with the sensor system.

Photochromism

Generally, PDAs can be tailor-made to be light-sensitive by grafting photo-responsive moieties into the headgroups of diacetylenes[327,398,419,420] or by doping photosensitive moieties that could interact with the headgroups of PDAs into the system.[421] However, PDA vesicles without functionalization of the headgroup could also be made light-sensitive *via* a combination of thin film hydration and supercritical CO_2 fluid treatment.[422] Importantly, the photo-wavelength for the stimulation of PDAs should be different from the 254 nm UV light used for the polymerization of diacetylenes to ensure control over the process. Upon irradiation with light, the conformational or structural change of the light-sensitive moieties could lead to the interruption of the PDA backbone, which may result in the color transition. Such a light-driven color transition could be used for, *e.g.*, encrypting information and anti-counterfeiting, where rapid and naked eye detection is needed.

---

[419] You, X.; Chen, X.; Zou, G.; Su, W.; Zhang, Q.; He, P. Colorimetric Response of Azobenzene-terminated Polydiacetylene Vesicles Under Thermal and Photic *Stimuli*. *Chem. Phys. Lett.* **2009**, 482, 129−133

[420] Li, J.; Jiang, H.; Hu, W.; Xia, H.; Zou, G.; Zhang, Q. Photocontrolled Hierarchical Assembly and Fusion of Coumarin-containing Polydiacetylene Vesicles. *Macromol. Rapid Commun.* **2013**, 34, 274− 279

[421] Sun, X.; Chen, T.; Huang, S.; Cai, F.; Chen, X.; Yang, Z.; Li, L.; Cao, H.; Lu, Y.; Peng, H. UV-induced Chromatism of Polydiacetylenic Assemblies. *J. Phys. Chem. B*, **2010**, 114, 2379−2382

[422] Yan, X.; An, X. Thermal and Photic Stimuli-responsive Polydiacetylene Liposomes with Reversible Fluorescence. *Nanoscale*, **2013**, 5, 6280−6283

Solution-Based Sensors

Vesicles and/or liposomes prepared by the self-assembly of amphiphilic diacetylenes in aqueous solution are the most commonly used form of PDAs for sensing. These two terms have been used somewhat interchangeably when referring to the nanoparticles composed of bilayers with an enclosed volume. Vesicles prepared from the self-assembly of diacetylenes exhibited extensive applications as sensors based on the typical blue-to-red color change and the enhancement of fluorescence upon stimulation.[355] As compared to PDA sensors in other forms, a critical advantage of such nanoparticles in aqueous solution is their mimicry of the cell membrane and applications in biological systems. In this context, a certain molar percentage of phospholipids [423,424] or surfactants[425,426] was often added to co-assemble with diacetylenes with the aim of increasing the fluidity of the artificial membrane structure with its preserved ability to polymerize. Membranes with a higher fluidity are thought to react more sensitively to external perturbations. Also, it was reported that the phospholipids or surfactants affected the sensing performance of the PDAs.[427,428]

Many PDA-based metal ion sensors were designed on the ability of transition metal ions to coordinate with certain ligands and form coordination complexes. The chelation between the metal ion and the ligand and the consequent influence on the backbone of PDAs results in the aggregation of PDAs leading to the optical transition.

Nowadays, there are increasing demands for the fast and accurate sensing of bacteria because of worldwide incidents like food poisoning and bioterrorism alerts. Traditional culture-based methods for bacterial sensing are time-consuming,

[423] Thet, N. T.; Jamieson, W. D.; Laabei, M.; Mercer-Chalmers, J. D.; Jenkins, A. T. Photopolymerization of Polydiacetylene in Hybrid Liposomes: Effect of Polymerization on Stability and Response to Pathogenic Bacterial Toxins. *J. Phys. Chem. B*, **2014**, 118, 5418−5427

[424] Kolusheva, S.; Shahal, T.; Jelinek, R. Peptide−Membrane Interactions Studied by a New Phospholipid/Polydiacetylene Colorimetric Vesicle Assay. Biochemistry 2000, 39, 15851−15859.

[425] Shin, M. J.; Kim, Y. J.; Kim, J. D. Chromatic Response of Polydiacetylene Vesicle Induced by the Permeation of Methotrexate. *Soft Matter*, **2015**, 11, 5037−5043

[426] Shin, Y. J.; Shin, M. J.; Shin, J. S. Permeation-induced Chromatic Change of a Polydiacetylene Vesicle with Nonionic Surfactant. *Colloids Surf. A*, **2017**, 520, 459−466

[427] Yadav, M. K.; Kumar, V.; Singh, B.; Tiwari, S. K. Phospholipid/Polydiacetylene Vesicle-based Colorimetric Assay for High-throughput Screening of Bacteriocins and Halocins. *Appl. Biochem. Biotechnol.* **2017**, 182, 142−154

[428] Kang, D. H.; Jung, H. S.; Lee, J.; Seo, S.; Kim, J.; Kim, K.; Suh, K. Y. Design of Polydiacetylene-phospholipid Supramolecules for Enhanced Stability and Sensitivity. *Langmuir*, **2012**, 28, 7551−7556

usually taking hours to days. To overcome this problem, numerous studies have pursued the fast and chromatic detection of bacteria using PDA vesicles.[383,429,430,431] Influenza virus is likely the most common virus that greatly affects our lives. Influenza virus has a lipid bilayer structure in which hemagglutinin (HA) lectin is anchored. HA binds with the α-glycosides of sialic acid on cell surface glycoproteins and glycolipids to initiate the viral infection. [432] Therefore, the most straightforward method for detecting influenza virus is to modify the headgroups of diacetylenes with sialic acid.[323,433,434] Alternatives include grafting influenza virus specific antibodies,[435,436,437] DNA,[438] or even peptides[439] to the headgroups of diacetylenes. For example, a highly specific and sensitive biosensor for the rapid detection of H1N1 influenza virus was developed by conjugating one of the virus specific peptide (PEP) to polymerized PDA vesicles (Figure 42 a).[439] Once H1N1 influenza virus was introduced, the PEP/PDA solution turned from blue to red appreciable at naked eye. An H1N1 virus nonspecific peptide was also introduced as a control study, without inducing any obvious color switch, thus indicating the specificity of

[429] Silbert, L.; Ben Shlush, I.; Israel, E.; Porgador, A.; Kolusheva, S.; Jelinek, R. Rapid Chromatic Detection of Bacteria by Use of a New Biomimetic Polymer Sensor. *Appl. Environ. Microbiol.* **2006**, 72, 7339− 7344

[430] Zhang, Y.; Fan, Y.; Sun, C.; Shen, D.; Li, Y.; Li, J. Functionalized Polydiacetylene-glycolipid Vesicles Interacted with *Escherichia Coli* Under the TiO_2 Colloid. *Colloids Surf. B,* **2005**, 40, 137−142

[431] Wu, W.; Zhang, J.; Zheng, M.; Zhong, Y.; Yang, J.; Zhao, Y.; Wu, W.; Ye, W.; Wen, J.; Wang, Q.; Lu, J. An Aptamer-based Biosensor for Colorimetric Detection of *Escherichia Coli* O157:H7. *PLoS One,* **2012**, 7, N. e48999

[432] Stencel-Baerenwald, J. E.; Reiss, K.; Reiter, D. M.; Stehle, T.; Dermody, T. S. The Sweet Spot: Defining Virus-sialic Acid Interactions. *Nat. Rev. Microbiol.* **2014**, 12, 739−749

[433] Deng, J.; Sheng, Z.; Zhou, K.; Duan, M.; Yu, C. Y.; Jiang, L. Construction of Effective Receptor for Recognition of Avian Influenza H5N1 Protein HA1 by Assembly of Monohead Glycolipids on Polydiacetylene Vesicle Surface. *Bioconjugate Chem.* **2009**, 20, 533−537

[434] Song, J.; Cheng, Q.; Zhu, S.; Stevens, R. C. "Smart" Materials for Biosensing Devices: Cell-mimicking Supramolecular Assemblies and Colorimetric Detection of Pathogenic Agents. *Biomed. Microdevices,* **2002**, 4, 213−221

[435] Dong, W.; Luo, J.; He, H.; Jiang, L. A Reinforced Composite Structure Composed of Polydiacetylene Assemblies Deposited on Polystyrene Microspheres and its Application to H5N1 Virus Detection. *Int. J. Nanomed.* **2013**, 8, 221−232

[436] Jeong, J.-p.; Cho, E.; Yun, D.; Kim, T.; Lee, I.-S.; Jung, S. Label-free Colorimetric Detection of Influenza Antigen Based on an Antibody-polydiacetylene Conjugate and its Coated Polyvinylidene Difluoride Membrane. *Polymers*, **2017**, 9, 127

[437] Jiang, L.; Luo, J.; Dong, W.; Wang, C.; Jin, W.; Xia, Y.; Wang, H.; Ding, H.; Jiang, L.; He, H. Development and Evaluation of a Polydiacetylene Based Biosensor for the Detection of H5 Influenza Virus. *J. Virol. Methods,* **2015**, 219, 38−45

[438] Park, M. K.; Kim, K. W.; Ahn, D. J.; Oh, M. K. Label-free Detection of Bacterial RNA Using Polydiacetylene-based Biochip. *Biosens. Bioelectron.* **2012**, 35, 44−49

[439] Song, S.; Ha, K.; Guk, K.; Hwang, S.-G.; Choi, J. M.; Kang, T.; Bae, P.; Jung, J.; Lim, E.-K. Colorimetric Detection of Influenza A (H1N1) Virus by a Peptide-functionalized Polydiacetylene (PEPPDA) Nanosensor. *RSC Adv.* **2016**, 6, 48566−48570

the peptide (Figure 42 b). Similar sensing strategies were also employed for other viruses, such as foot and-mouth disease virus.[440]

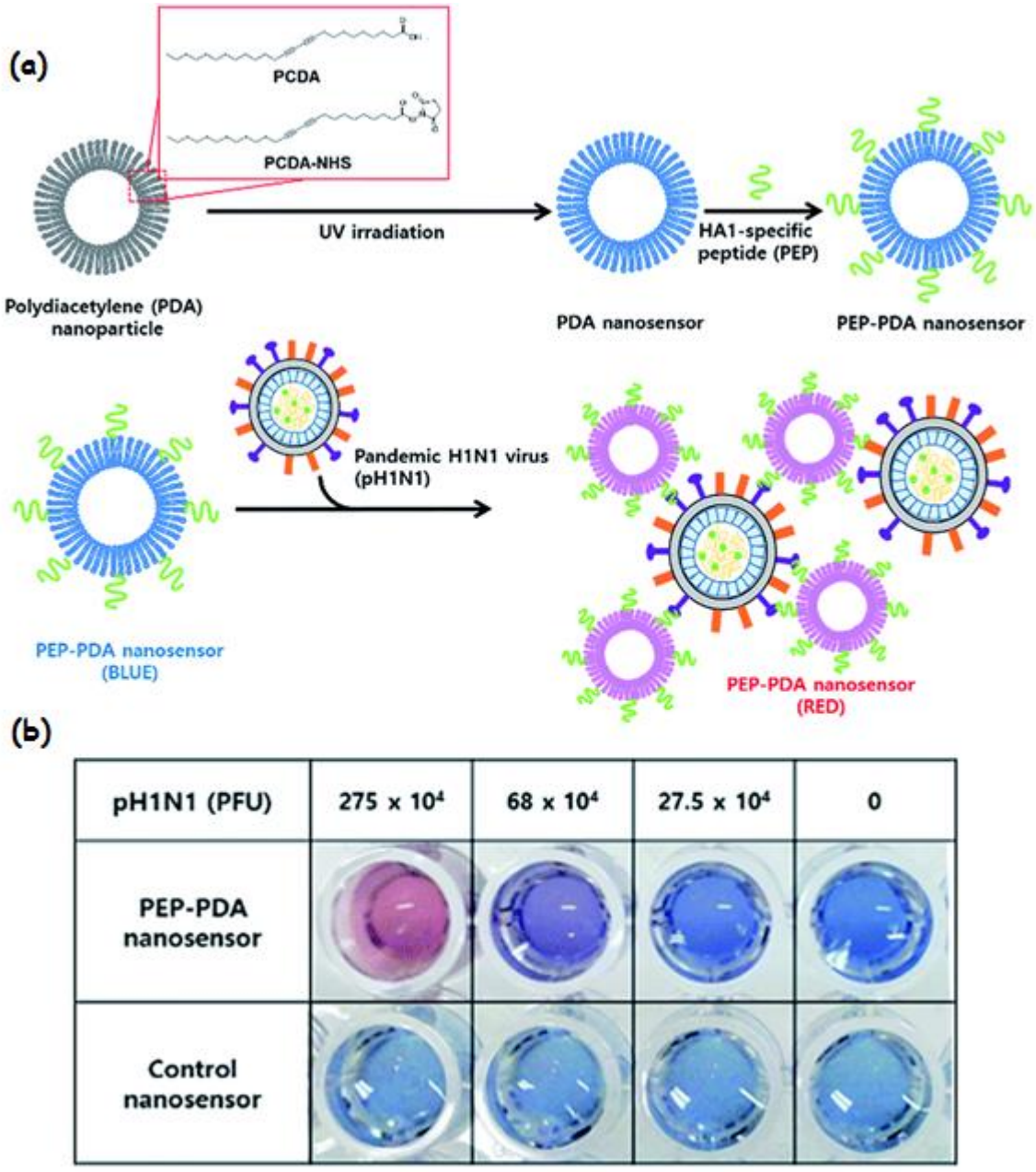

Figure 42. Peptide-modified PDA vesicles for the detection of H1N1 influenza virus. (a) Schematic illustration of the sensing process of PEP/PDA for H1N1 influenza virus. (b) Photographs of the PEP/ PDA and control nanosensor after addition of different concentrations of H1N1 influenza virus. Adapted with permission from ref 439.

[440] Jeong, J.P.; Cho, E.; Lee, S.C.; Kim, T.; Song, B.; Lee, I.S.; Jung, S. Detection of Foot-and-mouth Disease Virus Using a Polydiacetylene Immunosensor on Solid-liquid Phase. *Macromol. Mater. Eng.* **2018**, 303, 1700640

4.2 Aim of the work

Thymidylate synthase, thymidine phosphorylase (TP) and dihydropyrimidine dehydrogenase (DPD) take part in the metabolism of pyrimidines and are the target of 5-fluorouracil (5-FU), a strong chemotherapeutic agent commonly used to treat several solid tumors, such as breast,[441] colorectal[442] and skin cancer, where are overexpressed.[443] The proper dosage of 5-FU, that has a very narrow therapeutical window,[444] is strictly related to the level of these enzymes and unfortunately only about 25% of patients are treated with the appropriate dose of 5-FU, whereas approximately 15% of patients are overdosed (with severe toxic effects) and almost 60% of patients are under dosed (with a consequent reduced therapeutic efficacy of the drug).[445] Moreover, for patients who suffer of DPD deficiency (about 5-8% of cancer patients),[446] 5-FU can result lethal at the first administration and about 60% of patients treated with 5-FU are partially or borderline DPD deficient.[447] Hence it is evident the need of a fast, precise and cheap method to detect the level of the three target enzymes in patients that need 5-FU treatment. Currently screening methodologies with these characteristics do not exist. Actually, liquid chromatography and mass spectroscopy only enable to measure 5-FU content in the blood and require expensive and not widely available equipment, thus hindering the widespread diffusion of personalized dose management. The common gold standard approach for calibrating 5-FU drug therapy is based on body surface area estimation. However, variations up to 100 folds in the levels of 5-FU in plasma

[441] Winer, E.P. Oral 5-FU Analogues in the Treatment of Breast Cancer. *Oncology*, **1998**,12(7), 39-43

[442] Cunningham, D.; James, R. D.; Integrating the Oral Fluoropyrimidines into the Management of Advanced Colorectal Cancer. *Eur. J. Cancer,* **2001**, 37, 826-834

[443] Neubert, T.; Lehmann, P. Bowen's Disease–a Review of Newer Treatment Options. *Ther. Clin. Risk Manag.* **2008**, 4(5), 1085-1095

[444] Alvarez, P.; Marchal, J. A.; Boulaiz, H.; Carrillo, E.; Velez, C.; Rodrıguez-Serrano, F.; Melguizo, C.; Prados, J.; Madeddu, R.; Aranega, A. 5-Fluorouracil Derivatives: a Patent Review. *Expert Opin. Ther. Patents,* **2012**, 22(2) 107-123

[445] Saif, M. W.; Choma, A.; Salamone, S. J.; Chu, E. Pharmacokinetically Guided Dose Adjustment of 5-Fluorouracil: a Rational Approach to Improving Therapeutic Outcomes. *J. Natl. Cancer Inst.* **2009**, 101, 1543–1552

[446] Saif, M. W.; Syrigos, K.; Mehra, R.; Mattison, L. K.; Diasio, R. B. Dihydropyrimidine Dehydrogenase Deficiency (DPD) in GI Malignancies: Experience of 4-Years. *Pak. J. Med. Sci. Q.* **2007**, *23(6)*, 832-839

[447] Takimoto, C. H.; Lu, Z. H.; Zhang, R.; Liang, M. D.; Larson, L. V.; Cantilena, L. R. Jr; Grem, J. L.; Allegra, C. J.; Diasio, R. B.; Chu, E. Severe Neurotoxicity Following 5-Fluorouracil-based Chemotherapy in a Patient with Dihydropyrimidine Dehydrogenase Deficiency. *Clin. Cancer Res.* **1996**, 2, 477-481

between different subjects with the same body surface area can occur, thus often resulting either in the ineffectiveness or in severe side effects of the therapy.[445]

The aim of the investigation reported in this chapter is the development of PDA liposomes to detect the enzymes targeted by 5-FU. The formulation of the novel liposomes involves commercial lipids, namely 10,12-pentacosadiynoic acid (PCDA), a liposome-forming amphiphile commonly used as lipid matrix for PDA based-biosensors,[448] 1,2-dimyristoyl-*sn*-glycero-3-phosphorylcholine (DMPC) or 1,2-dioleoyl-*sn*-glycero-3-phosphocholine (DOPC), and one of three novel non-ionic amphiphiles (**11**, **12**, **13**, Figure 43). Based on previous investigations, where 5-FU functionalized lipids were shown capable of binding with TP both as monomers and when included in liposome formulations,[449,450] **11-13** were designed to bear a 5-FU moiety linked, through a hydrophilic polyoxyethylene spacer of 3, 4, or 6 units, to the hydrophobic tail containing a diacetylene unit (Figure 43), thus targeting the tumor biomarker enzymes. Different spacer lengths were chosen in order to investigate the influence of the 5-FU exposition to the bulk on the colorimetric response of the sensor. Due to the presence of the diacetylene function amphiphiles **11-13** can easily copolymerize with PCDA upon irradiation when embedded in PCDA liposome bilayers. The presence of phospholipids devoid of the diacetylenic function should not hinder polymerization because of lipids lateral mobility.

[448] Ji, E.; Ahn, D. J.; Kim, J. The Fluorescent Polydiacetylene Liposome. *Bull. Korean Chem. Soc.* **2003**, 24(5), 667-670

[449] Petaccia, M.; Condello, M.; Giansanti, L.; La Bella, A.; Leonelli, F.; Meschini, S.; Gradella Villalva, D.; Pellegrini, E.; Ceccacci, F.; Galantini, L.; Mancini, G. Inclusion of New 5-Fluorouracil Derivatives in Liposome Formulations for Cancer Treatment. *Med. Chem. Comm.* **2015**, 6, 1639-1642

[450] Petaccia, M.; Gentili, P.; Beˇsker, N.; D'Abramo, M.; Giansanti, L.; Leonelli, F.; La Bella, A.; Gradella Villalva, D.; Mancini, G. Kinetics and Mechanistic Study of Competitive Inhibition of Thymidinephosphorylase by 5-Fluoruracil Derivatives. *Coll. Surf. B. Biointerfaces,* **2016**, 140, 121–127

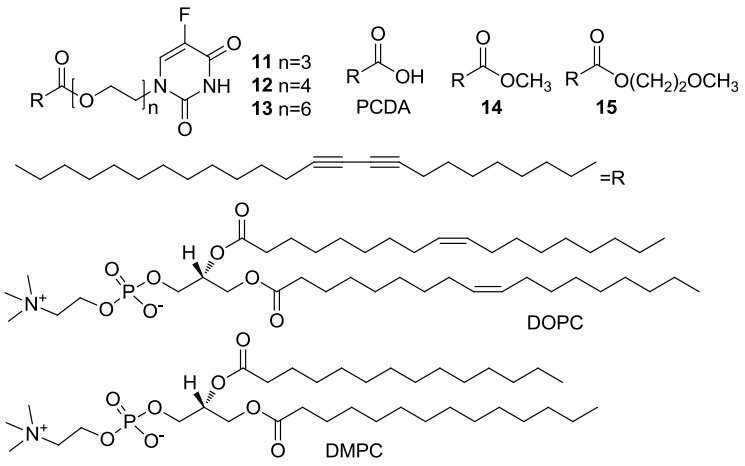

Figure 43**.** Liposomes components.

The sensor capability of the different formulations was evaluated on TP, chosen as model target enzyme because commercially available. Important parameters that can affect the sensor response to the protein can be lipid bilayer fluidity, modulated by the presence of a saturated (DMPC) or unsaturated (DOPC) phospholipid, as well as surface potential, modulated by the presence of methyl or ethyl ester of PCDA **14** and **15** (Figure 43). In fact, the interaction of the enzyme with liposomes membrane induces an electrostatic perturbation, due to the charged amino acids on the external surface of the protein, that is strictly affected by their surface potential.

4.3 Experimental section

4.3.1 Instrumentation

UV measurements were carried out on a Cary 50 UV−vis double beam spectrophotometer (Varian Australia PTY Ltd., Mulgrave, Vic., Australia). Liposomes were prepared using a Hielscher UP100-H ultrasonic processor with microtip probe (7 mm). ^{1}H and ^{13}C spectra (compounds **11-15**): Bruker 400; δ in ppm relative to the residual solvent peak of $CDCl_3$ at 7.26 and 77.0 ppm for ^{1}H and ^{13}C, respectively.

4.3.2 Materials

DOPC and DMPC were purchased from Avanti Polar Lipids (Alabaster, AL, USA). TP recombinant from Escherichia coli, BSA, phosphate-buffered saline tablets (PBS; 0.01 M phosphate buffer; 0.0027 M KCl; 0.137 M NaCl; pH 7.4), PCDA, PTFE syringe filters (porosity 0.8 μm and 0.45 μm) and all reagents employed for the synthesis of **11-15** (Figure 44 and Figure 45), were purchased from Sigma-Aldrich. All solvents and chemicals were used as purchased without further purification. Yields were not optimized. TLC: silica gel 60, F_{254}. Column chromatography (CC): silica gel 60, 70-230 mesh ASTM.

4.3.3 Methods

*Preparation of compounds **19-21**.*

The appropriate alcohol compound **16-18** (3 eq) was dissolved in CH_2Cl_2 (1 mL/mmol). The solution was cooled to 0°C, then CBr_4 (1 eq) and PPh_3 (1.1 eq) dissolved in CH_2Cl_2 (1 mL/mmol) were added dropwise. The solution was stirred for 2 h. The solvent was evaporated under reduced pressure and the residue was dissolved in water. The aqueous solution was filtered on paper and extracted once with CH_2Cl_2. The organic phase was dried over anhydrous Na_2SO_4 and evaporated under reduced pressure to give a yellowish oil that was washed several times with Et_2O. The organic solvent was separated by decantation to remove the yellow residue. The organic solution was evaporated again under reduced pressure to afford compounds **19-21**. Compound **19**: colorless oil, yield: 82%. ^{1}H-NMR ($CDCl_3$): δ 3.80 (t, 2H); 3.72-3.55 (m, 8H); 3.46 (t, 2H). Compound **20**: colorless oil, yield: 49%. ^{1}H-NMR ($CDCl_3$): δ 3.74 (t, 2H); 3.52-3.40 (m, 12H); 3.42 (t, 2H). Compound **21**: colorless oil, yield: 50%. ^{1}H-NMR ($CDCl_3$): δ 3.80 (t, 2H); 3.72-3.58 (m, 20H); 3.47 (t, 2H).

*Preparation of compounds **22-24***

5-FU (5 eq) was dissolved at r.t. in dry DMF (3 mL/mmol of 5-FU), then anhydrous K_2CO_3 (1 eq) and a small amount of 18-crown-6 were added. The solution was heated at 80° C and the appropriate bromine derivative **19-21** (1 eq) was added dropwise under nitrogen. The solution was stirred for 2 hours, then the solvent was

evaporated under reduced pressure and the residue was dissolved in $CHCl_3$ and filtered on paper to remove a white solid. The organic solvent was evaporated under reduced pressure and the resulting residue was purified by CC (SiO_2; $CHCl_3$/MeOH 9.5/0.5) to afford compounds **22**-**24**. Compound **22**: yellowish oil, yield: 49%. ^{1}H-NMR ($CDCl_3$): δ 7.55 (d, 1H); 3.92 (t, 2H); 3.74-3.61 (m, 10H). ^{13}C-NMR ($CDCl_3$): δ 157.80; 149.89; 141.18; 130.54; 72.54; 70.30; 67.32; 61.47; 48.45. Compound **23**: yellowish oil, yield: 31%. ^{1}H-NMR ($CDCl_3$): δ 7.60 (d, 1H); 3.88 (t, 2H); 3.71-3.58 (m, 14H). ^{13}C-NMR ($CDCl_3$): δ 157.60; 149.77; 140.41; 130.59; 72.70; 70.17; 61.56; 48.47. Compound **24**: yellowish oil, yield: 42%. ^{1}H-NMR ($CDCl_3$): δ 7.57 (d, 1H); 3.88 (t, 2H); 3.72-3.57 (m, 22H). ^{13}C-NMR ($CDCl_3$): δ 156.16; 149.67; 140.19; 130.40; 72.92; 70.27; 68.82; 62.03; 48.47.

*Preparation of amphiphiles **11-13***

The appropriate 5-FU derivative **22**-**24** (1 eq), PCDA (1 eq), previously dissolved in CH_2Cl_2 and filtered by 0.45 μm filter to remove polymerized monomers, DCC (*N*,*N*'-dicyclohexylcarbodiimide; 1.1 eq) and DMAP (4-dimethylaminopyridine; 0.015 eq) were dissolved at r.t. in CH_2Cl_2 (30 mL/mmol of PCDA). The solution was stirred till the complete disappearance of the starting material on TLC ($CHCl_3$/MeOH: 9.5/0.5), in about 3 hours. Then hexane was added to precipitate the urea derivative and the solution was filtered and evaporated under reduced pressure. The resulting residue was purified by CC (SiO_2; $CHCl_3$/MeOH 9.8/0.2) to afford amphiphiles **11**-**13**. Amphiphile **11**: white solid, Yield: 33%. ^{1}H-NMR ($CDCl_3$): δ 7.52 (d, 1H); 4.22 (t, 2H); 3.91 (t, 2H); 3.72-3.62 (m, 10H); 2.31-2.23 (m, 6H); 1.61 (m, 2H); 1.50 (m, 4H); 1.36-1.25 (m, 24H); 0.87 (t, 3H). ^{13}C-NMR ($CDCl_3$): δ 173.73; 157.42; 149.66; 141.15; 130.46; 77.04; 76.73; 70.57; 68.98; 65.32; 63.13; 48.36; 34.12; 31.90; 29.61; 28.85; 28.35; 24.85; 22.67; 19.17; 14.09. Amphiphile **12**: white solid, yield: 41%. ^{1}H-NMR ($CDCl_3$): δ 7.59 (d, 1H); 4.26 (t, 2H); 3.93 (t, 2H); 3.75-3.67 (m, 14H); 2.33-2.25 (m, 6H); 1.64 (m, 2H); 1.52 (m, 4H); 1.39-1.27 (m, 24H); 0.89 (t, 3H). ^{13}C-NMR ($CDCl_3$): δ 173.79; 156.97; 149.34; 141.07; 130.45; 77.12; 76.70; 69.23; 68.92; 63.27; 48.31; 34.17; 31.91; 29.40; 28.90; 28.86; 28.77; 28.33; 24.86; 22.68; 19.20; 14.11. Amphiphile **13**: white solid, yield: 53.5%. ^{1}H-NMR ($CDCl_3$): δ 7.56 (d, 1H); 4.24 (t, 2H); 3.90 (t, 2H); 3.75-3.60 (m, 22H);

2.32-2.24 (m, 6H); 1.59 (m, 2H); 1.49 (m, 4H); 1.39-1.26 (m, 24H); 0.86 (t, 3H). ^{13}C-NMR ($CDCl_3$): δ 173.69; 156.69; 149.32; 142.00; 130.81; 77.33; 76.70; 72.27; 70.63; 68.88; 65.38; 63.76; 61.66; 48.61; 33.75; 31.92; 29.63; 28.78; 28.32; 25.25; 22.82; 19.55; 13.91.

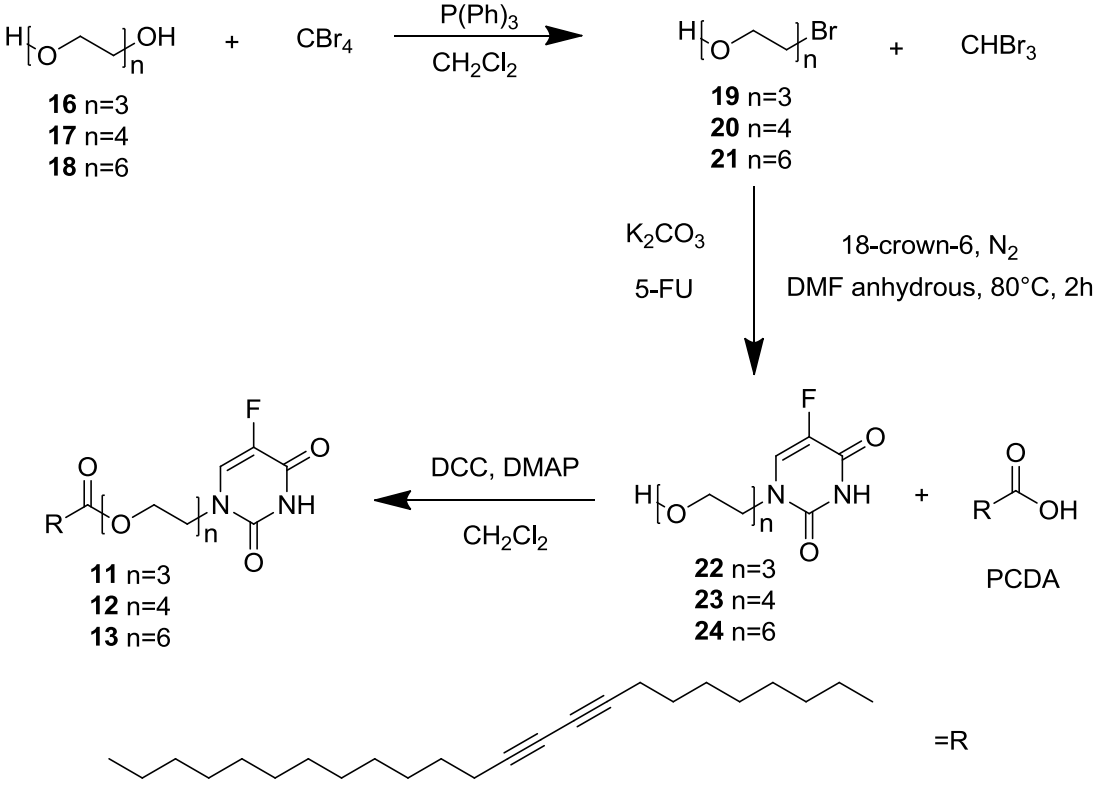

Figure 44**.** Synthetic pattern for the synthesis of amphiphiles **11-13**.

*Preparation of compounds **14** and **15***

2-Methoxyethanol, in the case of **14**, or MeOH in the case of **15** (10 eq), EDC (N-(3-dimethylaminopropyl)-N'-ethylcarbodiimide hydrochloride, 2.1 eq) and DMAP (0.010 eq) were added to a PCDA (1eq) solution in THF (3.5mL/mmol of alcohol) that was stirred for 18 h at room temperature. The solvent was evaporated under reduced pressure and the residue was dissolved in hexane. The pink solid residue (urea derivative) was separated by decantation and the organic phase was washed once with brine, dried on anhydrous Na_2SO_4 and evaporated under reduced pressure to afford the PCDA esters. Compound **14**: colorless oil, yield: 89%. ^{1}H-NMR ($CDCl_3$): δ 3.69 (s, 3H); 2.32 (t, 3H); 2.26 (t, 3H); 1.64-1.28 (m, 32H); 0.90 (t, 3H).

Compound **15**: colorless oil,yield: 70%. ^{1}H-NMR ($CDCl_3$): δ 4.24 (m, 2H); 3.61 (m, 2H); 3.41 (s, 3H); 2.35 (t, 2H); 2.25 (t, 4H); 1.64-1.27 (m, 32H); 0.90 (t, 3H).

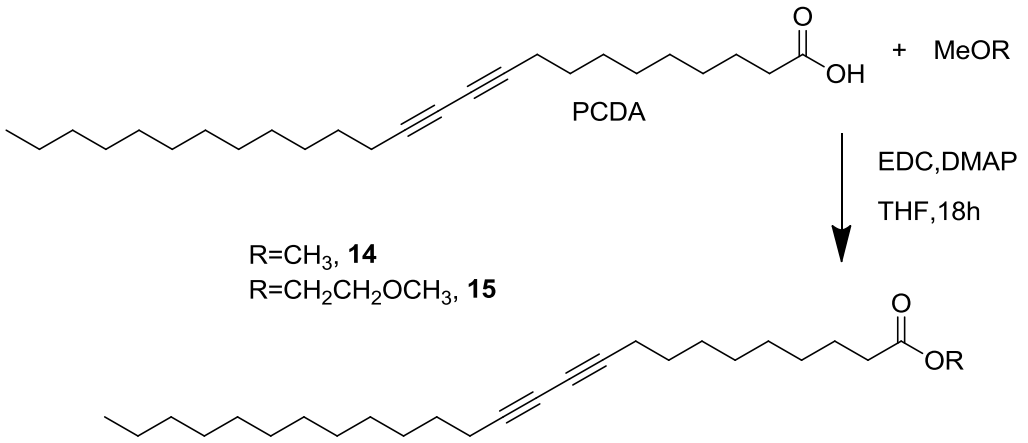

Figure 45. General procedure for the synthesis of **14** and **15.**

Liposomes preparation

Liposomes were prepared by a fast injection of lipids dissolved in DMSO at different molar ratios (Table 23) in 3 mL of 10 mM PBS buffer previously heated at 80 °C (final concentration=1 mM in total lipids). The solution was stirred at 80 °C for 15 minutes, then the suspension was sonicated for 20 minutes at 72 W and filtered with a PTFE syringe filter with 0.8 μm porosity. The solution was left overnight at 4°C and polymerized upon irradiation with UV light at 254 nm, for 5 minutes at room temperature.

Table 23. Composition of the investigated liposomal formulations.

PCDA/**11**(-**13**)	PCDA/PC/**11**(-**13**)[a]	PCDA/**14**(**15**)/**11**(-**13**)	PCDA/**14**(**15**)/**12**
9:1	5:4:1	5:4:1	4:5:1
9:0	6:4:0	6:4:0	6:3:1
			5.5:3.5:1

[a]PC, either DMPC or DOPC

DLS and Zeta potential measurements

DLS and electrophoretic mobility measurements were carried out at 25°C as explained above (see Chapter 2 section 1.3) on the samples without dilution directly soon after their preparation.

Evaluation of colorimetric response

The interaction of liposomes with TP and BSA was investigated by colorimetric tests: TP or BSA (at 1/1 molar ratio with **11-13**) were added to the samples that upon irradiation turned blue. The liposome suspensions in the presence of enzyme were left at room temperature for 1 hour to evaluate possible colorimetric change.

4.4 Results and discussion

4.4.1 Synthesis of amphiphiles

Amphiphiles **11–13** were prepared according to the synthetic pattern reported in Figure 44 starting from commercially available compounds **16–18.** that were reacted with CBr_4 in CH_2Cl_2, in the presence of $P(Ph)_3$, to give derivatives **19–21** that were successively reacted with 5 equivalents of 5-FU in the presence of a stoichiometric amount of K_2CO_3 and a catalytic amount of 18-crown-6 in anhydrous DMF under N_2 at 80 °C for 2 h to give 5-FU derivatives **22–24**. Amphiphiles **11–13** were prepared by reacting 5-FU derivatives **22–24** with commercial PCDA in the presence of a stoichiometric amount of DCC and a catalytic amount of DMAP in CH_2Cl_2. The molar ratios of these reactions have been optimized in order to reduce the quantity of the disubstituted compounds to a minimum. Esters **14-15** were prepared as illustrated in Figure 45 starting from commercial PCDA in the presence of a stoichiometric amount of EDC and a catalytic amount of DMAP in THF for 18 h.

4.4.2 Preparation of PDA liposomes

PDA liposomes prepared in 10 mM PBS polymerized quickly upon UV light irradiation and resulted stable for at least 1 year. Actually, a higher ionic strength hampered the polymerization and induced precipitation. This result is probably due

to the high concentration of cations that, interacting with the carboxylic groups of PCDA, affects the organization of the lipid bilayer thus disturbing the proper alignment of lipids required for the photopolimerization. In fact, as described in the introduction, the polymerization of diacetylenic function is topotactic and needs a well-defined topology of the monomers in terms of relative distances and angle between diacetylenic functions. In general, most formulations gave a high extent of polymerization as shown by the blue color of the obtained solution. However, in the case of liposomes formulated with any of PCDA ester derivatives, a blue solution was observed only in the presence of at least 55% of PCDA, whereas 50% and 40% of PCDA yielded a light color and a colorless solution, respectively. It is possible that a high amount of PCDA ester hinders lipid organization (in terms of distance and relative angles among the monomers) required for the occurrence of photopolymerization.

4.4.3 DLS and Zeta potential measurements

Liposomes size and zeta potential were evaluated by DLS measurements. The obtained results are reported in Table 24. All formulations feature a D_H among ≈ 100 and 150 nm. In samples containing PCDA esters 14 and 15 and a 5-FU derivative a minor smaller population (D_H among ≈ 60 nm) is also present, suggesting that the presence of these synthetic analogues together brings to a decrease of liposomes stability. As expected, in all cases a negative potential was observed.

Table 24. Liposomes dimensions and zeta potential. Similar results were obtained investigating analogue formulations containing 15 instead of 14 and/or 12 or 13 instead of 11, with the exception of the three samples reported in the bottom of the table.

Formulations	Size (nm)	Z-potential (mV)
PCDA	164±3	-39±3
PCDA/DMPC 6:4	145±5	-43±3
PCDA/DOPC 6:4	155±3	-38±3
PCDA/**11** 9:1	92±5	-49±5
PCDA/DMPC/**11** 5:4:1	158±4	-43±4
PCDA/DOPC/**11** 5:4:1	148±6	-37±5
PCDA/**14** 6:4	138±5	-45±4
PCDA/**14**/**11** 5:4:1	92±8	-51±8
PCDA/**14**/**12** 4:5:1	140±3	-40±3
PCDA/**14**/**12** 6:3:1	115±6	-55±6
PCDA/**14**/**12** 5.5:3.5:1	105±5	-53±5

4.4.4 Sensoring evaluation

The capability of the investigated formulations to give a colorimetric response upon the interaction with the target enzyme, TP, was investigated by adding an aqueous solution of TP to the aqueous suspension of liposomes in equimolar amount with respect to 5-FU derivative. Analogous experiments were carried out on BSA aqueous solution as negative controls (Table 25-26, Figure 46-47). PCDA and PCDA/PC formulations in the absence of 5-FU derivatives do not show any change of color upon addition of TP, whereas the same formulations give a colorimetric

response (from blue to light purple) upon addition of BSA, due to electrostatic unspecific interactions with the carboxylic groups of PCDA and/or the PEG polar spacers.

Table 25. Colorimetric response of 5-FU decorated PDA liposomes.

Formulations	UV	TP	BSA
PCDA/**11**(**12**,**13**) 9:1	blue	blue	purple
PCDA/DOPC/**11**(**12**,**13**) 5:4:1	blue	blue	purple
PCDA/DMPC/**11**(**12**,**13**) 5:4:1	blue	violet	pink

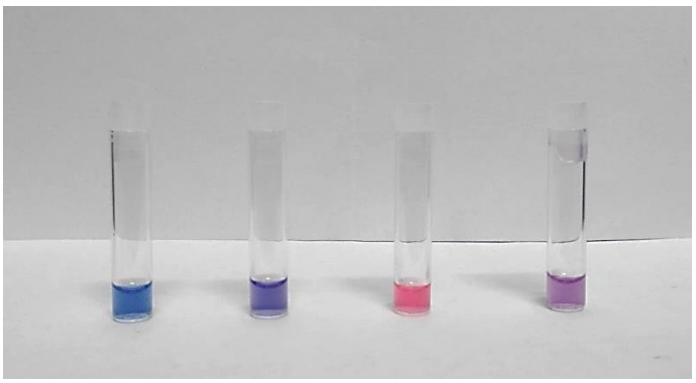

a. b. c. d.

Figure 46. Typical color variations of PDA liposomes: a. blue; b. violet; c. pink; d. purple.

PCDA/**11**(**-13**) formulations remained blue upon addition of TP while turned into an intense purple in the presence of BSA without any differences related to the different 5-FU derivative. Two hypotheses can explain this result: *i)* the binding of 5-FU with TP does not induce a conformational change in the polymer backbone; *ii)* 5-FU residues are embedded in the lipid bilayer. On the other hand, the strong electrostatic interactions promote the interaction with BSA and lipid rearrangement. Analogous results were observed in the case of PCDA/DOPC/**11**(**-13**) formulations.

On the other hand, in the case of PCDA/DMPC/**11**(**-13**) the blue liposome suspensions clearly turned into violet and pink upon the interaction with TP and BSA, respectively. It is possible that the higher fluidity of DOPC containing liposomes allows the 5-FU residues to embed in the lipid bilayer rather than keeping exposed to the bulk thus being able to interact with the target enzyme.

Table 26. Colorimetric tests in the presence of PCDA ester derivatives.

Formulations	UV	TP	BSA
PCDA/**14**(**15**)/**11**(**-13**) 5:4:1	blue	blue	violet
PCDA/**14**(**15**)/**12** 5:4:1	light violet	light pink	light violet
PCDA/**14**(**15**)/**11**(**13**) 4:5:1	colorless	-	-
PCDA/**14**(**15**)/**11**(**-13**) 6:3:1 and 5.5:3.5:1	blue	blue	violet

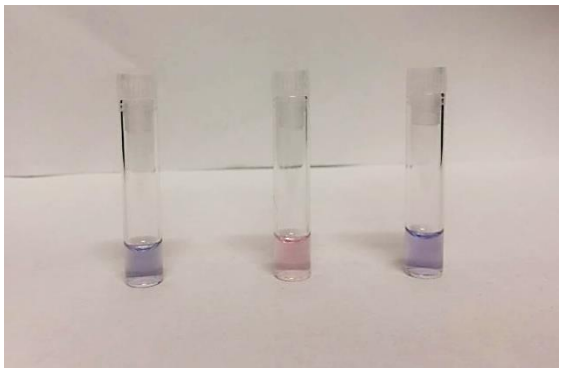

a. b. c.

Figure 47. Colorimetric evaluation. PCDA/**14**/**12** (5:4:1) liposomes: a. upon irradiation; b. upon interaction with TP; c. upon interaction with BSA.

Considering that all formulations gave a colorimetric response in the presence BSA (that we attributed to electrostatic interactions), we partially substituted PCDA with its ester derivatives in the attempt to reduce the negative charge on liposome surface. The intense blue color of the suspension of polymerized PCDA/**14**(**15**)/**11**(**13**) liposomes at 5:4:1 molar ratio was not affected by the interaction with TP whereas changed into violet upon addition of BSA. The trend is similar to that observed in the case of PCDA/**11**(-**13**) (blue to purple), however the change of color upon interaction with BSA is less marked, thus suggesting that the extent of electrostatic interaction plays a crucial role in the response of BSA. Interestingly, a specific response to TP, in the absence of any aspecific response to BSA, was observed in the case of PCDA/**14**(**15**)/**12** (5:4:1) formulations, though the change of color was not sharp, thus indicating a role of the PEG spacer of 5-FU derivative that can better expose the targeting residue to the interaction with TP. To solve this limitation we investigated liposomes in which the molar percentages of the components vary in the range of 10% (Table 23), but either the sensitivity of the system was strongly reduced (with PCDA at 60%) as or the solution was colorless (PCDA 40%) as previously mentioned.

These systems have a good potential to be used for the differential analysis; in fact some formulations changes color only in the presence of BSA, others show a different responce with TP and BSA. Future perspectives are the synthesis of PCDA and 5-FU derivatives analogues with different polar moiety to reduce unspecific interactions with the negative control.

4.5 Conclusions

Several PCDA and 5-FU derivatives were synthesized in order to use them in mixed liposomes for the development a colorimetric sensor for the dosage of TP enzyme. Our results demonstrate that either the fluidity of the bilayer and the polarity of the of the headgroup region play a crucial role in determining the sensoristic response of the system. The most promising results were obtained with PCDA/**14(15)**/**12** (5:4:1), even if the colorimetric variation is not so neat.

General conclusions

Liposomes are very versatile aggregates due to the possibility to functionalize and/or modulate their physicochemical properties to make them suitable for the aim to achieve.

In this thesis liposomes were investigated as drug delivery systems of natural substances (such as (+)-usnic acid and curcumin) and as biosensor for thymidine phosphorylase, a biomarker enzyme. The main focus of this work was to relate the properties of the aggregates to the molecular structure of the components.

The obtained results point out that also small variations in lipids chemical structure can affect *i)* the positioning of the loaded molecule in the bilayer and its pharmacological activity, *ii*) liposomes ability to interact with the biological environment and *iii*) their sensitivity/specificity as sensors. A crucial role is played by the fluidity of the bilayer together with lipid packing/organization. Moreover, the reported findings demonstrate that the charge of the polar headgroups is not the only parameter that controls the z-potential of the aggregates.

Another aspect that must not be neglected is the liposomes preparation methodology and the protocol for solute inclusion because can influence the stability and the homogeneity of the aggregates and the availability of the loaded molecules.

In conclusion, the subtle balance among all the investigated features determines liposomes physicochemical properties (thus their biological fate) and must always be evaluated altogether to have an overall view of the system.

Acknowledgments

At first, I would like to thank Dr. Luisa Giansanti, my PhD tutor, for all I have learned in these three years in the professional and personal matters and for giving me the possibility to always express myself.

I would like also to thank also Dr. Nora Ventosa and Dr. Jaume Veciana for giving me the opportunity to make an important and formative experience abroad and all the Nanomol group for welcoming me (in particular way Guillem and Mariana for their big help during my staying). In Barcelona I met fantastic people that I won't forget.

I am very grateful to all the people together with I worked or I spent my time at the University of L'Aquila during these three years; each of them helped and supported me in anyway.

At last but not least, I wish to thank my family, in particular way my parents, my husband and all my friends for always believing in me.

Finally, I want to thank me for the efforts made to achieve this important objective.